The Role of the Oncofetal Glycoprotein 5T4 in Ovarian Cancer Metastasis

A thesis submitted to the University of Manchester for the degree of Doctor of Philosophy in the Faculty of Medical and Human Sciences

2015

Saladin Sawan

School of Medicine

CONTENTS

Count Number: 56383 words

List of Figures

List of Tables

List of Appendices

ABSTRACT

The University of Manchester
Name: Saladin Sawan
Degree title: Doctor of Philosophy (PhD)
Theses title: The Role of the Oncofetal Glycoprotein 5T4 in Ovarian Cancer Metastasis
Date: February 13 2015

Ovarian cancer is the most lethal gynaecological cancer which frequently presents in advanced stages with the majority of patients succumbing to their disease. Cancer related mortality is generally caused by metastases, yet there is a paucity of information in the literature pertaining to investigations of the mechanisms involved in ovarian cancer metastasis.

5T4 is an oncofetal antigen; its expression in ovarian cancer has been previously found to be associated with advanced stages (cancer spread) and poor clinical outcome. Recent work in embryonic cells has suggested roles for 5T4 in both epithelial mesenchymal transition (EMT) and the functional cell-surface expression of the chemokine receptor CXCR4. In addition, Waif1, zebrafish homologous 5T4, was shown to inhibit canonical wnt signalling while activating the planar cell polarity (PCP) pathway. EMT, CXCR4-mediated chemotaxis and PCP pathway have all been implicated in cancer invasiveness and spread.

In this project several ovarian cancer cell lines have been investigated in terms of their phenotype as defined by the expression of 5T4, CXCL12 receptors (CXCR4 and CXCR7) and EMT markers (E-cadherin and N-cadherin), and their chemotactic response to CXCL12.

Two cell lines, SKOV-3 and Hoc-8, emerged as a useful model to investigate 5T4 biology further, the former expressed 5T4 and responded chemotactically to CXCL12 while the latter did not express 5T4 nor did it respond to CXCL12 in spite of showing surface CXCR4 expression.

5T4 knockdown in SKOV-3 cells abrogated the chemotaxis response to CXCL12, reduced non-directional cell motility and induced mesenchymal to epithelial transition. 5T4 overexpression in Hoc-8 promoted the reverse transition EMT and improved cell motility. In addition, 5T4 knockdown in SKOV-3 cells supressed non-canonical wnt signalling, and facilitated β-catenin dependent canonical pathway.

Analysis of 11 paired (primary & metastatic) human epithelial ovarian cancer samples showed higher 5T4 expression in the metastatic samples which was accompanied with a reciprocal change in the expression of cytokeratins and JNK expression.

Overall, this study has found 5T4 to be upregulated in metastatic ovarian cancers; also changes in its expression *in vitro* supported a metastatic phenotype making 5T4 a potential marker and a therapeutic target in metastatic ovarian disease.

DECLARATION

No portion of the work referred to in this thesis has been submitted in support of an application for another degree or qualification of this or any other university or other institute of learning.

COPYRIGHT STATEMENT

ACKNOWLEDGEMENT

I am deeply indebted to my supervisors, Professors Henry Kitchener and Peter Stern. Professor Stern's painstaking efforts converting me into a scientist, I hope, have been fruitful. The vivid memories of our discussions in my early PhD days are still alive. I have fond memories from my PhD years, and I hope I have managed to leave you with some good memories of your experience supervising me. I am ever so grateful for your hard work and commitment especially at those times when you could have chosen to have an easier life.

Prof Kitchener's support has guided my clinical and academic career over the last several years; I am very grateful for all you have done, directly and indirectly, to see me reach this point in my career.

I would like to acknowledge the help and support of my external supervisor Dr Eyad Elkord and advisor Dr Dave Gilham. I would also like also to thank all the present and past members of the Immunology Group in the Paterson Institute for Cancer Research for the great atmosphere during my PhD years which made me almost forget I was a clinician. Georgi Marinov, Andrzej Rutkowski, Kate Mulryan, Jian Li, Tom Southgate and Fernanda Castro; it was a real pleasure to know you all.

Special thanks to Owen McGinn for proofreading my thesis; your help and guidance particularly during the difficult times, which I encountered frequently, are much appreciated and made a huge difference. My sincere thanks also to Julie Brazzatti; our stimulating discussions and joint work on wnt signalling were very useful experiences. I am also grateful to Darren Roberts whose help in primary materials was clearly evident; you went out of your way to teach me all about staining and much of the block chemotaxis was built on your extensive experience. Debbie Burt's help during my MRes and PhD years at the Paterson was something I could always rely on; late or small samples for flow cytometry did not make you shy away from helping me out. Many more friends and colleagues at the Paterson have helped me in many ways; discussions, ideas, providing materials and making things happen; thank you all.

I would also like to thank Pat Caswell for the useful discussions and collaboration; I am glad further collaborative projects are progressing.

I am also grateful to the clinical team at St Mary's Hospital in Manchester especially Emma Crosbie whose work with Tom Southgate had led to this project. Rick Clayton, Cath

Holland and Saad Ali; your professional support and your efforts facilitating tissue collection are much appreciated.

The histopathologist team at Central Manchester Hospitals is remarkably pro research and they often did not mind providing fresh tissue samples even at late times or short notice; Rhona McVey, Gina Howarth, Richard Fitzmaurice and Godfrey Wilson; I am so grateful to you all. Many samples were provided or collected via BRC Biobank; thank you Jay Brown and Natalie Fyfe.

I would like also to thank the Core Facilities staff in the Paterson for their indispensable support and for the use of the state-of-the-art facilities in flow cytometry, microscopy and histology. Steve Bagley, Garry Ashton, Michelle Greenhalgh, Caron Abbey, Jeff Barry, Michael Hughes, and Kang Zeng, I am ever so grateful for your help all.

I am grateful to Sam Fletcher, Linsey Nelson and Carly Moseley for all their help including the final proof reading of this document.

I would also like to thank the administration teams in the University of Manchester and the Paterson Institute for Cancer Research not only for making the effort to simplify procedures and supporting this research project, but also for showing understanding during the difficult times I went through.

This work, and my PhD, would have not taken place without the generous funding from the Wigan & District Cancer Research Trust and William Walter Trust Fund.

Lastly but certainly not least, I am grateful to all women who took part in this research and other research studies. While you were going through the difficult time of cancer diagnosis and the impact of the emotional stress on your lives, you showed incredible generosity believing in the common good for the human race.

DEDICATION

To the remarkable women of Syria

I know, ovarian cancer is not really what is concerning you right now!

Saladin Sawan, Manchester 2015

ABBREVIATIONS

µM	micro Molar
7-AAD	7-Aminoactinomycin D
AA	Amino acid
ADP	Adenosine diphosphate
AF	AlexaFluor
AMP	Adenosine monophosphate
APC	Adenomatous polyposis coli
ARID1A	AT-rich interactive domain-containing protein 1A
Asp	Aspartic acid
ATCC	American Type Culture Collection
ATP	Adenosine triphosphate
B-ALL	B-cell acute lymphoblastic leukaemia
BAFF	B cell activating factor
BAR	β-catenin-activated reporter
BFA	Brefeldin A
bHLH	basic helix-loop-helix
BLAST	Basic Local Alignment Search Tool
bp	Base pair
BRAF	B-Raf proto-oncogene, serine/threonine kinase
BSA	Bovine serum albumin
BSB	Basic sorting buffer
CaCl2	Calcium chloride
cAMP	Cyclic adenosine monophosphate
CCR5	C-C chemokine receptor type 5
CCR7	C-C chemokine receptor type 7
CD26	Cluster of differentiation 26
cDNA	Complementary DNA
CEA	Carcinoembryonic antigen
CK	Cytokeratin
CK-1	Casein kinase-1
CTLA-4	Cytotoxic T-lymphocyte antigen 4
CTNNB1	β-catenin gene
CXCL11	Chemokine (C-X-C motif) ligand 11
CXCL12	Chemokine (C-X-C motif) ligand 12
CXCR3	Chemokine (C-X-C motif) receptor 3
CXCR4	Chemokine (C-X-C motif) receptor 4
CXCR7	Chemokine (C-X-C motif) receptor 7
DAB	3,3'-Diaminobenzidine
DAG	Diacyl glycerol
DAPI	4',6-diamidino-2-phenylindole
dATP	Deoxyadenosine triphosphate
ddH2O	Double distilled water
DEPC	Diethyl pyrocarbonate
DIC	Differential interference contrast (microscopy)
DiIC12(3)	1,1' Didodecyl-3,3,3',3'-tetramethylindocarbocyanine iodide
DKK	Dickkopf
D-MEM	Dulbecco’s Modified Eagle’s Medium
DMSO	Dimethyl sulfoxide

DNA	Deoxyribonucleic acid
DPA	Diprotin A
DPPIV	Dipeptidyl peptidase-4
dsDNA	Double stranded DNA
DVL	Dishevelled
EC_{50}	Half-maximal effective concentration
ECACC	European Collection of Cell Culture
ECM	Extra Cellular Matrix
EDTA	Ethylenediaminetetraacetic Acid
eGFP	Enhanced green fluorescent protein
EGFR	Epidermal growth factor receptor
EGTA	Ethylene glycol tetraacetic acid
ELISA	Enzyme-linked immunosorbent assay
EmGFP	Emerald green fluorescent protein
EMP	Epithelial mesenchymal plasticity
EMT	Epithelial mesenchymal transition
EOC	Epithelial Ovarian Cancer
ER	Epitope retrieval
ER	Endoplasmic reticulum
ERBB2	v-erb-b2 avian erythroblastic leukemia viral oncogene homolog 2
ERK	Extracellular Signal-Regulated Kinase
ES	Embryonic Stem
Fab	Fragment antigen-binding
FACS	Fluorescence-Activated Cell Sorting
FAP	Familial adenomatous polyposis
FC	Flow Cytometry
Fc	Fragment crystallisable
FCS	Fetal calf serum
FIGO	International Federation of Gynecology & Obstetrics
FITC	Fluorescein isothiocyanate
fMLP	N-formyl-methionyl-leucyl-phenylalanine
FOXO	Foxhead box transcription factor, group O
FSC	Forward scatter
FZD	Frizzled
GAIP	Gα interacting protein
GAP	GTPase activating protein
GAPDH	Glyceraldehydes-3-phosphate dehydrogenase
GDP	Guanosine DiPhosphate
GEF	Guanine exchange factor
GFP	Green fluorescent protein
GIPC	GAIP-interacting protein, C terminus
GPCR	G Protein-Coupled Receptor
GRK	G protein-coupled receptor kinase
GSK3	Glycogen synthase kinase 3
GTP	Guanosine TriPhosphate
H&E	Haematoxylin and eosin
HBS	HEPES-buffered saline
HBSS	Hank's balanced salt solution
HEK	Human embryonic kidney cells
HEPES	4-(2-Hydroxyethyl) piperazine-1-ethanesulfonic acid
HGF	Hepatocyte growth factor
HNPCC	Hereditary Non-Polyposis Colorectal Cancer

HOXA	Homeobox A
HRP	Horseradish peroxidase
HSP	Heat shock protein
IC	Intracellular
ICAM	Intracellular adhesion molecule
ICD	Intracellular domain
IF	Immunofluorescence
IFN	Interferon
IFN-γ	Interferon gamma
Ig	Immunoglobulin
IgG	Immunoglobulin G
IHC	Immunohistochemistry
Ile	Isoleucine
IMDM	Iscove's Modified Dulbecco's Medium
int-1	integrase-1
JNK	c-Jun N-terminus kinase
KD	Knockdown
kDa	Kilo Dalton
KO	Knock-out
KRAS	Kirsten rat sarcoma viral oncogene homolog
LacZ	β-galactosidase gene
LB	Lysogeny broth
LB Agar	Luria-Bertani Agar
LDL	Low density lipoprotein
LEF	Lymphoid enhancer factor
LFA-1	Lymphocyte function-associated antigen 1
LiCl	Lithium chloride
LIF	Leukemia inhibitory factor
LRP6	LDL receptor related protein 6
LRR	Leucine rich repeat
m5T4	Mouse 5T4
mAb	Monoclonal antibody
MAPK	Mitogen-activated protein kinase
MAPKK	MAPK kinase
MAPKKK	MAPKK kinase
MCS	Multiple cloning site
MDCK	Madin-Darby canine kidney cells
MDSC	Myeloid-derived suppressor cells
MEFs	Murine Embryo Fibroblasts
MEK	MAPK-ERK kinase
mES	Mouse embryonic stem
MET	Mesenchymal epithelial transition
MFI	Median fluorescence intensity
MFIR	Median fluorescence intensity ratio
MHC	Major histocompatibility complex
miRNA	micro RNA
MMP	Matrix MetalloProteinase
MMTV	Mouse mammary tumour virus
MOI	Multiplicity of infection
mRNA	Messenger RNA
MTOC	Microtubule-organizing centre
MTT	3-(4,5-dimethylthiazolyl-2)-2,5-diphenyltetrazolium bromide

MVA	Modified vaccinia Ankara
MVA-5T4	Modified Vaccinia Ankara encoding 5T4
nAb	Neutralizing antibody
NHS	National Health Service
NLS	Nuclear localisation signal
NS	Non-specific
NSCLC	Non-small cell lung carcinoma
Oct-4	Octamer-binding transcription factor 4
ORF	Open reading frame
OSE	Ovarian surface epithelium
P/S	Penicillin and streptomycin
PAGE	Polyacrylamide gel electrophoresis
PBMCs	Peripheral blood mononuclear cells
PBS	Phosphate buffered saline
PCP	Planar cell polarity
PCR	Polymerase chain reaction
PDK-1	PIP3-dependent protein kinase 1
PDZ	PSD-95 (postsynaptic density protein), Discs-large (Drosophila tumour suppressor), and ZO-1 (zonula Occludens-1)
PE	Phycoerythrin
PEG	Polyethylene glycol
PFA	Paraformaldehyde
PH	Pleckstrin homology
PhD	Doctor of Philosophy
PI	Phosphatidylinositol
PI3K	Phosphoinositide 3-kinase
PICR	Paterson Institute for Cancer Research
PIK3CA	Phosphatidylinositol-4,5-bisphosphate 3-kinase, catalytic subunit alpha
PIP2	Phosphatydlinositol-4,5-bisphosphate
PIP3	Phosphatydlinositol-3,4,5-trisphosphate
p-JNK	Phospho-JNK
PKB	Protein kinase B/Akt
PKC	Protein kinase C
PLC	Phospholipase C
PLD	Phospholipase D
PMS	N-methyl dibenzopyrazine methyl sulphate
PMSF	Phenylmethylsulfonyl fluoride
PP2A	Protein phosphatase 2A
PPC	Primary peritoneal cancer
pRb	Retinoblastoma protein
Pro	Proline
PtdIns	Phosphatidylinositol
PTEN	Phosphate and tensin homolog deleted on chromosome ten
PTX	Pertussis toxin
qPCR	Quantitative PCR
RBD	Ras-binding domain
RCC	Renal cell carcinoma
REC	Research Ethics Committee
RNA	Ribonucleic Acid
RNAi	Ribonucleic acid interference
ROCK	Rho-associated kinase
RPA	Ribonuclease protection assay

RPMI-1640	Roswell Park Memorial Institute growth medium
RT	Reverse transcription
SCLC	Small cell lung cancer
SD	Standard deviation
SDF-1	Stromal cell-derived factor-1
SDS	Sodium dodecyl sulphate
SEA	Staphylococcal enterotoxin A
SEM	Standard error of mean
Ser	Serine
sFRP	Secreted Frizzled-related proteins
SH	Src homology
SHIP	Src homology 2 domain-containing inositol 5-phosphatase
shRNA	Short hairpin ribonucleic acid
siRNA	Small interfering RNA
SKR	Specific knockdown ratio
SOC	Super optimal broth with catabolic repression
SSC	Side scatter
ssDNA	Single stranded DNA
SSEA-1	Stage-specific embryonic antigen-1
StMPM	Syncytiotrophoblast microvillous plasma membranes
SV40	Simian vacuolating virus 40
TAA	Tumour associated antigen
TBS	Tris buffered saline
TCF	T-cell factor
TEMED	Tetramethylethylenediamine
TGF-β	Transforming growth factor-beta
TIL	Tumour associated lymphocytes
TIP-2	Tax interacting protein 2
TIRF	Total internal reflection fluorescence (microscope)
TKR	Total knockdown ratio
TLR	Toll-like receptor
TM	Transmembrane
TNF-α	Tumour necrosis factor alpha
TOP/FOP	Optimal Tcf-binding site/Far-from-optimal Tcf-binding site
TP53	Tumour protein p53
TPBG	Trophoblast Glycoprotein
TRE	Tetracycline responsive element
Treg	T regulatory cell
uPAR	Urokinase receptor
UTR	Untranslated region
Val	Valine
VEGF	Vascular endothelial growth factor
VEGFR	Vascular endothelial growth factor receptor
Waif1	wnt-activated inhibitory factor 1
wg	wingless
WHIM	Warts, Hypogammaglobulinaemia, Infections, and Myelokathexis syndrome
WIF-1	WNT inhibitory factor-1
wnt	wg/int-1
WT	Wild type
X-gal	Bromo-4-chloro-indolyl-*ƒ*À-D-galactopyranoside
X^2	Chi squared
ZEB1	Zinc finger E-box-binding homeobox 1

Chapter 1

INTRODUCTION

Introduction

Epithelial ovarian cancer (EOC) is a common gynaecological cancer in which metastasis plays a detrimental role as EOC usually presents at advanced stages and has a high relapse rate contributing to the poor prognosis observed in this disease.

In addition to their roles in homeostasis and embryological development, several biological processes have been implicated in cancer spread such as epithelial mesenchymal transition (EMT), wnt signalling, and chemotaxis. The glycoprotein 5T4, which is expressed in the majority of ovarian cancers, has been implicated in these three processes.

This study aimed to explore whether 5T4 contributes functionally to ovarian cancer spread via possible roles in these biological processes. A better understanding of 5T4 role in ovarian cancer metastasis could help to develop new 5T4-based therapeutics or to improve the existing ones.

The following sections in this chapter review the current relevant knowledge of 5T4, epithelial ovarian cancer, chemotaxis, epithelial mesenchymal transition and wnt signalling.

1.1 The Oncofetal Glycoprotein 5T4

5T4 is an oncofetal glycoprotein, also known as trophoblast glycoprotein (TPBG) which was first described in 1988 by Hole and Stern[1]. Glycoproteins were purified from plasma membranes from human trophoblast syncytial microvilli and then were used as immunogens to raise antibodies which were selected on the basis of binding to trophoblasts and cancer cell lines but not normal peripheral blood mononuclear cells (PBMCs)[1]. 5T4 expression by several human cancer tissues was subsequently confirmed using immunohistochemistry[2].

The rationale was that oncofetal proteins are molecules expressed by both cancer cells and placental trophoblasts as these two types of cell share many properties including immune evasion and invasiveness[3]. While trophoblasts invade maternal endometrium to establish placentation which is essential for nutrient and gas exchange between maternal and fetal circulations[4], invasiveness is a hallmark of cancer which distinguishes it from benign tumours[5, 6].

1.1.1 5T4 Structure

5T4 is a heavily N-glycosylated protein with a molecular weight of approximately 72 kDa; the core protein after deglycosylation with N-glycanase is 42 kDa[7]. 5T4 is encoded, in humans, by the gene *TPBG* which is located on the long arm of chromosome 6 at q14-15[8].

5T4 is a 420 amino acid (AA) long trans-membranous protein; contains seven N-glycosylation sites and some seven leucine-rich repeat (LRR) motifs in the extracellular domain (**Figure 1.1**). LRR regions are found in proteins with diverse functional roles where LRR motifs serve to provide a structural framework which facilitates protein–protein interactions[9]. The short cytoplasmic tail of 5T4 contains a class I PDZ-binding motif (Ser-Asp-Val) which was shown to interact with TIP-2/GIPC[10]. TIP-2 is a protein that contains a PDZ domain, its interaction with 5T4 could provide a link between 5T4 and actin cytoskeleton.

Figure 1.1: 5T4 Structure

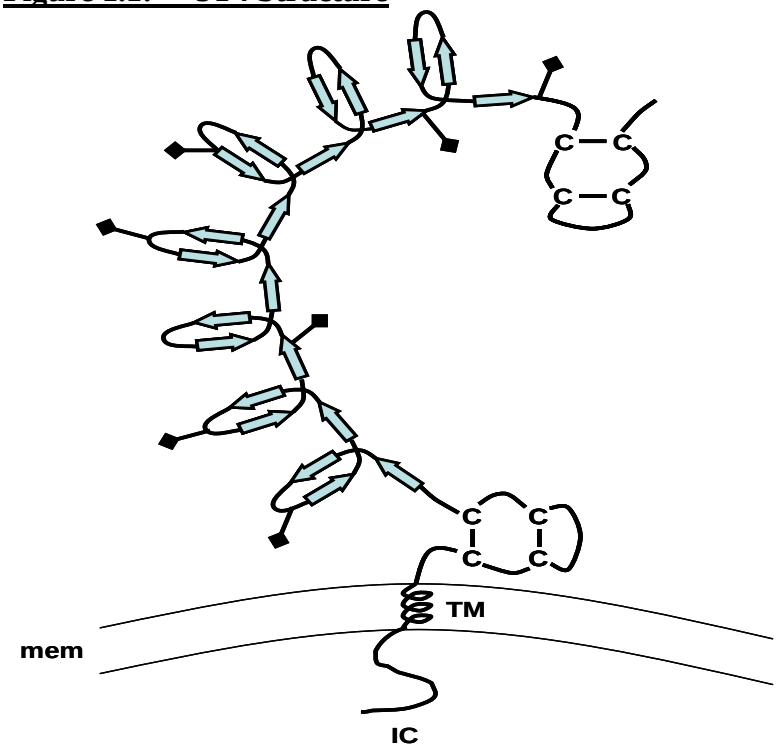

Schematic representation of 5T4 structure
Human 5T4 molecule consists of extracellular domain, trans-membranous domain (TM) and intra-cellular domain (IC). The extracellular domain comprises 7 leucine-rich repeats (arrows) and has 7 glycosylation sites (diamonds). After: Shaw *et al.*[7].

1.1.2 5T4 and Human Cancer

1.1.2.1 5T4 as a Tumour Associated Antigen (TAA)

Initial work documented the expression of 5T4 in a variety of epithelial cancer cell lines[1]. Subsequent studies on primary human neoplastic and non-neoplastic specimens confirmed the high expression of 5T4 in most malignant tumours with absent or low expression in normal and benign tissues[2]. 5T4 expression has since been found in a wide range of human cancers including cervical, gastric, colorectal, renal cell and ovarian cancers[11-14].

5T4 generally is not expressed by normal tissues in adults while some tissues have shown only limited expression such as: endometrium, cervical glands, gastric mucosal glands, and skin[2, 15].

This differential expression of 5T4 in malignant tumours but not in adult healthy tissues has identified it as a useful tumour associated antigen (TAA) with a potential use in the diagnosis and treatment of cancers.

Cancer treatment using TroVax® vaccine MVA-5T4 (Modified Vaccinia Ankara encoding 5T4) has been investigated in several clinical trials. Phase I/II studies in patients with colorectal cancer and renal cell cancer confirmed the presence of immune response against 5T4, the treatment was well tolerated with no side effects of concern[16]. Currently, a phase II clinical trial (TRIOC) is assessing the activity of TroVax® in relapsed asymptomatic epithelial ovarian cancers. Recruitment of 100 patients, randomised to receiving intramuscular TroVax® or placebo, is expected to be completed in November 2015[17].

Another approach has been tumour targeted superantigen (TTS) therapy utilising 5T4-targeted superantigen (SAg) with the rationale that this treatment can activate and recruit effector T cells into tumours[18]. ABR-217620 (naptumomab estafenatox, Anyara) is a fusion of a fragment antigen-binding (Fab) recognising 5T4 and a superantigen from staphylococcal enterotoxin A (SEA), a potent activator of human T cells. Anyara and its predecessor ABR-214936 (anatumomab mafenatox) have been shown to be safe and well tolerated in early phase clinical trials. Anatumomab mafenatox was associated with a prolonged survival in comparison to published data when it was used in a phase II trial in advanced renal cell cancer patients[19].

5T4 has been utilised as a TAA also in pre-clinical studies using 5T4 antibody tagged with active anti-cancer drugs (antibody drug conjugate: ADC). ADC therapeutics

are designed to deliver effective cytotoxic drugs into cancer cells which are selectively targeted by the TAA. An immunoconjugate of 5T4 antibody and calicheamicin, a potent cytotoxic drug, has shown an improved growth control in subcutaneous 5T4 positive tumour models in comparison to various controls[20]. More recently, the authors reported improved ADC technology by exploring other combinations of 5T4-antibody / linker / payload (active drug)[21]. A1mcMMAF is a conjugate of a humanised 5T4 antibody (A1) linked to the tubulin inhibitor monomethylauristatin F (MMAF) using a non-cleavable maleimidocaproyl (mc) linker. Xenograft studies suggested that A1mcMMAF was selectively delivered to 5T4 expressing cells, caused mitotic arrest, and inhibited tumour growth. A1mcMMAF was also well tolerated with no significant adverse events when it was administered in cynomolgus monkeys at 10 mg/kg[21].

1.1.2.2 5T4 and Metastasis

An elegant study conducted in colorectal and gastric cancers found that while more than 80% of cancers expressed 5T4 on cancer or stroma cells; it was the staining of cancer cells which correlated with cancer spread; 65% of patients with 5T4 expression on the tumour cells, but only 23% of those whose cancer cells did not stain for 5T4, had metastatic spread[22]. In another study in colorectal cancer patients, 5T4 expression by tumour cells was found to be an independent prognostic factor for poor prognosis regardless of age, sex, disease stage, and tumour site. Five year survival rate approached 75% in patients with negative staining of tumour cells but was only 22% in patients with positive staining for 5T4 in cancer cells[23].

Moreover, the 5T4 potential role in cancer spread was strengthened when a prospective study of gastric cancer patients showed that all 16 metastatic lesions in the regional lymph nodes investigated in this study stained positive for 5T4, this study also confirmed a correlation between positive staining for 5T4 with both cancer stage and poor prognosis[12].

The frequent association between 5T4 expression and cancer spread in these and other studies has posed the question of whether 5T4 has functional capabilities through which it contributes to epithelial cancer invasiveness and metastasis. The structure of 5T4 would support a potential functional role served by this protein given the fact that the several LRR motifs in the extracellular domain could form a platform for interaction with other extracellular proteins such as extracellular matrix (ECM) proteins; and the fact that the PDZ-binding domain in the intracellular tail and its link with the actin cytoskeleton indicate a possible role for 5T4 in cell morphology and motility.

Indeed, in recent years 5T4 expression has been implicated in three important biological processes, epithelial mesenchymal plasticity (EMP)[24], CXCL12-mediated chemotaxis[25] and wnt signalling[26]. These processes are pivotal in embryogenesis and organogenesis, and crucially, are thought to play important roles in tumourigenesis and cancer spread. Given the relevance of EMP, chemotaxis and wnt signalling to this study, they are reviewed in detail in the following sections in this chapter.

1.2 Epithelial Ovarian Cancer

1.2.1 Ovarian Cancer Epidemiology

Ovarian cancer is the sixth most common cancer in women worldwide[27]. In England there were approximately 6000 new cases of ovarian cancer in 2012[28], making it the second most common gynaecological cancer after endometrial cancer[29] **(Figure 1.2)**. It accounts for 4% of all cancers in women but it is responsible for 6% of cancer-related mortality, and for more deaths than all other gynaecological cancers combined[30] **(Figure 1.3).** In the UK, one in seventy women will develop ovarian cancer during her life time and one in a hundred will die of it[30].

Figure 1.2: Ovarian Cancer Incidence

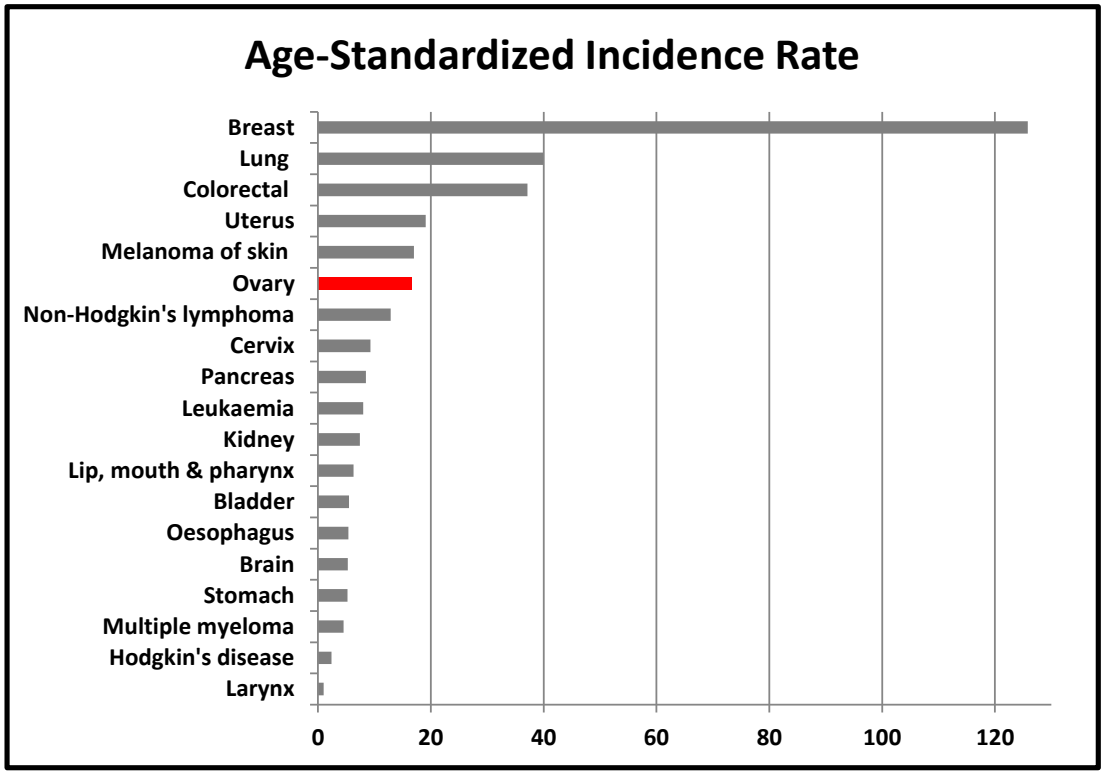

Age-standardised incidence rate for 21 common cancers in females in the UK
The incidence of ovarian cancer was 16.6/100,000 female population in 2008-2010. Incidence rate is calculated using the European Standard Population per 100000 females. Source: Office for National Statistics[29].

In humans, Epithelial ovarian cancer (EOC) **(Figure 1.4)** accounts for approximately 90% of all ovarian cancers[31]. EOC predominantly affects post-menopausal women with only 10% of cases in those under 45 years of age[32]. The number of cases are highest among women in their 60s and 70s, accounting for almost half the diagnoses[28] **(Figure 1.5)**. The less common ovarian sex cord and stromal tumours arise from granulosa cells and ovarian stroma, respectively; germ cell tumours are rare and affect young women[33].

Figure 1.3: Ovarian Cancer Mortality

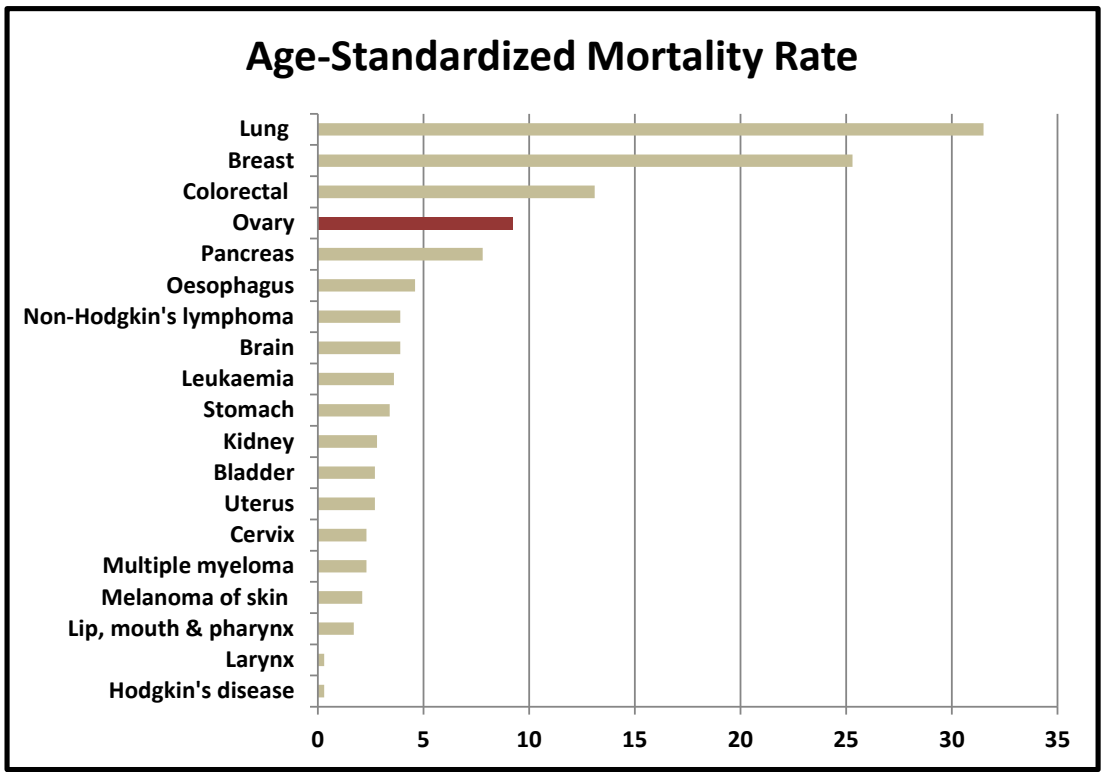

Age-standardised mortality rates for 21 common cancers in females in the UK

The mortality rate for ovarian cancer was 9.2/100,000 female population in 2008-2010. Mortality rate is calculated using the European Standard Population per 100000 females. Source: Office for National Statistics[29].

Figure 1.4: Epithelial Ovarian Cancer (EOC)

Epithelial ovarian cancer at laparotomy

A typical malignant appearance: complex cystic structures with multiple loculi and exophytic solid components; demonstrating the macroscopic heterogeneity of this disease. Source: from the world wide web.

Figure 1.5: Ovarian Cancer and Age

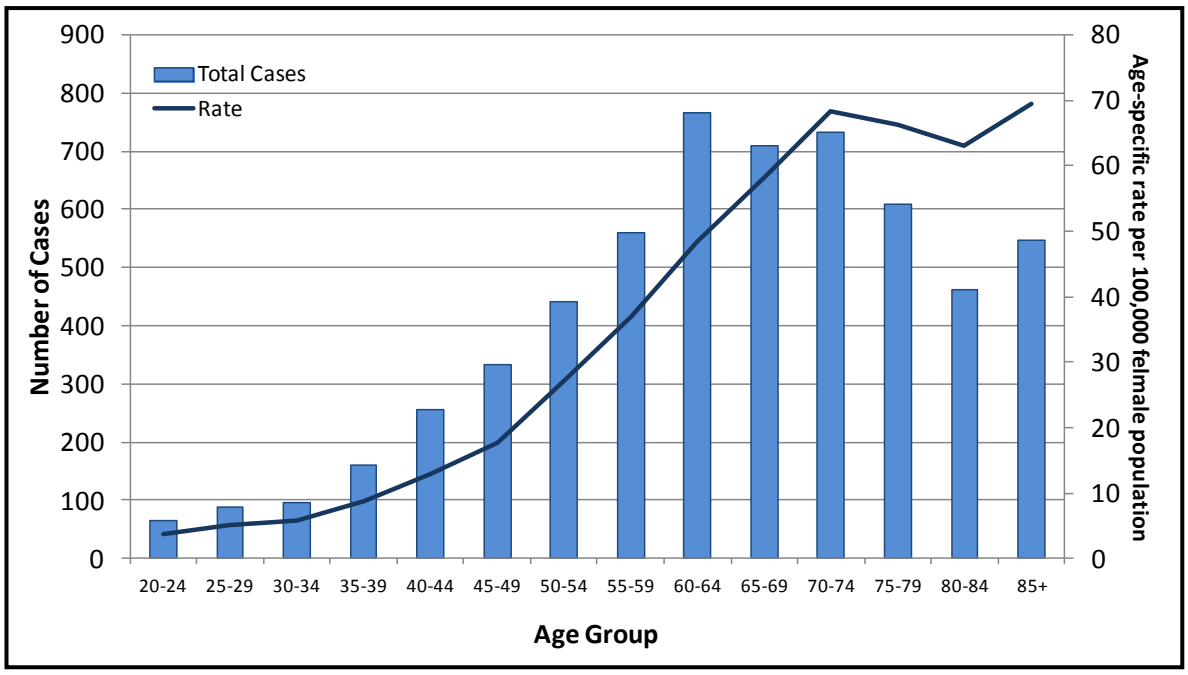

Age-specific incidence rates and numbers of cases diagnosed by age groups, England, 2009
Age-specific incidence rates rise steadily with age, peaking among women in their 70s and 80s. The numbers of cases are highest among women in their 60s and 70s, accounting for almost half of the diagnoses in 2009. Source: UK Cancer Information Service[28].

Most epithelial ovarian cancers are sporadic with an estimated 10% occurring in known familial ovarian cancer syndromes[31, 34, 35]. The two most common syndromes are the breast-ovarian cancer syndrome, which is caused by mutations in *BRCA1* and *BRCA2* (breast cancer 1 and 2) genes, and Lynch II syndrome (hereditary non-polyposis colorectal cancer: HNPCC) in which mutations in the DNA mismatch repair (MMR) genes occur with increased risk of ovarian, endometrial and colorectal cancers[36, 37]. Familial ovarian cancer syndromes generally carry better prognosis than sporadic disease and account for less than 1% of ovarian cancer related deaths[38].

1.2.2 Epithelial Ovarian Cancer Classification

EOC is morphologically classified by histopathological examination into several sub-types according to the World Health Organisation (WHO) criteria[39]. These include serous adenocarcinoma, 50-60% of all EOCs, which resembles the epithelium of the oviduct (fallopian tube), endometrioid adenocarcinoma resembling the endometrium, mucinous adenocarcinoma resembling the epithelium of endocervix, and clear cell carcinoma (mesonephrose-like)[31].

Serous EOC carries poor prognosis and tends to present as bilateral, high-grade, advance-stage disease[32, 40]. Serous ovarian cancer is divided further into high grade serous cancer (HGSC) and low grade serous cancer (LGSC), HGSC is 20 times more common

than LGSC[41, 42]. Some authors suggested that HGSC and LGSC are two distinct diseases which share little more than a similarity in their names[43]. Endometrioid EOC is similarly classified as high or low grade cancer[42]. Some authors consider high grade endometrioid as a variant of HGSC given the difficulty distinguishing between both tumours; it is therefore called by some 'HGSC with features of endometrioid carcinoma'[44, 45].

Hence, a two-type model was proposed almost a decade ago for EOC which has been gaining acceptance[46]. **Type I** EOC is composed of low grade serous, low grade endometrioid, clear cell and mucinous histological sub-types. The more aggressive **type II** includes high grade serous cancer and high grade endometrioid cancer[47]. Type I cancers arise from well identified precursor lesions such as endometriosis, benign and borderline tumours, they grow slowly, follow an indolent clinical behaviour where they are generally diagnosed at early stages and response poorly to chemotherapy. Type II cancers, on the other hand, are aggressive tumours, genetically highly unstable, progress rapidly, present at advanced stages and account for most EOC-related deaths[44, 45].

Gene alterations have been reported with varying frequency and specificity in EOC. However, mutations in *TP53* (tumour protein p53) are universal in HGSC while absent in LGSC. HGSC could also harbour *BRCA1* and *BRCA2* mutations while some LGSCs show mutations in *KRAS* (Kirsten rat sarcoma viral oncogene homolog) and *BRAF* (B-Raf proto-oncogene, serine/threonine kinase), and amplification of *ERBB2* (v-erb-b2 avian erythroblastic leukaemia viral oncogene homolog 2)[48-50]. *ARID1A* (AT-rich interactive domain-containing protein 1A) and *CTNNB1* (β-catenin) mutations are found in endometrioid cancers. Some clear cell cancers harbour *ARID1A* and *PIK3CA* (phosphatidylinositol-4,5-bisphosphate 3-kinase, catalytic subunit alpha) while mucinous cancers have *KRAS* mutation and *ERBB2* (*HER2*) amplification[40, 50-52].

Thus, in spite of being treated as a single disease, EOC exhibits a high degree of clinical, histological, and genetic aberration heterogeneity. What was initially seen as a single disease, then a disease with two sub-types, is increasingly viewed now as a group of biologically distinct diseases with recognisable genetic signatures[40, 45].

1.2.3 Epithelial Ovarian Cancer Aetiology and Cell of Origin

Epidemiological studies have suggested a link with the number of ovulatory cycles (incessant ovulation theory)[53], the risk of EOC increases in infertile women, late menopause and in those who never had children. The risk decreases with the number of pregnancies, breast feeding and the use of oral contraceptives[32, 54]. This theory could be supported further by the fact that there is no naturally occurring animal model of epithelial

ovarian cancer apart from aging hens which share frequent ovulation with humans[55, 56]. Environmental factors have also been suggested, since the risk in Japanese migrants to the United States was observed to increase to match that of the resident population[27, 57].

1.2.3.1 EOC Origin: Ovarian Surface Epithelium

Incessant ovulation theory suggests that EOC originates from ovarian surface epithelium (OSE). It proposes that EOC develops as a result of aberrant response to the repeated cycles of damage and repair occurring in OSE following ovulation which involves the rupture of mature follicles through ovarian epithelium[53].

Normal human OSE is a simple, flat-to-cuboidal, single cell layered epithelium which is separated from ovarian stroma with a thin collagen-rich zone called tunica albuginea **(Figure 1.6)**. OSE is embryologically derived from the coelomic mesothelium of the gonadal ridge. It forms part of the peritoneum and, similarly, it is unusual in that it is mesothelium with both mesenchymal and epithelial characteristics in the non-ovulating ovary[58, 59].

Figure 1.6: Ovarian Surface Epithelium (OSE)

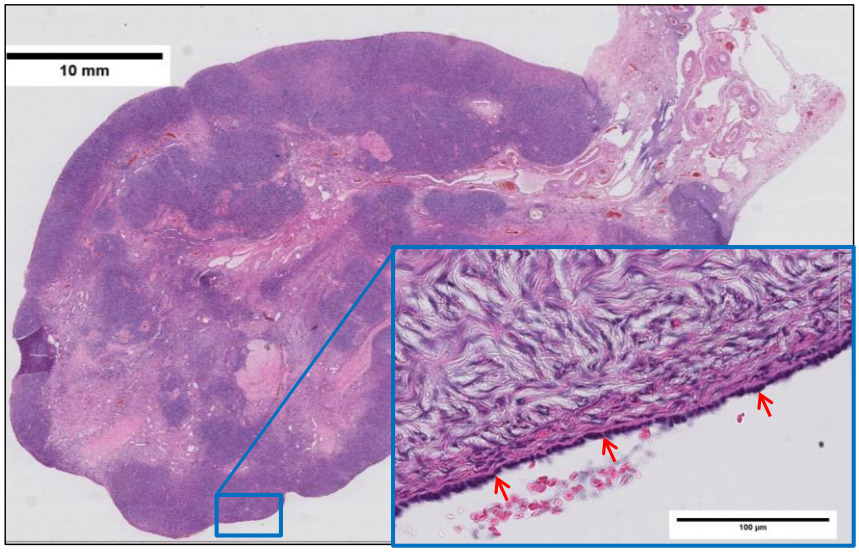

Ovarian surface epithelium (OSE): A section through a normal ovary with magnified OSE (red arrows) overlaying tunica albuginea, a collagenous zone separating OSE from ovarian stroma. Scale bar as labelled.

OSE is capable of acquiring epithelial or mesenchymal characteristics in certain conditions. During regenerative response, such as in postovulatory repair which follows the rupture (wounding) of ovarian surface during ovulation, OSE cells differentiate into fibroblast-like mesenchymal cells[60, 61]. In contrast, OSE acquires the characteristics of epithelium when it undergoes metaplasia, benign tumour formation or neoplastic changes[56]. Thus, unlike other epithelial cancers (cervical cancer for example), early ovarian cancer cells show more epithelial differentiation than their precursor cells (differentiating up)[62].

It has been hypothesised that OSE could become entrapped within ovarian stroma such as during ovulation, the rupture of mature follicles and the subsequent healing process. This could lead to the formation of inclusion cysts when OSE is completely engulfed within the stroma or ovarian clefts when surface epithelium invaginates into ovarian stroma but keeps a narrow connection with the peritoneal cavity. Some authors have hypothesised that OSE in these ovarian inclusion cysts and clefts could be the origin of EOC where epithelial cells are exposed in the confined vicinity to a microenvironment different from that of the physiological peritoneal cavity[63, 64].

This notion was supported by the observation that murine ovarian surface epithelium cell line (MOSEC) formed serous, endometrioid and mucinous cancers when transfected with the *homoeobx A* cluster genes: *Hoxa9*, *Hoxa10* and *Hoxa11* respectively prior to intraperitoneal inoculation into nude mice[65]. The authors also showed a distinct activation of *HOXA* genes which were found to be differentially expressed in human EOC sub-types in accordance with the patterns of Müllerian duct differentiation in a similar manner to what was shown in transfected MOSEC[65].

However, the origin of EOC is still elusive creating much debate among researchers and clinicians[66-69]. While the aforementioned *Hox* genes study shows that (murine) ovarian surface epithelial cells are capable of generating epithelial cancers resembling Müllerian epithelium, it does not prove that OSE is the origin of all EOCs[70].

1.2.3.2 EOC Origin: Non-Ovarian Sources

Accumulating data have indicated that at least some of EOCs originate from extra-ovarian tissues. For example, some ovarian cancers such as HGSC have been suggested to arise from the fimbrial portion of the ovarian tubes[71, 72]. Other EOCs have been linked to endometriosis such as clear cell and endometrioid cancers and borderline tumours[73].

There are several observations worth noting which cast doubt on the hypothesis that OSE is the origin of all EOC, and support a non-ovarian origin for HGSC. These observations include that OSE is a mesothelium while EOCs resemble Müllerian duct derived epithelia. This apparent "differentiation up" into non-ovarian tissues is unusual and necessitates metaplastic transformation of the mesothelial OSE into a Müllerian epithelium during or before malignant transformation[64, 69]. In addition, HGSC expresses PAX8[74, 75], a Müllerian marker, and not the mesothelium marker calretinin [76, 77]. Importantly, to date there has been no premalignant or precursor lesion found in OSE in spite of decades of extensive research[67].

Thus, the origin of EOC has been questioned and a non-ovarian origin for this disease was explored. In 1999 Dubeau proposed the 'secondary Müllerian system' as the origin of EOC[78]. He suggested that EOC originates from embryological remnants of Müllerian duct which are found scattered in the pelvis including ovaries, para-ovarian and para-tubal peritoneum. It was suggested that ovarian inclusion cysts are actual examples of this secondary Müllerian system rather than entrapped OSE[78, 79].

1.2.3.3 EOC Origin: Fallopian Tube

The attention was, however, shifted following the publication by Piek *et al.*[71] in 2001 which reported occult cancers and pre-malignant lesions, termed serous tubal intraepithelial carcinomas (STICs), in fallopian tubes prophylactically removed during risk reducing salpingo-oophorectomy from women carrying *BRCA* gene mutations[71].

Improved examination of the fimbria following the implementation of SEE-FIM protocol (Sectioning and Extensive Examination of the FIMbria)[80, 81] has increasingly provided evidence implicating the distal portion of the fallopian tube as a source for HGSC. Several studies have since reported STIC lesions in 4-17% of *BRCA* mutation carrier women[82-86]. In addition, STICs were also identified in 33-59% of sporadic EOC and primary peritoneal cancer (PPC) cases[87-92], importantly both the cancer lesions and their paired STICs harboured identical *TP53* mutations suggesting a clonal relationship[81].

Experimental evidence has established a carcinogenic sequence in the secretory cells of the fallopian tubes[93, 94] which strongly support the fallopian tube as an important source for EOC. This sequence is well defined genetically, molecularly and morphologically[93]; it progresses from 'p53 signature' cells, which are bland-looking cellular outgrowths in the fallopian epithelium with mutations in p53, to STIC lesions, which are genetically similar to p53 signatures, eventually leading to EOC[92]. Indeed, human fallopian tube secretory cells have been successfully immortalised, transformed, and when injected intraperitoneally in the immunodeficient NSG mice they resulted in disseminated tumours that resembled human HGSC on genetic analysis and immunological and histological examination[95].

More recently, Perets *et al.* developed a genetically engineered mouse model for HGSC in which *Trp53*, *Pten* with *Brca1* or *Brca2* were specifically deleted in fallopian tube secretory cells, which unlike ovarian cells express the transcription factor gene *Pax8*, utilising Cre-mediated recombination[96]. These mice developed invasive carcinomas which spread to peritoneum and ovaries and had molecular and morphological resemblance to

human HGSC. Cancers in these animals were prevented by early resection of fallopian tubes but not by removing uterus or ovaries confirming their origin in the fallopian tubes[96].

1.2.3.4 EOC Origin: Multiple Sites

Given that STIC lesions are not consistently present in HGSCs (20-60%)[87-92], could suggest that HGSCs, molecularly and aetiologically, constitutes several distinct diseases which share the anatomical location while having an origin in ovaries, fallopian tubes and peritoneum; hence the term pelvic serous cancer was coined[93].

Therefore the origin of EOC is currently thought to be from multiple sites **(Figure 1.7)**[97]. Authors on both sides of the debate currently accept that current evidence, as described in the previous paragraphs, supports that both fallopian tube and ovary can give rise to HGSC (summarised neatly by N Auersperg[67] and Crum *at el.*[93]).

Figure 1.7: Multiple Origins for EOC

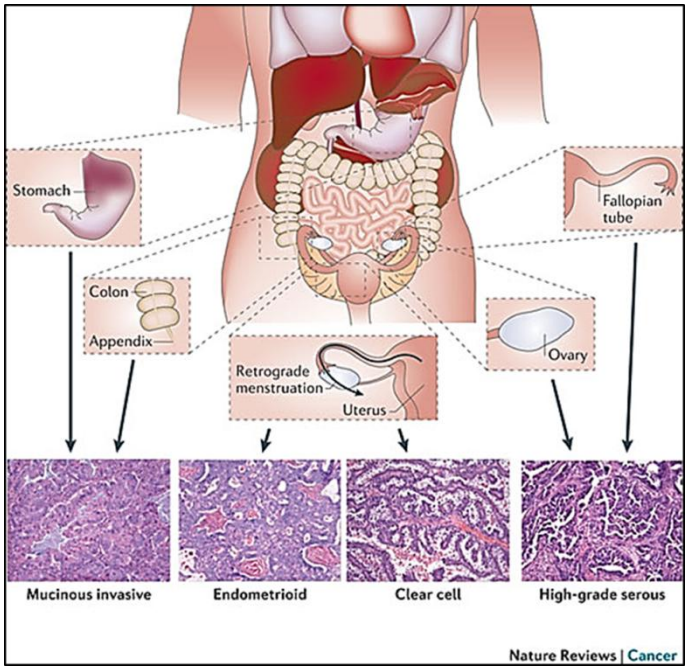

EOC can arise from several organs: Ovarian cancer is a collective term describing several invasive cancers that derived from different tissues in different organs. Most mucinous cancers are thought to originate in the gastrointestinal tract, endometrioid and clear cell cancers arise from endometriosis while HGSC has an origin in both the fallopian tube and the ovary, the relative contribution of those two organs is not clear. Reproduced with permission from Vaughan *et al.*[97].

It is thought, nevertheless, that fallopian tube cancers are under diagnosed, the current incidence of fallopian tube cancer is 1:50 compared to ovarian[87, 98-100], so is PPC which tend to be of the serous histology[101-103]. It follows that the stringent criteria for classification of pelvic serous cancer as endorsed by both WHO[39] and International Federation of Gynecology & Obstetrics (FIGO)[104, 105] are biased toward a default diagnosis of EOC while PPC is merely a diagnosis of exclusion (excluding ovarian and tubal cancers). Ovarian origin is assigned when the largest tumour mass involves the ovary with parenchymal involvement, tubal origin is determined when the ovary involvement is minimal and a transition from normal to STIC is established in addition to the presence of largest tumour mass in the tube[87].

1.2.4 Grading, Staging and Treatment

Ovarian cancer is staged and graded according to the International Federation of Gynecology & Obstetrics (FIGO)[104]. Ovarian cancer is graded as well differentiated (G1), moderately differentiated (G2) or poorly differentiated (G3). For the purpose of clinical management, ovarian cancer is staged on the basis of surgical findings into four main stages with further subdivisions **(Appendix 1)**[104]. In summary, stage I disease is limited to the ovaries, if the disease spreads to the pelvis it becomes stage II. The cancer is regarded as stage III or IV if the disease has spread outside the pelvis or given distant metastases respectively. FIGO has recently revised ovarian cancer stages[106]. However, since the samples used in this project were collected prior to this recent change, the 2009 stages will continue to be used here.

Current first line treatment for ovarian cancer is surgical debulking and platinum-based chemotherapy; for the small proportion of cancers with encapsulated unilateral disease (stage IA, low grade) surgical excision alone may suffice[107-111]. Current treatments achieve 90% five-year survival rate only when the disease is encapsulated and limited to the ovaries. Advanced disease is increasingly treated with six cycles neoadjuvant (prior to surgery) chemotherapy with interval surgical debulking after the third cycle[110]. Intraperitoneal chemotherapy for ovarian cancer is not routinely practiced in the UK, however, it was shown to improve survival but with high toxicity leading to less than half of women completing the treatment[112].

Some targeted therapies are in clinical use, bevacizumab which is an antibody against vascular endothelial growth factor A (VEGF-A) was found to benefit patients with advanced disease and incomplete surgical resection of tumour[113]. Several other therapies are at different phases of clinical trials such as pazopanib a VEGF receptor tyrosine kinase inhibitor (VEGF RTKi), and olaparib[114], a poly (ADP-ribose) polymerase (PARP) inhibitor, in patients with *BRCA* mutations[115].

Recurrent or relapsed ovarian cancer is largely incurable but may be managed with serial chemotherapy regimens[116, 117]. Cancer can be controlled for long term with some centres considering it as a 'chronic' disease[34, 116]; however, the outcome is generally related to the interval since last chemotherapy cycle. Secondary surgery has a place in selected cases with discrete recurrence which is being investigated in clinical trials (DESKTOP III), or to palliate bowel obstruction. Targeted therapies such as bevacizumab, pazopanib and olaparib are also being investigated in relapsed ovarian cancer[117-119].

1.2.5 The Role of Metastasis in Ovarian Cancer

A hallmark of epithelial ovarian cancer is the poor prognosis; overall five years survival rate is 43%, with only 6% of those with distant metastasis at diagnosis live for 5 years or longer[120]. Crucially, 70% of EOC cases present in advanced stages as symptoms at early disease are vague and non-specific resembling those of benign gastrointestinal or gynaecological conditions[27]. Therefore, there is an urgent need for new treatments if ovarian cancer outcome is to improve.

It is well recognised that a breakthrough in improving survival could be achieved when early diagnosis is feasible. However, the absence of defined precancerous lesions to screen for, the common occurrence of benign ovarian cysts particularly in pre-menopausal women, and the low prevalence rate in the community (1 in 2500) make screening for ovarian cancer an enormously challenging task[121-123]. Nevertheless, most cancer related deaths are caused by metastases; therefore, one possibility to improve the outcome of patients with this disease is targeting its spread.

EOC spreads primarily in two ways, to lymph nodes through lymphatics, and more commonly to peritoneal surface which is termed 'locoregional dissemination', a peculiar way of ovarian cancer dissemination[124]. Interestingly, peritoneum, which covers the abdominal cavity, is in continuity with ovarian surface epithelium and, similar to it, it is a mesothelium with epithelial and mesenchymal characteristics[58].

Peritoneal spread, also referred to as transcoelomic, is thought to occur by the shedding of cancer cells into the peritoneal cavity, multi-cell spheres or single cells, which are carried by the ascitic fluid within the abdominal cavity. Cancer cells must survive anoikis till establishing attachment to the mesothelium or the exposed extra cellular matrix (ECM) to form metastasis[124, 125]. The spread of peritoneal metastatic lesions are not even nor random, it is well recognised that peritoneal lesions have 'favourite' sites such as omentum, para-colic gutters, small bowel mesentery and diaphragmatic surface[126].

Several hypotheses have been proposed to explain this selectivity; such as that these are confined places with limited fluid movement. Others highlighted the importance of adipose tissues and milky spots in metastasis location[127]. The complex structure of omentum is an example, where blood capillaries end with glomerulus-like capillary beds with immune cell aggregates within and surrounding these structures to form milky spots. Both endothelial lining of terminal capillaries and the overlying mesothelium adapt to facilitate immune cell migration to and from the peritoneal cavity[127].

Blood borne distant metastases at presentation are uncommon in EOC. It is unclear whether this is a result of inherent properties of this cancer in which cancer cells lack the ability to form haematogenous metastasis or it is a result of patients dying of intraperitoneal progression before cancer is able to spread by blood. The obstacles for blood borne metastasis could be more challenging than those for dissemination within the peritoneal cavity; cells are required to disconnect from tumour mass, intravasate into blood vessels, survive the journey till reaching a distant organ where they extravasate into the tissues to establish growth and proliferation[128-130].

An interesting insight was provided from EOC patients who underwent palliative peritoneal-venous shunt formation to deal with depleting ascites; the majority of patients did not develop apparent distant metastasis in spite of 'injecting' millions of cancer cells into their blood stream[131]. While this could be the result of the inherent inability of this cancer to spread by blood, it could also be that the cells which survived in ascites are selected in a way which does not equip them with the characteristics required for haematogenous metastasis; the 'seed and soil' [131]. Interestingly, some centres where EOC is treated with repeated courses of chemotherapy courses have noticed an increase in the reported distant metastasis (Prof. G Jayson, Christie Hospital, personal communication). This clearly could have implication on future successful treatments aimed at intraperitoneal disease control.

Lymph node involvement in ovarian cancer increases by stage but is present in some cases where cancer is apparently limited to ovaries[132]. Robust data are difficult to acquire since lymph node removal (lymphadenectomy or lymph nodes sampling) is not performed routinely in all centres and it varies according to the assumed stage at laparotomy.

Nevertheless, peritoneal spread is still the detrimental factor in EOC sufferers, with patients doing worse than those with positive lymph nodes which resulted in FIGO revising the staging ladder recently. Therefore, addressing peritoneal disease is an immediate step in managing women with EOC. Not only is the disease diagnosed at advanced stages, which makes treatment difficult and occasionally not feasible, but patients generally succumb to bowel obstruction caused by intraperitoneal dissemination[34].

1.2.6 5T4 in Ovarian Cancer

A better understanding of the microenvironment and mechanisms involved in ovarian cancer metastases could lead to the development of therapeutics or diagnostics aimed at preventing or controlling cancer spread and, therefore, improving prognosis.

5T4 has been shown to be expressed in 71% of ovarian cancer tumours by immunohistochemical staining; and crucially 5T4 expression was correlated with the disease stage (cancer spread), grade (aggressiveness), the lack of responsiveness to chemotherapy, and poor prognosis[14]. A study of limited numbers revealed the absence of staining for 5T4 in normal human ovarian tissues; it is not clear, however, whether ovarian epithelium formed part of the investigated specimens[2].

These findings have encouraged the investigation of whether 5T4 has a functional role in human ovarian cancer spread. This could potentially recognise 5T4 as a diagnostic marker which could be used to identify sub-groups of patients who might benefit from alternative treatment strategies. More importantly, given the availability of 5T4-based therapeutics, this could potentially provide new treatment modalities in which 5T4 is targeted to control or eradicate cancer metastases.

1.3 Chemotaxis

Chemotaxis refers to cell migration along a concentration gradient of a chemokine. Chemokines are small proteins (70 – 130 amino acids) which may facilitate leucocyte trafficking and migration[133]. Chemokines are selectively secreted in different tissues and organs creating a concentration gradient with the highest levels present in the producing tissues. For example, leucocytes with the specific receptor migrate toward the tissues producing the corresponding ligand (e.g. infection site). It has been hypothesised that the distinct and multi-phasic lymphocyte migration pattern during their life cycle: lymphopoiesis, selective recruitment, and maturation, is finely tuned by the sequential changes in the functional expression of chemokine receptors and thus migration toward the different tissues producing the relevant ligands[134].

Chemokines generally exert their biological effect through a group of seven-transmembrane, G protein-coupled receptors (GPCR)[135]. There are more than 50 chemokines and 20 receptors known in humans; they are divided into four groups (C, CC, CXC and CX3C) according to the position of cysteine residues on the chemokine N-terminus[136]. Chemokines and their receptors are generally 'promiscuous' in that a chemokine could activate more than one receptor, and a receptor could interact with several chemokines **(Figure 1.8)**[137]. However, this happens only within each chemokine group such as CXC ligands with CXC receptors. For example CXCL12 has two receptors CXCR4 and CXCR7; CXCR7 also interacts with another ligand CXCL11 which has another receptor CXCR3. CXCR4 is unusual in that it is not known, to date, to interact with any chemokine other than CXCL12[135].

Chemokines can be defined as homeostatic or inflammatory according to their functional roles, but some chemokines exhibit dual roles[137]. Homeostatic chemokines are constitutively expressed and control leucocyte trafficking in immunosurveillance. By contrast inflammatory chemokine secretion is inducible and facilitates leucocyte recruitment to inflammatory sites[136]. Malfunction of chemokines or their receptors in leucocytes is associated with several disorders including immunosuppression and autoimmune diseases[133]. WHIM syndrome (Warts, Hypogammaglobulinaemia, Infections, and Myelokathexis) for example, is a rare disorder characterised by immunodeficiency, leucopoenia and neutrophil retention in bone marrow. This condition is an autosomal dominant disorder caused by truncation of the C terminus of the CXCR4 receptor which impairs leucocyte trafficking[138, 139].

Figure 1.8: The Chemokine Wheel

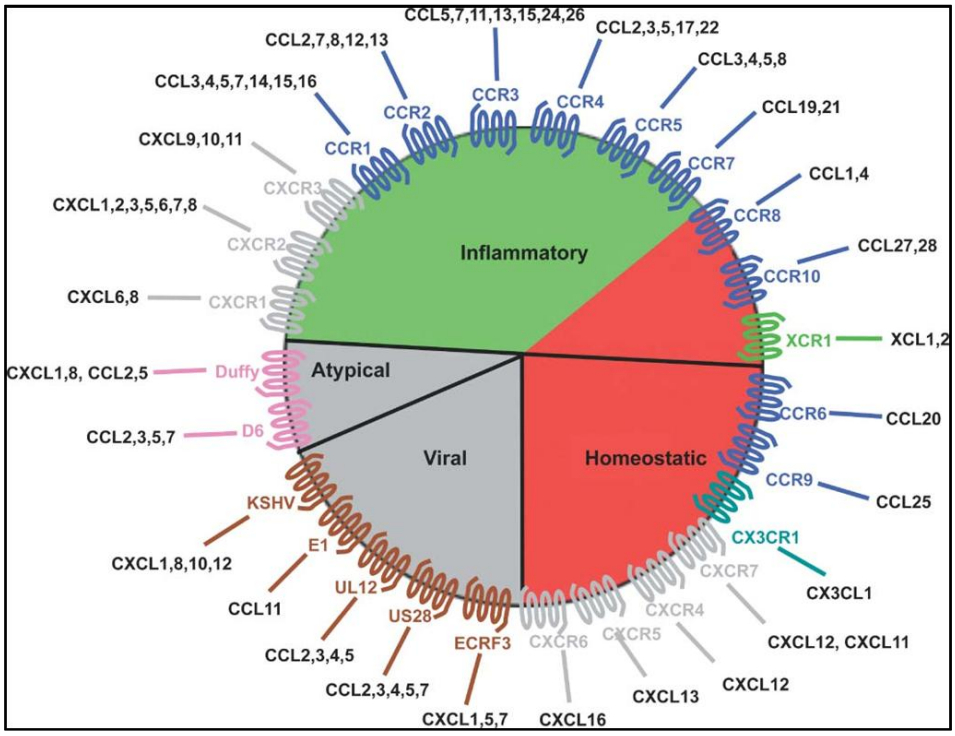

The chemokine wheel:
The 'inflammatory' chemokines are inducible and involved in all aspects of the immune response. The 'homeostatic' chemokines are involved in development and normal physiology. Atypical chemokine receptors are generally 'silent' and act as negative regulators of the systems, 'decoys' that reduce chemokine levels. Viral chemokines and receptors allow the pathogens to modulate immune responses to infection. Inflammatory, homeostatic and atypical chemokine receptors are all found in the tumour microenvironment. After Balkwill with permission[137]

1.3.1 CXCL12/CXCR4 Axis

CXCL12 is a homeostatic chemokine which is constitutively expressed by several tissues and its receptor CXCR4 is found in a wide variety of cells[140]. CXCR4 activation by CXCL12 results in multiple, mainly G protein dependent, signalling pathway activation. Influenced by the cell type and microenvironment, this can lead to several different cellular responses such as chemotaxis, enhanced survival, proliferation, intracellular calcium flux or transcription regulation[141]. Upon CXCL12 interaction, CXCR4 undergoes conformational changes leading to the exchange of guanosine diphosphate (GDP) with guanosine triphosphate (GTP) in the G protein complex; this results in disassociation of GTP-bound G_{α} sub-unit from $G_{\beta\gamma}$ dimer. This could lead to the activation of several downstream signalling pathways such as mitogen-activated protein kinase / extracellular signal-regulated kinase (MAPK /ERK)[136, 141].

The wide availability of both the receptor and the ligand (CXCL12 and CXCR4) would lead to constant activation of this axis across organs and tissues, a phenomenon is not supported by biological observations. This has led to the search for the mechanisms or molecules involved in the functional control of CXCL12/CXCR4 axis. Post-translational

inactivation of CXCL12 has been suggested in some studies; this includes the cleavage of selected amino acids at the N-terminus which are required for the functional interaction with CXCR4. Several molecules have been implicated in this process such as cathepsin G, CD26 (Dipeptidyl peptidase-4, DPPIV)[142-144] and several matrix metalloproteinases (MMPs)[145].

In addition, the bioavailability of the receptor CXCR4 can play a regulatory role in the chemotactic response to CXCL12. For CXCR4 to be functional it needs to be expressed on the cell surface and to be able to communicate extracellular signals into intracellular molecules. Holland *et al.* [146] found that some breast cancer cell lines which expressed CXCR4 on the cell surface failed to mount a response in spite of CXCL12 interaction with CXCR4; this seemed to be caused by the failure of G_{α} and G_{β} subunits to form heterotrimeric complexes with CXCR4[146].

Another mechanism through which chemokine receptors might influence cellular response is the formation of dimers. Recent evidence has demonstrated the capability of some receptors to form homodimers and heterodimers; these dimers usually have different functional roles from those of single receptors. For example, CXCR4/CCR2 heterodimerisation in primary leucocytes resulted in a cross inhibition where a specific antagonist to one receptor inhibited chemokine binding to the other receptor[147].

A recent study has shown that when CXCR4 and CXCR7, the newly described receptor for CXCL12[148], were co-expressed in overexpression experiment, they formed functional heterodimers, and that CXCR7 induced conformational changes in the CXCR4/G-protein complexes indicating a complex relationship between CXCR4 and CXCR7[149]. Functionally, this complex axis can be viewed in a simplified dual response model where CXCR7 activation plays a role in CXCL12-mediated cell survival and proliferation in contrast to CXCR4 response which mainly leads to chemotaxis[150, 151].

Taken together, these reports show the complexity of CXCL12/CXCR4/CXCR7 regulations and the many possible reasons of why cells might fail to respond to CXCL12 activation. Understanding these mechanisms and the roles of related molecules could be exploited to interfere in CXCL12/CXCR4 mediated cancer spread.

1.3.2 CXCL12/CXCR4/CXCR7 Axis and 5T4

The mechanisms through which cells can determine which receptor (CXCR4, CXCR7 or neither) to be activated by CXCL12 are not entirely clear. Receptor choice is likely to be microenvironment dependent, such as the type of expressed receptor and the presence of specific co-receptor proteins.

5T4 has recently been implicated in CXCR4 functional expression[25]. A comparative microarray analysis of undifferentiated and differentiating mouse embryonic stem (mES) cells, which were stratified according to 5T4 expression, has revealed significant changes in a large number of gene transcripts. These transcriptional changes which accompanied the expression of 5T4 included down-regulation of *Cd26* and upregulation of *Cxcl12* with no change observed in *Cxcr4* transcript[25].

CXCL12/CXCR4 function can be regulated through post-translational inactivation of CXCL12 which includes 'N-terminus processing' by CD26[144]. The fact that *Cxcl12* is upregulated and *Cd26* is down regulated in differentiating mES cells led to the investigation of whether 5T4, according to which these cells were stratified, is functionally implicated in CXCL12/CXCR4 mediated responses particularly those related to cell migration and survival.

Subsequently, Southgate[25] *et al.* utilising 5T4-knockout murine embryonic cells (mES cells and murine embryo fibroblasts (MEFs)) showed that 5T4 was required for the optimal surface functional expression of CXCR4[25]. In addition, the authors showed that in 5T4-knockout MEFs, CXCL12 exposure did not lead to ERK1/2 phosphorylation and this was not caused by disruption of MAPK/ERK pathway. 5T4 transmembrane domain was identified by the authors as necessary for the optimal surface expression of CXCR4 and chemotactic response to CXCL12. Crucially, CXCR7 surface expression was found to be independent of 5T4 expression on cell surface[25] suggesting a complex interplay between the components of this axis.

Given the evidence suggesting that CXCR4-mediated response to CXCL12 could lead to cell migration while CXCR7 activation could promote proliferation or survival[151]; the differential expression of 5T4 may be pivotal in the preferential biological response to CXCL12 in cancer cells, such as epithelial ovarian cancer cells, toward proliferation and growth or migration and spread.

1.3.3 CXCL12/CXCR4/CXCR7 Axis and EOC

Several chemokines have been implicated in cancer spread; in 2001 Muller *et al.*[152] reported that the receptors CXCR4 and CCR7 are highly expressed on human breast cancer cells, and crucially, their ligands (CXCL12, CCL21 respectively) played a role in determining the metastatic sites[152]. CXCL12/CXCR4 axis has since been implicated in more than 20 different cancers including epithelial ovarian cancer. It has also been shown that CXCL12 is present at high levels in lymph nodes, lungs, liver and bones; all are frequent destinations for human cancer metastases[139].

The potential role of CXCL12/CXCR4 axis in epithelial ovarian cancer is well established; several studies have linked CXCR4 expression with cancer spread and poor prognosis[153]. Scotton *et al.* used ribonuclease protection assay (RPA) to screen for mRNA of 14 different chemokine receptors (CXCR7 was not included) in six ovarian cancer cell lines and found that only CXCR4 mRNA was expressed in these cells; CXCR4 surface expression was also demonstrated on two cell lines (IGROV and Caov-3) using flow cytometry on live cells [154]. In addition, ascitic fluid from ovarian cancer patients was found to contain high levels of CXCL12[154]. This is an important observation since ascites could harbour cancer cells which have detached from the primary tumour, and it is thought to form a medium which facilitates cell transportation into different potential metastatic sites within the abdominal cavity. Importantly, mechanistic studies on ovarian cancer cell lines have demonstrated a role for CXCL12 in cell migration[155] and adhesion to peritoneal cells[156] *in vitro*.

These observations suggest a potentially important role for the CXCR4/CXCL12 axis in epithelial ovarian cancer spread for which metastasis constitutes a significant clinical problem. In certain cell types, 5T4 was found to be required for the optimal functional expression of CXCR4, in addition 5T4 is expressed by epithelial ovarian cancers particularly in those at advanced stages.

Taken together, the investigation of a functional role for 5T4 in epithelial ovarian cancer spread is an attractive option which could lead to selectively targeting CXCR4-mediated chemotaxis within the tumour since, unlike CXCR4, 5T4 expression in healthy adult tissues is limited.

1.4 Epithelial Mesenchymal Plasticity

Epithelial mesenchymal transition (EMT) is a term broadly used to describe the complex molecular, morphological and functional changes exhibited by epithelial cells transforming into a mesenchymal phenotype. During this process epithelial cells lose their intimate connections with the surrounding cells and with the extracellular matrix (ECM), replace their basoapical polarity with front-rear polarisation; thus becoming disperse and more motile[157, 158]. During EMT, cells show increased matrix metalloproteinase (MMP-2 and MMP-9) activities, lose epithelial markers (E-cadherin, cytokeratins) and acquire mesenchymal ones (N-cadherin, vimentin). Several EMT-inducing transcriptional factors act by binding to E-box elements in the *E-cadherin* (*CDH1*) promoter repressing its transcription. Transcriptional *E-cadherin* repressors include zinc finger proteins such as SLUG, SNAIL, ZEB1 (Zinc finger E-box-binding homeobox 1) and ZEB2, and the bHLH (basic helix-loop-helix) protein TWIST[159, 160].

There has been some objection to the current use of EMT in the literature as in many cases neither the starting cells are of the strict epithelial phenotype nor are the resultant cells mesenchymal. However, in most studies this term is a conceptual frame which refers collectively to the changing state of cells undergoing multiple transformations such as those described above[161, 162]. In addition, it is recognised that cancer cells during the processes of tumourigenesis and metastasis could transform repeatedly between epithelial and mesenchymal states. Recently the term 'epithelial mesenchymal plasticity' (EMP) has been coined to describe the dynamic changing state of cells undergoing epithelial mesenchymal transition (EMT) and mesenchymal epithelial transition (MET)[163].

1.4.1 EMT Sub-Types

The molecular and morphological changes occurring during EMT could vary according to the tissue type and to the biological process necessitating EMT. Recent efforts have been made to classify EMT into three sub-types based on the biological context in which EMT occurs[164].

Type I refers to EMT associated with implantation, embryogenesis and organogenesis. It does not cause fibrosis nor does it produce distant systemic cellular spread of the transformed cells[164]. This type of EMT is observed in many important developmental steps such as mesoderm formation from the primitive ectoderm, and neural crest and cardiac valve formation[159]. On the other hand **type II** EMT is seen in wound healing and tissue repair. This type aims to re-construct damaged tissues and is usually limited and associated with local inflammation. In the circumstances where chronic

inflammation develops and produces constant EMT stimulation, fibrosis and tissue destruction may occur[164]. **Type III** EMT which is seen in cancer development and spread is associated with abnormal cell growth and behaviour. A distinguishing feature of this type is that malignant cells could acquire invasive properties and metastasise[164]. Importantly cancer cells undergoing EMT may transform to different levels of morphological and molecular changes; for example while some cells would acquire a full mesenchymal phenotype and lose all epithelial markers, other cells would have mesenchymal and epithelial characteristics.

Despite the fact that these EMT sub-types correspond to different biological and functional contexts, they largely share the underlying patterns of differential expression of adhesion molecules and transcription factors mentioned earlier[164].

1.4.2 EMT and Epithelial Ovarian Cancer

Typically, E-cadherin expression diminishes in most epithelial cancers as tumour develops and importantly the absence of E-cadherin expression has been correlated with cancer metastasis and poor prognosis in several cancers[160]. Cancer cells disconnection from the surrounding cells and ECM could form an initial step in the cancer spread process, subsequent to which cancer cells might migrate in response to specific chemotactic signals[159, 165, 166].

E-cadherin is not usually expressed in normal ovarian surface epithelium (OSE) which is a mesothelium with epithelial and mesenchymal characteristics. OSE integrity is maintained by desmosomes, junctional proteins, integrins and N-cadherin but not E-cadherin[167]. Interestingly, a 'cadherin switch' from N-cadherin to E-cadherin takes place in well differentiated ovarian cancers, and ovarian epithelium lining inclusion cysts and epithelial clefts (both resulting from invagination of OSE into ovarian stroma possibly after ovulation)[168, 169]. Thus ovarian cancer is unusual in that cancer cells acquire E-cadherin expression during cancer development, this expression is decreased or lost in the less differentiated and more advanced disease[170, 171].

These observations are in keeping with the fact that well differentiated EOC exhibits a more committed epithelial phenotype than ovarian surface epithelium (differentiating up). The fact that the more advanced and less differentiated cancers show decreased expression of E-cadherin may indicate that EMT takes place in these cancers, a step which might be required for the spread of ovarian cancer.

1.4.3 EMT and 5T4

Embryonic stem cells during *in vitro* differentiation undergo changes resembling EMT process: cell surface E-cadherin to N-cadherin switch, increased vimentin expression, E-cadherin repressors (Snail and Slug proteins) upregulation, and increased cellular motility and matrix metalloproteinase (MMP-2 and MMP-9) activities[24, 172, 173]. 5T4, interestingly, appears to partake in cell differentiation as it was found to be transiently upregulated during embryonic stem cell differentiation while its absence is thought to be a suitable marker for cell pluripotency[174]. Similarly, 5T4 over-expression in murine epithelial cells resulted in reduced surface expression of E-cadherin, changes in cell morphology and alteration in cytoskeletal organisation[175]. 5T4 could function in metastasis through its influence on cytoskeletal organization, cell adhesion, and cell motility [175]. Taken together, these findings indicate that 5T4 expression may form an integrated component of the EMT process in both embryonic and epithelial cells *in vitro*.

Epithelial ovarian cancer has been shown to express 5T4 in some studies while others reported E-cadherin expression. This highlights the need for concomitant investigation of the expression of both 5T4 and E-cadherin (and other EMT markers) on the same human tissues. It is feasible that within the heterogeneous ovarian cancer mass, some cells express 5T4 while others express E-cadherin, and thus several cellular phenotypes co-exist within the tumour mass perhaps with different contributory functions to cancer biology. It is also important to note that EMT and its reverse transition, MET, are dynamic processes and thus 'snap shot' studies such as immunostaining of cancer tissues are unlikely to be sufficient for their evaluation. For example, a cell with an epithelial phenotype could be a cell which has just undergone an MET process such as establishing a metastatic lesion' or it could be a cell yet to undergo EMT. Similarly it is important to note that E-cadherin is one marker of many for EMT; E-cadherin alone is not sufficient to ascertain cell status as EMT involves complex multiple changes.

1.5 wnt Signalling

Nusse and Varmus published in 1982 a landmark discovery that mouse mammary tumour virus (MMTV) induced tumourigenesis by activating a gene they called *integrase-1* (*int-1*)[176]. Soon this was identified to be the homologous gene for the *Drosophila melanogaster* wingless gene (*Wg*) which had been extensively studied in developmental biology; *wg* and *int-1* were later fused to coin the name of wnt pathway[177]. Since, a plethora of developmental and cancer research has helped to uncover the complexity of this pathway identifying a vast number of different components involved in the cascades of wnt signalling[178].

Wnt pathways generally serve to transduce extracellular signals, it is composed of extracellular ligands and inhibitors, transmembrane receptors and co-receptors, and cytoplasmic cascades of protein-interactions leading to one of several identified outcomes[179]. Wnt signalling is broadly divided into canonical, β-catenin dependent, pathway **(Figure 1.9)**[180] and non-canonical, β-catenin-independent, pathways **(Figure 1.10)**[181] with evidence of feedback loops between the two forms of signal transduction[182].

Figure 1.9: The Canonical wnt Signalling Pathway

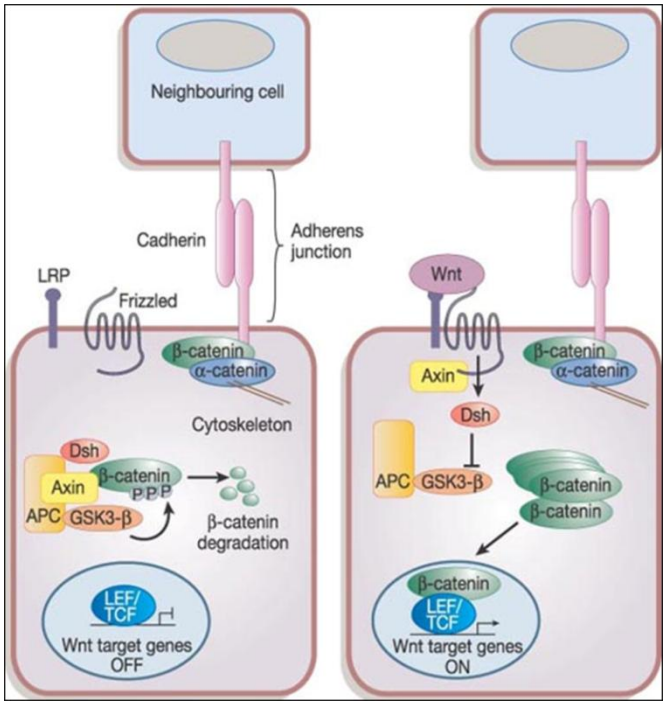

The canonical wnt signalling pathway: In the absence of Wnt signalling (left panel), β-catenin is in a complex with axin, APC and GSK3-β, and gets phosphorylated and targeted for degradation. β-Catenin also exists in a cadherin-bound form and regulates cell–cell adhesion. In the presence of Wnt signalling (right panel), β-catenin is uncoupled from the degradation complex and translocates to the nucleus, where its binds Lef/Tcf transcription factors, thus activating target genes. After Reya *et al*. with permission[180].

Generally, but not strictly, canonical wnt pathway regulates gene transcription while the non-canonical pathways modulate cellular function in non-transcriptional way[183]. Canonical wnt pathway is the more extensively studied and better characterised of the two.

In homeostasis, in the absence of wnt ligand activation, cytoplasmic β-catenin levels are maintained at low levels by the 'destruction complex' which phosphorylates β-catenin and thus targetes it for ubiquitination by proteasomes[184]. The destruction complex is primarily formed of Axin, adenomatous polyposis coli (APC), casein kinase-1 (CK-1) and glycogen synthase kinase-3 (GSK-3) proteins **(Figure 1.9)**[180, 185].

Figure 1.10: The Different wnt Signalling Pathways

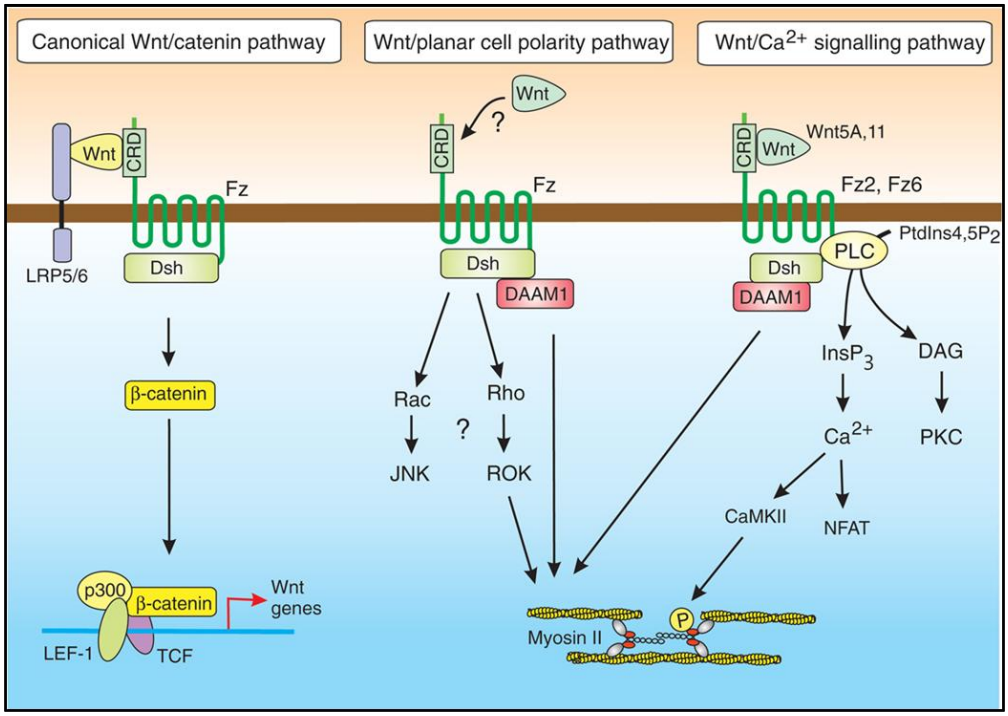

The signalling mechanisms used by the canonical and non-canonical wnt signalling pathways: All three signalling pathways are activated by frizzled (Fz) receptors that depend upon the dishevelled protein (Dsh) as part of the transduction mechanism to transfer information into the cell. Most is known about the canonical Wnt/β-catenin pathway with less information on the two non-canonical pathways. In the wnt/planar cell polarity (PCP) pathway, Dsh transfers information to the small GTP-binding proteins Rho and Rac. The wnt/Ca^{2+} signalling pathway is connected to the dishevelled-associated activator of morphogenesis 1 (DAAM1), which regulates actin formation. After Berridge with permission[181].

Activation happens when one of wnt ligands binds to the seven transmembrane receptor, Frizzled (FZD), in combination with a co-receptor, low density lipoprotein (LDL) receptor-related protein 5 or 6 (LRP5/LRP6). This leads to the activation of the intracellular dishevelled protein (DVL) which in turn, and in combination with phosphorylated and internalised LRP5/6, leads to inactivation of the destruction complex **(Figure 1.9)**. Cytoplasmic β-catenin thus escapes phosphorylation and accumulates to higher levels leading to its translocation to the nucleus where it acts as a transcription factor in combination with T-cell factor / lymphoid enhancer factor-1 (TCF/LEF) transcription factor family[182]. This has been exploited for designing reporter assays to study β-catenin activation such as TOP/FOP (optimal Tcf-binding site/Far-from-optimal Tcf-binding site) reporter assay and pBAR (β-catenin-activated reporter)[186-188].

There are 300 - 400 genes which were identified to contain wnt-responsive elements (WRE) and thus could act as target genes for the β-catenin-TCF/LEF-1 complex[189]. They include genes involved in cell cycle and proliferation such as c-myc (*MYC*), cyclinD1 (*CCND1*), vascular endothelial growth factor (*VEGF*), transforming growth factor-beta (*TGF-β*), interleukin-8 (*IL-8*) and several matrix metalloproteinases (*MMPs*)[182].

Signal transduction after wnt ligand activation independent of β-catenin is collectively known as the non-canonical pathway **(Figure 1.10)**[181]. There are several non-canonical pathways which are not entirely distinct with evidence that they overlap and intersect with each other[190]. One of the non-canonical wnt pathways is the planer cell polarity (PCP) pathway[191]. Initially it was described in developmental biology as the other arm of wnt signalling alongside β-catenin–dependent canonical pathway and was synonymous with the non-canonical activation[182, 192].

In PCP pathway, specific wnt ligands can bind to FZD receptors, without the involvement of LRP5/6, which recruits DVL[193]. The complex wnt/FZD/DVL binds to DVL-associated activator of morphogenesis (Daam1) leading to activation of the small GTPases RhoA family: Rac and Rho which ultimately activate c-Jun N-terminus kinase (JNK) and Rho-associated kinase (ROCK) respectively **(Figure 1.10)**[181, 194]. JNKs are activated by phosphorylation through the mitogen-activated protein kinase (MAPK) pathway[195]. Both activated ROCK and JNK can lead to cytoskeletal rearrangement and co-ordinated cell polarization within the plane of epithelial sheet through yet not fully understood mechanisms[179, 191].

Wnt proteins are approximately 40 kDa in size[185] with multiple cysteine residues and composed of 350-400 amino acids. Wnt proteins are subjected to post-translational modifications such as N-glycosylation and lipid-modification both of which are essential for their functional properties[183].

In humans, wnt proteins are encoded by 19 different genes and there are ten different FZD receptors[182]. Ligands can theoretically bind to any FZD receptor and activate any of the wnt pathways, with some ligands known to activate both canonical and non-canonical pathways while differences in the affinities of individual wnt proteins for different FZD receptors and co-receptors can influence the outcomes [196]. In general, however, ligands tend to primarily activate either canonical or non-canonical pathways and are thus classified into two groups. In mammals, canonical signalling is activated by WNT1, WNT3A, WNT8 and WNT8B, and non-canonical signalling is activated by WNT4, WNT5A and WNT11[197-200].

Wnt signalling pathways (canonical and non-canonical) are regulated by a large number of modulator molecules along the different steps of extra- and intra-cellular protein-interaction cascades[182, 183, 201, 202]. These include secreted Frizzled-related proteins (sFRPs), wnt inhibitory factor-1 (WIF-1) and Dickkopf (DKK) family. WIF-1 and sFRPs can antagonise wnt signalling, canonical and non-canonical, by directly binding to wnt ligands or FZD receptors. DKK proteins can bind to LRP5/6 and prevent the formation of wnt-FZD-LRP5/6 complex resulting in specific inhibition of canonical wnt signalling[203].

There is some evidence for negative feedback loops between the β-catenin pathway and the PCP pathway, with proteins upregulated by canonical wnt signalling such as protein naked cuticle (dNkd) and Dkk being inhibitors of canonical wnt signalling and activators of non-canonical wnt signalling[204-206]. β-catenin is also an important component of calcium-dependent intercellular adhesions where it is found in the cell membrane linking cadherins to cytoskeleton[207], however, evidence suggests that these are two separate distinct moieties of β-catenin with no signalling link[208].

Aberrant wnt signalling has been implicated in human disease including metabolic disorders, congenital abnormalities and cancer[185, 209-212]. Dysregulation in wnt pathways has been found in several solid cancers and leukaemia implicating wnt signalling in tumourigenesis and metastasis[213, 214]. Mutations in the tumour suppressor gene *adenomatous polyposis coli* (*APC)* were discovered in familial adenomatous polyposis (FAP) syndrome and colorectal cancer prior to elucidating their role in wnt signalling[215, 216]. Wnt ligands overexpression has been demonstrated in small cell lung cancer[217] and wnt antagonists (sFRPs) were found to decrease in expression in the head and neck squamous cell cancers[218]. In addition, FZD receptor overexpression was shown in gastric cancer[116], and the overexpression of LRP5 and LRP6 was found in breast cancer[219, 220].

1.5.1 wnt Signalling and Epithelial Ovarian Cancer

In epithelial ovarian cancer, mutations in *β-catenin* gene (*CTNNB1*) have been reported in half of studied endometrioid epithelial ovarian cancers. Less frequently, mutations were also found in *APC*, *AXIN1* or *AXIN2* in this histological sub-type[221]. While mutations in genes of the wnt signalling pathway are rare in serous (high and low grade), clear cell and mucinous ovarian cancers[222], nuclear staining of β-catenin has been reported in up to 59% of these tumours[223-226] which suggests a role for wnt signalling pathway in EOC in spite of the lack of evidence of gene aberration[227].

In one study using immunoblotting and immunohistochemistry, EOC samples were found to express more β-catenin and GSK3β than normal surface epithelium, benign or borderline tumours; β-catenin was confined to cell borders with no nuclear staining[228]. Another study found higher proportion of EOC specimens expressing WNT1 and WNT5A than benign tumours or normal ovaries; in addition the expression of FZD1 was less frequent in these cancer samples[229].

The non-canonical wnt pathways have not been investigated in cancer as extensively as the canonical pathway. Recently, WNT5A-induced non-canonical wnt signalling has been shown to enhance motility and invasive behaviour of melanoma, breast cancer, and gastric cancer cells[230-232]. In addition, WNT5A was found to be strongly expressed at the leading edge of non-melanoma skin cancers (squamous cell and basal cell cancers)[233]; WNT5A also enhanced directional migration of HaCat keratinocyte cells along its concentration gradient. This was accompanied with evidence of repression of canonical wnt signalling while it was a part of overall changes which boosted non-canonical wnt signalling[233]. Circulating tumour cells from pancreatic cancer patients were found to have significant enrichment for non-canonical wnt signalling components in 45% of cases suggesting a possible role for non-canonical signalling in pancreatic cancer metastasis[234].

In a large cohort (623 patients) of ovarian samples which included 230 benign controls, 86 borderline tumours and 307 EOC samples, it was found that WNT5A expression was significantly higher in the cancer samples with no significant difference between high grade serous and other sub-types of ovarian cancer. Using ovarian cell lines the authors found that WNT5A stimulation resulted in decreased canonical signalling and upregulation of genes related to the non-canonical pathway. WNT5A stimulation also resulted in an increase of vimentin and SNAILl expression and a reduction in E-cadherin expression suggesting an epithelial to mesenchymal transition[235]. However, another study reported that WNT5A expression was lower in EOC samples compared to ovarian surface or fallopian tube epithelium and WNT5A antagonised wnt canonical pathway in EOC cells and induced cellular senescence[236]. The reason of the marked discrepancy of WNT5A expression reported in this and the aforementioned study is not clear.

The wnt inhibitor secreted frizzled related protein 4 (sFRP4) was found to be down regulated in EOC[237]. In another study, sFRP4 inhibited WNT3A-induced canonical wnt signalling in ovarian cancer cells, caused a reduction in cell motility, and resulted in increased expression of E-cadherin and reduced expression of vimentin and TWIST (mesenchymal to epithelial changes: MET)[238].

The DKK family of wnt inhibitors act largely by binding to LRP5/6 co-receptors so preventing interaction with FZD and thus abrogating canonical signalling[203]. Both elevated and decreased levels of DKK1 have been reported in a variety of cancers such as breast, colon, myeloma and melanoma in different studies[239]. However, in ovarian serous cancer DKK1 expression was shown to be elevated and correlated with poor outcome[240].

1.5.2 5T4 and wnt Signalling

Recently it has been demonstrated that the 5T4 zebrafish homologue, *wnt-activated inhibitory factor 1* gene (*Waif1*), is a target for canonical wnt signalling during the different stages of zebrafish embryo development (gastrula, somitogenesis and organogenesis)[26]. Waif1 expression was found to be directly regulated by Wnt8. Furthermore, Waif1 was found to act as a negative feedback modifier to canonical wnt signalling in zebrafish and frog embryos. Waif1 appeared to compete with Dkk1 for Lrp6 binding resulting in the augmentation of the non-canonical wnt PCP signalling pathway[26] likely by increasing the availability of Dkk1 to bind with the co-receptor Glypican 4 member Knypek (Kny, a Dally-like homolog). Kny is an extracellular heparan sulfate proteoglycan (HSPG) which had been shown to modulate the propagation and the range of action of Dkk1[241].

The crystal structure at 1.8 A° resolution for the extracellular domain of Waif1 confirmed the expectations of heavily glycosylated core protein containing eight (rather than the previously thought seven) leucine-rich repeats (LRRs)[242]. The authors identified Tyr325, Lys76 and Phe97 to be essential for the inhibition action of Waif1 on the canonical wnt signalling[242].

Thus, 5T4 may promote cancer cell invasion by enhancing non-canonical wnt signalling. Research into 5T4 as a wnt modifier in human EOC could shed more light on whether it has a role in the molecular regulation of wnt pathway and on the mechanisms of cancer invasion.

1.6 Study Aims

Tumour dissemination within the peritoneal cavity is typical of epithelial ovarian cancer and is largely responsible for the high mortality rate in this disease. The oncofetal glycoprotein 5T4 is expressed in the majority of ovarian cancers while it shows low or absent expression in normal adult tissues. The expression of 5T4 appears to mark a switching state (or response) in three important biological processes: epithelial to mesenchymal transition, planar cell polarity wnt response and chemotactic response to CXCL12. 5T4, therefore, can be associated with cells becoming more motile and migratory. It is possible that 5T4 has a functional role in the spread of ovarian cancer through one or more of these processes.

1.6.1 Research Hypothesis

5T4 plays a functional role in epithelial ovarian cancer spread through its role in:

1) CXCL12/CXCR4-CXCR7 chemotaxis axis
2) EMP
3) Wnt signalling

1.6.2 Research Outline

This study investigated whether 5T4 has a role in the spread of ovarian cancer by exploring its functional contribution to EMT, PCP and chemotaxis in ovarian cancer cell lines. Subsequently, the expression of the relevant proteins was investigated in normal and malignant ovarian samples. This project explored in ovarian cancer cell lines:

- Morphological and 5T4-related molecular cell phenotypes
- Chemotactic response to CXCL12
- Manipulation of 5T4 expression by overexpression and knockdown
- Epithelial/mesenchymal phenotype and cell motility
- Response to canonical and non-canonical wnt ligands

In addition, ovarian surface epithelium, primary and metastatic ovarian cancer samples were compared using immunohistochemistry in terms of the expression of:

- 5T4
- CXCL12 receptors: CXCR4 and CXCR7
- Epithelial/mesenchymal markers: E-cadherin, cytokeratins, N-cadherin and vimentin
- wnt pathway proteins: β-catenin, DKK-1, JNK and phopsho-JNK

The following chapter details the methodology used to achieve these aims.

Chapter 2

MATERIALS AND METHODS

Materials and Methods

Several experimental methods have been implemented in this study to investigate a role for 5T4 in ovarian cancer spread including flow cytometry, immunofluorescence, immunohistochemistry and chemotaxis assays. Experiments were conducted initially on established cell lines and the generated findings were subsequently explored in primary human ovarian cancer tissues. In addition 5T4 knockdown experiments were performed using shRNA and lentiviruse in established cell lines.

2.1 Cell Lines

Eight ovarian cancer cell lines were used in this study, they were obtained sequentially as the experimental investigations progressed; new cell lines with specific characteristics were further obtained to address emerging questions. A complete list of all cell lines used in this project is in **Table 2.1**. SKOV-3, OVCAR-3 and Caov-3 cell lines were obtained previously in our laboratory from the American Type Culture Collection (ATCC). These cell lines were used in the preliminary experiments leading to this project. Subsequently the following cell lines were obtained: TOV-112D (ATCC), TOV-21G (ATCC), OV-90 (ATCC), Hoc-8 (our laboratory archive, established by J Filmus[243]) and A2780 (European Collection of Cell Culture (ECACC), provided by Dr P Caswell).

Table 2.1: EOC Cell Lines

Cell Line	Supplier	Origin	Histopathology subtype	Recommended media	Growth media
SKOV-3	ATCC, HTB77	Ascites	Adenocarcinoma, Ovary	McCoy's 5a	RPMI
OVCAR-3	ATCC, HTB161	Ascites	Adenocarcinoma, Ovary	RPMI	RPMI
Caov-3	ATCC, HTB75	Tumour	Adenocarcinoma, Ovary	DMEM	RPMI
TOV-21G	ATCC, CRL11730	Tumour	Clear cell carcinoma, Ovary	MCDB 105 / Medium 199	RPMI
TOV-112D	ATCC, CRL11731	Tumour	Endometrioid, ovary	MCDB 105 / Medium 199	RPMI
OV-90	ATCC, CRL11732	Ascites	Serous (high grade), ovary	MCDB 105 / Medium 199	RPMI
Hoc-8	Dr J Filmus	Ascites	Serous (high grade), ovary	RPMI	RPMI
A2780	ECACC	Tumour	Adenocarcinoma, Ovary	RPMI	RPMI

A complete list of epithelial ovarian cancer cell lines used in this study[243-245].

On acquisition, Cell lines were handled according to the suppliers' instructions in terms of thawing, culturing and stock-freezing. Several different growth media were recommended for culturing these cell lines. This imposed a practical challenge since an essential part of this project was the investigation of chemotaxis and cell motility for which phenol red-free medium was required and this was commercially available only in RPMI or DMEM formats. Hence all cell lines were investigated, and subsequently maintained, in RPMI growth media. This had an added advantage of simplifying procedures and making comparisons between cell lines less complicated by eliminating the possible effect of varying growth media and the inconsistency of growth factors and other molecules contained in these media. **Table 2.1** shows all cell lines, histological sub types, recommended media and the used growth medium.

It could be argued that cell biology and behaviour could be influenced by changing the growth media from the recommended ones; this should not be an issue in this study since the results are clearly presented as of those cell lines grown in RPMI. In addition, this study was concerned with exploring the role of 5T4 on the expression of specific molecules and on certain biological functions rather than studying the phenotype and behaviour of a particular cell line per se.

All cell lines were regularly checked for mycoplasma infection and contamination as tested by human cell line authentication service in the Paterson Institute for Cancer Research (PICR). There were no infections recorded during this project period and all authentication results were as predicted by suppliers' data ruling out cross contamination. However, Hoc-8 cell line failed to amplify using AmpFLSTR® Identifiler® PCR Amplification Kit (Applied Biosystems) on two occasions and further attempts to amplify it were abandoned. There are several recognised reasons which could explain why amplification using this kit might fail such as degradation, inhibition, or low copy numbers[246]. The authenticity of this cell line was particularly questioned since it is not available commercially and typically it is obtained by passing from one research group to another which could increase the chances of contamination. Nevertheless, the scientific value of this line to this study is less dependent on its origin and more related to its molecular phenotype.

2.1.1 Cell Culture

All cell lines were cultured in a standardised complete growth medium which is made of RPMI-1640 (sigma, R0883) supplemented with 10% heat-inactivated fetal calf serum (FCS) (Biosera, batch: 2020071), 2 mM L-glutamine (Sigma, G7513), 100 U/ml

penicillin and 100 μg/ml streptomycin (P/S) (Gibco, Invitrogen, 15140). Fetal calf serum was purchased in a large quantity of the same batch and stored for later use. This allowed experiments to be conducted under constant serum contents of molecules and substrates and not to be subjected to varying contents of different serum batches which could have influenced experimental results.

Cells were generally split when reaching 80-90% confluence on microscopic examination (usually every 3-5 days according to the cell line). Detachment of adherent cells was achieved by removing growth medium, washing with phosphate buffered saline (PBS) and then applying 40 μl/cm^2 (3 ml for T75 flask) of 0.05%/0.02% solution of trypsin/EDTA (Ethylenediaminetetraacetic acid, Sigma, T3924) for 3-5 minutes at 37˚C followed by suspension in 10% serum-supplemented medium to quench trypsin activity. Cells were then centrifuged at 1500 rpm (revolutions per minute) for 5 minutes (universal 320 centrifuge, Hettich zentrifugen), the pellet was then washed with warm PBS. Cells were then counted using haemocytometer (C-chip, Digital Bio) for live cell counting by trypan blue (Sigma, T8154) exclusion method. Cells were suspended in 15 ml complete growth medium and seeded in T75 Falcon cell culture treated flask (Corning, 430641) with a density of $15x10^3$-$30x10^3$ cell/cm^2 (varied by cell line) and kept in an incubator (Binder, Wolf Lab) which maintained humidified atmosphere of 5% CO2 at 37˚C. 24 hours later growth medium was replaced with fresh one.

Cells were used during this project at low passage number (< 10 passages) and replaced with frozen stocks periodically. At early passages, aliquots of each cell line were cryopreserved for future use. One to two million cells (according to the cell line) were suspended in cryopreservation medium containing FCS and dimethyl sulphoxide (DMSO, Sigma, D8418) in 9:1 volume ratio in cryogenic vials (Sigma, V7634) which were placed in propranolol freezing box (Nalgene, 5100-0001) which was placed in -80˚C freezer. This provided gradual, gentle drop in temperature of 1˚C/minute, cell aliquots were then stored in liquid nitrogen. A record of cells was kept which included the date of freezing, the number of cells, the passage number and the used growth media.

When using frozen cells out of stock or when acquired from suppliers, cryopreserved cells were rapidly thawed in a 37˚C water bath and washed in 15 ml of the recommended growth medium (pre-warmed to 37˚C), then were suspended in 15 ml recommended growth medium in T75 cell culture flask and incubated till cells became adherent (12 -24 hours) when media were replaced with fresh ones.

2.2 Flow Cytometry

Flow cytometry (FC) was used to phenotype cell lines using indirect staining technique (using primary and secondary antibodies) on live unfixed cells to explore cell surface expression of 5T4, CXCR4, CXCR7, CD26, E-cadherin and N-cadherin.

2.2.1 Reagents and Optimisation

Primary antibodies were chosen on the basis of published literature and our laboratory experience **(Table 2.2)**. To determine the optimal concentration of each antibody, they were initially tested by serial dilutions, guided by the manufactures' instructions, on cells known to express the relevant protein.

Table 2.2: Primary Antibodies Used in FC

Target	Type	Supplier	Reference	Clone	Concentration
5T4	Mouse IgG1	Stern *et al.*	used in 5T4 discovery	H8	1µg/ml
CXCR4	Rabbit polyclonal IgG	Abcam	ab2074		5µg/ml
CD26	Mouse IgG2b	Santa Cruz	SC-7633	202.36	2µg/ml
CXCR7	Rabbit polyclonal IgG	Abcam	Ab72100		4µg/ml
CXCR7	Mouse IgG1	ChemoCentryx		11G8	1µg/ml
E-cadherin	Mouse IgG2a	Invitrogen	13-5700	SHE78-7	5µg/ml
N-cadherin	Rabbit polyclonal IgG	Santa Cruz	SC-7939	H-63	2µg/ml

A complete list of primary antibodies used in flow cytometry in this study.

Generally during optimisation steps the relevant negative and positive controls were used to ascertain specificity and sensitivity for the staining technique. This included using unstained cells (omitting primary and secondary antibodies) which served as negative control and to gauge background autofluorescence. In addition, the relevant isotypes and both primary and secondary antibodies were used separately to uncover any non-specific staining or other protein interactions such as Fc (fragment crystallisable) receptor non-specific binding. Also, cell lines known to express certain markers were used as positive controls to rule out false negative staining; similarly cells known to lack the expression for each antibody were used as negative controls for staining to eliminate false positive staining. Therefore, the antibodies used in this study were confirmed to be suitable for the use in flow cytometry.

Negative control isotypes were all obtained from Dako and each was used at the same concentration of the corresponding primary antibody. These were mouse IgG1 (X0931), mouse IgG2a (X0943), mouse IgG2b (X0944) and rabbit polyclonal IgG (X0936).

2.2.2 Flow Cytometry Technique

Cell lines at 80–90% confluence were washed with warm PBS, trypsinised and, when detached, suspended in complete medium and centrifuged as described above. The resultant pellet was washed with cold PBS twice, cells were counted and then suspended in flow cytometry staining buffer (1% bovine serum albumin (BSA), Sigma, 05482) at $1x10^6$ cell/ml concentration. 200 µl of cell suspension in staining buffer was then placed in a Falcon polystyrene round bottom test tube (5 ml, BD Biosciences, 352058) and incubated for 60 minutes at 4˚C. Four tubes were prepared; one contained a primary antibody **(Table 2.2)**, a second contained the relevant isotype at the same concentration, while the other two tubes were left plain one to serve as unstained cells control while the other to be incubated with the secondary antibody only.

Subsequently, cells were washed twice in cold staining buffer and suspended in 200 µl staining buffer containing the relevant secondary antibody at 3/1000 concentration (6 µg/ml) for 30 minutes, in the dark at 4˚C. AlexaFluor 488 specific secondary antibodies (raised in goat) were used in all single colour flow cytometry experiments as in **Table 2.3**. Cells were then washed three times in staining buffer and suspended in 200 µl flow cytometry analysis buffer (0.5% BSA, 0.1% sodium azide (Sigma, 58032) in PBS).

Table 2.3: Secondary Antibodies Used in FC

Dye	Host animal	Target	Supplier	Reference	Concentration
Alexa Fluor 488	Goat	Mouse IgG1	Invitrogen	A-21121	6µg/ml
Alexa Fluor 488	Goat	Mouse IgG2a	Invitrogen	A-21131	6µg/ml
Alexa Fluor 488	Goat	Mouse IgG2b	Invitrogen	A-21141	6µg/ml
Alexa Fluor 488	Goat	Rabbit IgG	Invitrogen	A-11034	6µg/ml
Alexa Fluor 633	Goat	Rabbit IgG	Invitrogen	A-21071	6µg/ml

A complete list of secondary antibodies used in flow cytometry in this study.

Samples were processed using BD FACSCanto II machine which was kept under regular maintenance by suppliers and its performance was checked prior to each use at least once daily by using the supplied tracking beads according to the manufacturer's instructions. Data were acquired using BD FACSDiva software provided with FACSCanto II machine. After running the set up steps, detector voltages for forward scatter (FSC) and side scatter (SSC) checked and adjusted using unstained cells so cells can be viewed within

the dot plot graph; gating then was applied around live cells to ascertain the capture of surface expression of studied molecules.

Cells stained for the matched isotype were used to adjust the detector voltage for active fluorescence, usually FITC (Fluorescein isothiocyanate), so the graph was placed in the first log. Following that, cells stained with primary antibody and those stained with secondary antibody alone were processed. Therefore, in each experiment, four samples were analysed; unstained, secondary antibody only, primary and secondary, and isotype and secondary.

2.2.3 Data Analysis and Statistics

Data from $25x10^3$ cells were captured in each tube, data then were stored and later analysed using FlowJo software (version: 7.6.1). Each experiment was conducted independently at least three times and average results were presented[247-249].

Firstly, graphs were visually examined for the uniformity (homogeneity) of staining; this was uni-modal for all antibodies in all cells apart from OV-90 cell line (see later paragraphs). Subsequently, Median Fluorescence Intensity Ratio (MFIR) was calculated; MFIR of staining for a given antibody in a cell line is the ratio of the median fluorescence intensity (MFI) obtained when that antibody is used to the MFI when the matched isotype is used. The median was used in this project, rather than the mean, as the fluorescence intensity results, as expected, were not normally distributed and recorded on a logarithmic scale for which median analysis is a more suitable option[250, 251].

The MFIR was used to reflect the degree of 'peak shift' resulting from using a primary antibody in comparison to using the matched isotype. Hence, if staining with a primary antibody did not result in a peak shift from that of the isotype staining, MFIR would equal 1 indicating the lack of surface expression of the studied molecule[252-254]. It was decided in this project that MFIR values $\leq 1 \pm 0.25$ would be considered negative staining. MFIR hence provided a useful tool to numerically distinguish positive from negative staining, in addition it allowed meaningful comparisons between different results which were used in result presentation.

2.2.4 Multicolour Flow Cytometry

OV-90 cells showed heterogeneity for expression of 5T4 and CXCR4, hence double staining flow cytometry was used to explore the presence of any relationship between 5T4 and CXCR4 expression in these cells. Primary antibodies used in double staining were the same of those used in single colour flow cytometry and at the same concentrations

(Table 2.2). Alexa Fluor 488 (AF488 goat anti mouse IgG1) was used for 5T4 as a secondary antibody which could be seen on FITC channel; Alexa Fluor 633 (AF633 goat anti rabbit) was used for CXCR4 and was seen on APC (allophycocyanin) channel.

Simultaneous incubation with antibodies was used in this study, where the staining steps followed essentially those of single antibody staining however both primary antibodies were added simultaneously at the appropriate step and also both secondary antibodies were added together at the appropriate time. Simultaneous staining was possible because optimisation experiments demonstrated that antibodies did not cross react when added together. During optimisation, cells incubated with 5T4 primary antibody were stained with the secondary antibody used for CXCR4 (AF633 goat anti rabbit) alone or in combination with secondary antibody used for 5T4 (AF488 goat anti mouse IgG1). Similarly cells incubated with CXCR4 antibody were stained with the secondary antibody used for 5T4 (AF488 goat anti mouse IgG1) alone or in combination with secondary antibody used for CXCR4 (AF633 goat anti rabbit).

In addition, in multicolour flow cytometry cells were stained for each antibody separately with the routine controls i.e. unstained cells and secondary alone staining as this was required for calculating fluorescence compensation. Fluorescence compensation was performed at the beginning of each double staining experiment utilising the automatic calculation property provided by the FACSDiva software; the parameters were then applied to the entire FC experiment performed.

2.2.5 Fluorescence-Activated Cell Sorting

Cell sorting was required on two occasions in this project; following 5T4 knockdown experiments to select cells with reduced 5T4 expression, and in exploring OV-90 cells which were heterogeneous for 5T4 and CXCR4 expression. Fluorescence-activated cell sorting (FACS) was used for both purposes and it followed primarily the techniques of single colour flow cytometry for knockdown cells, and double-staining flow cytometry for OV-90 cells. However all steps were performed in cabinet hood to maintain sterility and sodium azide was omitted.

In brief, cells were harvested at 80% confluence, washed with cold PBS twice and counted. A small proportion of cells (about $0.5x10^6$) were left unstained while the remaining cells were indirectly stained for 5T4 (and CXCR4 in case of OV-90 cells). Primary and secondary antibodies were used in FACS at 10 fold concentration of that used in the routine flow cytometry since cell concentration here was ten times of that used in

flow cytometry. In addition, cells were stained with 7-Aminoactinomycin D (7AAD, Invitrogen, A1310) for viability at 5 µl/ml.

Cells were subsequently washed and kept in filter-sterilised Basic Sorting Buffer (BSB) at concentration of $10x10^6$ cell/ml. BSB is made of calcium-free, magnesium-free PBS, EDTA (1mM), HEPES (25 mM, PH=7.0) and heat-inactivated FBS (1%). Cells were then submitted on ice in polypropylene 5 ml tubes (BD, 352063) for cell sorting.

Unstained cells were used to set forward (FSC) and side (SSC) scatters voltages. Live cells were gated as those negative for 7AAD. Within live cells those expressing the lowest 5T4 levels were selected and collected into cold heat-inactivated FBS (100%) in the case of 5T4 KD studies. For OV-90 three groups of cells were obtained according to 5T4 and CXCR4 expression (detailed later).

Sorted cells in 100% FBS were transferred on ice to our laboratory where they were seeded in warm growth media in a T75 cell culture flask and incubated as routine cell culture practice. When reached 80-90% confluence, cells were passaged and two or three vials with $1\text{-}2x10^6$ cells were cryopreserved.

2.3 Immunofluorescence Staining

Immunofluorescence (IF) staining was used in conjunction with flow cytometry to characterise cell phenotype in terms of expression of 5T4, E-cadherin, cytokeratins, N-cadherin and vimentin. Unlike FC which requires detachment of cells from each other and from the culture surface; in situ IF had the advantages of staining cells with minimal disturbance. Another advantage of IF was that it allowed studying structural changes such as actin cytoskeleton and vimentin, and it was a useful means to investigate subcellular location of β-catenin i.e. nuclear, cytoplasmic or membranous.

2.3.1 Surface Markers Staining

Cells were harvested at 80% confluence and then suspended in complete growth medium at concentration of $25x10^3$ cell/ml; cells were then seeded in glass-bottom 24 well imaging plates (PAA Laboratories, PAA21315231X) at 1ml/well. The plate was then kept in the cell culture incubator (Binder, Wolf Lab) which maintained a humidified atmosphere of 5% CO2 at 37˚C as per routine cell culturing explained earlier. Cells were left in the incubator for 36-72 hours till the desired cell confluence was achieved. When exposure to specific molecules was under investigation, the growth media were replaced at this stage with fresh complete growth media supplemented with the molecule and left for the required time in the cell culture incubator.

Cells were then fixed by adding 120 µl of 37% fresh paraformaldehyde (PFA) solution (Sigma, 158127), to achieve final concentration of 4%, for 10 minutes at room temperature (RT). Cells were then washed with PBS twice for 5 minutes each. Cells were then permeabilised by adding 0.1% triton X-100 (Sigma, T8787) in PBS for 10 min at RT. This step was omitted when staining for cell surface expression of 5T4, N-cadherin and E-cadherin.

Cell proteins were then blocked by incubating cells with 10% normal goat serum (Cell Signalling Technologies, 5425S) in PBS for two hours at RT. Triton X-100 at 0.1% concentration was added at this step if required. Subsequently, goat serum was removed and cells were incubated with the relevant primary antibody **(Table 2.4)** or the matched isotype at the required concentration in PBS overnight at 4˚C.

Negative control isotypes were all from Dako and used at the same concentration of the corresponding primary antibody. These were mouse IgG1 (X0931), mouse IgG2a (X0943), mouse IgG2b (X0944) and rabbit polyclonal IgG (X0936).

Table 2.4: Primary Antibodies Used in IF

Target	Type	Supplier	Reference	Clone	Concentration
5T4	Mouse IgG1	Stern et al.	used in 5T4 discovery	H8	2µg/ml
E-cadherin	Mouse IgG2a	Invitrogen	13-5700	SHE78-7	4µg/ml
N-cadherin	Mouse IgG1	BD Biosciences	BD610920	32/N-Cadherin	5µg/ml
Vimentin	Mouse IgG1	Leica Biosystems	VIM-V9-L-CE	V9	0.125µg/ml
Cytokeratins	Rabbit polyclonal IgG	Abcam	Ab9377	Anti-wide spectrum	10µg/ml
B-catenin	Mouse IgG1	BD Biosciences	BD610154	14/Beta-Catenin	1µg/ml

A complete list of primary antibodies used in immunofluorescence in this project.

Cells were then washed with PBS three times, 5 minutes each, and incubated with relevant secondary antibody **(Table 2.5)** for 2 hours in the dark at RT. Nuclei were then counterstained with DAPI (4′,6-Diamidino-2-phenylindole dihydrochloride, Sigma, D9542) at 1 µg/ml concentration for 15 minutes at RT in the dark also.

Finally, cells were washed three times in PBS, 5 minutes each, and preserved by covering cells with several drops of ProLong Gold antifade reagent (Invitrogen, P36934). Plates were then kept in the dark (black boxes) at 4˚C in the fridge until they were imaged in the following 24 hours.

Table 2.5: Secondary Antibodies Used in IF

Dye	Host animal	Target	Supplier	Reference	Concentration
Alexa Fluor 488	Goat	Mouse IgG1	Invitrogen	A-21121	6µg/ml
Alexa Fluor 488	Goat	Mouse IgG2a	Invitrogen	A-21131	6µg/ml
Alexa Fluor 488	Goat	Rabbit IgG	Invitrogen	A-11034	6µg/ml
AF-488 Phalloidin		Cytoskeleton	Invitrogen	A12379	3 units (15µl)/well

A complete list of secondary antibodies used in immunofluorescence in this study.

2.3.2 Microscopy

A Time Lapse system with Axiovert 200M microscope stand was used to screen and capture images (bright field, green and blue). The system utilises a Plan-Apochromat 10x, 20x and 40x objective lenses. Illumination was achieved using a 300W Xenon system (Sutter Instruments) which presented the system as an even field of illumination in addition to the appropriate neutral density and Schott filters to modulate the light source. Wavelength selection was achieved using external filter wheels, (Sutter Instruments) and

the ET-Sedat set, (Chroma). Images were captured utilising the CoolSNAP HQ (Photometrics) camera with an axial resolution of 150 nm using the MS-2000 stage (Applied Scientific Instrumentation). The system was fully controlled and automated via Metamorph software (Molecular Devices). All of the data sets were stored and analysis was carried out using ImageJ software (National Institute of Health, USA, ImageJ 1.48g).

Plates were kept in dark by transferring in a black box and maintained at low temperature (4˚C) when not being imaged. First, all cells in each well were examined and then several representative images (at least four areas with total > 100 cells) were captured for presentation; experiments were performed at least three times.

The same capture parameters were used for each antibody and its matched isotype and for all cell lines when their expression was subjected to comparison such as 5T4-KD cells and parental cells. Capture parameters were primarily the settings of the software used including gain, exposure time and magnification power.

Images were named appropriately on capture and stored on the system to be processed for presentation and comparison using ImageJ software, again same parameters for this software were used to allow valid comparisons.

2.4 Cell Motility and Chemotaxis Assays

Several methodologies were considered to investigate cell motility and cell migration. Each technique has its advantages and disadvantages, however, FluoroBlok® assay (BD Bioscience) was chosen in this study as it was relatively easy to utilise with a reasonable reproducibility. This technique was developed further in this project by incorporating in situ cell counting offered by microplate scanner (Thermo Scientific Cellomics HCS) which is a novel technique used in this study.

2.4.1 Method Overview

FluoroBlok® assay, like other insert-based methods, utilises the established principles of Boyden's chambers method[255] in evaluating cell migration through a porous membrane separating two chambers one above and one below the membrane; cells are usually placed in the top chamber. Practically this is achieved by using a well (from a multiwell plate) as the bottom chamber; while a device called insert is secured on the top hanging inside the well. The insert is a specially designed hollow cone with a base formed by a porous membrane. The insert has a height which is smaller than that of the used well so the bottom of the insert does not come in contact with the inner aspects of the well instead it allows for a small space in between to be filled with the solution to which the cells migration is observed.

Both chambers are filled with solutions which varied according to the experimental design. In its simplest settings both chambers would contain the same solution which is made of the recommended growth medium for the cells under investigation. In this instance, cells migration between two identical media across the membrane would provide a useful means to studying cell motility. Alternatively, medium in either chamber could be supplemented with molecules under investigation to illustrate their effect on cell migration. In this project, CXCL12 was often added to the lower chamber to explore its chemotactic effect on cells placed in the upper chamber; in this design the only difference between the contents of upper and lower chambers (apart from the cells themselves) is the molecule under investigation (i.e. CXCL12).

Cells after migration typically attached to the inferior surface of the membrane and only negligible number were observed to 'drop' down and settle on the bottom of the well. These cells were counted indirectly by fluorescence intensity (or directly using plate scanner) as the outcome of each experiment and comparisons were made between the varying experimental conditions.

2.4.2 FluoroBlok® Cell Migration Assay

In early versions of insert methods, which used transparent membranes, cell counting was achieved by removing cells which did not migrate and remained inside the insert by mechanical means such as cotton buds; then physically cutting the membrane off the insert edges, turning it downside up and then staining cells and performing direct counting under light confocal microscope. This technique was deemed in this study to be unsatisfactory since it was not certain that all cells which did not migrate could be removed by using cotton buds. Hence these cells could be mistaken for and counted as migrated cells given the transparent nature of the membrane used. In addition, the manual handling of the membrane during cutting could result in cell detachment and subsequent loss of cells. Furthermore, once membranes were cut they tended to twist and curl which made focusing by microscope to count the cells a rather challenging task.

For these reasons, FluoroBlok® inserts (BD Bioscience, 351152) were used in this project. FluoroBlok inserts have the advantage of utilising coloured light-tight polyethylene terephthalate (PET) membranes which block light transmission within the range of 490-700nm. Staining cells with an appropriate fluorescent dye and using microplate bottom reader (FLUOStar Omega, BMG labtech) allowed the detection of only the cells which migrated through the membrane. The detected fluorescence intensity reflected the number of migrated cells in each insert and this subsequently was used for comparisons among the different settings within each experiment.

2.4.2.1 Optimisation

Several initial experiments were performed to determine the optimal experimental conditions including cell density, serum concentration, cell staining and pre-experiment cell condition. Given the significant price of FluoroBlok inserts, flat bottom 96 well plates (BD, 353072) were used to determine the initial optimal conditions since the growth surface for these wells (0.32 cm^2) are similar to those of the inserts. Subsequently, when the conditions were narrowed down, FluoroBlok inserts were used to 'fine-tune' the optimal conditions.

The first step was to determine the cell density at which cells were spread evenly at the bottom of the insert without being too sparse or overcrowded. This was a condition where a large number of cells are available to migrate without creating unnecessary competition for the finite number of pores. In addition, the lowest serum concentration without compromising cell viability was sought. This was thought to be required to be able

to illustrate CXCL12-mediated chemotaxis which might be otherwise masked by the background cell motility in higher serum concentrations.

For each cell line, a range of cell densities ($5x10^3$, $10x10^3$, $25x10^3$, $50x10^3$ and $100x10^3$ cells/well) in combination with varying serum concentrations (0%, 0.5%, 1%, 3%, 5% and 10%) were tested. Seeded cells were examined by confocal microscope at three time points; (1) immediately after seeding reflecting the start of chemotaxis experiment; (2) 2-3 hours later corresponding to the start of data recording in the chemotaxis experiment; and (3) at 12 hours which is the time length required for chemotaxis assay. The results of these experiments indicated that $50x10^3$ or $100x10^3$ cells/well in 0.5%-1% serum were the suitable conditions for cell lines in this project.

Other experiments revealed that it was important to starve cells of serum overnight prior to chemotaxis assays to be able to better demonstrate the chemotactic response to CXCL12. One explanation is that depriving cells of the constant stimulation by the various growth factors, cytokines and chemokines, usually present in FCS, before the chemotactic experiment might help to unmask CXCL12 chemotactic response.

2.4.2.2 Experiment Steps

Cells grown in the relevant growth medium in T75 flasks were starved of serum overnight at 80-90% confluence by replacing the medium with serum-free RPMI-1640 after a wash with PBS. The following day, cells were washed with PBS and trypsinised then washed with phenol-red free RPMI (Sigma, R7509) containing 1% serum to quench trypsin. Phenol red was avoided as it could interfere with the signal detection by the microplate reader. Cells were then washed twice with PBS and stained with 1,1' - Didodecyl - 3,3,3',3' - tetramethylindocarbocyanine iodide (DiIC12(3), AnaSpec, 84902) at a final concentration of 10 µg/ml for 30 minutes at room temperature in dark. DiIC12(3) is a lipophilic tracer which stains cellular membrane; it was used given its low toxicity and minimal effects on cell viability.

The accompanying 24 well plate (BD Biosciences, 353504) was blocked with 1% BSA/PBS for three hours immediately before commencing the experiment. FluoroBlok inserts with pores size of 8 µm were then placed carefully in the correct position in the wells. Subsequently, 300 µl assay medium containing $50x10^3$ cells (or $100x10^3$ cells for some cell line) were placed in each insert; the multiwell plate was then placed in cell culture incubator maintaining 5% CO2/ 37˚C humidified atmosphere for two hours to allow cells to settle.

1000 µl medium was then added to the wells (lower chambers) carefully to avoid air bubbles forming beneath the membrane. In each experiment the media added to the lower chamber were; (1) identical to that in the upper chamber (negative control), (2) supplemented with 10% serum (positive control) or (3) supplemented with 100 ng/ml CXCL12 (R&D Systems, 350-NS), (when response to CXCL12 was investigated); each was done in triplicates. In addition three wells were prepared in the exact manner as negative control, however, without cells in the upper chamber to serve for calculating background fluorescence. Background fluorescence was likely to vary from one experiment to another and therefore it was adjusted for during analysis.

The plate containing the inserts was then placed in a microplate bottom reader (FLUOStar Omega, BMG labtech) which maintained atmosphere of 5% CO2/ 37˚C, and data were recorded over night with the appropriate excitation and emission wave length (544 nm and 590 nm respectively) at 20 minutes intervals.

2.4.2.3 Data Handling

An advantage of FluoroBlok technology in addition to avoiding traditional cell counting methods, is that it permitted the continuous live monitoring of cell migration by recording the fluorescence signal at the inferior aspects of the insert membrane as cells travelled through the pores while allowing the experiment to continue. In the traditional, microscope-based cell count assays, it was necessary to terminate experiments to be able to obtain any results.

Live monitoring of cell migration provided more insight into cell migration behaviour in each experimental setting over time; nevertheless this imposed a statistical challenge in interpreting the generated data since the continuously recorded values are not statistically independent variables per se and the direct use of the common statistical tests (such as student t test) was deemed inappropriate[256, 257]. The use of ‘summary statistics’ is encouraged for this type of data, specifically slope analysis (regression coefficient) is recommended for data of the kind obtained in our experiments (so–called growth pattern line)[257].

Since experiments were performed in triplicates in these studies, the recorded fluorescence intensity was summarised by calculating the mean at each time point of the triplicates, this resulted in one set of data representing each experimental setting. The ‘true’ fluorescence intensity was then calculated by subtracting the mean of the background fluorescence from the mean of the recorded values of each experimental setting (CXCL12 for example). The slope of the line of means, the migration slope, was then calculated as

the regression coefficient over 10 hours (a usual time for the assay). Thus the migration slope was a summary statistic representing cell migration in a given experimental condition and was used, therefore, to compare migration outcomes among experiments.

While FluoroBlok technique helped to overcome the need for physical counting of cells and while it made it possible to compare results obtained from the same cell line within the same experiment, it imposed new questions about comparing results obtained from different cell lines or from different experiments where the relationship between recorded fluorescence intensity and cell number is less clear. Initially, this was resolved by expressing results in relative terms to inherent cell motility i.e. results obtained when inserts separating two identical media. For example, cell migration along CXCL12 concentration gradient would be expressed as 125% when the migration slope of cells migrated toward CXCL12 is 1.25 fold of cell motility migration slope in the same experiment. These relative values were then used to compile results obtained by different experiments or to compare cell lines.

Several factors could affect these values and cause variation particularly among different cell types and from one experiment to another such as confluence status prior to the assay, the number of cells obtained from the flask at the start of experiment, affinity to the dye (DiIC12(3)), and the presence of cell membrane debris which stain with DiIC12(3) and could pass freely through the 8µm pores. In addition, it was found that dye uptake varied among the different cell lines when fluorescence intensity was measured by flow cytometry. In one experiment Hoc-8, OVCAR-3, Caov-3 and SKOV-3 cells were stained with DiIC12(3) and fluorescence intensity was measured using flow cytometry. This revealed MFI of 35375, 54002, 65337 and 86080 (arbitrary fluorescence units) respectively, that is 41%, 63% and 76% in comparison to SKOV-3 (respectively), which would make comparing absolute results, obtained by FluoroBlok, between cell lines unhelpful.

Some researchers attempted to establish cell number/fluorescence unit formulas to use in converting fluorescence data into cell numbers. This was explored by seeding known numbers of cells on the insert membranes after placing the inserts upside down (so cells are seeded on what is the inferior surface of the membrane if it were in the correct position). Cells are allowed to settle and adhere; inserts are then placed in the correct position in a multiwell plate prior to reading the fluorescence intensity by a plate bottom reader. A line representing cell numbers to fluorescence intensity units was then drawn and used for cell calculation subsequently. This was felt to be an inaccurate representation of

what actually happens when cells migrate through pores and therefore was not used in this study. Furthermore, in spite of a robust standardised methodology for conducting this assay; it could not be ascertained that cell uptake of the fluorescence dye does not vary from one experiment to another.

The need to compare different cell lines was becoming more crucial in this project and simple FluoroBlok® method was no longer sufficient given the difficulty in converting the recorded fluorescence intensities into actual cell numbers.

2.4.3 Plate Scanner Cell Counting

During the later months of this project, a new machine, plate scanner (Thermo Scientific Cellomics HCS) was acquired in our institute which offered the opportunity of microscopically imaging cells in situ and to automatically count cell numbers by programming the operating software. This plate scanner was taken advantage of to show that migrated cells can be counted accurately in situ. For the first time it became possible to count migrating cells reliably and with little physical disturbance to cells.

2.4.3.1 Methodology

The initial steps for experiments were identical to those conducted using FluoroBlok inserts in FLUOStar Omega plate bottom reader explained earlier. However, after recording data for 12 hours, the experiment was stopped and plates were processed for cell count by the plate scanner.

The plate was taken to cell culture cabinet and 37% PFA was added to both the bottom and the top chambers for final concentration of 4%, for 60 minutes at room temperature; this fixed cells to the insert membrane. Subsequently, DAPI was added without changing media for final concentration of 1µg/ml for 30 minutes at room temperature and in dark. The plate was then read by the scanner which was programmed to count the stained nuclei. The area of the membrane which was covered by the plate scanner consisted of 36 fields totalling 1.3 cm^2 which was 43 % of the entire insert bottom surface. This is approximately the same surface area which was generally scanned by the plate reader.

In addition, it was possible to count the number of seeded cells at the start of each chemotaxis experiment. An equal volume of the cell suspension and therefore the same cell numbers as those placed in the top chamber of the insert was placed in a well of 96 well plate with a growth surface area identical to the inner surface of the membrane of the insert. The 96 well plate was placed in the incubator for the length of the chemotaxis

experiment, fixed with PFA, stained with DAPI and read by plate scanner with the same settings (the same surface area with the same ratio of the entire surface). This methodology provided not only the number of migrated cells but the number of cells at the beginning of the experiment. Therefore, it proved to be a powerful tool which allowed comparison across experiments and different cell lines with increased confidence.

2.5 5T4 Knockdown in SKOV-3 Cells

SKOV-3 cell line was found in this project to express 5T4 and to respond chemotactically to CXCL12 (result chapters). Therefore, this cell line was chosen to investigate the effect of 5T4 knockdown on cell phenotype and functional properties.

2.5.1 Lentivirus-based KD

Given the nature of functional experiments involved in this project, it was sought to obtain a stable knockdown of 5T4 for which lentivirus-based methodology was utilised. This was done in collaboration with Dr Mark Holland from the Children's Cancer Group in the Paterson Institute for Cancer Research (PICR).

BLOCK-iT™ kit was purchase from Invitrogen which contained the required buffers and reagents. When dealing with viruses appropriate measures and suitable working cabinets were used according to PICR biosafety procedures and suppliers' instructions. The following steps were used to make 5T4-KD lentivirus and to use it in SKOV-3 cells.

2.5.1.1 Sequence Determination

Pre-miRNA single stranded DNA (ssDNA) oligonucleotides to knock down 5T4 expression were designed and purchased from Life Technologies (Invitrogen). Sequences were generated by algorithm-based software (Invitrogen's RNAi Designer) according to manufacturer's instructions (BLOCK-iT™ Pol II miR RNAi Expression Vector Kits).

Four pairs of single stranded oligonucleotide were supplied; each pair consisted of one top and one bottom oligonucleotide. They have the reference numbers: Hmi417656, Hmi417657, Hmi417658 and Hmi417659. As a negative control lacZ (β-galactosidase) double-stranded oligonucleotide was used (provided with the kit).

2.5.1.2 Annealing into Double-Stranded Oligonucleotides

Oligonucleotides were supplied lyophilized, each diluted in DEPC (Diethylpyrocarbonate)-treated water (Ambion, Life Technologies; AM9920) to a final concentration of 200 µM. The corresponding top and bottom oligonucleotides of each pair were mixed together in the supplied annealing buffer, heated to 95˚C for 4 minutes then allowed to cool to room temperature for 10 minutes; this annealed each top and bottom single stranded oligonucleotides in each pair into double stranded oligonucleotides (ds-oligo) which in turn were diluted in DEPC-treated water to a final concentration 10nM and stored at -20˚C for later use. The formation and integrity of ds-oligos were confirmed by using Bioline HyperLadder V marker (BIO-33057) on 4% agarose gel where the LacZ (which was supplied as double stranded oligonucleotide) used as a positive control.

2.5.1.3 Generation of Expression Clones:

2.5.1.3.1 Cloning Double Stranded Oligonucleotide into Expression Vector

Each of the four double stranded oligonucleotides designed to knock down 5T4 expression in addition to LacZ duplex was mixed separately with ligation buffer (provided in the kit) and linearised pcDNA 6.2-GW/EmGFP-miR (expression vector provided in the kit). For negative control DNase/RNase-Free water (without oligonucleotide or expression vector) was used. All samples were mixed with T4 DNA ligase and left at room temperature for 5 minutes then placed on ice prior to transforming *E-coli*.

2.5.1.3.2 Transforming *E.coli* for Selection

2 µl of each ligation reaction was added separately to One Shot® TOP10 chemically competent *E.coli* (provided in the kit), mixed and incubated on ice for 15 minutes, followed by heat shock at 42˚C for 30 seconds, then back on ice. 250 µl S.O.C. medium (provided in the kit) was added and the mixture incubated at room temperature for 1 hour with shaking. 150 µl of each transformation mixture was then plated on pre warmed Luria-Bertani (LB) agar plates containing 50µg/ml spectinomycin (Sigma; S4014) and incubated at 37˚C overnight. Spectinomycin was used for selection since pcDNA™6.2-GW/EmGFP-miR vector contains Spectinomycin-resistance gene.

Colonies grew on all transformation plates, except for the negative control (water only ligation) plates. For each plate 5 colonies were picked and cultured overnight in LB medium with 50 µg/ml spectinomycin; plasmids were then isolated using miniprep kit (QIAGEN; 27104) which was performed by PICR core facility and confirmed to have the correct sequences using the forward and reverse primers provided in the Invitrogen kit.

2.5.1.4 Creating Entry Clones for the Use with pLenti6/V5-DEST

This was performed by following the manufacturer's instructions of the BLOCK-iT™ Lentiviral Pol II miR RNAi Expression System with EmGFP (Life technologies; K4938-00). Briefly, the resultant expression vectors cannot be used directly with the pLenti6/V5-DEST destination vector as pcDNA™6.2-GW/EmGFP-miR expression vector contains attB sites. Therefore, Gateway® BP recombination reaction with pDONR 221 vector was done first to generate the attL sites. This entry clone then was transferred by Gateway® LR recombination reaction into pLENTI6/V5-DEST vector to generate the complete lentivirus construct.

Lentivirus produced from LacZ oligonucleotide henceforth will be called lenti-LacZ while lentiviruses produced for 5T4 knockdown will be named lenti-56, lenti-57, lenti-58 and lenti-59 (keeping the reference numbers of original ssDNA sequences).

2.5.1.5 Producing Lentivirus in 293FT Cells

Lentivirus stocks were generated using 293FT Producer cell line provided in ViraPower™ Lentiviral Packaging Mix kit (Life Technologies, K4975-00). 293FT were cultured as instructed in Dulbecco's Modified Eagle's Medium (DMEM; Sigma, D6546) supplemented with 10% FCS and 0.5 mg/ml G418 (Life Technologies; 10131-035). Each pLenti6 construct was separately mixed with ViraPower solution (provided in the kit) in 1.5 ml DMEM first, then with lipofectamine 2000 (Life Technologies; 11668-027) in DMEM. Subsequently, DNA-lipofectamine complexes were added to trypsinised 293FT cells, incubated for 24 hours then media were changed to complete growth media.

Virus-containing supernatants were harvested at 48 hours, media were replaced and virus harvested again at 72 hours. 48 and 72 hours' virus-containing supernatants were mixed, centrifuged at 3000 rpm and filtered through 0.45 μm low protein binding filter (Millipore, DS2944EN00). Lentivirus titration revealed low concentration, therefore concentration was optimised by centrifuging through Vivaspin-20 (GE Healthcare Life Sciences; 28-9323-63) at 2000 g for 90 minutes at room temperature; samples were then frozen and stored in aliquots at -80˚C.

2.5.1.6 SKOV-3 Cell Line Transduction

SKOV-3 cells were seeded in 6 well cell culture plates (Corning Life Sciences; 3516) at a density $2x10^5$ cells/2ml/well in complete RPMI growth medium (sigma, R0883) and incubated in humidified 5% CO2, 37˚C atmosphere (Binder incubator, Wolf Lab). 48 hours later when cells reached 70% confluence, media were replaced with fresh ones mixed with polybrene (Sigma; H9268) and one of the lentiviruses for each well (lenti-LaZ, lenti-56, lenti-57, lenti-58 and lenti-59) at Multiplicity of Infection (MOI) ratio of 3. One well served as a no transduction control. Media were replaced with fresh ones 24 hours later, cells were harvested, and transduction efficiency and 5T4 knockdown efficacy were checked by two colour flow cytometry after staining for 5T4 using AF546-tagged goat secondary antibody (Invitrogen; A-21123).

SKOV-3 cells transduction was good as judged by green fluorescent protein (GFP) expression, however, 5T4 expression was only mildly affected even after cell sorting. **(Figure 2.1)**. Given the low knockdown efficacy obtained by lentivirus and the length of time taken to reach the final results, lentivirus-based knockdown was abandoned and

shRNA technology was used. First GFP-expressing plasmids were used as the presence of GFP was thought to offer an easy and convenient way to judge transfection during optimisation steps. Subsequently, stable knockdown was achieved by using shRNA tagged with antibiotics resistance gene.

Figure 2.1: 5T4 Knockdown Using Lentivirus

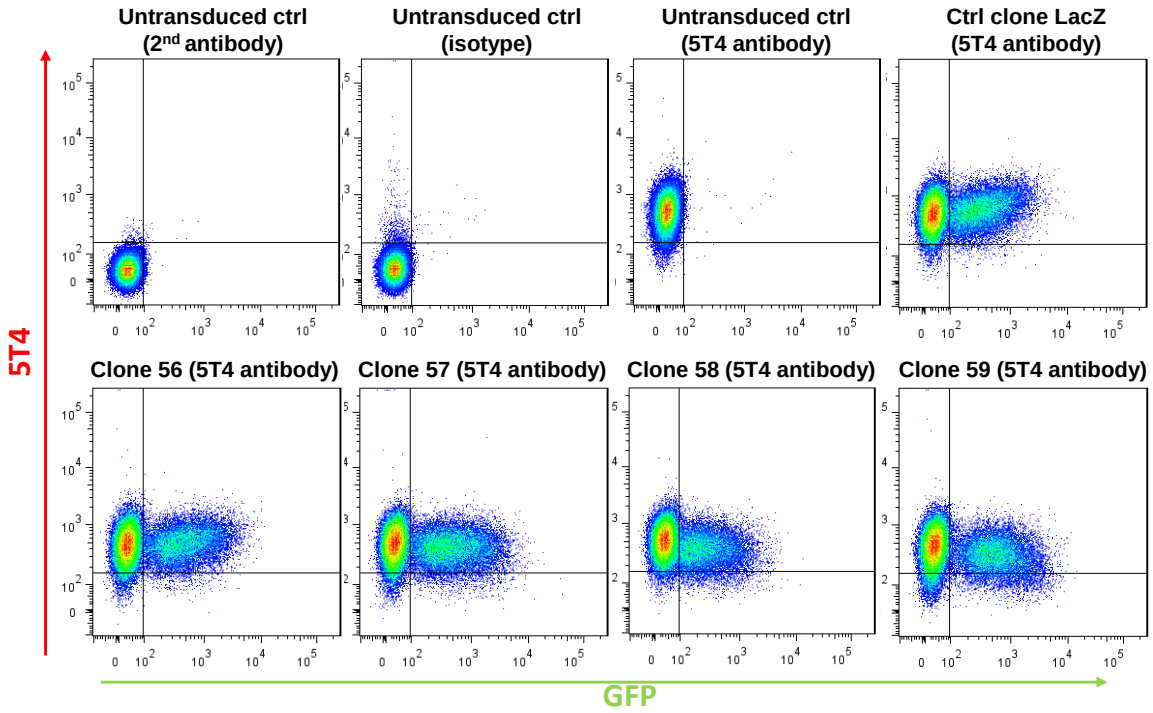

Double staining flow cytometry of 5T4 lentivirus knockdown in SKOV-3 cells: cell transduction with virus was successful as judged by GFP expression, however 5T4 expression remained high in the transduced cells when compared to the control knockdown LacZ.

2.5.2 Short Hairpin RNA Plasmids

Short hairpin RNA (shRNA) plasmids were designed using an experimentally validated algorithm which is based on BLAST search and supplied by QIAGEN (SABiosciences). Four different SureSilencing shRNA plasmids and one negative control were provided. The negative control shRNA was a non-targeting scrambled sequence (Ref: 20060802). The sequences of the inserts are in **Table 2.6**.

Table 2.6: shRNA Sequences

shRNA clone	Insert sequence	Named SKOV cells after transfection
Clone 1	CCATCCCTGCAAACCTCTTAT	SKOV-C1
Clone 2	CACCTGGACTTAAGTAATAAT	SKOV-C2
Clone 3	ACCTCAGTCCCTTCGCTTTCT	**SKOV-C3**
Clone 4	CTGGACTGTGACCCGATTCTT	SKOV-C4
Control clone	GGAATCTCATTCGATGCATAC	**SKOV-CC**

The sequences of four active and one scrambled shRNA clones used to knock 5T4 expression down, and the names given to cells after transfecting SKOV-3 cell line.

Each plasmid was supplied in two forms, one containing GFP gene (336314KH10229G) which expressed GFP as a marker; and one containing puromycin-resistance gene (336314KH10229P) which expressed puromycin-N-acetyltransferase. Each vector expressed shRNA under the control of U1 promoter and GFP gene with CMV promoter upstream or puromycin-resistance gene with SV40 promoter upstream **(Figure 2.2)**.

Figure 2.2: shRNA Plasmids Structure

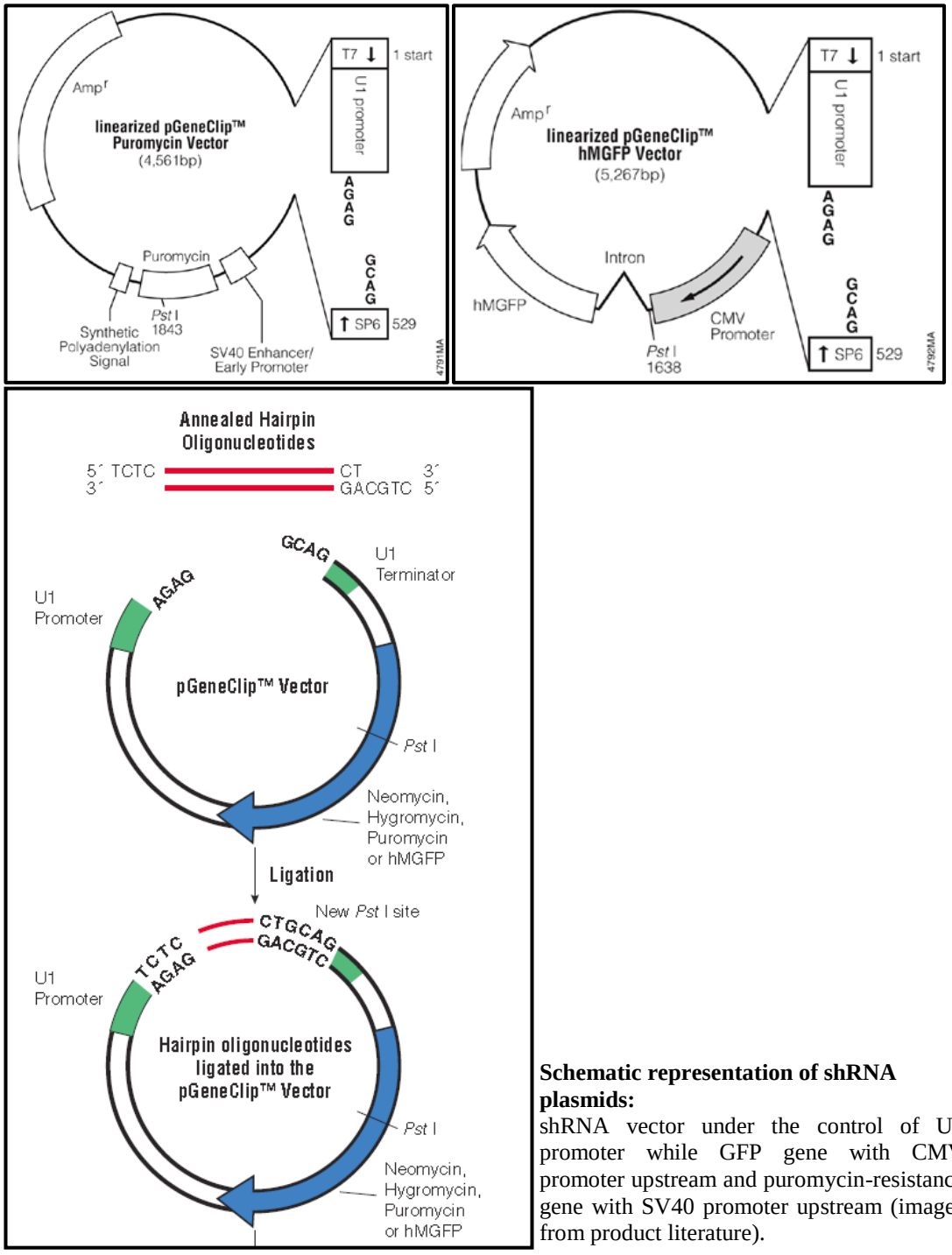

Schematic representation of shRNA plasmids:
shRNA vector under the control of U1 promoter while GFP gene with CMV promoter upstream and puromycin-resistance gene with SV40 promoter upstream (images from product literature).

GFP-expressing plasmids were used during optimisation steps given the ability to check transfection efficiency and KD efficacy in a relatively short period. Once the optimal conditions were achieved, plasmids containing puromycin-resistance gene were used for stable 5T4 KD.

2.5.2.1 Plasmid Preparation for Transfection

Plasmids were supplied in transformation grades and therefore they were first amplified in bacteria for storage and transfecting cell lines. This was performed according to suppliers' instructions (SureSilencing^{TM} shRNA Plasmids; Ref:1019A). This included two steps: plasmid amplification using *E.coli* transformation and plasmid purification. The same steps were performed in preparing GFP-expressing plasmids and plasmids containing puromycin-resistance gene.

2.5.2.1.1 Plasmid Amplification

Plasmid were shipped on ice, 1 µl of each plasmid solution was mixed with 100 µl competent DH5α *E.coli* (Invitrogen; 18258-012) and incubated on ice for 30 minutes. Then cells were heat-shocked for 45 seconds at 42˚C to be placed back on ice for 2 minutes. 250 µl S.O.C. medium (Invitrogen; 15544-04) was added to each tube, mixed by gentle tumbling and incubated at 37˚C with gentle shaking for 1 hour. 300 µl of each transfection mixture was pipetted on LB agar plate supplemented with ampicillin to a final concentration of 50 µg/ml, spread evenly and incubated overnight upside down at 37˚C. The following day, a single, smooth-edged colony was picked with a sterile glass rod for each plasmid; mixed with 2 ml LB medium with ampicillin (50 µg/ml) and incubated with shaking (200 rpm) for four hours at 37˚C till turbidity was first observed in the tubes. 200 µl of transfected *E.coli* was then mixed with LB medium with ampicillin (50 µg/ml) in a 500 ml sterile flask, incubated overnight with shaking (200 rpm) at 37˚C.

2.5.2.1.2 Plasmid Purification

QIAGEN-tip 500 (Ref: 10063) was used according to its instructions to purify plasmids. Briefly; *E.coli* culture media were centrifuged at 6000 g for 15 minutes at 4˚C (4K15 LaborZentrifugen, Sigma). The bacteria pellet was then suspended in 4 ml Buffer P1 (provided in the kit) supplemented with RNase A (provided in the kit); then 4 ml Buffer P2 (provided in the kit) was added to the mixture in a sealed tube, mixed thoroughly and incubated at room temperature for 5 minutes. Then 4 ml ice-cold Buffer P3 (provided in the kit) was added, mixed thoroughly and incubated on ice for a further 5 minutes.

The final mixture was then centrifuged in polypropylene tubes at 20000 g for 30 min at 4˚C. The supernatant was then removed promptly and centrifuged again at 20000 g for

15 min at 4˚C. Subsequently it was equilibrated in a QIAGEN-tip 500 by applying 4 ml Buffer QBT (provided in the kit), and allowing the columns to empty completely by gravity. QIAGEN-tips were then washed twice in 10 ml of Buffer QC (provided in the kit) before plasmids were eluted with 5 ml Buffer QF (provided in the kit). Plasmids were then precipitated by adding 3.5 ml isopropanol (0.7 volumes, room temperature), mixed and centrifuged at 15000 g for 30 minutes at 4˚C. The supernatant was decanted and pellets were then washed with 2 ml of ethanol (70%, room temperature), and centrifuged at 15000 g for 10 minutes. The supernatant was decanted and the pellets were air dried for 10 minutes, and then re-dissolved in Tris-EDTA (TE) buffer (Signa, 93283).

Plasmid concentration was then determined using Nanodrop device (Thermo scientific) according to manufactures instructions, and plasmid stored at -20˚C for later transfection use.

2.5.2.2 Optimisation Steps Using GFP-Expressing Plasmids

The optimisation experiments sought to evaluate several variables such as cell density, transfection medium, transfection reagent, and reagent/DNA ratio. The aim was to determine conditions which provided low cell toxicity with a reasonable transfection efficiency (the proportion of cells expressing GFP) and best knockdown efficacy (reduction in 5T4 expression).

Knockdown ratio is another variable considered during optimisation steps. The total knockdown ratio (TKR) is defined as the proportion of cells in which 5T4 expression is successfully knocked down out of all transfected cells while specific knockdown ratio (SKR) refers to the proportion of cells in which 5T4 expression is successfully knocked down out of cells expressing GFP. This discrepancy between transfection and knockdown results from the fact that shRNA is expressed under a different promoter from the marker gene (GFP or puromycin) in the used plasmids.

Two colour flow cytometry after staining for 5T4 using AF546-tagged goat secondary antibody (Invitrogen; A-21123) was used to evaluate transfection efficiency (GFP expression) and 5T4-knockdown efficacy (AF546).

Preliminary work with the plasmids revealed that plasmid clone 3 resulted in the best knockdown efficacy; therefore it was used, along with the control clone, during optimisation to evaluate the different methods. However, once optimal conditions were determined all clones were used and results were in keeping with clone 3 being the most efficacious in knocking down 5T4 expression.

The methodology during experimentation is summarised here however it is described in detail later in this chapter. Briefly, cells were seeded at the desirable density in 6 well plates (Corning Life Sciences; 3516), 36 hours later transfection reagent prepared according to the manufactures' instructions, was added and mixed with the selected plasmid. Cells then were incubated for the desirable period which varied with different methods before changing media to complete growth media and the cells then were harvested after specific periods, stained for surface 5T4 and assessed by flow cytometry for transfection efficiency (GFP expression) and KD efficacy (5T4 expression).

2.5.2.2.1 Preparing Cells:

SKOV-3 cells were obtained during log-growth phase and cultured in 6 well cell culture plates (Corning Life Sciences; 3516) at $150x10^3$ cells/2ml a well in complete growth media. This concentration was used since it was found after preliminary optimisation experiments to provide cells at 70% confluence after 36 hours.

2.5.2.2.2 Choosing Transfection Reagent

Several transfection reagents were used to determine the best methodology in knockdown experiments. These are Transit-2020 (Mirus; MIR5400), Lipofectamine LTX (Invitrogen; 15338-100), FuGeNE 6 (Roche; 11814443001), X-tremeGENE 9 (Roche; 06365787001), and calcium phosphate. At this stage the reagent/DNA ratio recommended by the suppliers for each reagent was used, incubated with cells overnight and cells harvested 24 hours later for analysis **(Figure 2.3-A)**.

2.5.2.2.2.1 Transit-2020

Experiments revealed that Transit-2020 when used at reagent/DNA ratio of 7.5µl/2.5µg, as recommended by the manufactures, caused severe cell toxicity in SKOV-3 cells with very few cells surviving the experiment and therefore its use was ruled out.

2.5.2.2.2.2 Calcium Phosphate

1M $CaCl_2$ (Sigma; C5670) was prepared in double distilled water (ddH2O). Separately, **medium I** was made of 50 ml DMEM; Gibco; 12491-015) with 1.25 ml 1M HEPES (Sigma, H3375) then PH was adjusted to 7.1, **medium II** was made of 50 ml DMEM supplemented with 10% fetal calf serum, with 1.25 ml 1M HEPES then PH was adjusted to 7.9. This established methodology was used at a medium/DNA ratio of 100µl/1µg. 950 µl medium I was mixed with 10 µg plasmid and 50 µl $CaCl_2$, left for 10 minutes at room temperature. Cells growing in 6 well plates at 70% confluence had their media replaced with 200 µl medium II and then 50 µl of medium I/DNA mix was added

and mixed by rocking across the plate. Then it was incubated overnight and medium was changed to complete growth medium the following day.

The transfection efficiency was low using this methodology at 5.1% with only 1.5% cells showing reduction in 5T4 expression **(Figure 2.3-A)**. These results were deemed unsatisfactory and hence the use of calcium phosphate was abandoned in this project.

2.5.2.2.2.3 Lipofectamine LTX

Only 3.3% of cells expressed GFP protein and only 1.2% demonstrated reduction in 5T4 expression **(Figure 2.3-A)**. Clearly this showed very low transfection efficiency when using the recommended reagent/DNA ratio of 2µl/2.5µg; therefore this reagent was not used in this project.

2.5.2.2.2.4 X-tremeGENE 9

This reagent was used at the recommended reagent/DNA ratio of 3µl/1µg. While it was very effective reagent resulting in 67.3% transfection efficiency only 19.4% of SKOV-3 cells showed reduction in 5T4 expression making the specific knockdown ratio to be 28.8% **(Figure 2.3-A)**.

2.5.2.2.2.5 FuGENE 6

FuGENE 6 was used initially at the recommended reagent/DNA ratio of 3µl/1µg. While it was a fairly effective reagent resulting in 17.7% transfection efficiency but it produced the highest specific knockdown ratio (36.2%) among our panel of reagents **(Figure 2.3-A)**.

X-tremeGENE 9 reagent yielded the highest transfection efficiency but the ratio of cells which showed reduction in 5T4 expression (specific knockdown ratio) was higher with FuGENE 6. Therefore, the subsequent optimisation steps aimed at improving transfection efficiency in FuGENE 6.

Figure 2.3: shRNA Transfection Optimisation

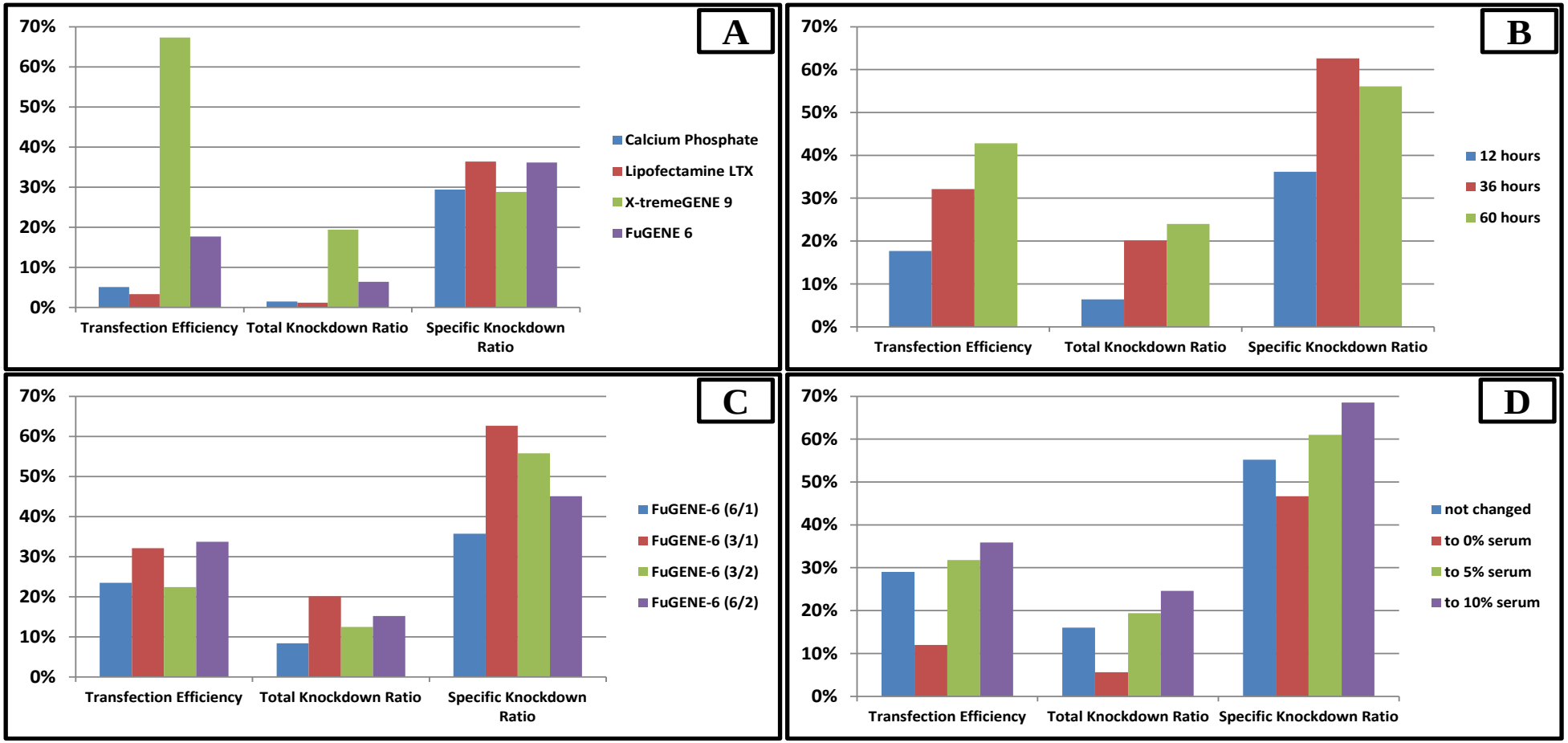

Transfection optimisation experiments in SKOV-3 cells as measured by two colour flow cytometry. Cell count used to calculate the percentage of cells expressing GFP in relation to the total cell number (transfection efficiency) and the percentage of cells with reduced 5T4 expression in relation to the total cell number (total knockdown ratio) or to cells expressing GFP (specific knockdown ratio). **A: selection of transfection reagent.** Several commercially available reagents were evaluated; FuGENE 6 produced the highest specific knockdown ratio, Lipfectamine LTX showed similarly high ratio but on the background of a lower transfection efficiency. **B: the role of incubation time with FuGENE 6 transfection mixture in SKOV-3 cells.** Incubation with the transfection mixture for 36 hours provided the highest specific knockdown ratio. **C: selection of FuGENE 6/DNA ratio in SKOV-3 cells:** 3/1 revealed the highest specific knockdown ratio. **D: changing growth media prior to Transfection** to fresh complete growth media revealed the highest specific knockdown ratio.

2.5.2.2.3 Length of Incubation with FuGene-6 Transfection

The FuGENE 6 reagent/DNA mixture was replaced with complete growth media after 12, 36 or 60 hours. As shown in **Figure 2.3-B**; incubation for 60 hours resulted in higher percentages of cells expressing GFP (42.8%) and showing reduction in 5T4 expression (24%) in comparison to incubation for 36 hours (32.1%, 20.1% respectively) or 12 hours (17.7%, 6.4% respectively). However, the specific knockdown ratio when incubation was limited to 36 hours was higher (62.6%) when compared to incubation for 12 or 60 hours (36.1 and 56.1% respectively). Therefore, cells were incubated with transfection mixture for 36 hours prior to replacing media in this project.

2.5.2.2.4 FuGENE 6/DNA Ratio

All previous optimisation steps were performed using a FuGENE 6 reagent/DNA ratio of 3µl/1µg as recommended by manufactures. Therefore, several other ratios were evaluated: 6µl/1µg, 3µl/1µg, 3µl/2µg and 6µl/2µg. The same steps detailed above were followed including incubation with transfection mixture for 36 hours. 3µl/1µg ratio demonstrated to be the most effective one as shown in **Figure 2.3-C** as it resulted in the higher specific knockdown ratio.

2.5.2.2.5 Pre-Transfection Conditions

Transfection was initially performed at 70% confluence of SKOV-3 cells seeded at $150x10^3$ density without changing growth media. However, this was compared to changing growth media, just prior to adding FuGENE 6 transfection mixture, to one supplemented with 10% serum, 5% serum or no serum. Replacing with complete growth medium prior to transfection improved both transfection efficiency and specific knockdown ratio **(Figure 2.3-D)**; therefore this was included in the subsequent experiments.

The overall conclusion from using GFP-tagged clone 3 shRNA was that cells should be used at confluence of 70% with changing media to fresh complete growth media and using a FuGENE 6/DNA ratio of 3µl/1µg with incubation for 36 hours **(Figure 2.4)**. These findings were then used to perform knockdown using puromycin-resistance gene containing plasmids.

2.5.2.2.6 Puromycin Effective Concentration

Cell lines have different levels of resistance to antibiotics; therefore prior to transfection, the minimum puromycin concentration required to kill untransfected cells was determined. This was done by exposing SKOV-3 cells to several concentration levels of puromycin as recommended by the manufacturers of the knockdown kit (SABiosciences,

1019A). Puromycin dihydrochloride (Sigma, P9620) was diluted in sterile distilled water and stored at concentration 100 µg/ml at -20˚C. To establish transfection dose of puromycin (this is the concentration during transfection experiments), SKOV-3 cells were seeded in a 6 well plate (Corning Life Sciences; 3516) at the same density used for transfection and when they reached 25% confluence (the level at which puromycin would be added after transfection), growth media in each well were changed to fresh ones supplemented with puromycin at one of the following final concentrations: 10 µg/ml, 8 µg/ml, 6 µg/ml, 4 µg/ml, 2 µg/ml, 1 µg/ml or 0 µg/ml.

Figure 2.4: 5T4 Knockdown Using GFP-tagged shRNA

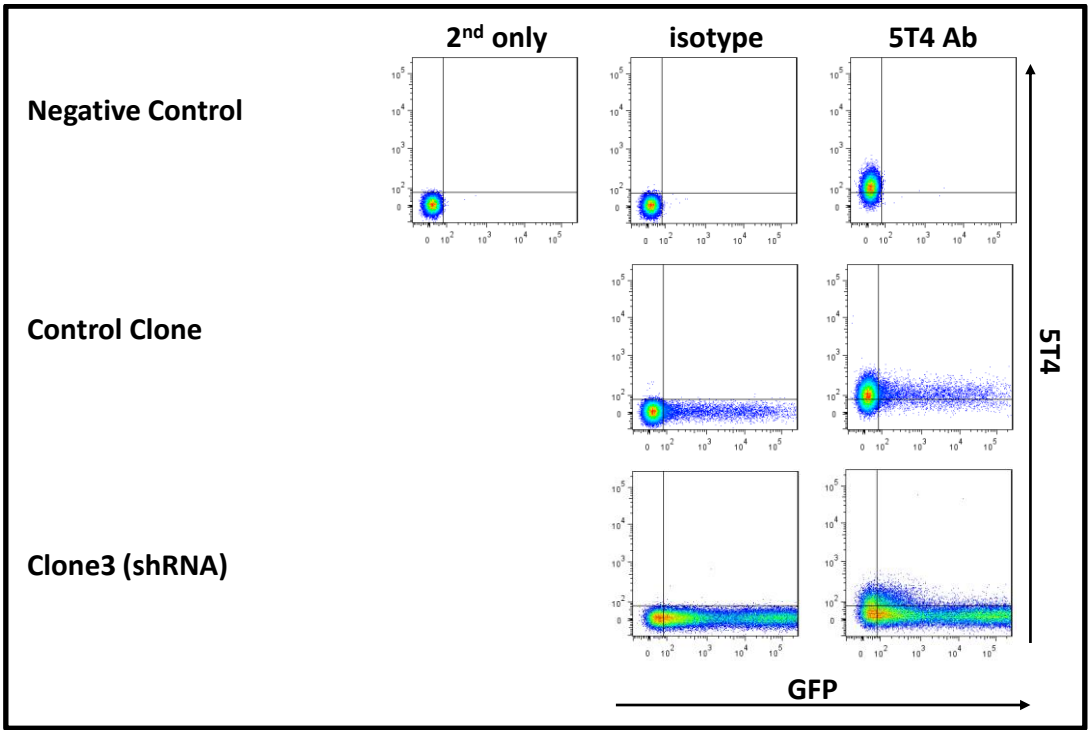

Double staining flow cytometry of optimisation experiments of 5T4 knockdown in SKOV-3 cells using GFP-tagged shRNA plasmid. 5T4 expression remains high in spite of a successful transfection as judged by GFP expression.

Puromycin at 2 µg/ml was found to be the minimum concentration which killed all untransfected SKOV-3 cells within 72 hours while the well without puromycin reached full confluence; therefore this dose was used subsequently in the transfection experiments **(Figure 2.5)**.

It is recognised that lower levels of antibiotics are required if added to cells at the seeding time; therefore the maintenance dose of puromycin was established by adding puromycin at one of the following final concentrations in the growth media at the time of seeding cells: 2 µg/ml, 1 µg/ml, 0.5 µg/ml or 0 µg/ml. This revealed that the maintenance dose of puromycin required for SKOV-3 culture is 1 µg/ml.

Figure 2.5: Selection of Puromycin Effective Concentration

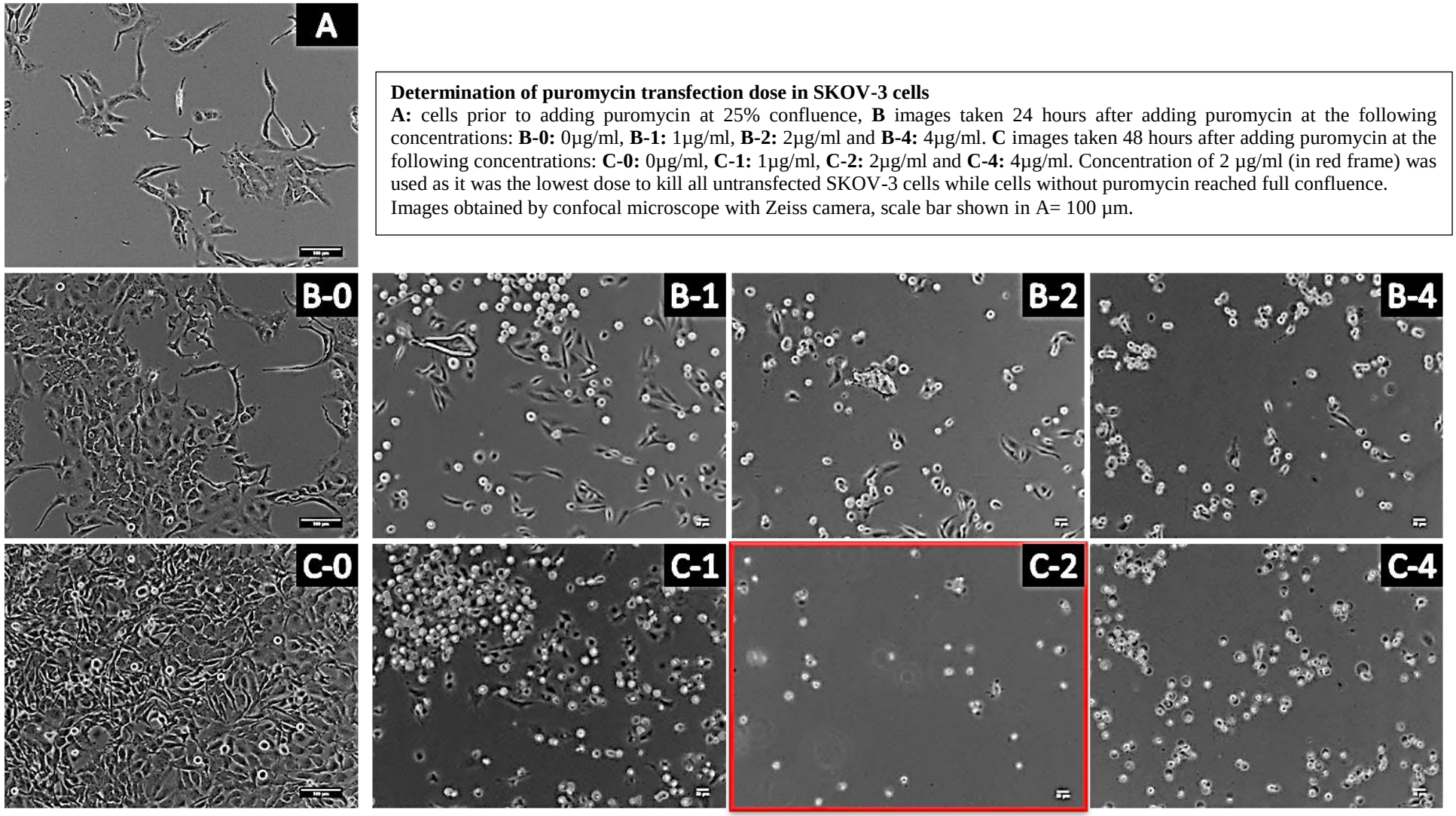

Determination of puromycin transfection dose in SKOV-3 cells
A: cells prior to adding puromycin at 25% confluence, **B** images taken 24 hours after adding puromycin at the following concentrations: **B-0:** 0µg/ml, **B-1:** 1µg/ml, **B-2:** 2µg/ml and **B-4:** 4µg/ml. **C** images taken 48 hours after adding puromycin at the following concentrations: **C-0:** 0µg/ml, **C-1:** 1µg/ml, **C-2:** 2µg/ml and **C-4:** 4µg/ml. Concentration of 2 µg/ml (in red frame) was used as it was the lowest dose to kill all untransfected SKOV-3 cells while cells without puromycin reached full confluence. Images obtained by confocal microscope with Zeiss camera, scale bar shown in A= 100 µm.

2.5.2.3 Transfection

As concluded from the optimisation experiments, SKOV-3 cells were seeded in 6 well plates (two plates) at $150x10^3$ cell/200µl/well and incubated until 70% confluence was reached when the growth media were changed to fresh complete growth media.

Six tubes were prepared where each tube contained 3 µl FuGene-6 was diluted in 97 µl Opti-MEM I reduced serum medium (Gibco; 31985) and incubated at room temperature. Then 1 µg DNA of each shRNA plasmid (four KD clones and one control clone) was added to each FuGene-OptiMEM tube while one tube was left without plasmid to serve as the mock transfection control.

The transfection mixture now containing FuGene-plasmid complex was mixed thoroughly and incubated at room temperature for 30 minutes. The content of transfection mixture tubes were added drop wise to wells of one plate while the other one left untransfected to serve as a control for cell toxicity. The plates rocked gently to mix the mixture with the newly added fresh medium, then returned to the incubator. After incubating SKOV-3 cells with the transfection mixture for 36 hours (as established in the optimisation experiments), cells were trypsinised and seeded at a density of 25% confluence ($250x10^3$ cell/well). Two plates were made where puromycin (final concentration 2 µg/ml) was added to wells in one plate whilst the other plate served as a control.

All cells in the puromycin-free plate grew at the expected rate, whilst cells in the plate where puromycin was added showed cell death; suggesting toxicity to the untransfected cells. All cells in the well with mock transfection died after 72 hours as expected**.**

Subsequently, cell colonies were allowed to grow, growth media were replaced every 2-3 days whilst maintaining puromycin concentration at 2 µg/ml. After ten days selected transfected cells were established when they were expanded to be subsequently analysed for 5T4 expression. Cells were sorted for the lowest 5T4 expression using FACS as detailed earlier in this chapter. Aliquots of transfected cells from all plasmids were stored in freezing media for later use and kept in liquid nitrogen.

2.6 5T4 Overexpression in Hoc-8 Cells

Hoc-8 cell line was found in this project to lack 5T4 expression, therefore it was chosen to investigate the effect of 5T4 neo-expression on cell phenotype and functional properties.

5T4 overexpression in Hoc-8 cells was performed in our laboratory by Dr B Thomas as detailed in her PhD thesis[258]. Briefly, full length 5T4 cDNA was cloned into a constitutive expression vector under CMV promoter which contained neomycin resistance gene to enable selection for stable expression. An empty vector was used as negative control. Subsequently cells were cultured at dilution of 0.5 cell / well and single colonies were chosen and analysed for 5T4 expression. Cells from one colony with high 5T4 expression were chosen in this project (termed Hoc-5T4), whilst parental cells (Hoc-8) were used for comparison.

2.7 Immunohistochemistry in Primary Human Tissues

This study was approved by the North West 8 Research Ethics Committee (REC reference number: 10/H1013/66, **Appendix 2**). It received the approval of the Research and Development Department of Central Manchester University Hospitals NHS Foundation Trust and it was sponsored by the University of Manchester. Under this ethics approval it was possible to collect samples from patients treated at Central Manchester Hospitals and to acquire samples from BRC Biobank allocated in Central Manchester Hospitals.

In total 11 paired ovarian cancer specimens and five normal ovarian samples were stained by immunohistochemistry (IHC) using Leica BOND-MAX robotic platform (Leica BIOSYSTEMS) utilising Bond Polymer Refine Detection kit (Leica, DS9800). Bond Polymer Refine Detection is a biotin-free, polymeric horseradish peroxidase (HRP)-linker antibody conjugate system for the detection of bound primary mouse or rabbit antibodies. This detection system avoids the use of streptavidin and biotin, and therefore it could eliminate non-specific staining caused by endogenous biotin.

Formalin-fixed paraffin-embedded (FFPE) tissues were cut on acquisition into 5 µm sections, mounted on glass slides (Thermo scientific, 10144633). Sections were then preserved in a thin layer of wax and kept at room temperature for later use when all samples were available for staining. Thus all samples were stained at the same time for any given antibody, which reduced any potential variation that could have been caused by multiple experiments.

Tissue sections were assigned codes so the researcher was blinded during staining and scoring to whether a tissue section was primary or secondary cancer; this gave more credibility and robustness to the results.

2.7.1 Optimisation Steps

Given the automated nature of BOND-MAX platform, there were generally two main optimisation steps required, the epitope retrieval (ER) method and primary antibody concentration.

Primary antibodies were diluted in Bond dilution solution. It was anticipated that the required concentration is considerably lower than that recommended for traditional methods of immunohistochemistry (IHC). Several concentrations were tested for each antibody ranging around 1/10 of the suppliers' recommended concentration. BOND-MAX uses a supplied solution for ER, optimisation steps aimed at defining the time and PH. For

all antibodies 20 minutes was used with both PH 6 and PH 9 with each tested concentration at 98˚C. For each antibody the optimal concentration with PH 6 was used if it was effective, otherwise the optimal concentration with PH 9 was chosen.

2.7.2 Experimental Steps

For each experiment, data of the number of sections to be stained, the required epitope retrieval method, the primary antibody and its concentration, and the matched isotype were entered to software program of Leica BOND-MAX robotic platform. These data were determined previously during optimisation steps. BOND-MAX then created a protocol specific to that experiment and generated printed adhesive labels to be used on slides.

Tissue sections preserved in thin wax layer were baked at 60˚C for 15 minutes while maintained on side to allow wax to drop. Slides were then labelled with the labels generated by BOND-MAX when programmed for the relevant staining experiment. Slides were then placed in the robotic arms, secured in the platform and the robot was started to commence staining.

The automated platform then followed the created protocol. This, briefly, included dewaxing of tissue sections with Bond dewax solution, hydrated with decreasing concentration of alcohol then washed with Bond wash solution. Bond epitope retrieval (ER) solution then was added at the predetermined PH (6 or 9) for 20 minutes then washed with Bond wash solution. Sections were then incubated with hydrogen peroxide to block endogenous peroxidase activity and then washed with Bond wash solution. Primary antibody or matched isotype then was applied diluted in the supplied dilution solution for 15 minutes. Sections were then washed and Post Primary Reagent was added, washed again before adding Polymer solution. Sections were washed again with Bond wash solution and deionised water, mixed DAB (3,3'-Diaminobenzidine) Refine solution was then added. Sections were washed with deionised water, haematoxylin was added and finally sections were washed with deionised water followed with Bond wash solution then deionised water. Section samples were also stained with haematoxylin and eosin (H&E).

Sections were then removed from the robotic platform, manually dehydrated through increasing concentrations of alcohol, immersed in xylene and coverslips were mounted manually. Slides were allowed to dry and then were scanned with Leica SCN400 slide scanner (Leica Microsystems). Images were then stored and viewed with SlidePath Gateway LAN software (Leica Microsystems).

Table 2.7 contains a list of all primary antibodies used in IHC with the concentration and epitope retrieval method. There was no need to use secondary antibodies as Bond Polymer refine Detection kit (Leica, DS9800) was used. Isotype controls were all provided by DAKO, mouse monoclonal IgG1 (X0931), mouse monoclonal IgG2a (X0943), mouse monoclonal IgG2b (X0944), and rabbit polyclonal IgG (X09336).

Table 2.7: Primary Antibodies Used in IHC

Target	Type	Supplier	Reference	Clone	Concentration	Epitope retrieval
5T4	Mouse IgG1	R&D Systems	MAB4975	524731	1 µg/ml	PH 9
CXCR4	Rabbit monoclonal IgG	Abcam	Ab124824	UMB2	2.34 µg/ml	PH 6
CXCR7	Mouse IgG1	MBL	K0223-3	9C4	4 µg/ml	PH 6
Cytokeratins	Rabbit polyclonal IgG	Abcam	Ab9377	Anti-wide spectrum	2 µg/ml	PH 9
E-cadherin	Mouse IgG2a	Invitrogen	13-5700	SHE78-7	4 µg/ml	PH 6
Vimentin	Mouse IgG1	Leica Biosystems	VIM-V9-L-CE	V9	0.06 µg/ml	PH 6
N-cadherin	Mouse IgG1	BD Biosciences	BD610920	32/N-cadherin	1.25 µg/ml	PH 6
B-catenin	Mouse IgG1	BD Biosciences	BD610154	14/Beta-Catenin	0.125 µg/ml	PH 6
Dkk-1	Mouse IgG2b	R&D Systems	MAB10962	141135	1.5 µg/ml	PH 9
JNK	Rabbit poly IgG	R&D Systems	AF1387		10 µg/ml	PH 9
pJNK	Rabbit poly IgG	R&D Systems	AF1205		2 µg/ml	PH 9

A complete list of primary antibodies used in immunohistochemistry in this study[259, 260].

2.7.3 IHC Scoring

Once staining of all tissue sections with all studied antibodies and corresponding isotypes was completed, they were scanned under the same settings to allow comparison between slides. Images were then stored and viewed with SlidePath Gateway LAN software. A semi-quantitative method [261-263] was then used to score staining as detailed in chapter 7 which includes a working example. Data was processed using SPSS to probe statistical significance; the paired t test was used when comparing results obtained from the same patient such as comparing scoring of primary cancer with that of metastatic samples, or comparing normal ovarian surface epithelium to epithelium of ovarian clefts. Otherwise, the independent (two sample) t test was used to compare unrelated samples and the X^2 test was used for changes in the staining between primary and secondary tumours.

2.8 Chapter Discussion

The aims of this project as set out in the introduction chapter were explored in established cell lines and primary human tissues. The methodology was broadly concerned with probing protein expression and cell motility functional assay. A detailed discussion of the advantages and limitations of the methodology is presented in the final chapter of this report.

The following result chapters present the data obtained in this project starting with the selection of cell lines and phenotype characterisation.

Chapter 3

RESULTS:

Cell Phenotype and Chemotactic Response

Phenotype Characterisation and Chemotactic Response in Ovarian Cancer Cell Lines

3.1 Aim

To identify epithelial ovarian cancer cell lines which express both 5T4 and CXCR4 and to investigate a chemotactic response to CXCL12 in these lines.

3.2 Introduction

5T4 expression has been previously found to correlate with clinical outcome and cancer stage in epithelial ovarian cancer (EOC)[14]. It is not clear, however, if 5T4 has a functional role in the spread of EOC *in vitro*.

Previous work has suggested a role for 5T4 in the functional expression of CXCR4 on cell surface in murine embryonic stem (mES) cells[25] and demonstrated a reduction in *Cd26* transcript during mES cells differentiation which accompanied neo-expression of 5T4. CXCR4 is a receptor for CXCL12 and CD26 is known to inactivate CXCL12 by proteolysis[144]. In addition, CXCR7 has been uncovered as a CXCL12 receptor[148]; response through CXCR7 is thought to primarily promote cell growth while CXCL12 activation of CXCR4 can lead to chemotaxis. However, these observations were not investigated in adult human ovarian cancer cells in terms of expression or functional relationship. This is explored in this chapter.

3.3 5T4 Expression and Phenotype of EOC Cell Lines

Three EOC cell lines were chosen initially to determine cell phenotype; these were SKOV-3, Caov-3 and OVCAR-3. These cell lines were chosen as they were commonly investigated in the relevant literature[264]. In addition, preliminary data in our laboratory suggested a chemotactic response in SKOV-3 cells toward CXCL12.

Flow cytometry (FC) on live cells was used to investigate the surface expression of 5T4, CXCR4, CXCR7 and CD26. All three cell lines were found to express 5T4 **(Figure 3.1)**; SKOV-3 and Caov-3 showed equal expression levels as measured by median fluorescence intensity ratios (MFIR), 12 and 11.8 respectively; while OVCAR-3 expression was approximately half of that (MFIR= 6.5).

Figure 3.1: EOC Cell Lines Phenotype

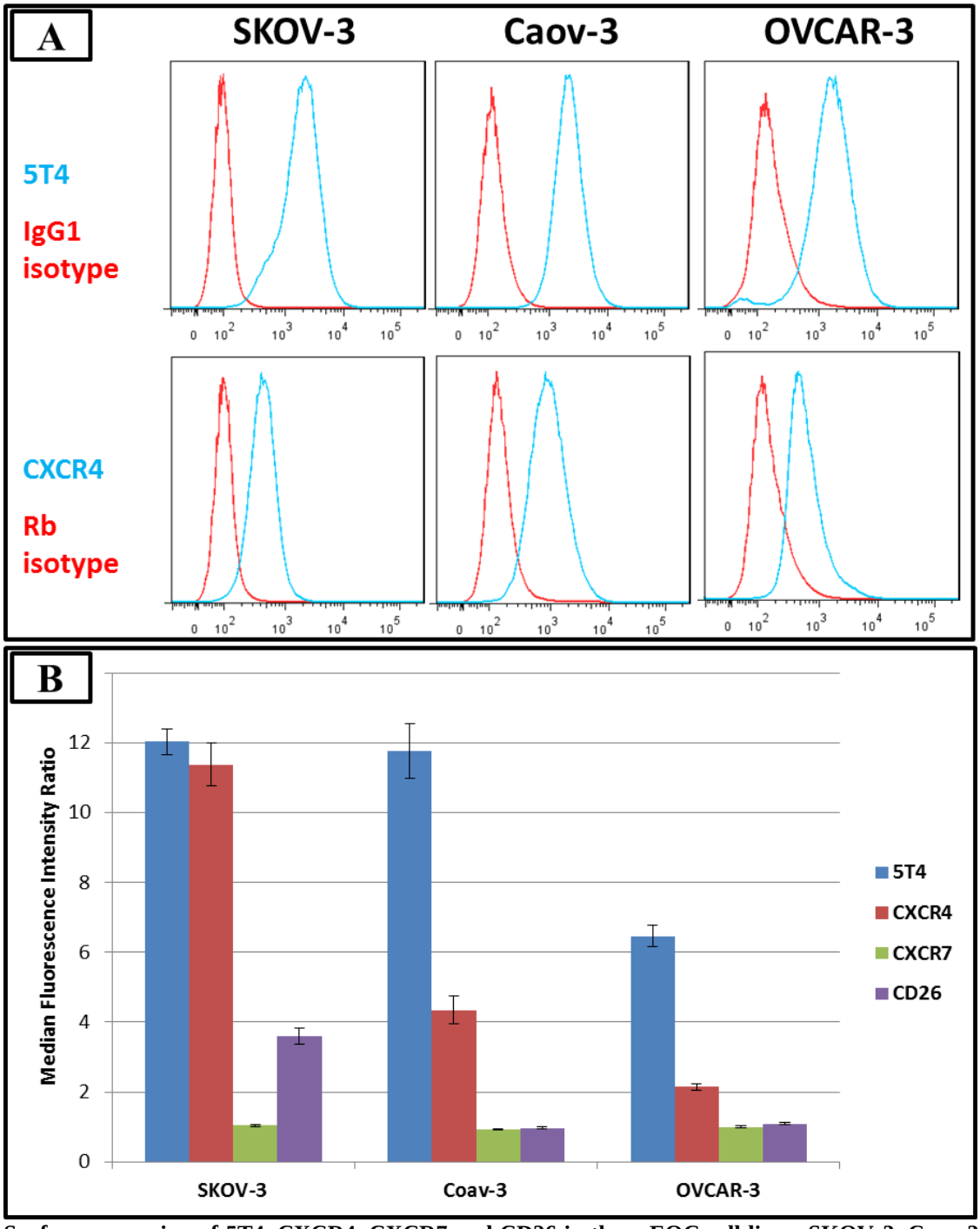

Surface expression of 5T4, CXCR4, CXCR7 and CD26 in three EOC cell lines: SKOV-3, Coav-3 and OVCAR-3 as measured by flow cytometry

A: Flow cytometry results of a representative experiment of the surface expression of 5T4 and CXCR4 in SKOV-3, Caov-3 and OVCAR-3. **B:** Results represent average MFIR obtained by flow cytometry of three independent experiments each included analysis of $25x10^3$ cells. OVCAR-3 expressed less 5T4 than the other two cell lines, while SKOV-3 expressed more CXCR4 and was the only cell line to express CD26. None of these cells expressed CXCR7 (MFIR=1). Error bars = standard error of mean (SEM).

SKOV-3 cells expressed the highest levels of surface CXCR4 followed by Caov-3 and OVCAR-3 (MFIR: 11.4, 4.4 and 2.2 respectively). SKOV-3 expressed CD26 (MFIR= 3.6) while both Caov-3 and OVCAR-3 were negative (MFIR 1.0 and 1.1 respectively). None of these cell lines expressed CXCR7 (MFIR 1.0, 0.9 and 1.0 respectively).

3.4 Chemotactic Response to CXCL12

Since all these cell lines; SKOV-3, Caov-3 and OVCAR-3 expressed both 5T4 and CXCR4, it was important to investigate if CXCR4 was functional in these cells. Therefore, the chemotactic response to CXCL12 was investigated using FluoroBlok® inserts. These experiments were conducted in triplicates; the top chamber media, which contained the cells, were identical in all experimental conditions (phenol red-free RPMI with 1% FCS). The lower chambers contained media which were: (1) identical to top chamber contents as a control to compare to, (2) supplemented with 10% FCS as a positive control, or (3) supplemented with 100 ng/ml CXCL12.

Results are expressed as migration slopes relative to those in the unsupplemented control condition. SKOV-3 cells showed a chemotactic response to CXCL12 **(Figure 3.2)** where the mean of migration slopes increased from 1368 to 1752 (28% increase, *P=0.02*, paired t test) when CXCL12 was present in comparison with 1% FCS alone. However, both Caov-3 and OVCAR-3 cells did not show chemotactic response toward CXCL12 **(Figure 3.2)**. The mean of migration slopes toward migration media with or without CXCL12 were respectively 330 and 340 (*P=NS*, paired t test) for Caov-3 cells, and 35 and 31 (*P=NS*, paired t test) for OVCAR-3 cells.

SKOV-3 cells were found to express 5T4 and CXCR4 on cell surface, and showed a chemotactic response to CXCL12. Whether the receptor CXCR4 was required for this chemotactic response was subsequently investigated. SKOV-3 cells were incubated with the CXCR4 antagonist AMD3100 (Octahydrochloride; Sigma, A5602) at 1µg/ml for 60 minutes prior to chemotaxis assays; this led to abrogation of the chemotactic response to CXCL12 with no effect on SKOV-3 migration toward 1% serum **(Figure 3.3)**. This demonstrated that SKOV-3 chemotactic response toward CXCL12 is CXCR4-mediated.

Since SKOV-3 was the only cell line in this panel to express CD26 which could cleave CXCL12 inhibiting its effect; diprotin-A (Ile-Pro-Ile) a CD26 inhibitor was tested in SKOV-3 migration assays. SKOV-3 cells were incubated in 10 µM diprotin-A (Sigma, I9759) which was also added to migration media. Diprotin-A did not change SKOV-3 cells chemotactic response to CXCL12 nor did it affect their migration toward 1% serum **(Figure 3.4)**. Therefore diprotin-A was not used in the subsequent experiments on SKOV-3 migration.

Figure 3.2: Chemotaxis in EOC Cell Lines

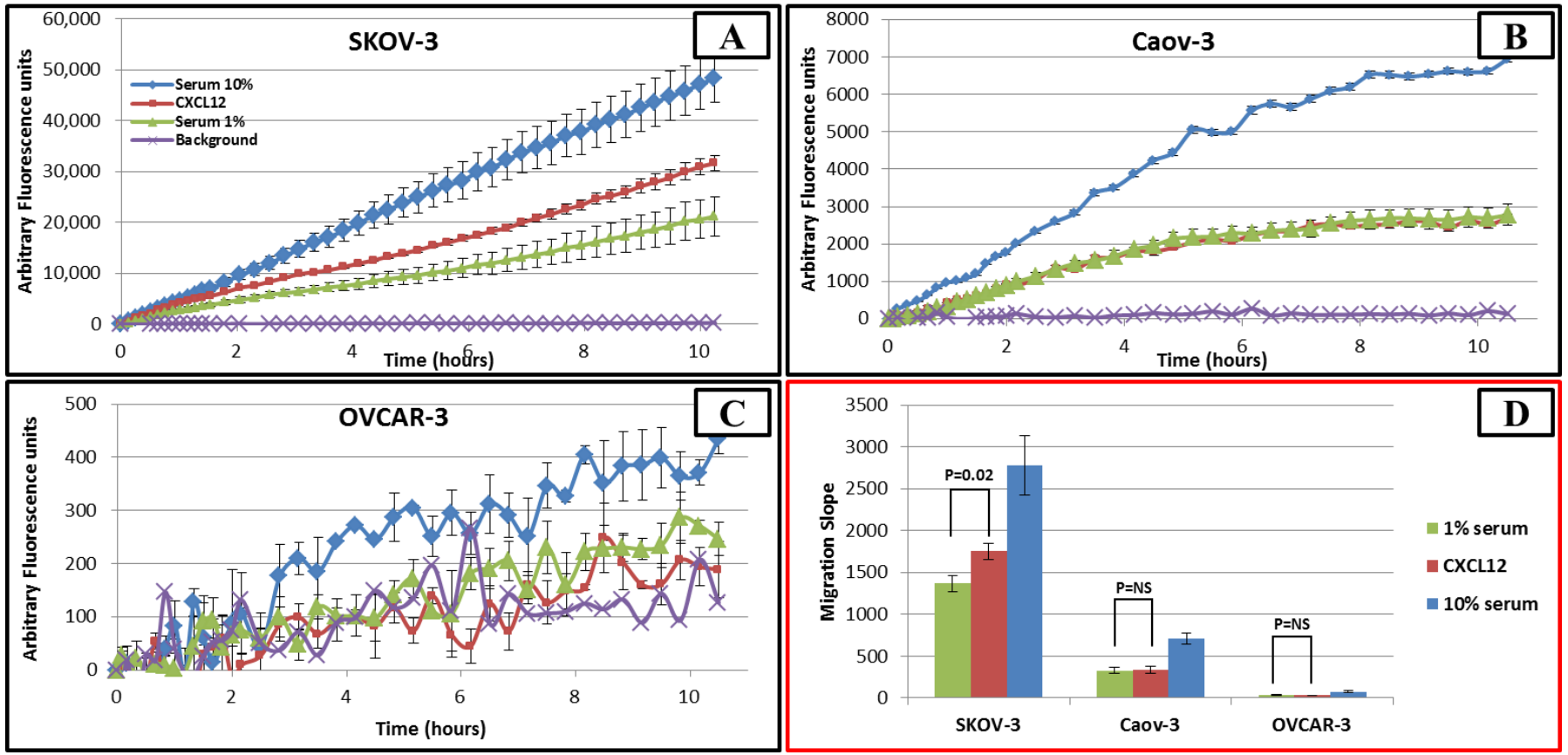

FluoroBlok Chemotaxis assay in SKOV-3, Caov-3 and OVCAR-3 cells.

A: a representative experiment showing a chemotactic response to CXCL12 in SKOV-3 cells *; **B & C**: representative experiments demonstrating the lack of chemotactic response to CXCL12 in Caov-3 and OVCAR-3 respectively*. **D:** quantitative summary graph of three independent experiments showing a chemotactic response in SKOV-3 to CXCL12 but not in Caov-3 or OVCAR-3. A, B and C: Lines show fluorescence intensity values over the experiment period (11hours), values represent average of triplicates, error bars= SEM. Migration slopes were used for comparison. D: Bars represent the averages of three independent experiments of migration slopes over the experiment period, error bars= SEM.

*Fluorescence intensity is measured using arbitrary units which varied between cell lines as a result of several factors (detailed in paragraph 2.4.2.3). In this figure, fluorescence intensity values differed widely necessitating the use of different scales on the y axes to present each cell line data which in turn might give an artificial impression of varying shapes of the data curves. These graphs, therefore, should not be used for direct comparison; instead the migration slopes as in D were used to compare migration results (paragraph 2.4.2.3).

Figure 3.3: Blocking CXCR4 in SKOV-3 Chemotaxis Assay

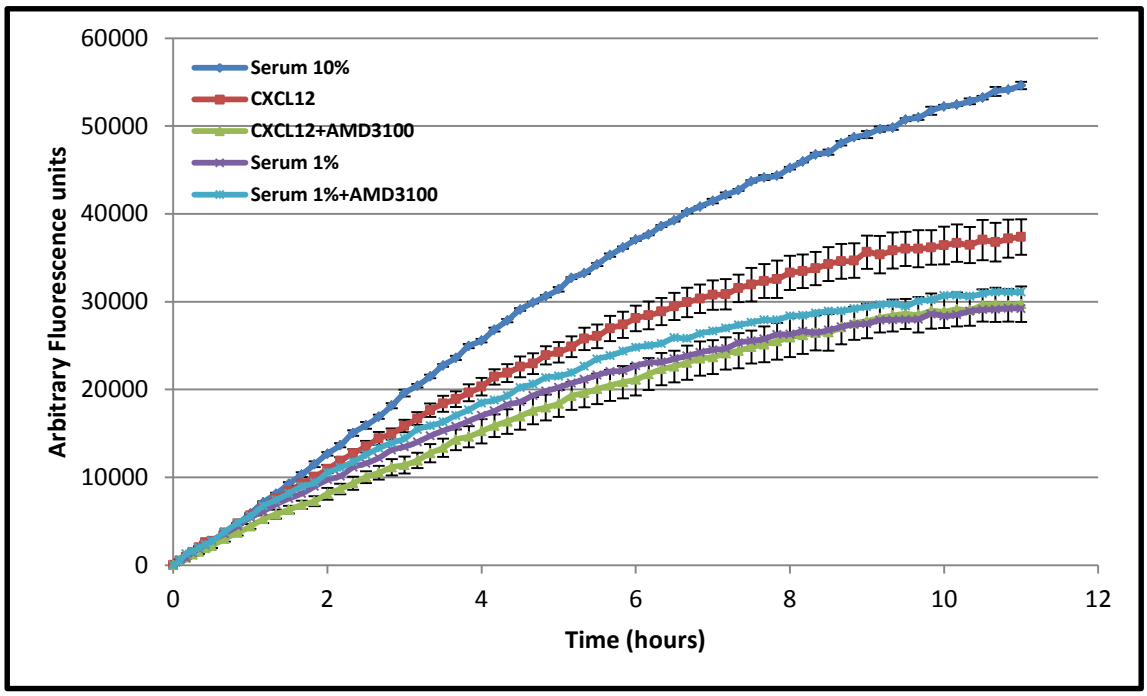

FluoroBlok Chemotaxis assay of AMD3100 role on SKOV-3 migration.
While AMD3100 (a CXCR4 antagonist) did not affect SKOV-3 cells migration toward 1%, cells lost their chemotactic response to CXCL12 when incubated with AMD3100. This supports that SKOV-3 chemotactic response to CXCL12 is CXCR4-mediated. Cells migrated toward 10% serum-supplemented medium as expected, which served as a positive control.
Lines show fluorescence intensity values over the experiment period (11hours), values represent average of triplicates in a representative experiment, error bars= SEM.

Figure 3.4: CD26 Inhibition in SKOV-3 Chemotaxis Assay

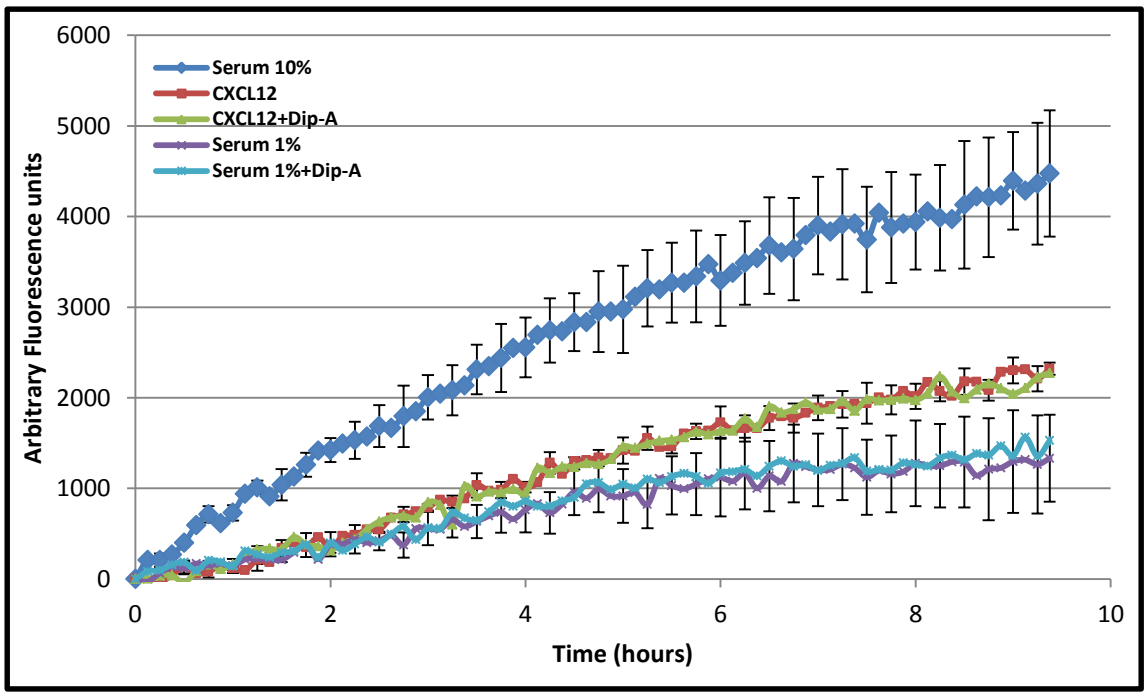

FluoroBlok Chemotaxis assay of diprotin-A in SKOV-3 migration:
A representative experiment showing that diprotin-A did not change SKOV-3 chemotaxis response to CXCL12 or migration toward 1% serum.
Lines show fluorescence intensity values over the experiment period (10hours), values represent average of triplicates, error bars= SEM.

3.5 Additional EOC Cell Lines

The chemotactic response to CXCL12 by SKOV-3 cells was only moderate averaging about 28% increase in migration slope over the basic cell migration toward 1% serum. To explore a functional role for 5T4 in CXCR4/CXCL12 chemotactic response, additional EOC cell lines were searched aiming to obtain cell lines which lacked 5T4 expressions and others which had higher chemotactic response to CXCL12.

OV-90 cell line was established from the aggressive high grade serous cancer and it was anticipated to demonstrate a chemotactic response to CXCL12. TOV-21G cell line was established from an ovarian clear cell cancer and was reported in the literature to express CXCR4. In contrast TOV-112D originated from the less aggressive endometrioid ovarian cancer, and its expression of CXCR4 was reported in the literature to be low. Hoc-8 cell line was established from a high grade serous adenocarcinoma and was found previously to be 5T4 negative by flow cytometry in our laboratory. A2780 cells are known to be reasonably motile and often used in migration assays; the histological type of their original tumour is not clearly documented.

3.5.1 OV-90 Cells

OV-90 cells showed an overall low mean expression of 5T4 (MFIR =1.4), CXCR4 (MFIR = 2.8) and CD26 (MFIR = 1.4) but were negative for CXCR7 (MFIR = 1.1) **(Figure 3.5)**. Initial chemotaxis experiments in this cell line showed no chemotactic response to CXCL12 **(Figure 3.6)**.

Figure 3.5: OV-90 Cell Phenotype

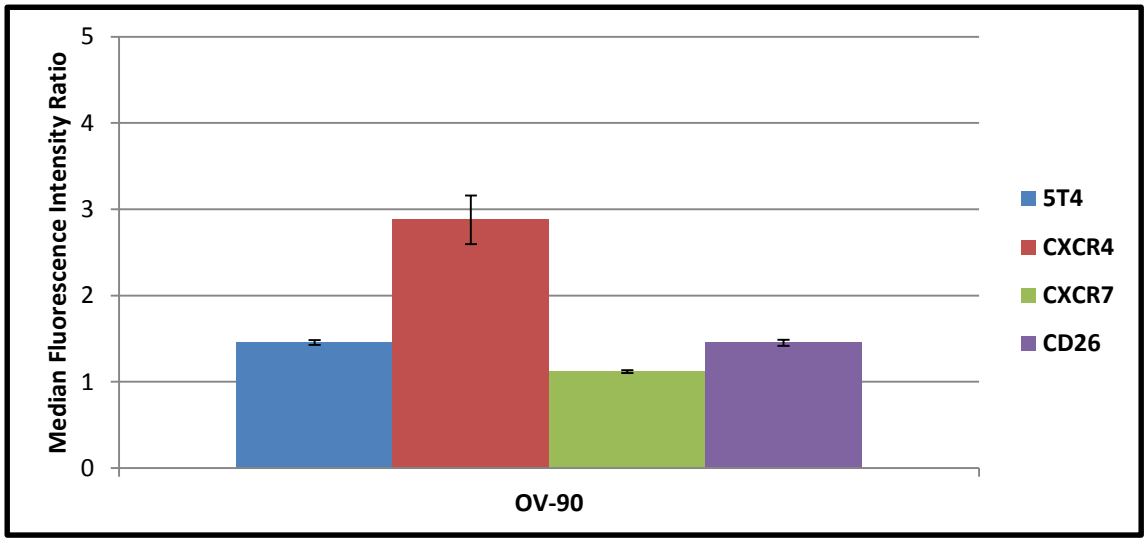

Surface expression of 5T4, CXCR4, CXCR7 and CD26 in OV-90 cells as measured by flow cytometry: Generally OV-90 cells expressed low levels of 5T4, CD26 and CXCR4 and were negative for CXCR7 (see also **Figure 3.7**).
Results represent average MFIR obtained by flow cytometry of three or more independent experiments each included analysis of $25x10^3$ cells, error bar= SEM.

Figure 3.6: Chemotaxis in OV-90 Cells

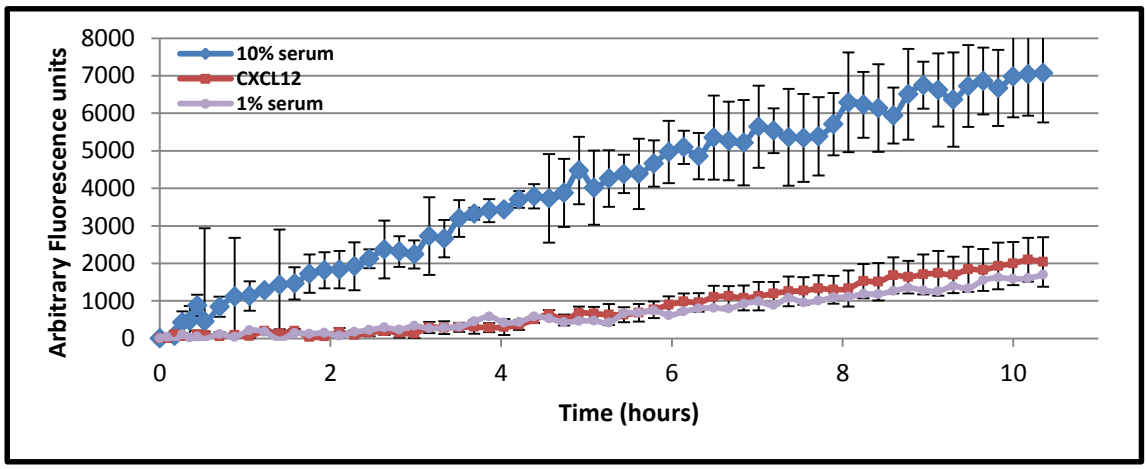

FluoroBlok Chemotaxis assay in OV-90 cells:
A representative experiment showing that OV-90 cells did not respond chemotactically to CXCL12. Lines show fluorescence intensity values over the experiment period (11hours), values represent average of triplicates, error bars= SEM.

However, OV-90 cells were heterogeneous in terms of the surface expression of 5T4 and CXCR4 (bimodal), and 3 sub-groups could be identified when double staining flow cytometry was used **(Figure 3.7-A)**. 35% of OV-90 cells did not express CXCR4 or 5T4, about half expressed CXCR4 but not 5T4 and about 15% of the cells expressed both molecules. Interestingly, very few cells (<1%) expressed 5T4 and did not express CXCR4 **(Figure 3.7-A)**.

These findings indicated that it might be possible to isolate OV-90 cells which lack the surface expression of 5T4 to compare their phenotypic and functional properties with 5T4 positive cells. Therefore, OV-90 cells were sorted according to their 5T4 and CXCR4 surface expression by Fluorescence Activated Cell sorting (FACS) **(Figure 3.7-A)**. Several attempts to isolate CXCR4 negative cells were unsuccessful; however cell populations positive for both 5T4 and CXCR4 (OV-902), cells negative for 5T4 (OV-900), and cells with low 5T4 surface expression (OV-901) were obtained **(Figure 3.7-A)**.

Results from sorted cells showed that OV-900 did not express 5T4 (MFIR = 1.2) but had low levels of CXCR4 (MFIR = 1.7) ($5T4^{-}CXCR4^{low}$). OV-901 showed low levels of 5T4 (MFIR = 1.8) while expressed CXCR4 (MFIR = 3.7) ($5T4^{low}CXCR4^{+}$). However, OV-902 expressed both 5T4 (MFIR = 3.7) and CXCR4 (MFIR = 3.3) ($5T4^{+}CXCR4^{+}$). None of these sorted cell lines expressed CXCR7 (MFIR = 1.0 in all) and only OV-902 expressed CD26 (MFIR = 2.8) **(Figure 3.7-B)**.

Figure 3.7: FACS in OV-90 Cells

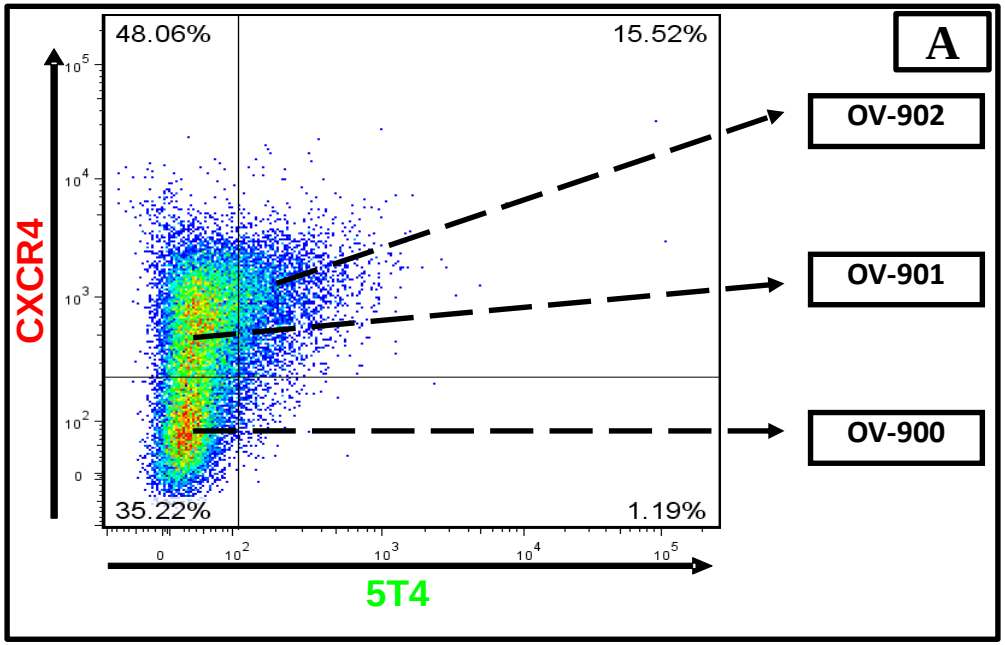

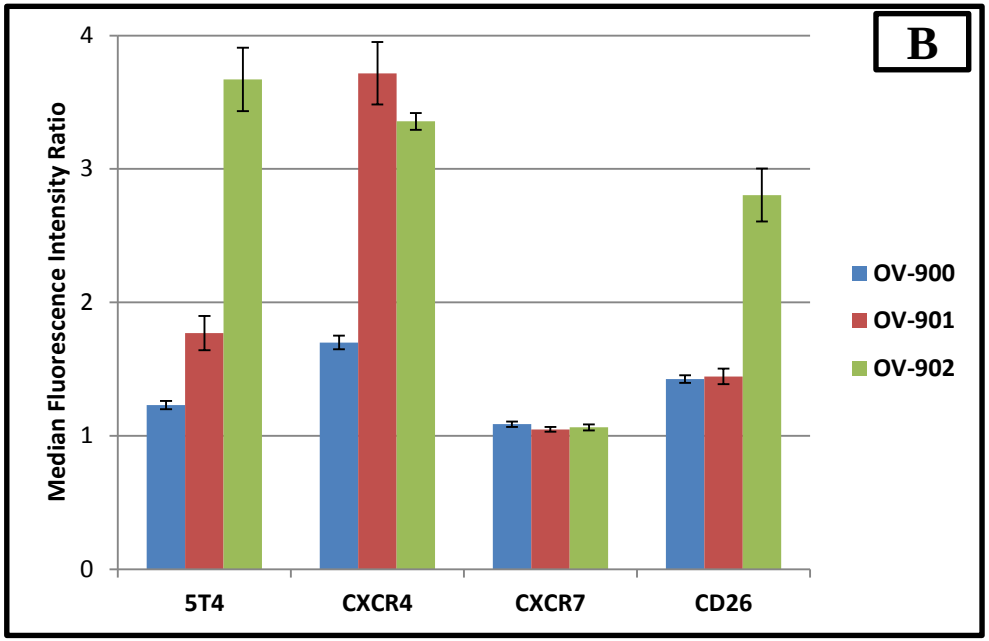

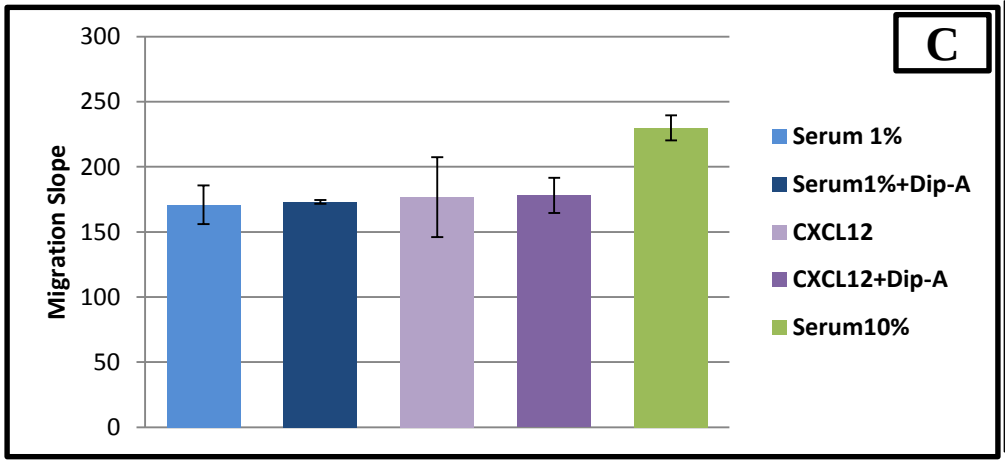

Fig 3.7-A: Surface expression of 5T4 and CXCR4 in OV-90 by two colour flow cytometry. OV-90 showed low levels of both 5T4 and CXCR4 but importantly was the only cell line in our panel to show heterogeneity in the expression of both markers. This cell line was subsequently sorted by FACS into three sub-groups: OV-900, OV-901 and OV-902 according to 5T4 and CXCR4 expression.

Fig 3.7-B: Surface expression of 5T4, CXCR4, CXCR7 and CD26 in sub-populations after sorting OV-90 cell lines as measured by flow cytometry. Results represent average MFIR obtained by flow cytometry of three or more independent experiments each included analysis of $25x10^3$ cells, error bar= SEM.

Fig 3.7-C: FluoroBlok Chemotaxis assay in OV-902 cells. There was markedly low cell motility and migration toward 10% serum, as well OV-902 did not respond chemotactically to CXCL12, incubation with diprotin-A did not improve response to CXCL12. Bars represent the averages of three or more independent experiments of migration line slopes over the experiment period (12hours), error bars= SEM.

Chemotaxis assays in OV-902 cells ($5T4^{+}CXCR4^{+}$) showed, similar to the parental cell line (OV-90), a lack of chemotactic response to CXCL12 where the means of migration slopes toward media with or without CXCL12 were respectively 171 and 177 (*P=NS*, paired t test). Furthermore, incubation with diprotin-A (CD26 inhibitor) did not result in a chemotactic response (migration slope means 177 vs. 178, *P=NS*, paired t test) **(Figure 3.7-C)**.

Conducting further experiments on the sorted cells was hampered by the fact that they were phenotypically unstable, as cells with different molecular phenotypes were generated after several passages **(Figure 3.8).** Noticeably, OV-902 ($5T4^{+}$ $CXCR4^{+}$) produced cells which lacked the expression of both markers and OV-900 ($5T4^{-}$ $CXCR4^{low}$) produced cells which expressed higher CXCR4 levels but remained negative for 5T4.

3.5.2 TOV-112D and TOV-21G Cells

TOV-112D expressed high levels of cell surface 5T4 (MFIR = 21.9) but low levels of surface CXCR4 (MFIR = 2.1); interestingly it expressed relatively high levels of CD26 (MFIR = 8.6) and low levels of CXCR7 (MFIR = 1.7) **(Figure 3.9-A)**. TOV-112D cell lines did not respond to CXCL12, perhaps not surprisingly given the low CXCR4 expression, even when incubated with diprotin-A which inhibits CD26 **(Figure 3.9-B&D)**.

TOV-21G expressed moderate levels of cell surface 5T4 (MFIR = 4.8) and CXCR4 (MFIR = 2.3) but was negative for both CXCR7 (MFIR = 1.0) and CD26 (MFIR = 1.0) **(Figure 3.9-A).** In addition, TOV-21G cells failed to show a chemotactic response to CXCL12 **(Figure 3.9-C&D)**.

3.5.3 A2780 and Hoc-8 Cells

A2780 cells showed cell surface expression of 5T4 (MFIR = 8.9) and CXCR4 (MFIR = 6.7) comparable with SKOV-3 cells. A2780 cells did not express CD26 (MFIR = 1.0) and, like SKOV-3, they did not express CXCR7 (MFIR = 1.0). Chemotactic assays in A2780 cells did not show a chemotactic response to CXCL12 **(Figure 3.10)**.

Hoc-8 cells did not express 5T4, CD26 or CXCR7 and expressed moderate levels of CXCR4 (MFIR: 1.0, 1.0, 1.0 and 3.3 respectively). Chemotactic assays in Hoc-8 cells did not show a chemotactic response to CXCL12 **(Figure 3.10)**.

Figure 3.8: Instability of OV-90 Sub-Type Populations

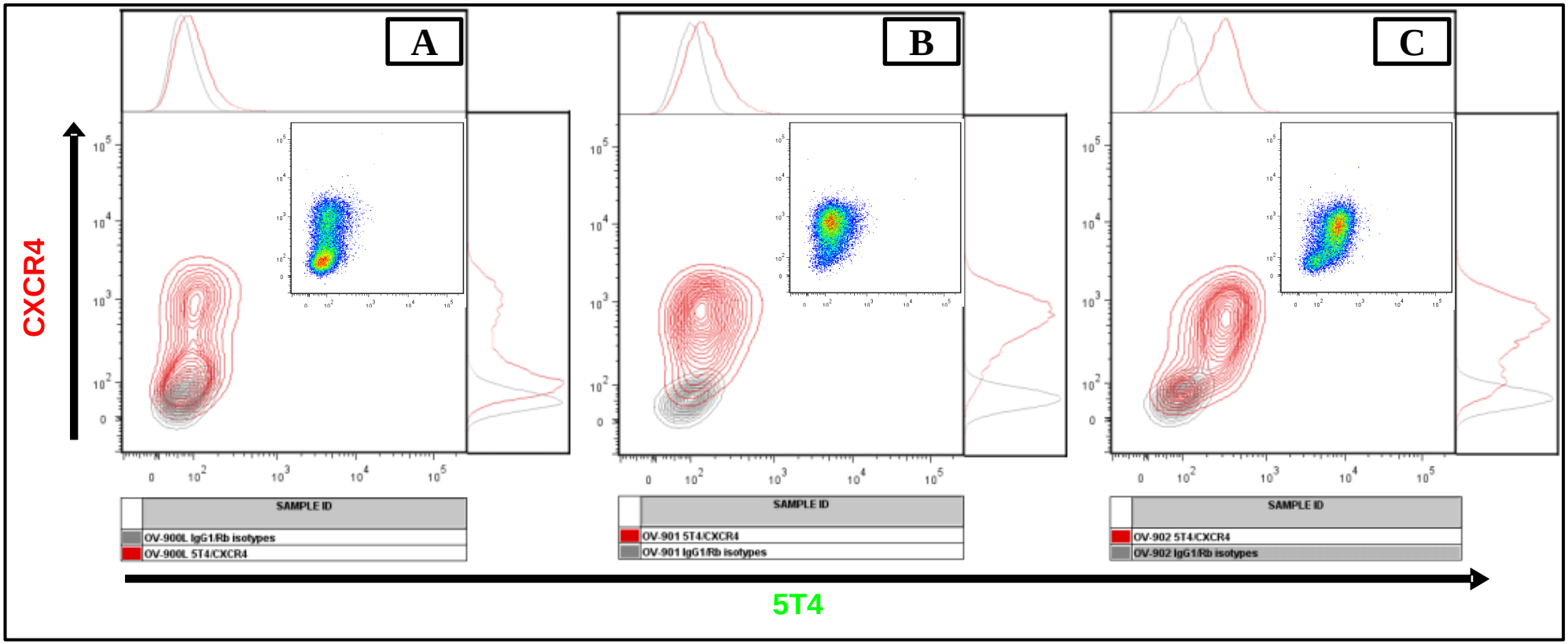

Instability in OV-90s cells by two colour flow cytometry

These three sub-populations which were initially produced from OV-90 cells according to their expression of 5T4 and CXCR4 did not maintain their phenotype and increasingly higher proportion of cells with different phenotype were generated while passaging cells. **A:** OV-900 cells which were originally sorted as $5T4^{-}CXCR4^{low}$ produced cells expressing higher CXCR4 levels. **B:** OV-901 cells which were initially obtained as $5T4^{low}CXCR4^{+}$ generated $CXCR4^{-}$ cells. **C:** OV-902 ($5T4^{+}CXCR4^{+}$) produced cells which lacked the expression of both 5T4 and CXCR4. This data was obtained from cells subjected to five passages from the time of FACS.

Figure 3.9: Phenotype and Chemotaxis in EOC Cell Lines (1)

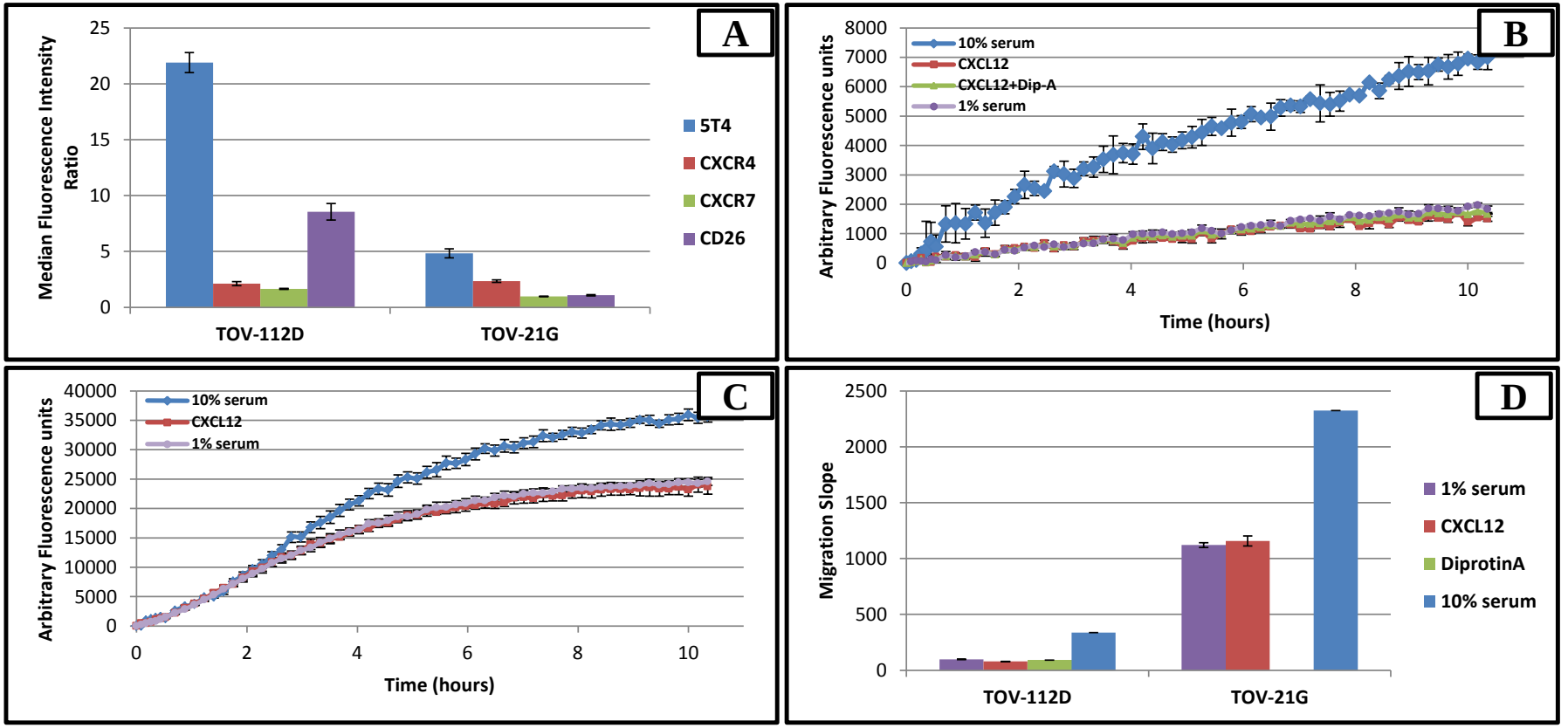

Phenotype and chemotactic response in TOV-112D and TOV-21G cell lines:

A: TOV-112D cells expressed high levels of 5T4 while TOV-21G showed moderate levels. Both cell lines showed low levels of CXCR4. TOV-112D cells expressed high levels of CD26 and were positive for CXCR7; TOV-21G cells did not express CXCR7 nor CD26. **B:** TOV-112D cells migrated in equally toward CXL12 and 1% serum suggesting a lack of chemotactic response as measured by FluoroBlok methodology. Incubation with diprotin-A did not improve response to CXCL12. **C:** similarly TOV-21G cells failed to respond chemotactically to CXCL12. **D:** summary quantitative graph of migration and chemotactic response, while both cell lines did not show chemotactic response to CXCL12, TOV-112D cells had significantly lower cell motility than TOV-21G.

A: Results represent average MFIR obtained by flow cytometry of at least three independent experiments each included analysis of $25x10^3$ cells, error bar= SEM. B and C: Lines show fluorescence intensity values over the experiment period (11hours), values represent average of triplicates, error bars= SEM. D: Bars represent the averages of three or more independent experiments of migration line slopes over the experiment period, error bars= SEM

Figure 3.10: Phenotype and Chemotaxis in EOC Cell Lines (2)

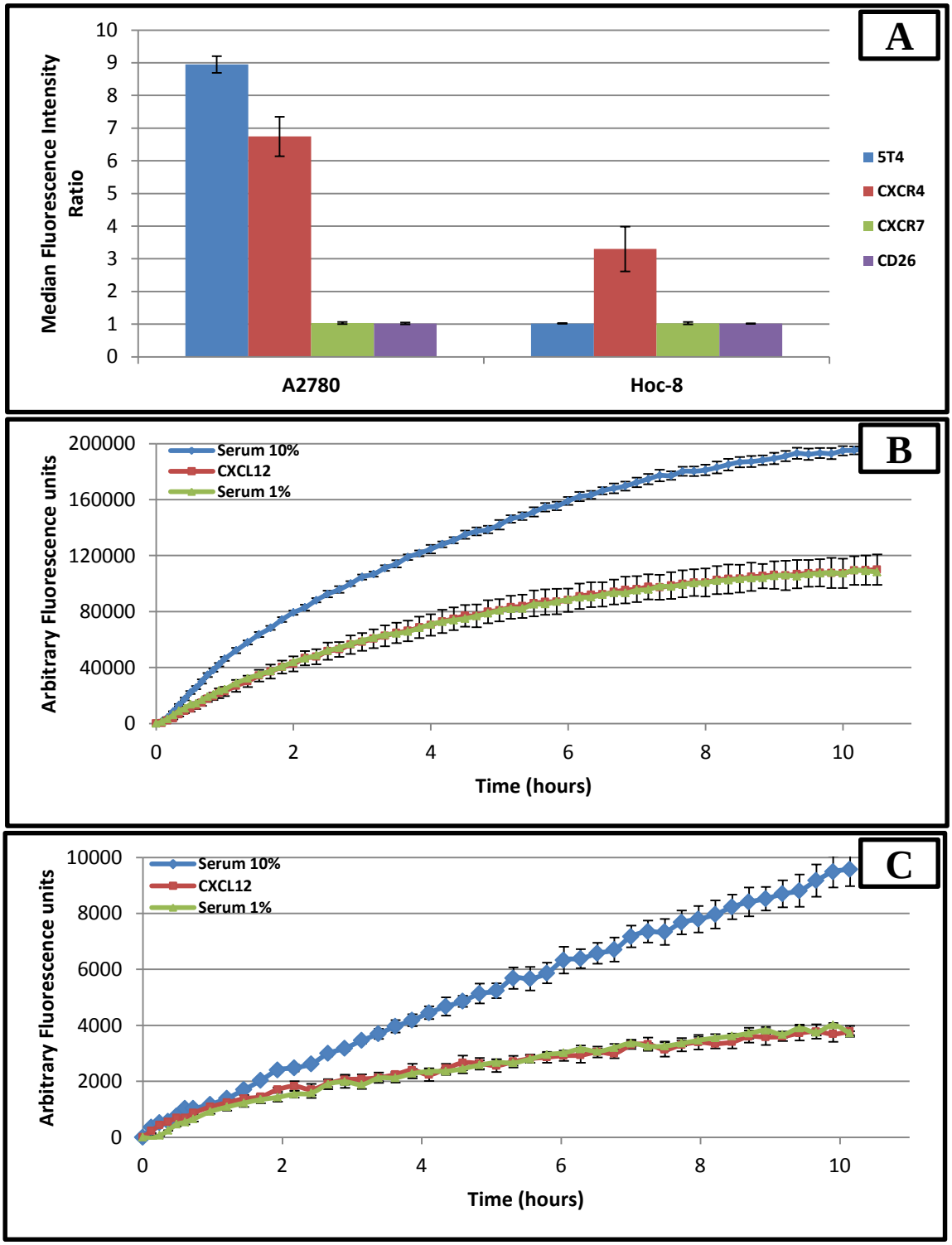

A: Surface expression of 5T4, CXCR4, CXCR7 and CD26 in A2780 and Hoc-8 cell lines as measured by flow cytometry. A2780 cells expressed 5T4 and CXCR4 while Hoc-8 cells were negative for 5T4 and expressed moderate amount of CXCR4. Both cell lines were negative for CD26 and CXCR7. Results represent average MFIR obtained by flow cytometry of three or more independent experiments (of $25x10^3$ cell each), error bar= SEM. **B: FluoroBlok Chemotaxis assay in A2780 cells**. A2780 cells migrated in equally toward CXCL12 and 1% serum suggesting a lack of chemotactic response. **C: FluoroBlok Chemotaxis assay of Hoc-8 cells**. Hoc-8 cells showed a lack of chemotactic response to CXCL12.
B&C: Lines show fluorescence intensity value over the experiment period (11hours), values represent average of triplicates, error bars= SEM.

3.6 Chapter Discussion

In this chapter the surface expression of 5T4, CXCL12 receptors: CXCR4 and CXCR7, and the CXCL12 inactivating peptide CD26 was explored using flow cytometry on live cells in eight EOC cell lines: SKOV-3, Caov-3, OVCAR-3, OV-90, TOV-112D, TOV-21G, A2780 and Hoc-8. In addition, a FluoroBlok® method was utilised to investigate the chemotactic response to a CXCL12 gradient in these cell lines. **Table 3.1** summarises the phenotype and chemotactic response in these cell lines.

Table 3.1: Summary of MFIR in EOC Cell Lines

Cell line	5T4	CXCR4	CXCR7	CD26	CXCL12 chemotaxis
SKOV-3	12	11.4	1	3.6	Yes
OVCAR-3	6.5	2.2	1	1.1	No
Caov-3	11.8	4.4	0.9	1	No
OV-90	1.4	2.8	1.1	1.4	No
TOV-112D	21.9	2.1	1.7	8.6	No
TOV-21G	4.8	2.3	1	1	No
A2780	8.9	6.7	1	1	No
Hoc-8	1	3.3	1	1	No

Marker expression in the eight cell lines studied in this study using flow cytometry expressed as median fluorescence intensity ratio (MFRI), and chemotactic response to CXCL12.

All of the studied EOC cell lines were found to express 5T4 with the exception of Hoc-8 which was negative. 5T4 expression in these cell lines was found at varying levels, with MFIR ranging from 1.4 (OV-90 cells) to 21.9 (TOV-112D cells). Although 5T4 expression in these cell lines has not been previously reported, these results are not surprising and are in keeping with previous data from our laboratory. In addition, the positive cell surface expression of 5T4 is consistent with the methodology followed in 5T4 discovery and subsequent validation of its expression when it was found to be expressed by most cancer cell lines[1, 3].

TOV-112D cells were found to be the only cell line in this study to show surface expression of CXCR7 (MFIR = 1.7). The function of CXCR7 in TOV-112D as a receptor for CXCL12 or CXCL11 was not investigated in this project; future research could explore these aspects including any potential role for 5T4 in modulating such function.

CXCR7 cell surface expression has not previously been reported in any of these cell lines, possibly because CXCR7 has only recently been identified as a CXCL12 receptor. One study, however, did report CXCR7 transcript, but not protein in SKOV-3 cells[265]. It is possible that CXCR7 in SKOV-3 cells does not get translated into protein or it might be that CXCR7 protein exists within the cell and not on the cell surface. In addition, concerns

have been raised lately regarding the validity of CXCR7 antibodies used in the reported literature[259]. It is relevant that the authors of this paper had a potential commercial conflict of interest, but the use of the antibody utilised in this chapter (Ab72100) was not assessed in that particular paper by flow cytometry. In addition, results obtained using this antibody (Ab72100) were separately confirmed in this project using the antibody suggested by the authors (clone 11G8).

CD26 surface expression was shown in SKOV-3, OV-90 and TOV-112D (MFIR respectively: 3.6, 1.4 and 8.6) while the other cell lines were found to lack CD26 surface expression. A literature review has revealed that SKOV-3 expressed CD26 at low levels as determined by flow cytometry, which was in keeping with our results[266]. There has been no reported data concerning CD26 expression in the other cell lines studied here.

All cell lines studied showed surface expression of CXCR4, MFIR ranged from 2.1 in TOV-112D cells to 11.4 in SKOV-3 cells. CXCR4 has been extensively investigated in the literature; its expression has been reported in A2780 cells using immunofluorescence and Western blotting[267]; CXCR4 at transcription level was identified in OVCAR-3[268] while flow cytometry confirmed CXCR4 expression in SKOV-3 and Caov-3 cells[269]. CXCR4 expression in all studied cell lines in this project is consistent with the published data and in keeping with the recognised diverse expression of CXCR4 in human cancers and cell lines given its role in cell motility and invasion[140].

It was possible to demonstrate a chemotactic response to CXCL12 only in SKOV-3 cells under the experimental conditions used in this project. This was a CXCR4-mediated response as blocking CXCR4 with AMD3100 in SKOV-3 cells abrogated their chemotactic response. There have been no published reports investigating the chemotactic response to CXCL12 in any of the cells studied in this project apart from SKOV-3 and Caov-3. In keeping with these results Giri et al reported a chemotactic response to CXCL12 in SKOV-3 cells[270], while Caov-3 cells did not migrate toward CXCL12 in an invasion assay in another study[155].

Given the fact that all cell lines migrated toward 10% serum-supplemented media more than they did toward 1% serum in this project, it is reasonable to hypothesise that the lack of response to CXCL12 is not a result of global malfunction of cellular motility since fetal calf serum contains several growth factors and chemokines[271, 272].

The concurrent surface expression of 5T4 and CXCR4 on several of the studied cell lines without a chemotactic response to CXCL12 could suggest that there is no obligate

link between cell surface phenotype and functional response indicating a non-functional CXCR4 surface expression. This apparent lack of response could be a consequence of methodology limitation in elucidating small scale responses in some cells. It is also plausible to suggest that the high cell motility in some cells such as A2780 could mask any chemotactic response to CXCL12 while in other cells, such as OVCAR-3, the low cell motility might contribute functionally to the lack of measurable chemotaxis. While future research could improve on methodology by further optimisation or utilising other techniques, it is still possible that these cells might have developed chemotactic response through different chemotactic axes which may or may not be 5T4 dependent. Another explanation is that while CXCR4 is functional it is the interaction with CXCL12 which is lacking. This could be caused by CXCL12 modification which is a recognised signal regulation process as detailed in the introduction chapter. Proteolysis by CD26 is one of these processes, however, inhibiting CD26 activity with diprotin-A did not restore chemotactic response to CXCL12 in TOV-112D cells nor did it improve the chemotactic response in SKOV-3 cells.

There are several reported methods for assessing chemotaxis in cell lines which include generally two dimensional and three dimensional studies[273-275]. While this project used a 2D based chemotaxis assay, 3D based techniques could be of value in future research and might elucidate further aspects of the potential role of 5T4 in cell biology in ovarian cancer.

The FluoroBlok® technique was chosen as it offers continuous cell motility monitoring as well as generating end results without interference or the need to terminate experiments; which is required in the traditional Boyden's methodology. FluoroBlok® was modified later to include in situ cell counting by taking advantage of a plate scanner, this novel technique provided actual cell count, which enabled increasingly reliable comparisons between experiments of the different cell lines.

FluoroBlok® inserts could be utilised for invasion assays where the porous membrane is covered by a thin layer of a substance such as laminin or collagen to 'resemble' cell invasion of ECM. In this project there was no attempt to perform these studies given the peculiar nature of ovarian cancer spread within the peritoneum which does not require invasion, at least initially. Cells shed off the primary tumour into the peritoneal cavity; they then attach to the peritoneal mesothelial cells or to the exposed basement membrane between dispersed cells caused by the distended abdomen resulting from accumulating ascites.

Another chemotaxis technique is the Ibidi microslide[275] microfluidics method which was tested in this project and found to be unhelpful. A major disadvantage is that number of the experimental chambers is limited to three. When these chambers are used for repeats of the same experimental setting it is not possible to do any comparative experiments simultaneously. In addition, the need for time lapse microscopy for an extended time, typically overnight, meant increasing cost and time limitation.

To conclude, in this chapter several EOC cell lines were phenotyped and investigated in terms of chemotactic response to CXCL12. The results obtained in this chapter are in keeping with published reports. Two cell lines, SKOV-3 and Hoc-8, emerged from this part of the project as a useful model to investigate further 5T4 biology. SKOV-3 expressed 5T4 and responded chemotactically to CXCL12, a response which was CXCR4-mediated (5T4 positive, CXCL12 responsive); while Hoc-8 cells lacked 5T4 expression and did not respond chemotactically to CXCL12 (5T4 negative, CXCL12 unresponsive) **(**

Figure 3.11**)**. These two cell lines were thereafter used in the following chapter to knock down 5T4 expression in SKOV-3 and overexpress 5T4 in Hoc-8 cells to investigate whether or not 5T4 has a role in the observed chemotaxis response.

Figure 3.11: SKOV-3 and Hoc-8 a Useful Model

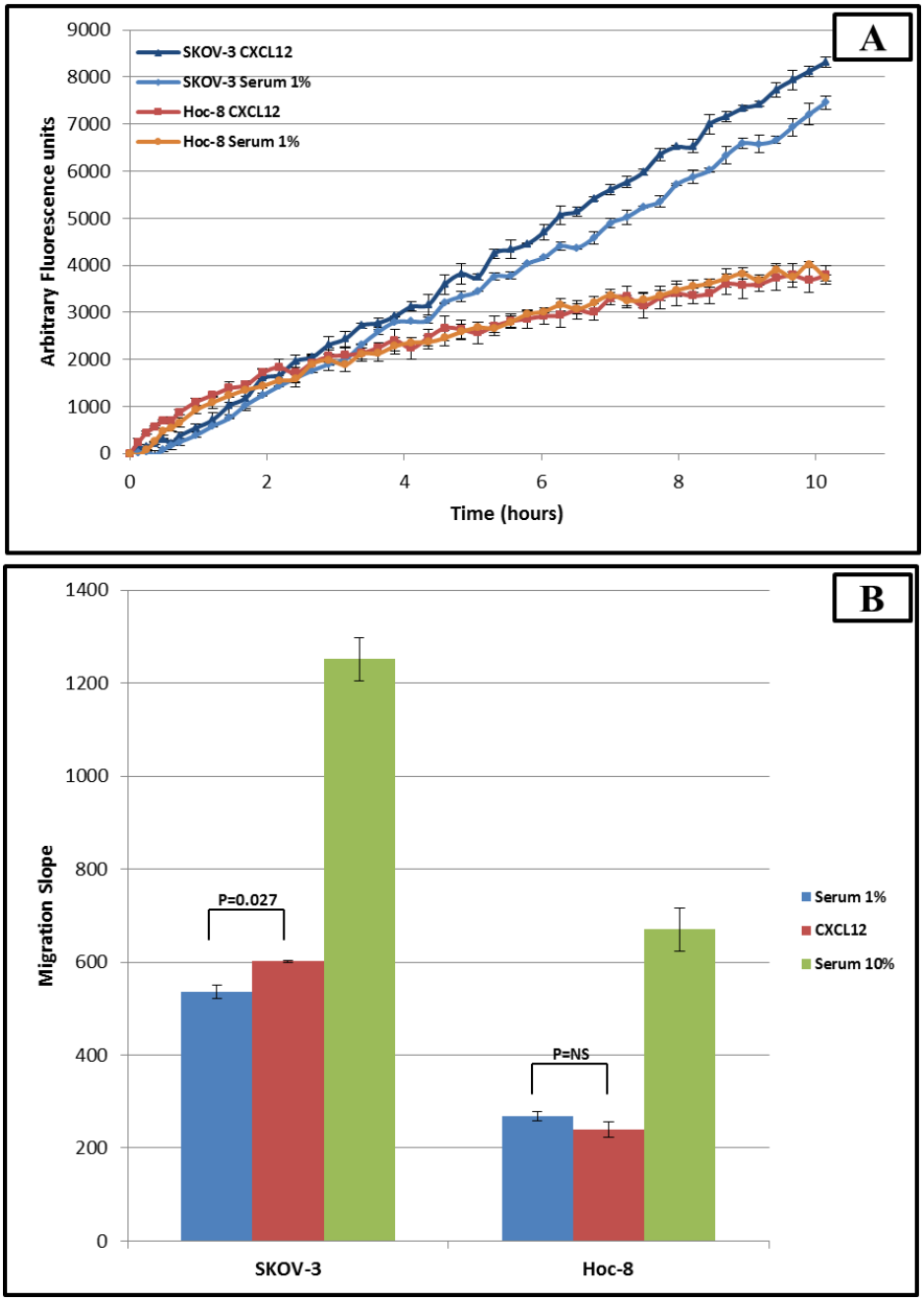

FluoroBlok Chemotaxis assay in SKOV-3 and Hoc-8 cells.
SKOV-3 and Hoc-8 cell lines emerged as a useful model to investigate 5T4 biology. **A:** an example experiment showing chemotactic response to CXCL12 in SKOV-3 cells and the lack of response in Hoc-8; Lines show fluorescence intensity values over the experiment period (11hours), values represent average of triplicates, error bars= SEM. **B:** summary quantitative graph of migration and chemotactic response, generally Hoc-8 cells had lower cell motility and lower response to 10% serum than SKOV-3. SKOV-3 responded chemotactically to CXCL12 while Hoc-8 did not. SKOV-3 data is shared with **Figure 3.2.**
Bars represent the averages of migration line slopes of triplicates in a single simultaneous chemotaxis assay, error bars= SEM.

Chapter 4

RESULTS:

5T4 Knockdown and Overexpression: Chemotaxis

5T4 Knockdown and Overexpression: Phenotype and CXCL12 Chemotaxis

4.1 Aim

To explore the consequences of manipulating 5T4 expression in SKOV-3 and Hoc-8 cells on the chemotactic response to CXCL12 and on the expression of selected markers (CXCR4, CXCR7 and CD26).

4.2 Introduction

Experiments in the previous chapter led to identifying two cell lines which could be investigated further to explore 5T4 biology. These are Hoc-8 which lacked 5T4 expression and did not respond to CXCL12 chemotactically; and SKOV-3 which expressed 5T4 and showed a chemotactic response to CXCL12. Therefore, experiments to knock 5T4 down in SKOV-3 were performed in addition to 5T4 overexpression in Hoc-8.

4.3 5T4 KD in SKOV-3

Stable 5T4 knockdown was achieved using short hairpin RNA (shRNA). Briefly, SKOV-3 cells were incubated with the transfection mixtures each containing one of four shRNA plasmids designed for 5T4 knockdown or a control plasmid. Transfected cells were then selected by culturing in puromycin-supplemented growth media (final concentration 2µg/ml) shRNA clone 3 emerged as the most efficacious at reducing 5T4 expression out of the four clones used to knock 5T4 down in SKOV-3 cells **(Figure 4.1)**.

However, a small proportion of these cells expressed moderate levels of 5T4 and therefore they were sorted using FACS to select cells which expressed low 5T4. Hence, the sorted cells which were stably transfected with clone 3 (**SKOV-C3)** were used in this study to explore 5T4 biology. Untransfected cells (**SKOV-3**) and those transfected with the control clone (**SKOV-CC**) had their expression of 5T4 unchanged **(Figure 4.1)**. These cells generally showed no heterogeneity in their phenotype or behaviour and hence they were not clone-selected.

Figure 4.1: 5T4 Knockdown in SKOV-3 Cells

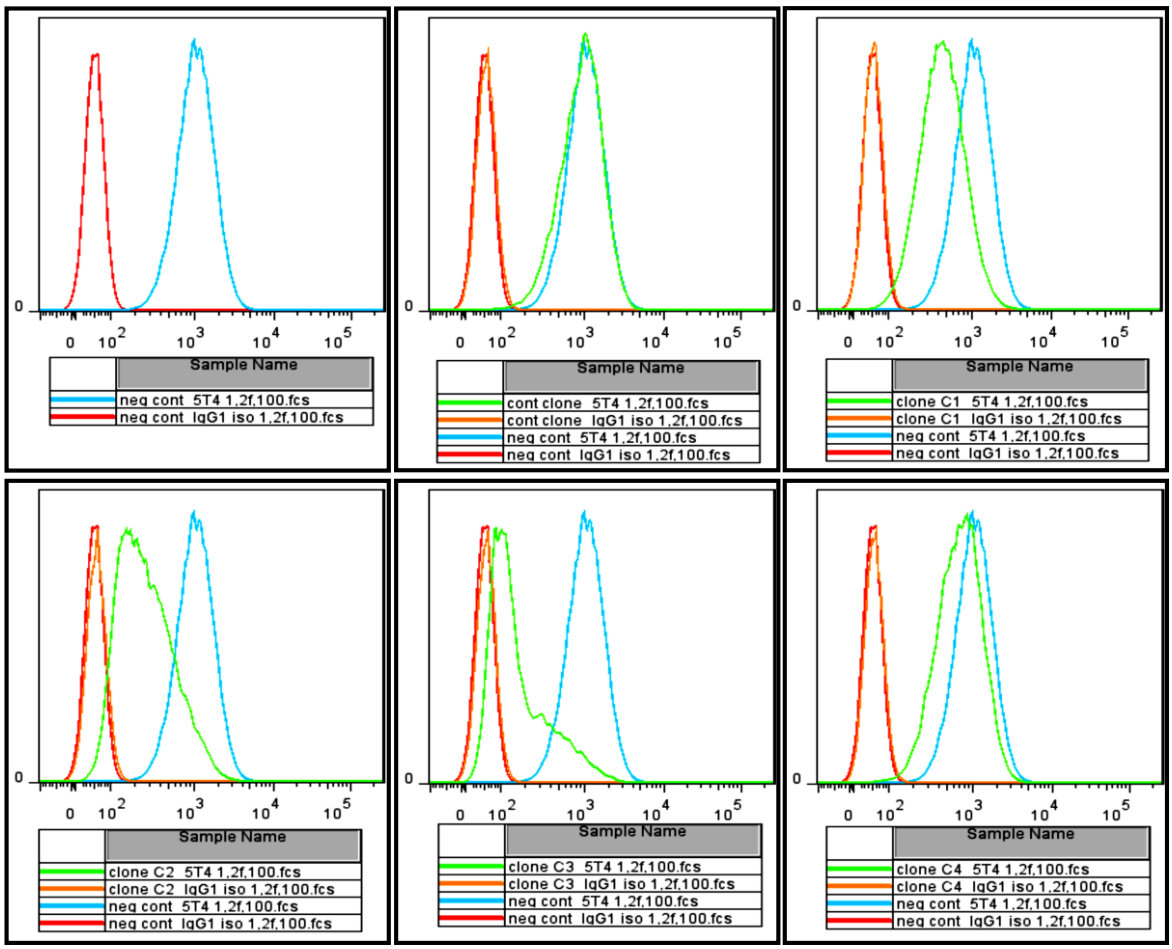

5T4 KD in SKOV-3: Flow cytometry results of a representative experiment of surface expression of 5T4 in SKOV-3 cells after transfection with four active shRNA plasmids and one scrambled control. Clone 3 (middle bottom picture) was the most effective clone, however a small proportion of cells expressed more 5T4 than others demonstrated by the long tail of the histogram. Clone-3 transfected cells were subsequently purified using FACS.

4.3.1 5T4 KD Resulted in Lower CXCR4 Levels

Flow cytometry on live cells showed that surface 5T4 expression in SKOV-C3 cells was on average 21% of that of the paternal cell line (MFIR: 2.4 and 11.4 respectively, $P < 0.0001$, t test). The KD control cells (SKOV-CC) maintained similar levels of 5T4 expression (MFIR = 11.5) **(Figure 4.2)**. Interestingly, CXCR4 surface expression in SKOV-C3 cells was reduced to 70% of that in SKOV-3 cells as measured by flow cytometry on live cells (MFIR: 8.6 and 12.2 respectively, $P = 0.01$, t test). There was no significant change in CXCR4 expression in SKOV-CC (MFIR = 11.6) **(Figure 4.2)**.

4.3.2 5T4 KD Has No Measurable Effect on CXCR7 and CD26 Expression

The parental, control and knockdown cells all remained negative for CXCR7 (MFIR: 1.0 for all, *P = NS*, t test) as measured by flow cytometry. On the other hand, all three cell lines expressed surface CD26 with no statistically significant difference (MFIR: 3.0, 2.3 and 2.2 respectively, *P = NS*, t test) **(Figure 4.2)**.

Figure 4.2: 5T4 Knockdown and Cell Phenotype

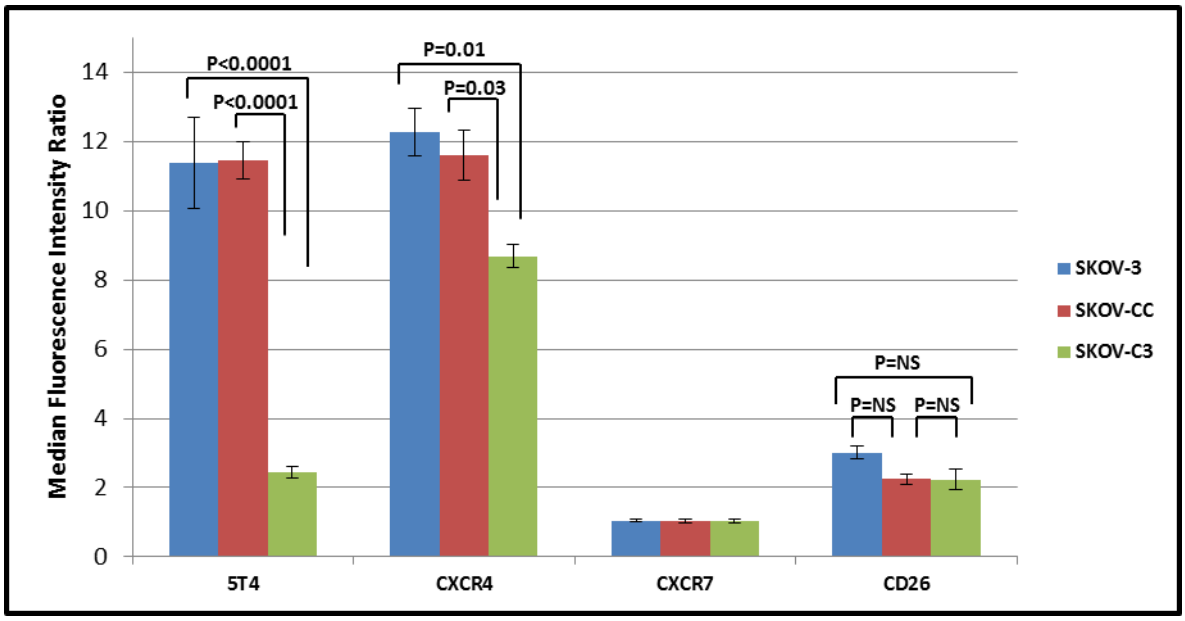

5T4 KD in SKOV-3 and its effect on surface expression of CXCR4, CXCR7 and CD26as measured by flow cytometry. Results represent average MFIR obtained by flow cytometry of at least three independent experiments each included analysis of $25x10^3$ cells. 5T4 expression was reduced by 80% in SKOV-C3 with no change in its expression in SKOV-CC. SKOV-C3 also expressed less CXCR4 and there were no significant changes in the expression of CXCR7 or CD26. Error bars = standard error of mean (SEM).

4.3.3 KD Negates Response to CXCL12

The use of a plate microscopic scanner (Thermo Scientific Cellomics HCS) to count migrated cell numbers in FluoroBlok chemotaxis assay, as detailed in the materials and methods chapter, provide an additional tool to define the magnitude of chemotactic response to CXCL12 in SKOV-3 cells.

Both SKOV-3 and SKOV-CC cells responded chemotactically to CXCL12. There was a 10% increase over their respective migration toward 1% serum (111.0%, *P < 0.0001*, and 112.9% *P < 0.0001*, respectively, paired T test) **(Figure 4.3-B)**. This response disappeared in SKOV-C3 cells which migrated in similar numbers toward 1% serum with or without CXCL12 (99.5%, *P = NS*, paired t test). The migration and chemotaxis response of all three cell lines were not influenced by incubation with diprotin-A (CD26 inhibitor) **(Figure 4.3-B)**.

Figure 4.3: 5T4 Knockdown and Chemotaxis

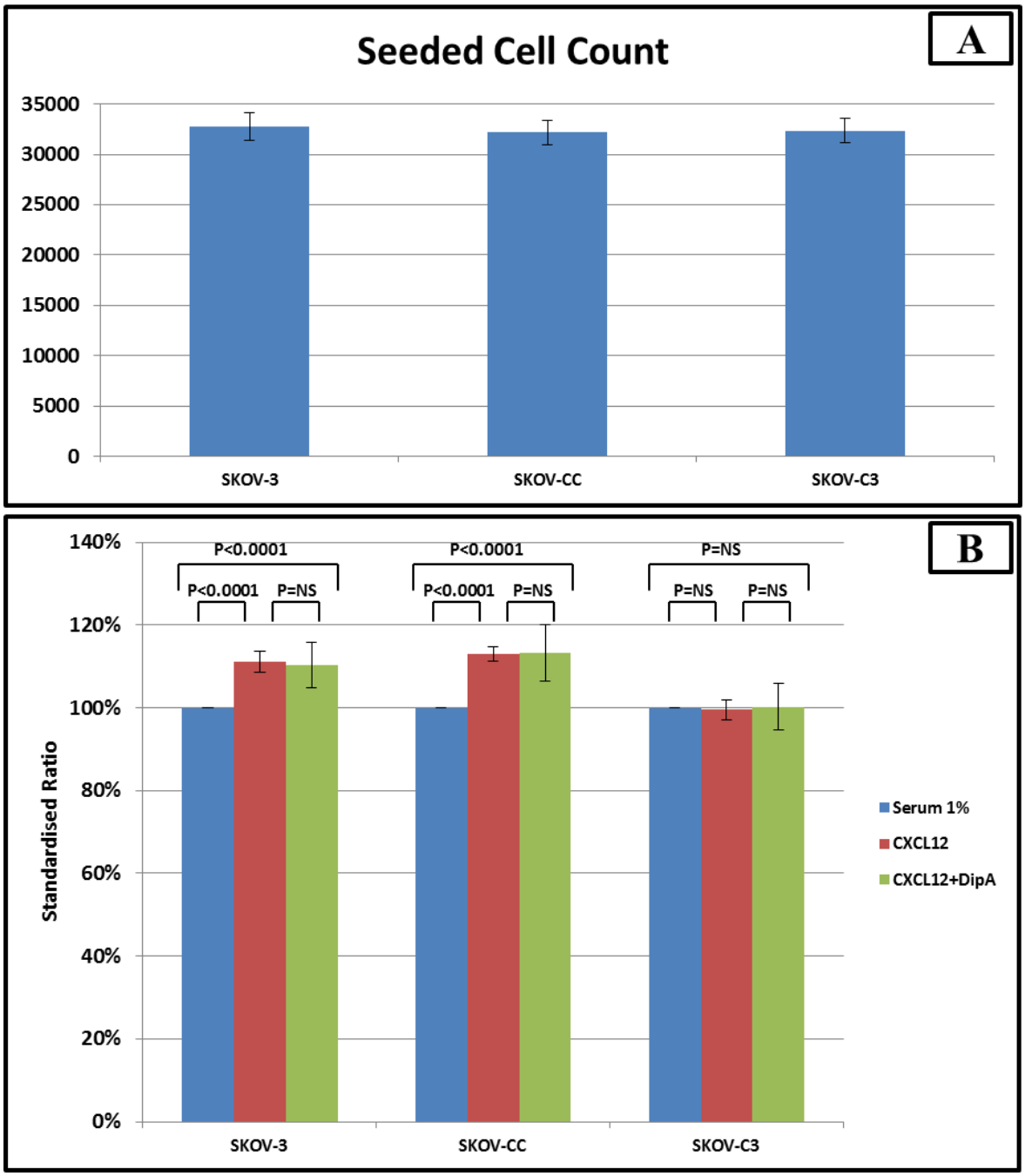

Modified FluoroBlok Chemotaxis assay in SKOV-3, SKOV-CC and SKOV-C3.
In this chemotaxis assay the outcome is expressed as cell numbers counted by fluorescence-based plate scanner. **A:** shows no difference in the numbers of cells seeded at the start of chemotaxis assays[#]. Results represent average cell count of at least three independent experiments, error bar= SEM. **B:** Both the parental (SKOV-3) and knockdown control (SKOV-CC) cells showed a chemotactic response to CXCL12 which was abrogated in the knockdown cells (SKOV-C3). Incubation with diprotin-A did not affect the outcome in any of these cell lines. Results represent standardised percentage ratio***** to the number of cells migrated to 1% serum in each experiment averaged of at least three independent experiments, error bar= SEM.

[#] Cells of the three cell lines seeded at the start of each chemotaxis experiment in 96 well plate where the growth surface equals that of the FluoroBlok insert growth surface (0.3 cm^2); this provided an accurate measure of the number of cells assayed. The area scanned by the plate scanner was 0.13 cm^2 (43% of growth are) which explains the apparent discrepancy in cell count.
***** The standardised percentage ratio is calculated according to formula: (number of migrated cells / number of cells migrated to 1% serum)x100.

4.4 Overexpression in Hoc-8

5T4 overexpression in Hoc-8 cells was performed previously in our laboratory (by Dr B Thomas) where a full length 5T4 cDNA was cloned into a constitutive expression vector under CMV promoter. Cells from one clone with high 5T4 expression were used in this project (termed Hoc-5T4), while parental cells (Hoc-8) were used for comparison.

4.4.1 Cell Phenotype

5T4 surface expression was confirmed in Hoc-5T4 cells by flow cytometry on live cells while Hoc-8 cells did not express 5T4 (MFIR: 36.8 and 1.0 respectively, $P < 0.0001$, t test) **(Figure 4.4)**. CXCR4 surface expression increased also by 41% (MFIR: 4.1 and 5.8 respectively) but this did not reach statistical significance. Both Hoc-8 and Hoc-5T4 cells remained negative for CXCR7 (MFIR: 1.0 and 0.9 respectively) and CD26 (MFIR: 1.0 and 1.1 respectively) **(Figure 4.4)**.

Figure 4.4: 5T4 Overexpression and Hoc-8 Phenotype

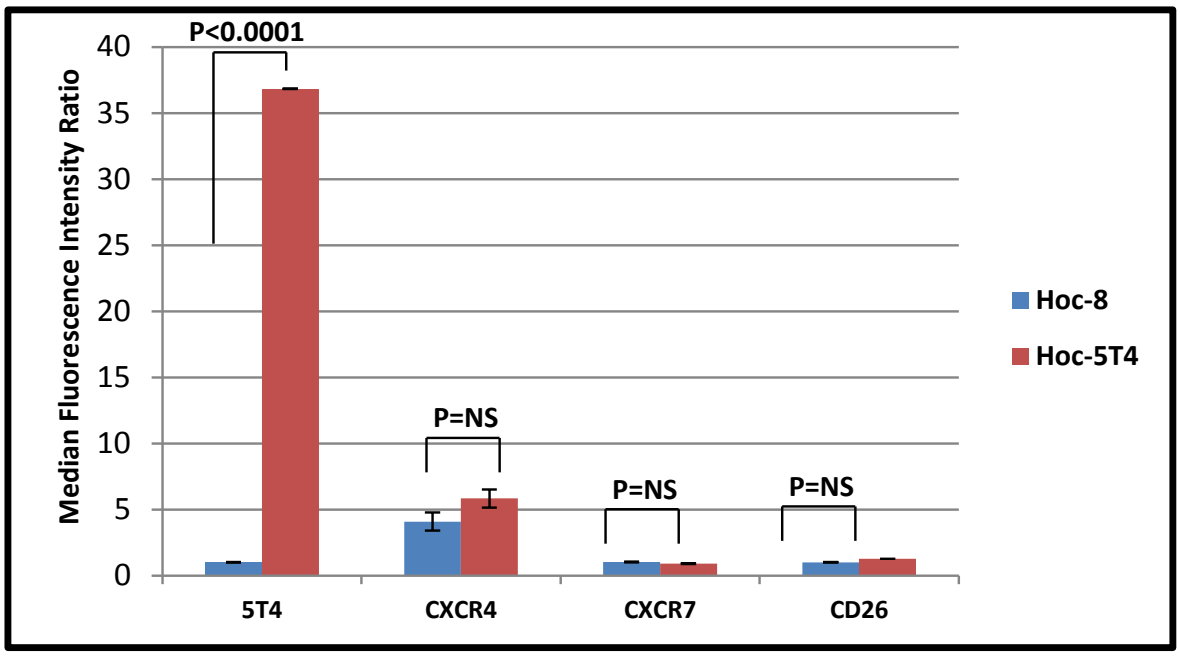

Surface expression of 5T4, CXCR4, CXCR7 and CD26 in Hoc-8 and Hoc-5T4 cells
5T4 was successfully over-expressed in Hoc-8 cells, the new cell line with stable 5T4 expression (Hoc-5T4) expressed high levels of 5T4. CXCR4 surface expression increased but this did not reach statistical significance. Both Hoc-8 and Hoc-5T4 cells remained negative for CXCR7 and CD26.
Results represent average MFIR obtained by flow cytometry of at least three independent experiments, error bar= SEM.

4.4.2 Chemotactic Response to CXCL12

In spite of successfully expressing high levels of surface 5T4, Hoc-5T4 cells failed to respond chemotactically to CXCL12 **(Figure 4.5)**.

Figure 4.5: 5T4 Overexpression and Chemotaxis

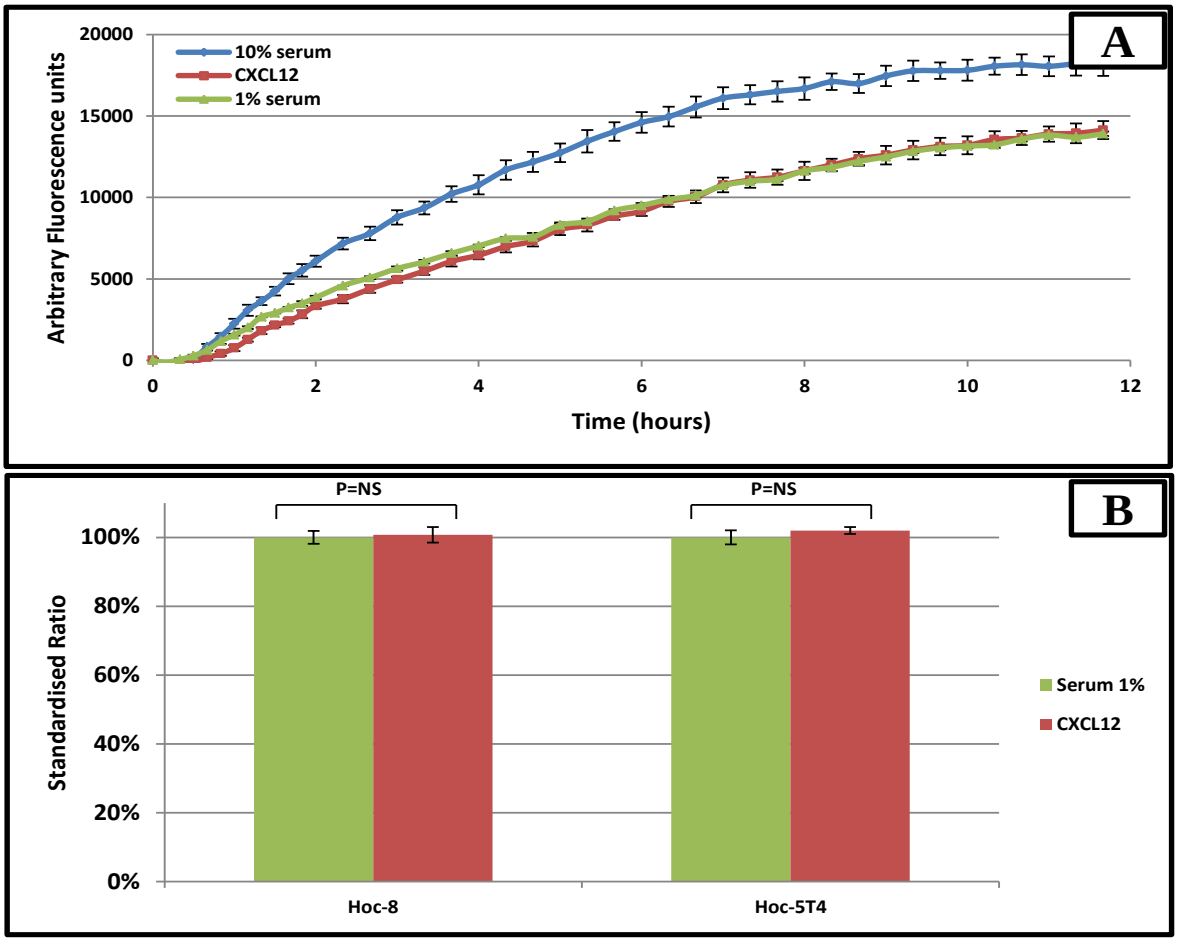

FluoroBlok Chemotaxis assay of Hoc-5T4 cells. Hoc-5T4 cells migrated in equally toward CXL12 and 1% serum suggesting a lack of chemotactic response to CXCL12. Hoc-8 Cells, however, migrated toward 10% serum-supplemented medium which served as a positive control. Lines show fluorescence intensity value over the experiment period (12hours), values represent average of triplicates, error bars= SEM.
B: Modified FluoroBlok chemotaxis assay in Hoc-8 and Hoc-5T4 cells both cell lines did not show chemotactic response toward CXL12. Results represent average cell count standardised ratio as measured using plate scanner of at least three independent experiments, error bar= SEM.

4.5 Chapter Discussion

In this chapter two cell lines were used to explore the consequences of the manipulation of 5T4 expression: SKOV-3 which is 5T4 positive and responds chemotactically to CXCL12 and Hoc-8 which is 5T4 negative and does not respond chemotactically to CXCL12. 5T4 was successfully knocked down in SKOV-3 cells and overexpressed in Hoc-8 cells by plasmid transfection.

5T4 knockdown in SKOV-3 cells resulted in an 80% reduction in 5T4 surface expression. CXCR4 surface expression was also reduced in the 5T4-KD SKOV-C3 cells and importantly there was a loss of the chemotactic response to CXCL12 under the tested experimental conditions in these cells.

This study did not examine whether the reduction in CXCR4 surface expression was transcriptional or post translational; this would be however worthy of investigating in future studies. An extensive effort by Dr G Marinov in his PhD research in our laboratory[276] was unsuccessful in identifying a direct link between 5T4 and CXCR4 expression and he concluded that other proteins such as receptor associated molecules might be involved[276]. Indeed, similar to other GPCR receptors, other co-receptors or modulator proteins might play a crucial role in CXCR4 function[277-279].

Whether or not 5T4 has a direct functional role in the abrogation of CXCR4-mediated chemotactic response is not clear. In spite of the fact that the results from only one construct were reported here, our published research in other cell lines using the same construct showed similar results **(Appendix 3)**[280]. Nonetheless, future research utilising multiple constructs for 5T4 knockdown could help to exclude 'off target' effects. Another strategy could be the use of knockout techniques in cell lines[281, 282] which are currently under investigation in our laboratory. Achieving 5T4 KO in cancer cell lines and utilising rescue experiments by reintroducing truncated, full length or mutated forms of 5T4, accompanied with signal transduction studies, could unravel its potential role in CXCR4 expression and function, and which domains of 5T4 are required for these functions.

In contrast to observations in SKOV-3 cells, it was not possible to demonstrate a chemotactic response to CXCL12 in 5T4-expressing Hoc-8 cells. This could have resulted from the fact that the high cell motility observed in Hoc-8 cells masked any relatively small chemotactic response; 30% of seeded Hoc-8 cells migrated to identical media in comparison with 10% of SKOV-3 cells. Further optimisation of the experimental conditions such as a reduction in the serum concentration in the migration media might be

required to investigate whether or not the inherent cell motility in Hoc-5T4 cells could mask a chemotactic response to CXCL12.

The discrepancy in the results obtained from 5T4 knockdown versus 5T4 neo-expression could theoretically be explained as follows; when 5T4 is constitutively expressed it serves specific functions which would be affected by the reduction of its expression. Cells which survive without expressing 5T4 might not, however, be dependent on its function. Such cells might have developed alternative 5T4-independent pathways or paralogue proteins to accommodate for 5T4 loss. This possibility was investigated by Dr A Rutkowski[283] in his PhD research in our laboratory in which he discovered a 5T4 paralogue gene (*PL5*), however attempts to isolate the putative protein were largely unsuccessful[283].

CXCR7 surface expression was found not to be influenced by 5T4 overexpression in Hoc-8 cells or 5T4 KD in SKOV-3 cells, as both cells remained CXCR7 negative. This is in keeping with the findings in mES, where both WT and 5T4KO, differentiating and undifferentiated cells showed no change in CXCR7 expression[25]. Interestingly, it was shown that CXCR7 expression in MEFs was upregulated in 5T4KO animals by flow cytometry and Western blotting. However, the same study reported that 5T4 KD had no effect on CXCR7 levels in H1048 SCLC[280].

Taken together, this suggests a complex relationship between 5T4 and CXCL12 function and receptor expression which is possibly context dependent and the 5T4 role in cancer cells is different from that in embryological cells. It is also plausible to hypothesise that 5T4 function could be dependent on the presence of a 'machinery' of other molecules without which 5T4 expression (or overexpression) is redundant.

5T4 neo-expression in Hoc-8 cells was performed by Dr B Thomas in her PhD research in our laboratory[258], where clone selection was performed by limiting dilution. Dr Thomas used an empty vector as a control for 5T4 transfection and reported no change in 5T4 expression (cells remained negative). Empty vector transfected Hoc-8 cells were not available for my study hence only parental and 5T4 expressing cells were used in the relevant studies. Whilst this is clearly a less than optimal control, the results obtained from overexpression experiments, however, were largely negative (no detectable difference between parental and 5T4-expressing cells) which makes the role of this control less crucial.

To conclude, in this chapter the two cell model, SKOV-3 (5T4 positive, CXCL12 responsive) and Hoc-8 (5T4 negative, CXCL12 unresponsive) was used to explore 5T4

biology. 5T4 knockdown in SKOV-3 and 5T4 neo-expression in Hoc-8 were achieved successfully. While 5T4 KD resulted in a reduction in surface expression of CXCR4 and abrogated CXCR4-mediated chemotactic response to CXCL12, 5T4 neo-expression in Hoc-8 did not manifest detectable consequences on CXCR4 function.

Chapter 5

RESULTS:

5T4 Knockdown and Overexpression: EMP

5T4 Knockdown and Overexpression: Epithelial-Mesenchymal Plasticity

5.1 Aim

To explore the role of 5T4 expression in epithelial mesenchymal plasticity (EMP) in epithelial ovarian cancer cell lines.

5.2 Introduction

5T4 expression was found to be transiently upregulated during *in vitro* differentiation of murine embryonic stem cells[174]. Cells during differentiation undergo changes resembling EMT process such as cell surface E-cadherin to N-cadherin switch, increased vimentin expression, and increased cellular motility[173]. Other studies reported that 5T4 over-expression in murine epithelial cells resulted in a reduced surface expression of E-cadherin, changes in cell morphology and alteration in cytoskeleton organisation[175].

This research has looked in the previous chapters into the role of 5T4 in the chemotactic response via CXCR4/CXCL12 axis. This will be further investigated as to whether 5T4 has a role in EMP by evaluating the consequences of 5T4 knockdown and 5T4 overexpression on the relevant cell morphology and inherent cell motility.

5.3 SKOV-3 and 5T4 KD Experiments

5.3.1 5T4 and Cell Morphology in SKOV Cell Lines

The change in cell shape was one of the most immediate observations made after 5T4 knockdown experiments in SKOV-3 cells. Unlike the parental SKOV-3 cells which were spindle-like elongated cells, the 5T4-KD SKOV-C3 cells looked flat and broad under bright field confocal microscope **(Figure 5.1)**. This indicated that SKOV-3 cells, which had mesenchymal morphology, might have acquired an epithelial appearance subsequent to 5T4 knockdown. The control knockdown cells (SKOV-CC) maintained the parental mesenchymal appearance which suggested that the change in cell shape is potentially a direct consequence of 5T4 knockdown.

Figure 5.1: 5T4 Knockdown and Cell Morphology

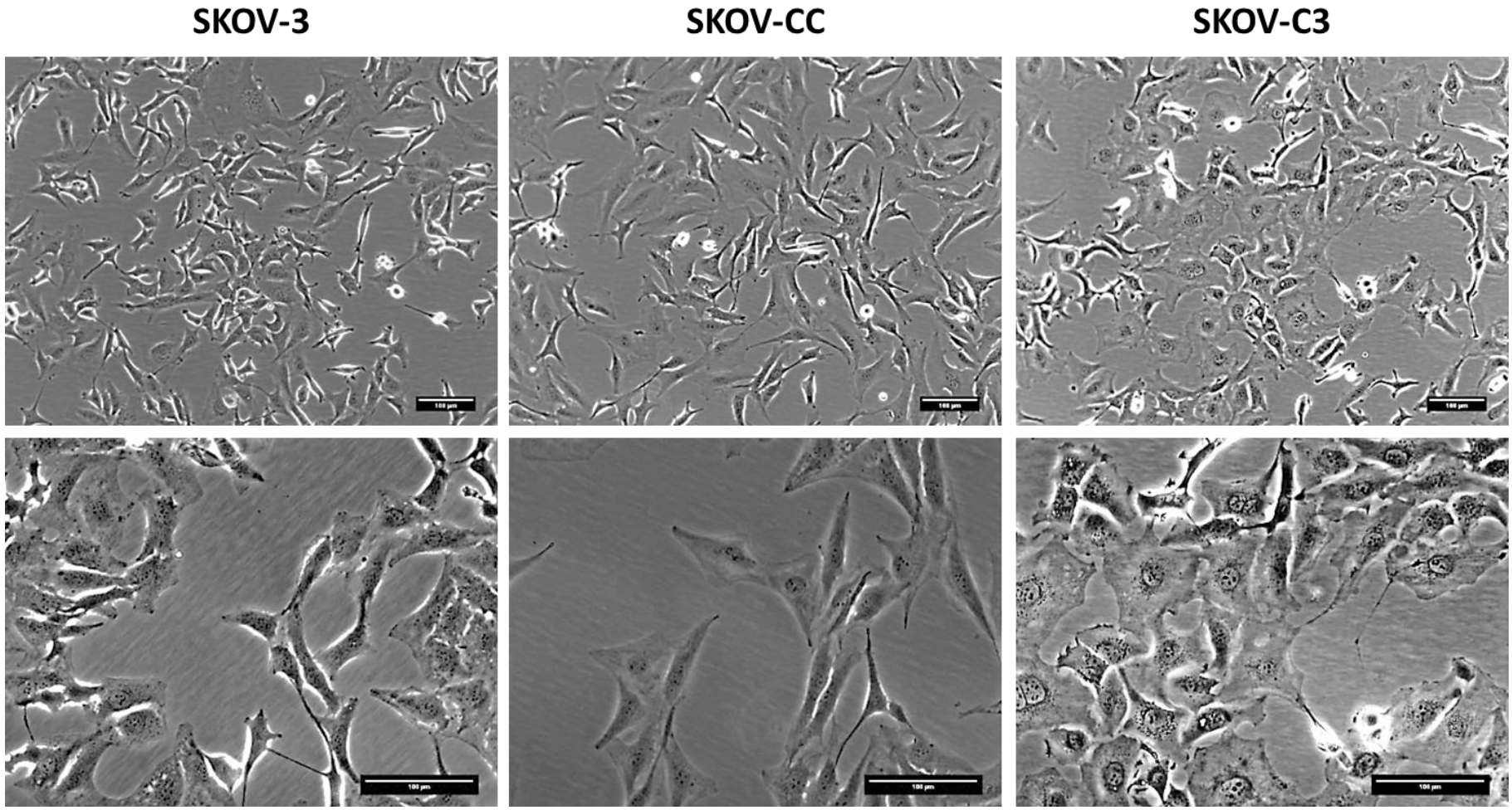

Morphological changes resulting from 5T4 knockdown.
5T4 knockdown in SKOV-3 cells resulted in changing cell appearance from the spindle-like mesenchymal shape (SKOV-3) to a broad epithelial phenotype (SKOV-C3), cells transfected with the control clone (SKOV-CC) maintained 5T4 expression levels and cell morphology.
Top row images 10X magnification, bottom row images 20X magnification. Images obtained by confocal microscope with Zeiss camera, scale bar= 100 µm.

5.3.2 5T4 and EMP Phenotype in SKOV Cell Lines

5.3.2.1 Flow Cytometry Studies

Switching between E-cadherin and N-cadherin is one of the frequently observed molecular changes accompanying transition between epithelial and mesenchymal phenotypes. Therefore, the expression of these markers was explored in SKOV-3, SKOV-CC and SKOV-C3 cell lines by flow cytometry on live cells. 5T4 surface expression dropped from MFIR 11.4 in SKOV-3 and SKOV-CC cells to MFIR 2.4 in SKOV-C3 cells ($p<0.0001$, t test). This reduction was accompanied by a trend of reduced N-cadherin expression with MFIR of 3.1, 2.9 and 1.8 for SKOV-3, SKOV-CC and SKOV-C3 respectively, however this change did not strictly reach statistical significance ($p=0.06$, t test). Flow cytometry showed that all three cell lines remained negative for E-cadherin (MFIR = 1.0 for all cell lines) **(Figure 5.2)**.

Figure 5.2: 5T4 Knockdown and EMP by FC

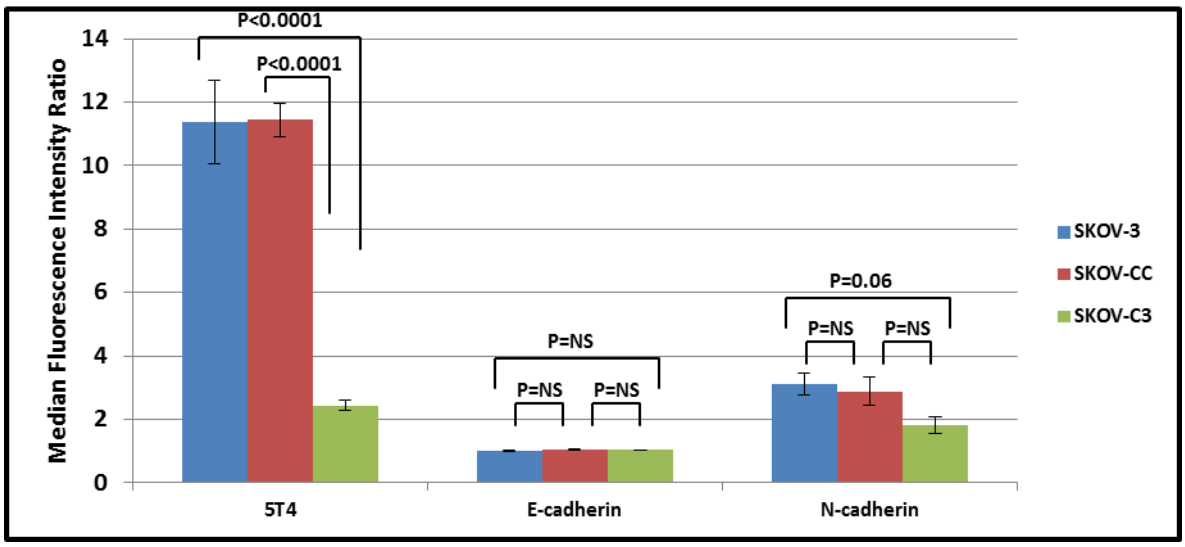

The effect of 5T4 knockdown on surface expression of E-cadherin and N-cadherin in SKOV-3 cells measured by flow cytometry on live cells

While there was no change in E-cadherin surface expression after 5T4 knockdown, there was a decrease in N-cadherin expression but this did not reach a statistical significance. 5T4 data are shared with **Figure 4.2.** Results represent average MFIR obtained by flow cytometry of at least three independent experiments, error bar= SEM.

5.3.2.2 Immunofluorescence Staining

Flow cytometry staining requires trypsinisation to generate cell suspensions which could affect some surface markers in addition to disconnecting cells from each other and from attachment to growth substrate. This could lead to a failure to detect some changes in molecular expression. Therefore, immunofluorescence staining on cells fixed in situ (in situ IF) was used to study SKOV cell lines. Transition between epithelial and mesenchymal phenotypes could include changes in the expression of markers other than E-

cadherin and N-cadherin. Hence, in situ IF was used to investigate the expression of N-cadherin, vimentin (mesenchymal markers), E-cadherin, cytokeratin (epithelial markers) and 5T4. Since several cytokeratins could be expressed by cells, some with organ specificity, pan cytokeratins antibody was used as a marker for epithelial phenotype in IF. As detailed in the materials and methods chapter, IF studies included at least three independent experiments for each study. A complete assessment of each well was performed with a confocal microscope to investigate homogeneity of the staining, then four random areas were chosen for picture capture to enable data analysis and figure presentation (≥ 100 cells each experiment).

In situ IF showed that both SKOV-3 and SKOV-CC cell lines stained strongly for 5T4 while the staining was faint in SKOV-C3 **(Figure 5.3)**.The epithelial markers E-cadherin and pan cytokeratins were not expressed by SKOV-3 or SKOV-CC cells while the 5T4-KD SKOV-C3 cells expressed both markers however this was limited to some and not all SKOV-C3 cells **(Figure 5.3)**.

There was no detectable difference in the expression of N-cadherin among the three cell lines **(Figure 5.3)**. However, the expression of the mesenchymal marker vimentin in SKOV-C3 was markedly different from the expression in SKOV-3 and SKOV-CC **(Figure 5.3)**. Vimentin in the parental and control cells was evenly diffused in the cytoplasm while it was concentrated around one pole of nuclei in the knockdown cells.

In addition, cells from the three cell lines (SKOV-3, SKOV-CC and SKOV-C3) were cultured in identical conditions, fixed with fresh paraformaldehyde and stained with phalloidin to probe actin cytoskeleton structural organisation. Both parental and control cells showed ‘stress fibres’ arrangements of the cytoskeleton typical of mesenchymal phenotype while the knockdown cells SKOV-C3 lacked these arrangements **(Figure 5.4)**. This observation supports further that 5T4 knockdown in SKOV-3 cells produced changes suggestive of mesenchymal epithelial transition (MET).

Figure 5.3: 5T4 Knockdown and EMP by IF

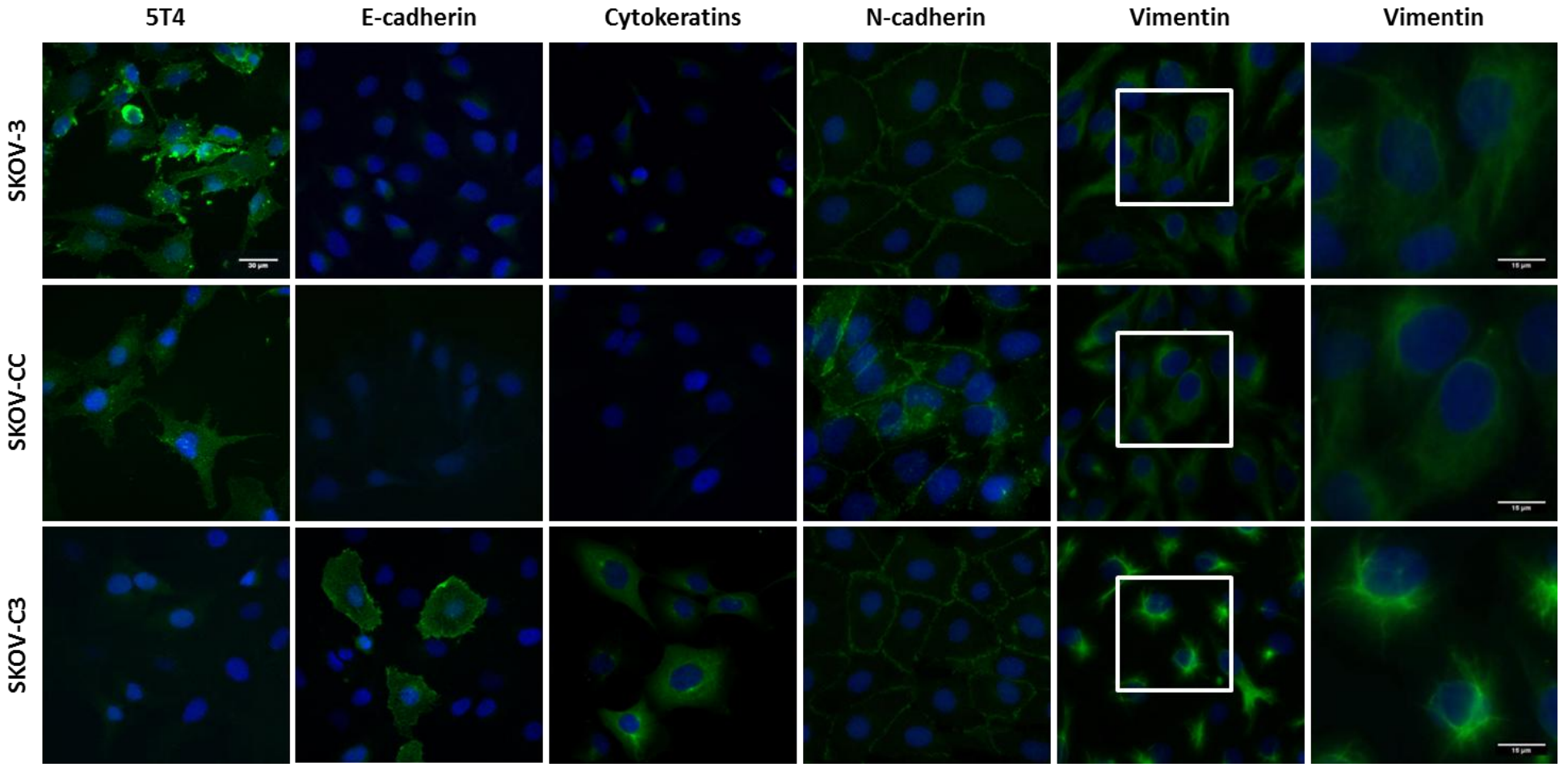

In situ immunofluorescence for EM markers in SKOV cell lines.
Cells from the three cell lines (SKOV-3, SKOV-CC and SKOV-C3) were cultured in identical conditions, fixed with 4% PFA at 80% confluence and stained for the different markers. SKOV-C3 cells expressed less 5T4 and more E-cadherin and cytokeratins, all cells expressed N-cadherin and vimentin however the distribution of vimentin was confined to one pole of nuclei in SKOV-C3 cells while was evenly diffused in the cytoplasm in the other two cell lines. Representative images of three independent experiments; scales bar: 30µm (15 µm far right images).Images captured with Axiovert 200M microscope mounted with CoolSNAP HQ camera.

Figure 5.4: 5T4 Knockdown and Actin Cytoskeleton

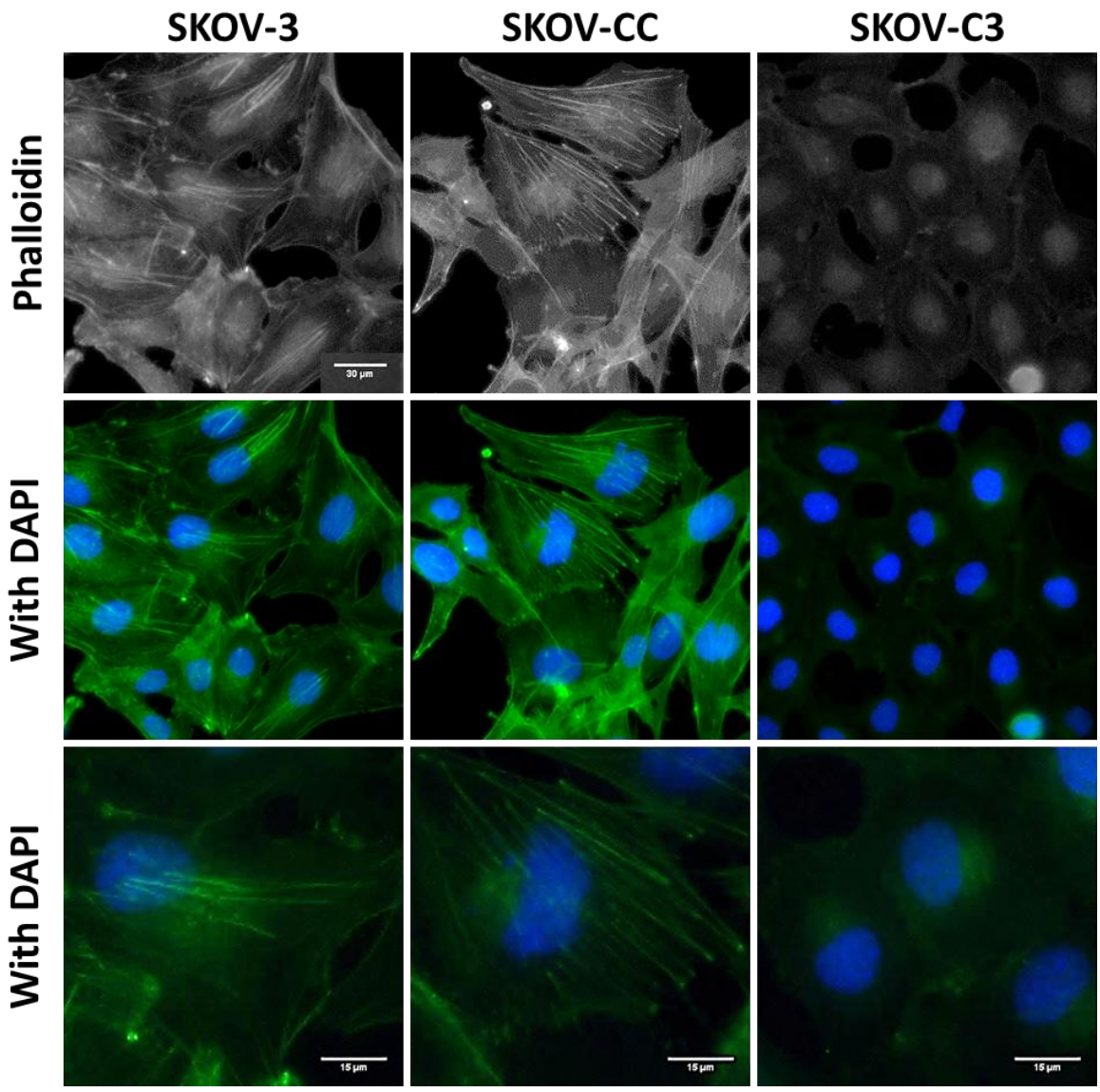

In situ immunofluorescence staining of actin cytoskeleton.
Cells from the three cell lines (SKOV-3, SKOV-CC and SKOV-C3) were cultured in identical conditions, fixed with fresh 4% PFA at 80% confluence and stained with AF-488 phalloidin. Both parental and control cells showed 'stress fibre' organisation of the actin cytoskeleton typical of mesenchymal phenotype while the knocked down cells lacked this arrangement of the cytoskeleton. Representative images of three independent experiments, scales bar: 30µm (15 µm bottom row images).Images captured with Axiovert 200M microscope mounted with CoolSNAP HQ camera.

5.3.3 Cell Motility

The modified FluoroBlok® chemotaxis assay was used as, unlike the traditional FluoroBlok technique, it allowed actual cell counting of migrated cells. Cell motility was measured in this project by the number of cells which migrated through the insert membrane when the bottom chamber contained medium identical to that in the top chamber (1% serum in SKOV experiments). In the previous chapter it was demonstrated that 5T4 knockdown in SKOV-3 cells abrogated the chemotactic response to CXCL12. There was also a distinct effect on cell motility which resulted from 5T4 knockdown.

SKOV-C3 cell motility was lower than that in SKOV-3 and SKOV-CC (5.5%, 12.0% and 12.1% of seeded cells respectively) **(Figure 5.5)**; this was a reduction by 0.55 fold (*p<0.0001*, t test). Migration to 10% serum was more profoundly affected (8.5%, 32.9% and 30.6% respectively) which was a reduction by 0.74 fold (*p<0.0001*) **(Figure 5.5)**.

Figure 5.5: 5T4 Knockdown and Cell Motility

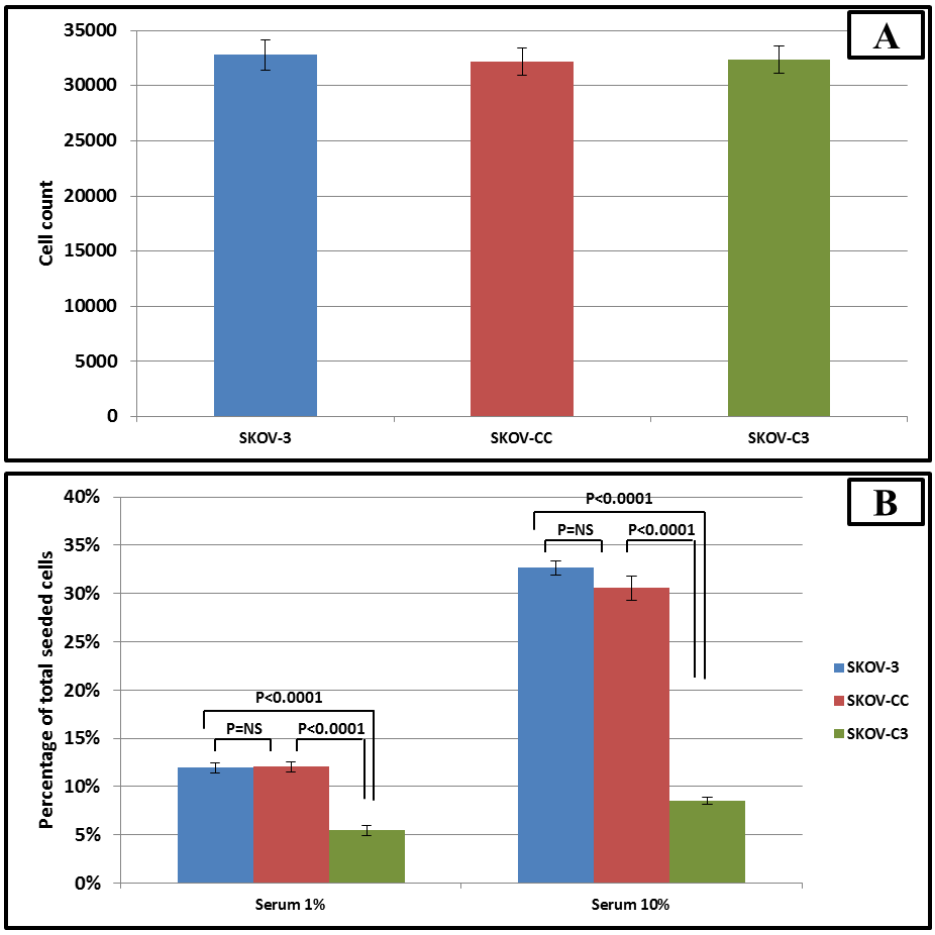

Modified FluoroBlok Chemotaxis assay in SKOV-3, SKOV-CC and SKOV-C3.
A: shows no difference in the number of cells seeded at the start of chemotaxis assays. Results represent average cell count of at least three independent experiments, error bar= SEM. **B:** Cell motility (migration to 1% serum) in SKOV-C3 cells was lower (5.5% seeded cells) than cell motility in SKOV-3 and SKOV-CC (12.0% and 12.1% respectively). Migration to 10% serum was more profoundly affected (32.9%, 30.6% and 8.5%, SKOV-3, SKOV-CC and SKOV-C3 respectively). Results represent average percentage of seeded cells of three independent experiments, error bar= SEM.

Taken together, these results suggest that 5T4 knockdown in SKOV-3 cells negated the chemotactic response to CXCL12 and also caused a general reduction in cell motility. These results support the findings of flow cytometry, immunofluorescence and bright field microscopy which showed that 5T4 knockdown in SKOV-3 produced molecular and morphological changes resembling an epithelial phenotype.

5.4 Hoc-8 and 5T4 Overexpression Experiments

5.4.1 5T4 and Cell Morphology in Hoc Cell Lines

Neo-expression of 5T4 in Hoc-8 cells did not induce noticeable morphological changes during culturing in complete growth media supplemented with 10% serum in keeping with the observation of Dr B Thomas in her PhD thesis[258]. However, when cells were serum-starved, the 5T4-expressing Hoc-5T4 cells became elongated and spindle shaped consistent with mesenchymal phenotype while Hoc-8 cells remained flat and broad **(Figure 5.6)**.

Figure 5.6: 5T4 Overexpression and Cell Morphology

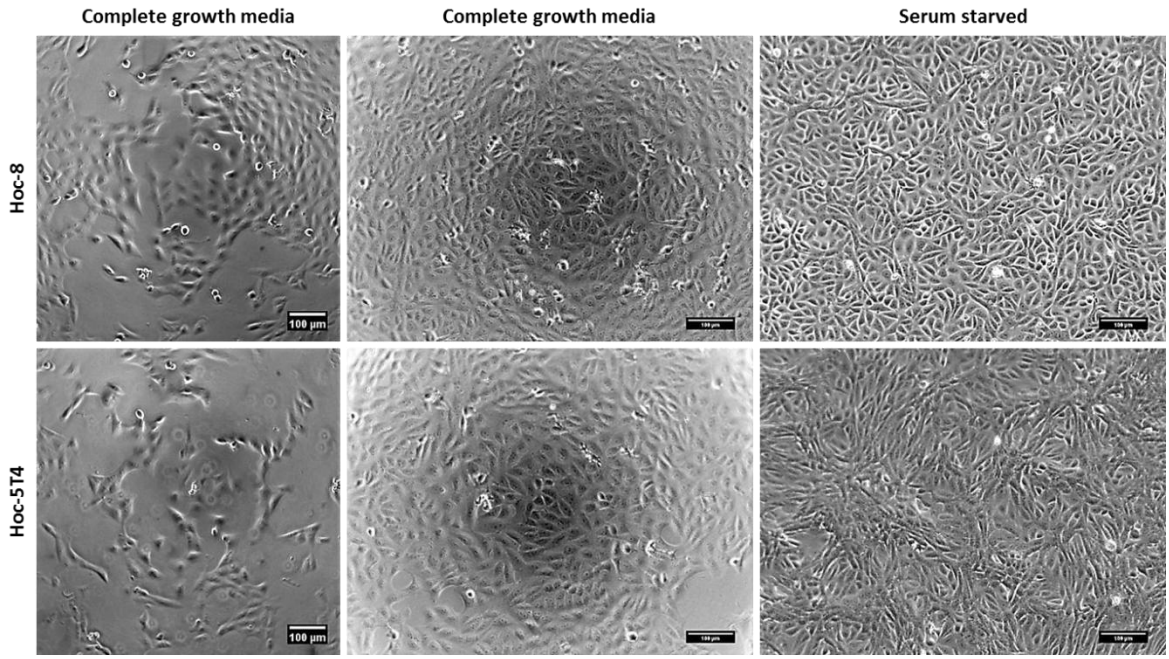

Morphological changes resulting from 5T4 overexpression
5T4 overexpression in Hoc-8 cells did induce morphological changes when cells cultured in complete growth media (10% serum) at low density (left images) nor at full confluence (middle images). When growth media were serum-free Hoc-5T4 cells became spindle-like suggesting mesenchymal changes while Hoc-8 cells maintained their broad shape.
Images obtained by confocal microscope with Zeiss camera, scale bar= 100 µm.

5.4.2 5T4 and EMP Phenotype in Hoc Cell Lines

5.4.2.1 Flow Cytometry Studies

The expression of E-cadherin and N-cadherin was explored in Hoc-8 and Hoc-5T4 cell lines by flow cytometry on live cells. Hoc-8 did not express 5T4 (MFIR=1) while as shown before Hoc-5T4 cells expressed high levels of 5T4 (average MFIR=36.8). This was accompanied by an increase in N-cadherin expression as measured by average MFIR from 1.5 in Hoc-8 cells to 5.3 in Hoc-5T4 cells (*p=0.01*, T test). Both cell lines were negative for E-cadherin with no detectable changes after 5T4 overexpression **(Figure 5.7)**.

Figure 5.7: 5T4 Overexpression and EMP by FC

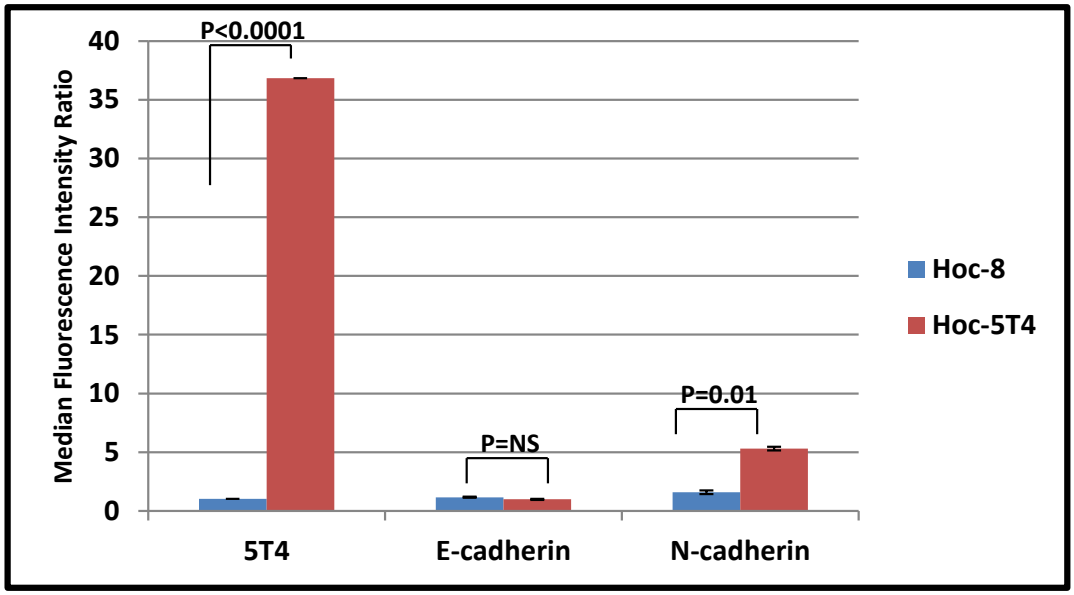

The effect of 5T4 overexpression on surface expression of E-cadherin and N-cadherin in Hoc-8 cells measured by flow cytometry

Hoc-5T4 cells expressed 5T4 as expected; while there was no change in E-cadherin surface expression after 5T4 over expression, there was a statistically significant increase in N-cadherin expression. 5T4 data are shared with **Figure 4.4**

Results represent average MFIR obtained by flow cytometry of at least three independent experiments, error bar= SEM.

5.4.2.2 Immunofluorescence Staining

Hoc-8 cells did not stain for 5T4 while Hoc-5T4 cells stained unevenly ranging from faint to strong positive **(Figure 5.8)**. Hoc-8 cells expressed the epithelial markers E-cadherin which was limited to some but not all cells while the 5T4 expressing cells Hoc-5T4 did not express E-cadherin **(Figure 5.8)**. Both cell lines Hoc-8 and Hoc-5T4 expressed N-cadherin and vimentin **(Figure 5.8)**.

Both Hoc-8 and Hoc-5T4 cell lines when stained with phalloidin showed mixed staining of actin cytoskeleton with no distinct difference in the actin structure. However, occasionally 'stress fibres' appeared more pronounced in Hoc-5T4 cells **(Figure 5.9)**.

Figure 5.8: 5T4 Overexpression and EMP by IF

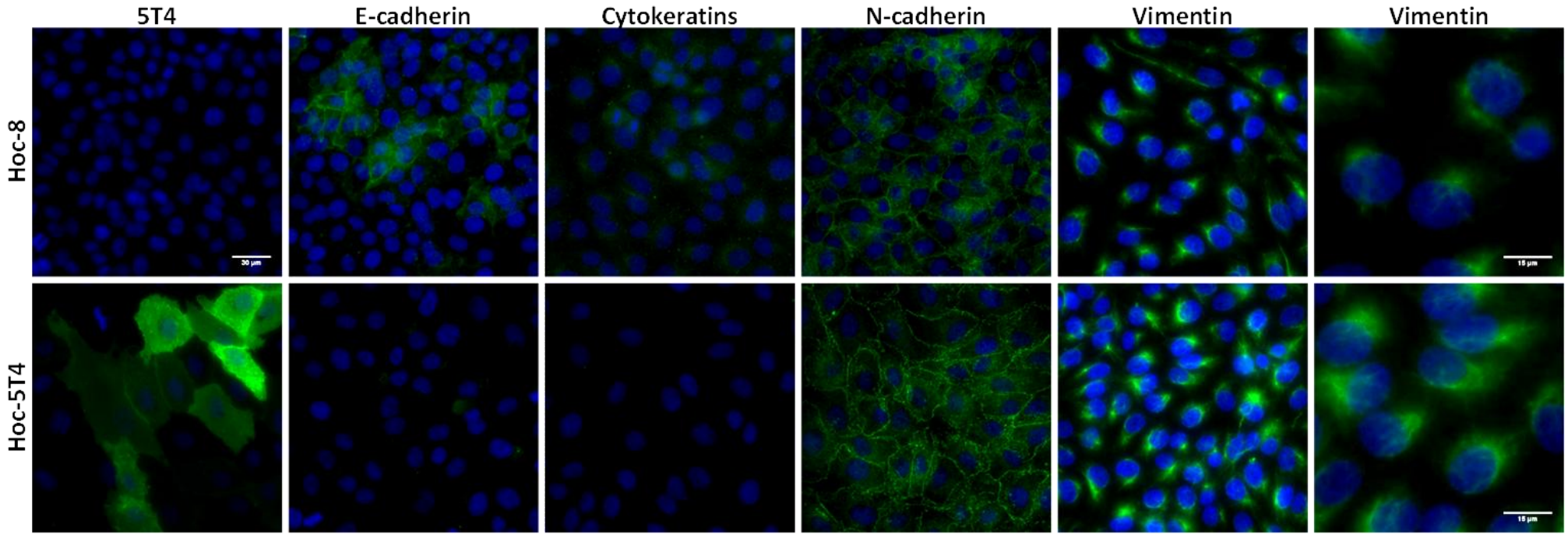

In situ immunofluorescence for EM markers in Hoc cell lines.

Cells from both cell lines (Hoc-8 and Hoc-5T4) cultured in identical conditions, fixed with 4% PFA at 80% confluence and stained for the different markers. Hoc-5T4 cells expressed 5T4 as expected albeit unevenly while Hoc-8 did not stain for 5T4. Hoc-5T4 lost E-cadherin expression which was present in Hoc-8 cells with no significant difference in other EMT markers.

Representative images of three independent experiments , scales bar: 30µm (15 µm far right images).Images captured with Axiovert 200M microscope mounted with CoolSNAP HQ camera, full panel of each marker staining in M&M chapter.

Figure 5.9: 5T4 Overexpression and Actin Cytoskeleton

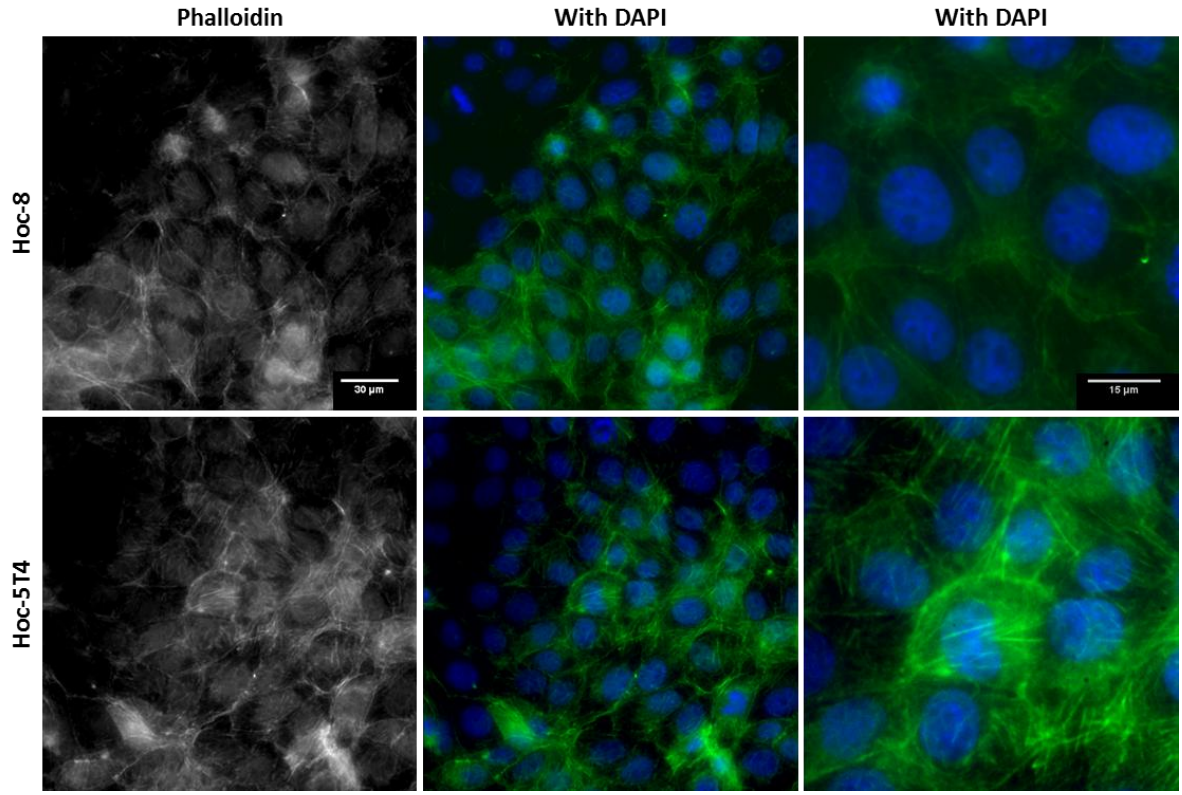

In situ immunofluorescence staining of cytoskeleton .
Hoc-8 and Hoc-5T4 cells were cultured in identical conditions, fixed with fresh 4% PFA at 80% confluence and stained with AF-488 phalloidin. Both cell lines seem to show occasionally 'stress fibre' organisation of the cytoskeleton which were more prominent in Hoc-5T4 cells. Representative images of three independent experiments, scales bar: 30µm (15 µm far right images).Images captured with Axiovert 200M microscope mounted with CoolSNAP HQ camera.

5.4.3 Cell Motility

In the previous chapter it was shown that in spite of successful overexpression of 5T4 in Hoc-5T4 cells this did not translate into a chemotactic response to CXCL12. However, chemotaxis assays revealed an increase in cell motility (cell migration to 1% serum) in Hoc-5T4 cells in comparison to Hoc-8 cells (31% to 40% of seeded cells, *P=0.005,* t test) **(Figure 5.10)**. In addition cell migration toward 10% serum increased in Hoc-5T4 compared to Hoc-8 cells from 39% to 47% of seeded cells (*P=0.03,* t test) **(Figure 5.10)**.

Figure 5.10: 5T4 Overexpression and Cell Motility

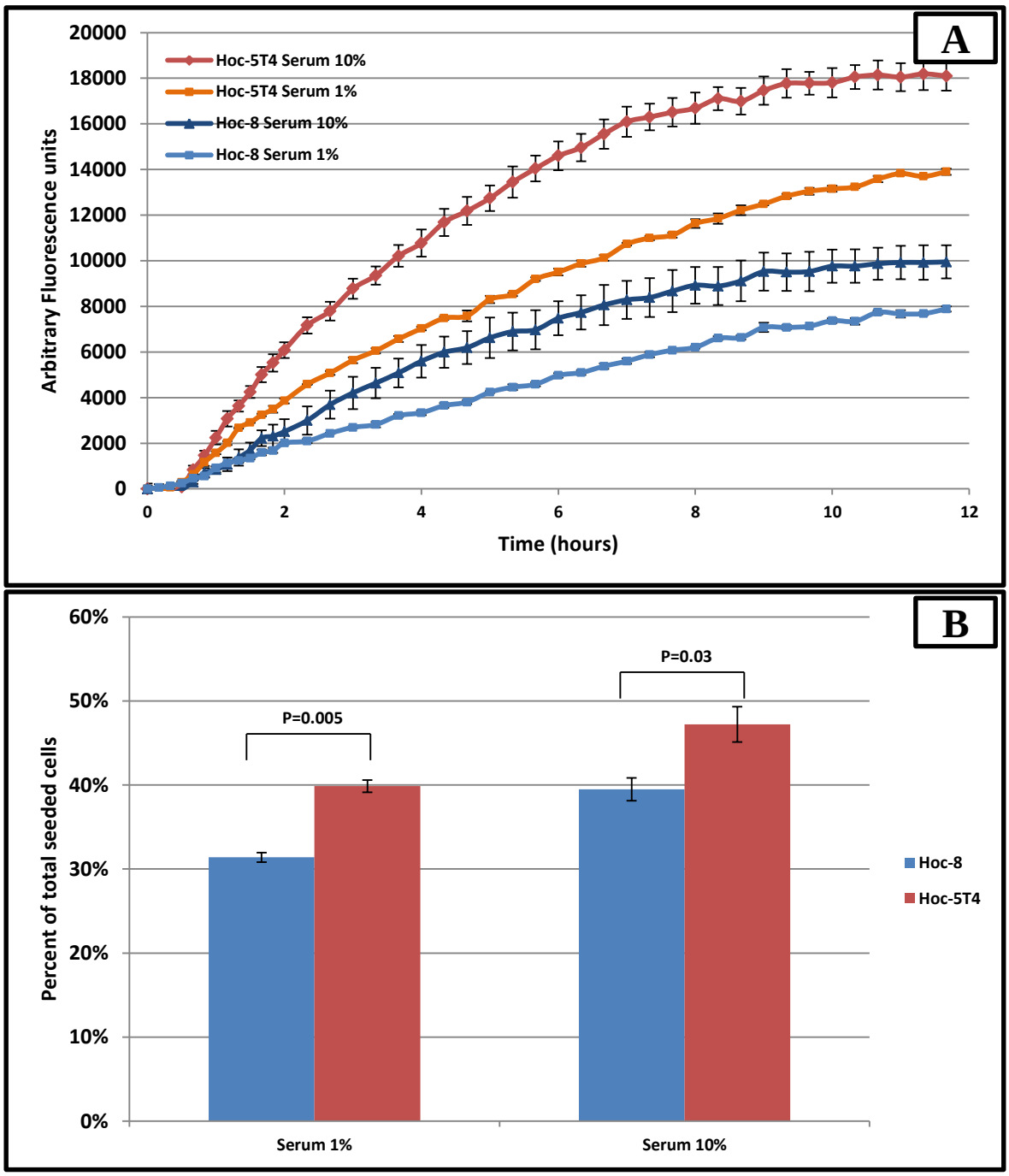

A: FluoroBlok Chemotaxis assay in Hoc and Hoc-5T4 cells
Hoc-5T4 cells migrated more toward 1% serum and 10% serum than Hoc-8 cells demonstrating a higher cell motility. Lines show fluorescence intensity value over the experiment period (12hours), values represent average of triplicates, error bars= SEM.

B: Modified FluoroBlok chemotaxis assay in Hoc-8 and Hoc-5T4 cells
Results confirming the findings in A but with actual cell number allowing for direct comparison. Results represent average percentage of seeded cells of three independent experiments, error bar= SEM.

5.5 Chapter Discussion

The effect of 5T4 expression on cell motility has been demonstrated in this chapter for the first time in human cancer cells; 5T4 knockdown in SKOV-3 cells resulted in a reduction in cell motility by 55%; and 5T4 neo-expression in Hoc-8 improved the already high motility by 30%.

The possibility that these changes in cell motility could be mediated by alterations in the cellular epithelial mesenchymal plasticity in both cell lines was explored. 5T4 knockdown in SKOV-3 cells was accompanied by evidence of a mesenchymal to epithelial transition (MET) as demonstrated by the following observations; cells adopted a flattened, broad morphology, substantively lost N-cadherin expression, expressed E-cadherin and cytokeratins, and showed re-arrangements of vimentin and the actin cytoskeleton **(Table 5.1)**. On the other hand, 5T4 neo-expression in Hoc-8 resulted in the expression of N-cadherin and the loss of E-cadherin expression; the effects on cytokeratin and vimentin, however, were less evident than those observed in SKOV-3 cells. **(Table 5.1)**.

Table 5.1: Summary of 5T4 Expression and EMP Phenotype

Marker	Method	SKOV-3	SKOV-C3	Hoc-5T4	Hoc-8
5T4	**FC (MFIR)**	11.4	2.4	36.8	1 (negative)
E-cadherin	**FC (MFIR)**	1 (negative)	1 (negative)	1 (negative)	1 (negative)
	IF	Negative	Positive*	Negative	Positive*
Cytokeratins	**IF**	Negative	Positive*	Negative	Positive*
N-cadherin	**FC (MFIR)**	3.1	1.8	5.3	1.5
	IF	Positive	Positive	Positive	Positive
Vimentin	**IF**	Cytoplasmic	Nuclear pole	Nuclear pole	Nuclear pole
Cytoskeleton	**IF**	Stress fibres	Diffuse	Stress fibres	Stress fibres
Cell motility	**(cell %)**	11.9%	5.4%	40%	31%
Migration to 10% serum	**(cell %)**	32.9%	8.5%	47%	39%
Shape		Spindle-like	Broad, flat	Spindle-like (0% serum)	

Summary of cell phenotype and cell motility changes following 5T4 KD and overexpression experiments. The bottom raw shows the impression of the overall phenotype whether epithelial or mesenchymal for each cell line. *: expression present in some cells only.

E-cadherin expression was demonstrated by in situ immunofluorescence in some but not all 5T4-KD SKOV-3 cells. It was not however detected using flow cytometry; where all cells appeared homogenous with a negative single peak histogram (MFIR = 1.0). The failure to detect E-cadherin expression by FC is likely to be caused by a removal or masking (proteolysis or conformational) of the specific epitope during cell detachment by trypsin. The same antibody (clone SHE78-7, Invitrogen) was successfully used during optimisation to detect E-cadherin by FC on H146, a small cell lung cancer (SCLC) cell line, which grows in suspension. The effect of trypsin on E-cadherin detection by FC was

shown in H146 cells as MFIR dropped from 20.4 to 4.7 when an extra step was added in which cells were incubated with trypsin for 3 minutes prior to FC staining.

Nonetheless, the selected upregulation of E-cadherin expression subsequent to 5T4 knockdown in SKOV-3 cells is an interesting observation, the reason for this limited expression in some cells is unclear. Given the fact that there is a broad spectrum within the epithelial mesenchymal phenotypes, 5T4 knockdown might produce cells which are at different stages of this spectrum and hence some, but not all cells, are at the epithelial end; a phenomenon known as the 'community effect'[284-286]. This is supported further by the type of staining observed in Hoc-8 cells which are constitutively negative for 5T4 and showed a similar pattern of staining for E-cadherin.

Another possible explanation is that 5T4-KD SKOV-C3 cells generally still express 5T4 (knock down and not a knock out) and only those cells which expressed 5T4 below a specific threshold level could potentially express epithelial markers. This could be investigated further by immunofluorescence co-staining for E-cadherin and 5T4 in future studies. Alternatively, one could perform limiting dilution experiments to select cells which are expressing E-cadherin and subsequent investigation of their expression stability versus cells which remained negative for E-cadherin could be attempted; FACS is not a suitable technique for this selection since E-cadherin was not detected on these cells by flow cytometry.

The exact mechanism by which 5T4 expression manipulation influences EMP was not explored in depth in this study. The involvement of other proteins is possible since 5T4 has the potential to interact with the actin cytoskeleton via the PDZ-binding domain in its C-terminus[10].

Epithelial mesenchymal plasticity (EMP) in the studied lines was investigated in this project by exploring the expression of selected epithelial (E-cadherin, cytokeratin) and mesenchymal (N-cadherin and vimentin) markers in addition to changes in the arrangements of cytoskeleton. While these are not the only markers of EMP, they are the most commonly used in the literature[157]. Other markers could be used in future research such as E-cadherin repressor proteins (SLUG SNAIL and TWIST) which could help to elucidate the mechanism by which 5T4 expression affects EMP. Such research could explore whether 5T4 expression manipulation has an effect on the expression of any of these repressor proteins and subsequently investigate 5T4 involvement in the mechanism leading to such expression changes.

Other than our published report **(Appendix 3)**[280] there has been no previous research into 5T4 KD in any cell type, nor have there been studies of the effect of 5T4 expression manipulation in ovarian cancer cells previously. The results presented here are in keeping with the relevant literature which mainly investigated 5T4 and EMT in murine (including 5T4 knockout) and human embryonic cells, such as the transient upregulation of 5T4 during embryonic stem cell differentiation which resembles EMT[24, 172, 174, 287]. Other reports were limited to overexpression studies; overexpression of full length 5T4 in CL-SI murine mammary cells or MDCK (Madin Darby canine kidney) epithelial cells resulted in increased motility with varying effect on cell morphology and attachment[175].

Consistent with that, 5T4 neo-expression in Hoc-8 cells resulted in increased cell motility but changes in EMT markers were less profound than the reciprocal changes observed by 5T4 KD in SKOV-3 cells. This could be a result of a selective developmental process whereby cells develop to function independent of 5T4, perhaps by expressing a paralogue protein; hence the expression of 5T4 would manifest with limited changes according to the availability of other proteins. The observation that serum starvation induced morphological changes in Hoc-5T4 cells which were not present at 10% serum could indicate that any 5T4 effect is context dependent, and future research could explore cell morphology and motility in serum-starved Hoc-8 and Hoc-5T4 cells.

Interestingly, Hoc cells regardless of their expression of 5T4 are generally very motile. For example, 39% of seeded Hoc-8 cells which did not express 5T4 migrated toward 1% serum in comparison with only 5% in SKOV-C3 cells which expressed low levels of 5T4. This high motility could explain the small increase in cell motility resulting from the overexpression of 5T4. It is plausible also that this high motility might have masked any possible chemotactic response to CXCL12.

Interestingly, induction of 5T4 expression in MDCK cells using truncated forms of 5T4 cDNA revealed a separable role for 5T4 in cell morphology and cell motility; the cytoplasmic domain was necessary to abrogate actin/cadherin-containing contacts but it did not affect motility[175]. This raises the possibility as to whether other pathways are involved in 5T4-mediated changes. One possible mechanism is the activation of the wnt non-canonical pathway, PCP, by 5T4 since 5T4/Waif1 was shown to block wnt canonical and activate non-canonical signalling in zebrafish embryo and HEK293T cells[26].

In this chapter, in situ IF provided a useful tool to explore protein expression and intracellular filament arrangement of actin cytoskeleton and vimentin in ovarian cancer

cells. Data have been presented in this study in a descriptive manner and no attempts were made to quantify the staining intensity.

Quantification in IF could be achieved by presenting the outcomes by the change in cell ratios or in the fluorescence intensities as calculated using ImageJ software for example. Descriptive analysis was chosen here since cells generally appeared to stain in a uniform pattern, and showed homogeneous morphology and molecular expression. In addition, concomitant quantitative data obtained by FC studies were in keeping with, and supported further, the results obtained by in situ IF.

Similarly, cell morphology under bright field confocal microscope was visually judged as prolonged shape or broad appearance. There were no attempts to measure cell diameter or volume in a quantitative manner which could have further supported the conclusions drawn in this chapter.

To conclude, in this chapter the two cell model, SKOV-3 (5T4 positive) and Hoc-8 (5T4 negative) were used by 5T4 KD in the first and 5T4 neo-expression in the second to show a link for 5T4 expression with cell motility and epithelial / mesenchymal phenotype. The findings of 5T4 KD experiments in general, and 5T4 overexpression in human ovarian cancer cells in particular, are novel in this study. While the results were not completely reciprocal, they were in keeping with the known published properties of 5T4. One possible mechanism by which 5T4 expression might exert its effect is modulating wnt response. Therefore, the following chapter investigates the role of 5T4 in wnt signalling in EOC cells.

Chapter 6

RESULTS:

5T4 Knockdown and Overexpression: wnt Signalling

5T4 and Wnt Signalling in Ovarian Cell Lines

6.1 Aim

To explore whether wnt signalling response in ovarian cancer cell line is influenced by 5T4 expression and whether such a response is associated with changes in cell motility.

6.2 Introduction

Wnt response is generally categorised into three pathways; one canonical involves nuclear translocation of β-catenin, and two non-canonical (β-catenin-independent) pathways: planer cell polarity (PCP) which is widely implicated in cell motility and calcium pathway[182]. In a recent study, 5T4 homolog in zebrafish (Waif1) was shown to negatively regulate canonical wnt signalling and to enhance the non-canonical wnt PCP pathway in zebrafish development[26]. Non-canonical wnt signalling generally enhances motility and invasive behaviour and thus 5T4 may also promote cancer spread by enhancing non-canonical Wnt signalling in EOC.

Wnt ligands are primarily canonical or non-canonical according to the wnt signalling pathway they mainly stimulate. In this project WNT3A and WNT5A were chosen to explore canonical and non-canonical pathways respectively in relation to 5T4KD in SKOV cell lines.

6.3 β-catenin Nuclear Translocation

In situ immunofluorescence was used to investigate the subcellular location of β-catenin in response to activation with wnt ligands. Lithium chloride (LiCl), an inhibitor of GSK3, was also used to stabilise cytoplasmic β-catenin and demonstrate β-catenin nuclear translocation.

SKOV-3, SKOV-CC and SKOV-C3 were seeded separately in complete growth media in glass-bottom 24 well plates At 80% confluence the growth media were replaced with fresh complete media supplemented with lithium chloride 50 µM (Sigma, 203637), WNT5A, 100 ng/ml (R&D systems, 645-WN), WNT3A, 100 ng/ml (R&D systems, 5036-WN) or left unsupplemented.

β-catenin staining appeared to be membranous with no significant nuclear staining when cells were not exposed to wnt ligands or LiCl **(Figure 6.1)**. However, with exposure to LiCl for 30 minutes all three cell lines showed translocation of β-catenin into nuclei confirming the integrity of wnt canonical pathway in these cells **(Figure 6.1)**. Exposure to WNT5A for six hours did not result in a significant nuclear staining of β-catenin suggesting that WNT5A has no canonical role in these cell lines at the studied concentration. Importantly, while WNT3A did not exhibit canonical stimulation in the parental (SKOV-3) or control (SKOV-CC) cells, it resulted in β-catenin transposition in the 5T4-KD cells (SKOV-C3) **(Figure 6.2)**.

6.4 Canonical wnt Response in 5T4-KD Cells is Dose Dependent

All three cell lines were incubated, at 80% confluence, for six hours with WNT3A at increasing concentration in complete growth media: 0, 10, 50, 100, 500 ng/ml. There was no nuclear immunofluorescence staining of β-catenin at any concentration in the 5T4-expressing parental (SKOV-3) or control (SKOV-CC) cells. However, increasing fluorescence intensity of nuclear β-catenin was shown as WNT3A concentrations increased with no apparent advantages for concentrations over 100 ng/ml **(Figure 6.3)**.

Figure 6.1: 5T4 Knockdown and β-catenin Nuclear Translocation (1)

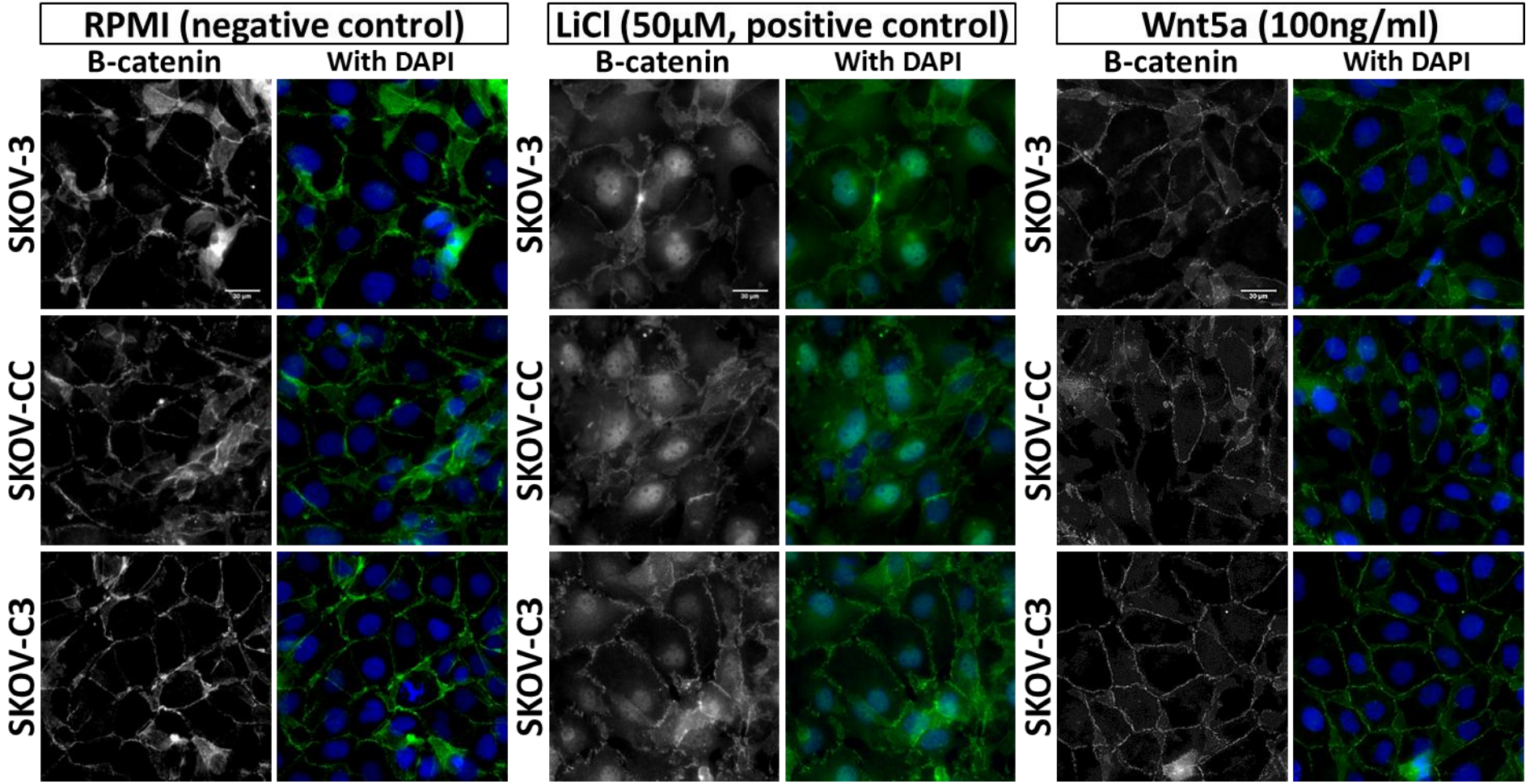

β-catenin translocation in SKOV cell lines. (also see Fig 6.2):

All three SKOV cells showed membranous and no nuclear staining for β-catenin when the growth media replaced with fresh RPMI with or without WNT5A. Exposure to lithium chloride (GSK3 inhibitor) resulted in strong nuclear staining for β-catenin as expected which confirmed the integrity of canonical wnt signalling pathway in all three cell lines as well as the validity of the staining method. Representative images of three independent experiments, scale bar: 30µm. Images captured with Axiovert 200M microscope mounted with CoolSNAP HQ camera.

Figure 6.2: 5T4 Knockdown and β-catenin Nuclear Translocation (2)

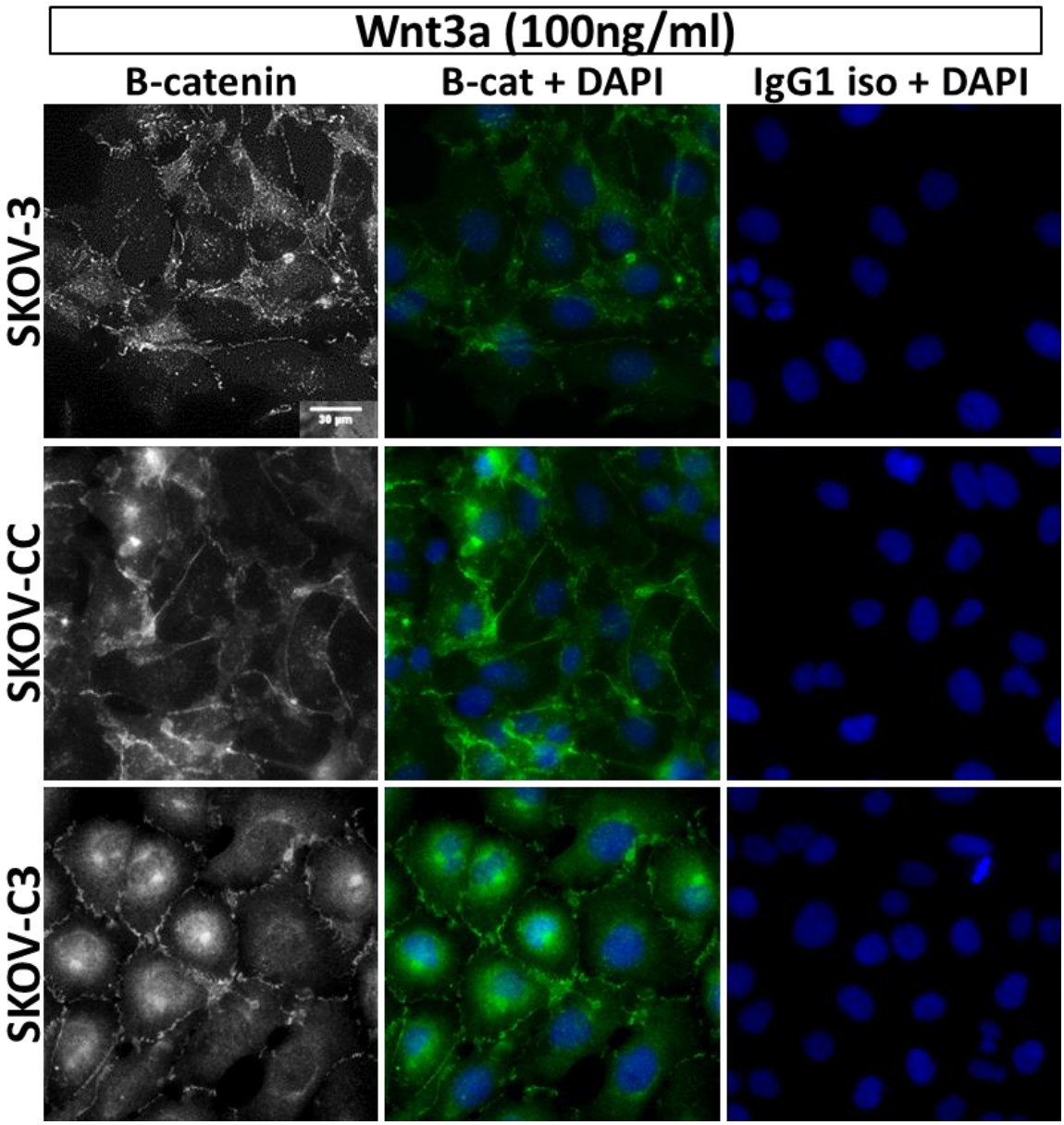

Wnt canonical signalling in SKOV cell lines. (also see Fig 6.1):
Exposure of SKOV-3, SKOV-CC and SKOV-C3 cell lines to recombinant WNT3A resulted in nuclear accumulation of β-catenin in the 5T4-knocked down cells only and not in the control or parental cells suggesting a role for 5T4 in inhibiting canonical wnt signalling in these cell lines.
Representative images of three independent experiments, scales bar: 30µm.Images captured with Axiovert 200M microscope mounted with CoolSNAP HQ camera.

Figure 6.3: β-catenin Nuclear Translocation: a Dose Effect

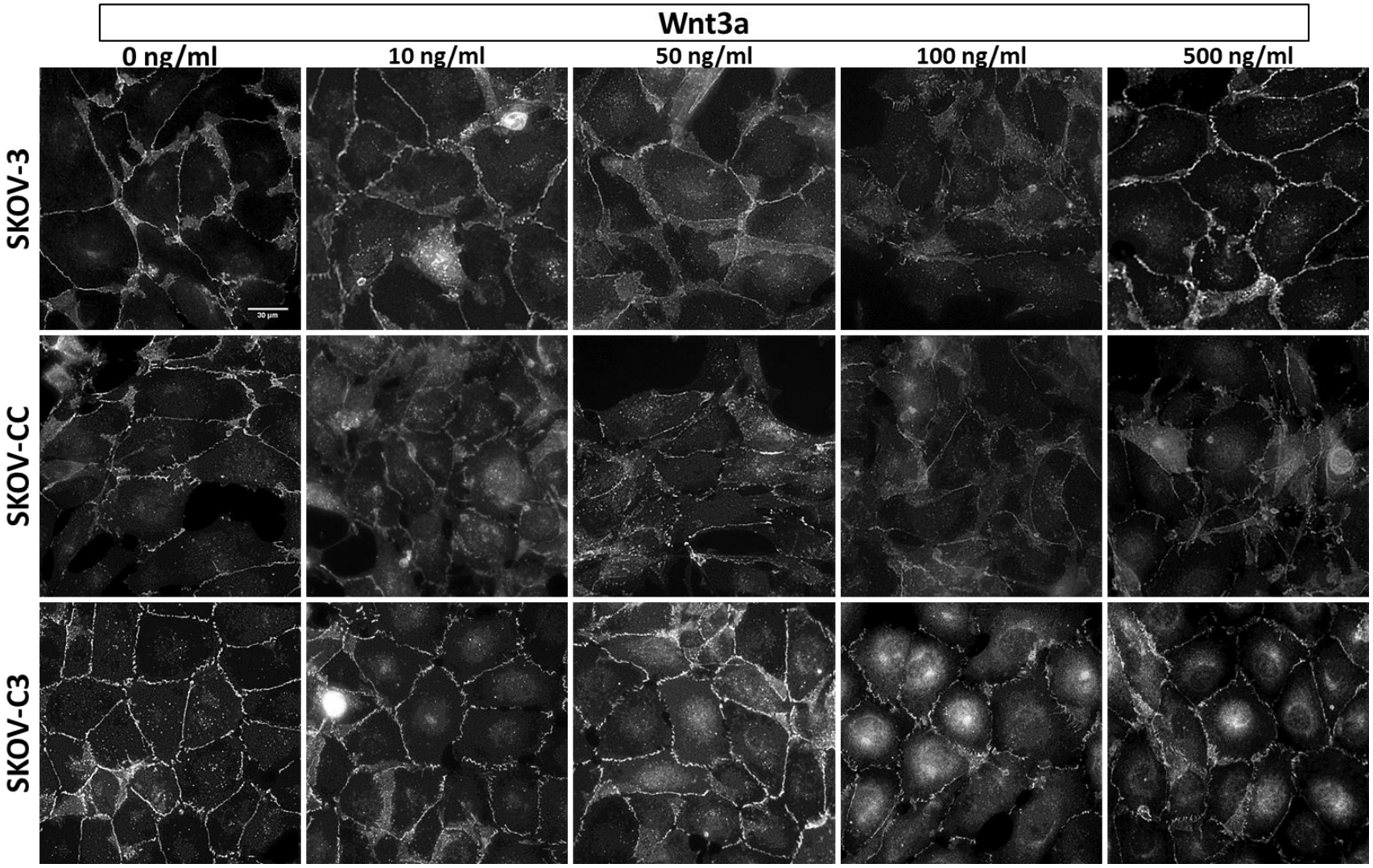

Dose effect of WNT3A in SKOV cell lines: Exposure of SKOV-3, SKOV-CC and SKOV-C3 cell lines to recombinant WNT3A at concentrations: 0, 10, 50, 100 and 500ng/ml showed no apparent effect in the control and parental cells at all concentrations. In the 5T4-knocked down cells there was nuclear accumulation of β-catenin which increased as WNT3A concentration increased up to 100ng/ml with no advantage for a higher concentration. Representative images of three independent experiments, scales bar: 30µm.Images captured with Axiovert 200M microscope mounted with CoolSNAP HQ camera.

6.5 WNT5A Increased Cell Motility in 5T4-Expressing Cell Lines

Cell motility was measured using modified FluoroBlok® assay where a plate scanner was used to count the number of cells migrated though the insert membranes. Cells were seeded in the upper chamber and left to settle for 4 hours while kept in cell culture incubator, then cells were incubated with WNT3A (100 ng/ml) or WNT5A (100 ng/ml) for 30 minutes prior to commencing the assay.

Cell motility was unaffected in all cell lines when incubated with WNT3A (98%, 99% and 97% for SKOV-3, SKOV-CC and SKOV-C3 respectively, *P = NS*, paired t tests) **(Figure 6.4)**. However, WNT5A resulted in a modest but statistically significant increase in cell motility in SKOV-3 cells (106%, *P = 0.048*, paired t test) and SKOV-CC cells (112%, *P = 0.001*, paired t test), while it did not have an effect on the 5T4-KD cells (SKOV-C3) **(Figure 6.4)**.

Figure 6.4: 5T4 Knockdown and Response to WNT5A

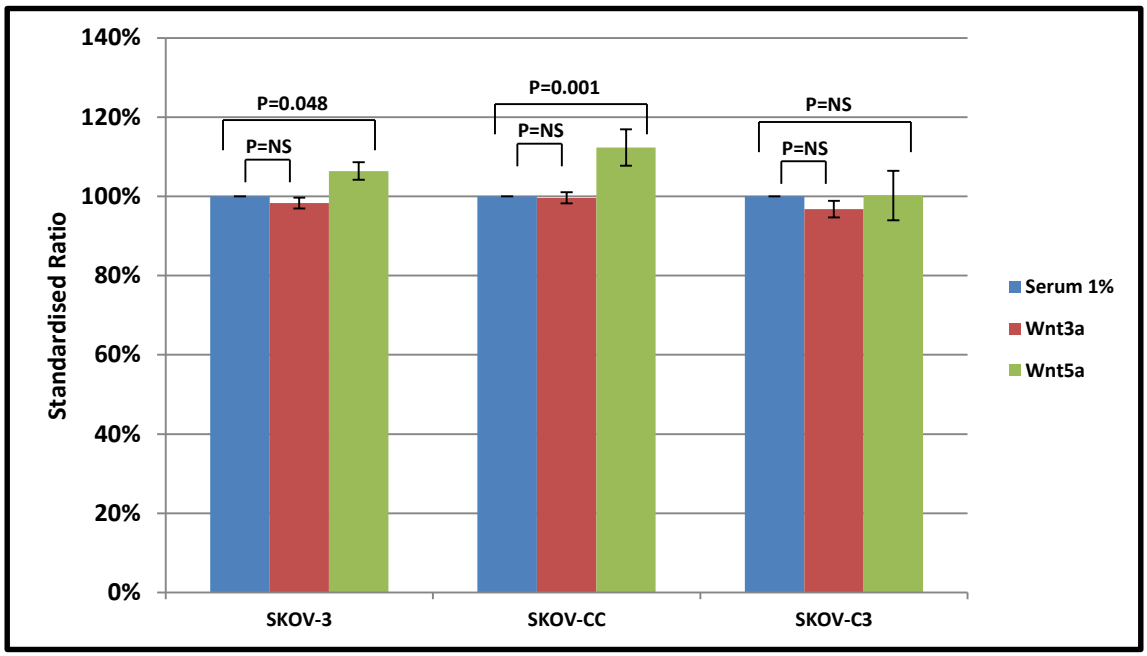

Wnt stimulation and cell motility in SKOV-3, SKOV-CC and SKOV-C3.
Both the parental (SKOV-3) and control (SKOV-CC) cell lines showed increased cell motility when incubated with WNT5A (100ng/ml) while the motility of 5T4-knocked down cells (SKOV-C3) was not changed. Incubation with WNT3A (100ng/ml) did not affect cell motility in all cell lines. Results represent standardised percentage ratio to the number of cells migrated to 1% serum in each experiment averaged of at least three independent experiments, error bar= SEM.

In addition, when WNT5A was added to the bottom chamber only, and not to the seeded cells in the top chamber cell motility remained unchanged in SKOV-3, SKOV-CC and SKOV-C3 cells (99%, 101% and 100% respectively) **(Figure 6.5)**. This suggested that WNT5A effect on 5T4-expressing cells was not a chemotactic one.

Figure 6.5: Response to WNT5A Is Not Chemotactic

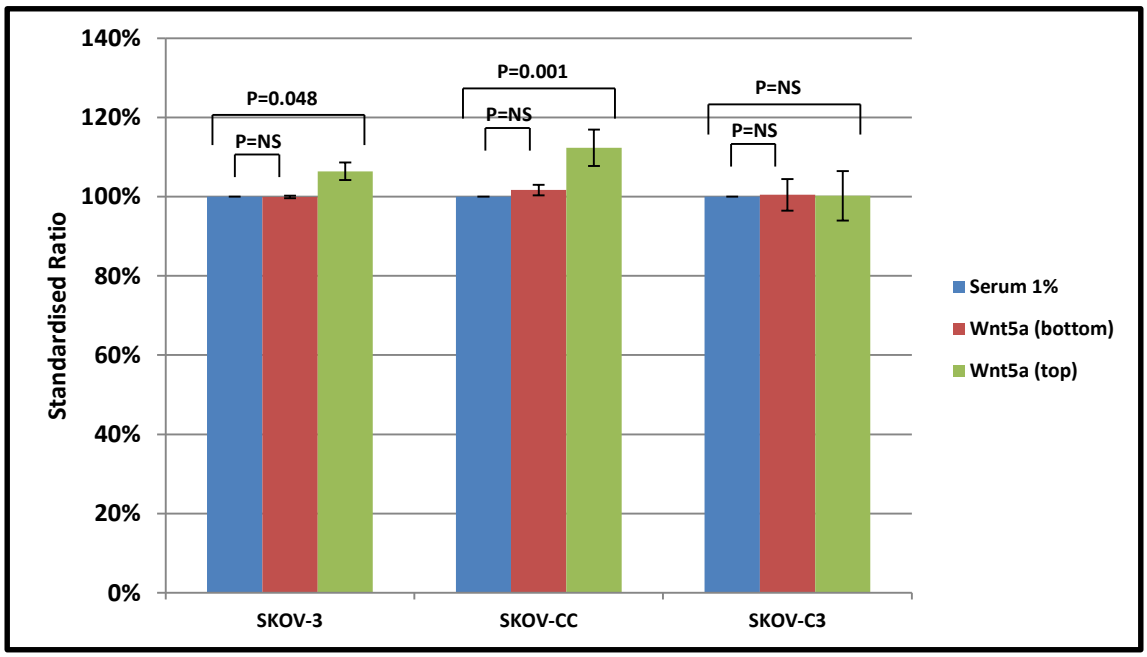

WNT5A is not a chemoattractant in SKOV-3, SKOV-CC and SKOV-C3.
While incubating cells in the top chamber of the chemotaxis assay increased cell motility in SKOV-3 and SKOV-CC cells, adding WNT5A only to the bottom chamber did not have an effect on cell motility suggesting that WNT5A is not a chemoattractant. WNT5A did not affect SKOV-C3 migration whether it is placed in the top or bottom chamber.
Results represent standardised percentage ratio to the number of cells migrated to 1% serum in each experiment averaged of at least three independent experiments, error bar= SEM

6.6 Wnt5a and CXCL12 Combined Effect: Exploratory Work

In a previous chapter it was observed that 5T4-expressing cell lines (SKOV-3 and SKOV-CC) but not 5T4-KD cells (SKOV-C3) responded chemotactically to CXCL12. Given the observations in this chapter that WNT5A improved cell motility in 5T4-expressing cells, the combined effect was investigated in two preliminary experiments which were not repeated given the time constraints.

In the first experiment, cells were incubated with WNT5A at 100 ng/ml concentration prior to routine CXCL12 chemotaxis assay. Cells migrated in larger numbers toward CXCL12-supplemented media when incubated with WNT5A than they did when the experiment media lacked CXCL12 or WNT5A. This was observed only in 5T4-expressing cells and not in 5T4-KD cells **(Figure 6.6)**, which raised the question whether there is an additive effect on cell migration when CXCL12 and WNT5A were used simultaneously in 5T4-expressing cells.

Figure 6.6: Possible Additive Effect for CXCL12 and WNT5A

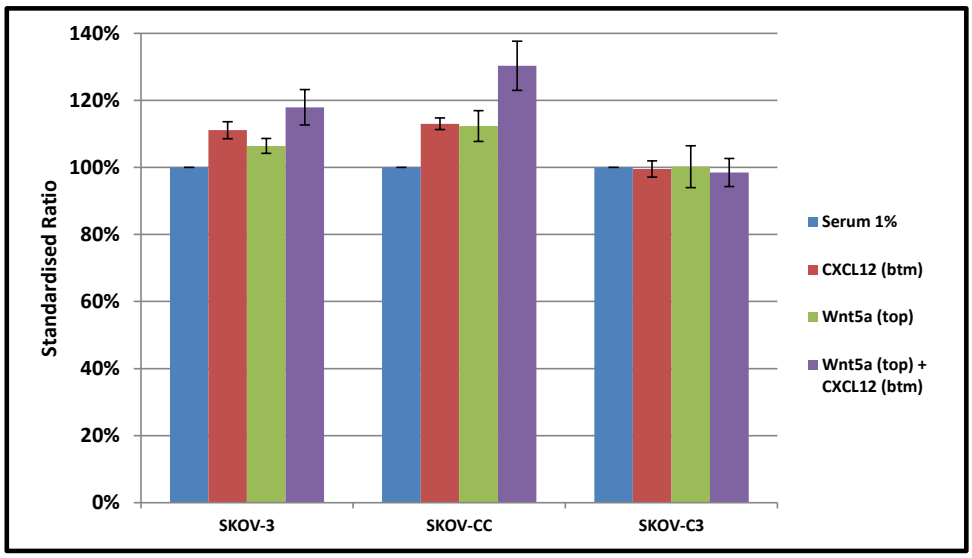

WNT5A and CXCL12 in SKOV-3, SKOV-CC and SKOV-C3.
When using CXCL12 as a chemoattractant to SKOV-3 and SKOV-CC cells incubated with WNT5A cell migration was increased. As expected the knockdown cells SKOV-C3 were unresponsive.
Results represent standardised percentage ratio to the number of cells migrated to 1% serum from **a single experiment**, error bar= SEM.

In the second experiment the optimal WNT5A concentration was explored in the presence of constant CXCL12 concentration of 200 ng/ml. It was observed that both cell motility and chemotactic response to CXCL12 improved as the WNT5A concentration increased from 0, 50 to 100 ng/ml with no added benefit with a concentration of 250ng/ml **(Figure 6.7)**.

Figure 6.7: CXCL12 and WNT5A Dose Effect

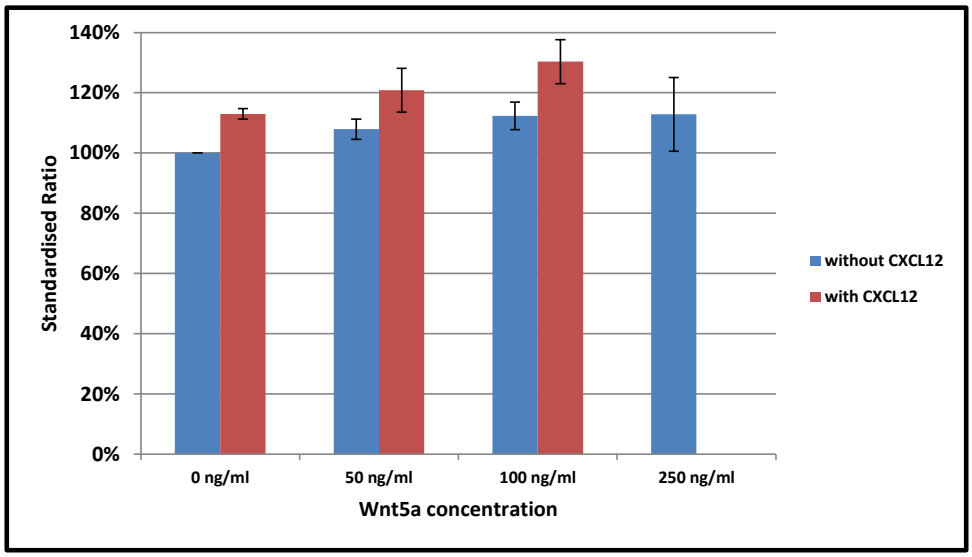

WNT5A concentration response in SKOV-CC cells.
Both cell motility and chemotaxis toward CXCL12 improved as WNT5A concentration increased up to 100ng/ml. There was no additional improvement when a higher concentration (250ng/ml) was used.
Results represent standardised percentage ratio to the number of cells migrated to 1% serum from **a single experiment**, error bar= SEM.

6.7 5T4 Overexpressing and wnt Response

The consequences of 5T4 overexpression in 5T4-Hoc-8 cells were investigated in terms of β-catenin nuclear translocation and cell motility. While untreated Hoc-8 and Hoc-5T4 cells showed mainly membranous β-catenin on IF staining, both cell lines demonstrated β -catenin translocation when incubated with lithium chloride **(Figure 6.8)**. However, both cell lines maintained the membranous position of β-catenin and failed to show nuclear translocation when exposed to WNT5A or WNT3A **(**Figure 6.9**Figure 6.8)**. In addition, WNT5A did not improve cell motility in Hoc-8 or Hoc-5T4 cells **(Figure 6.9)**.

Figure 6.8: 5T4 Overexpression and β-catenin Nuclear Translocation

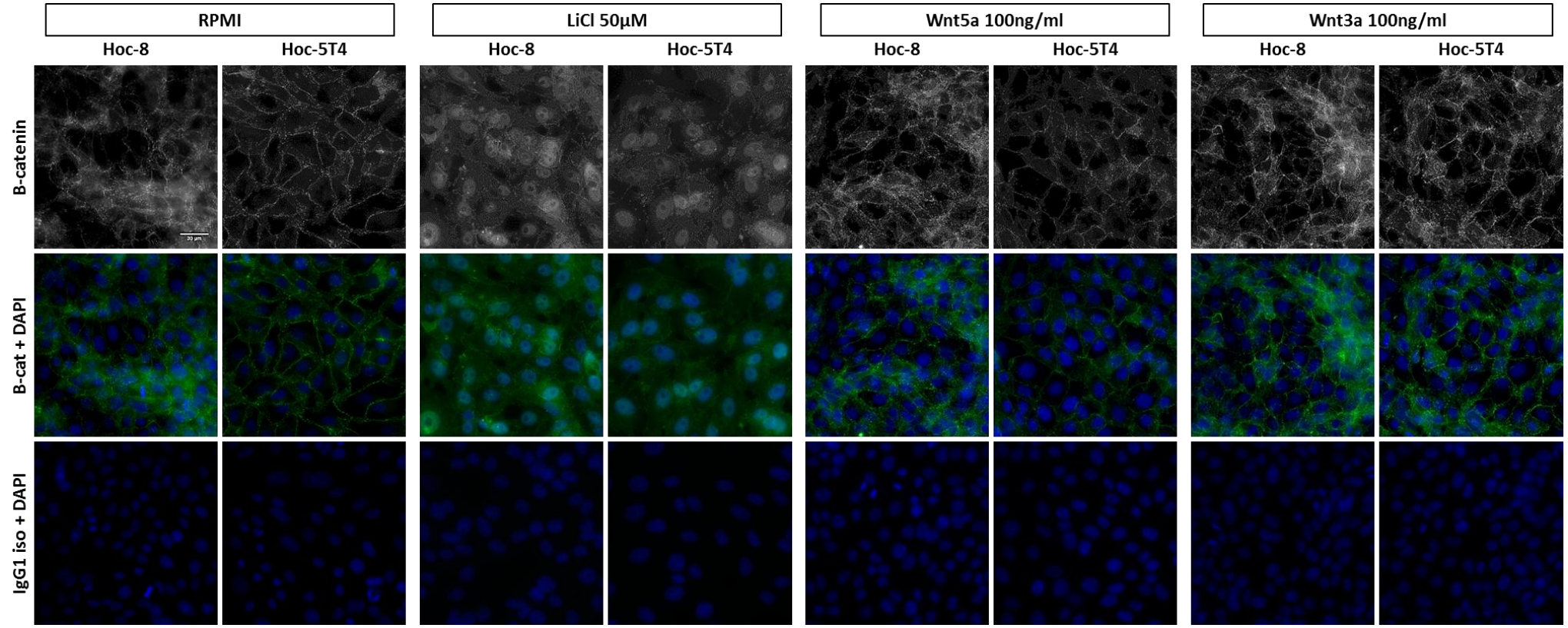

β-catenin in Hoc cell lines.

Both Hoc-8 and Hoc-5T4 cell lines showed membranous and no nuclear staining for β-catenin when the growth media replaced with fresh RPMI with or without WNT5A or WNT3A. Exposure to lithium chloride (GSK3 inhibitor) resulted in strong nuclear staining for β-catenin which confirmed the integrity of canonical wnt signalling pathway in both cell lines as well as the validity of the staining method.

Representative images of three independent experiments, scale bar: 30µm. Images captured with Axiovert 200M microscope mounted with CoolSNAP HQ camera.

Figure 6.9: 5T4 Overexpression and Non-Canonical wnt Reponse

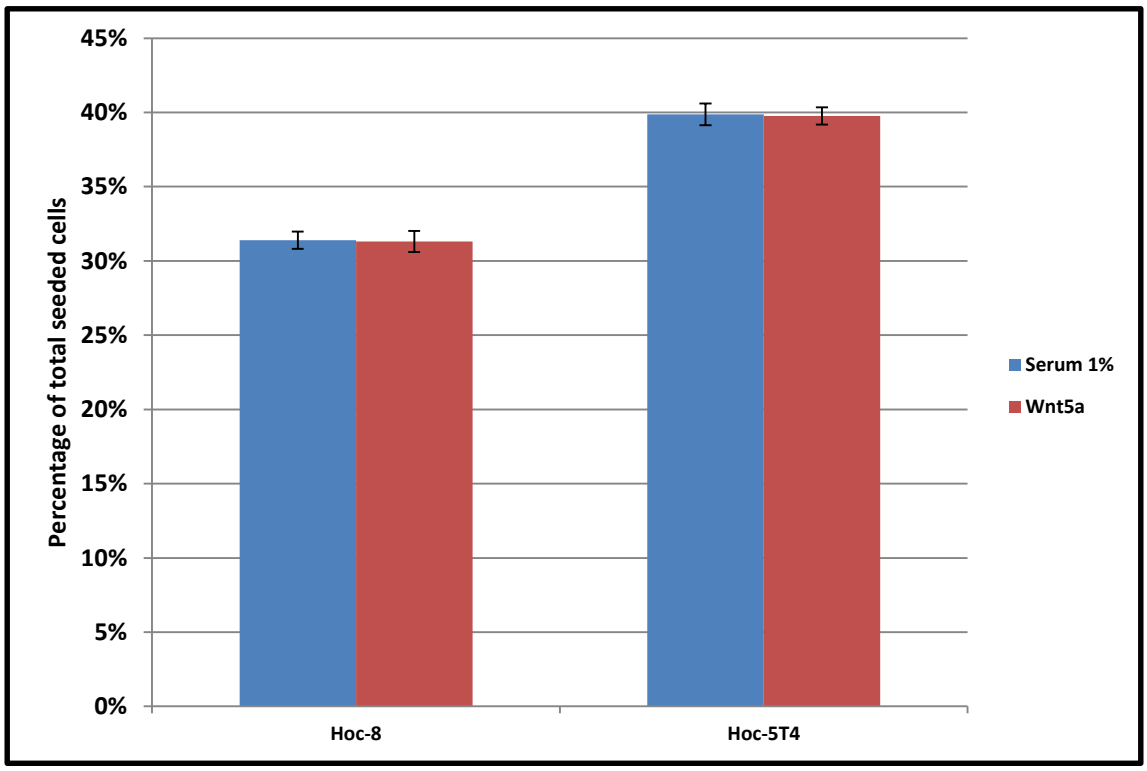

WNT5A and cell motility in Hoc-8 and Hoc-5T4.
While 5T4 overexpression improved cell motility in Hoc-8 cells, incubation with WNT5A did not result in change in cell motility.
Results represent standardised percentage ratio to the number of cells migrated to 1% serum in each experiment averaged of at three independent experiments, error bar= SEM.

6.8 Chapter Discussion

This chapter explored the effect of the manipulation of 5T4 expression on wnt response in EOC utilising Hoc-8 cells and their 5T4-expressing derivative (Hoc-5T4) as well as SKOV-3 cells and their 5T4-KD derivative (SKOV-C3).

The intracellular canonical wnt signalling pathway was confirmed intact in all three SKOV cell lines as demonstrated by β-catenin nuclear translocation in response to LiCl. The 5T4 expressing ovarian cancer cells, SKOV-3, did not show β-catenin nuclear translocation when stimulated with WNT3A, a response which was rescued when 5T4 expression was knocked down. β-catenin nuclear translocation suggested a canonical response which was confirmed in parallel research in our laboratory using a pBAR reporter assay **(Figure 6.10) (Appendix 4)**[288].

Figure 6.10: 5T4 KD and β-catenin Nuclear Activity: pBAR Reporter Assay

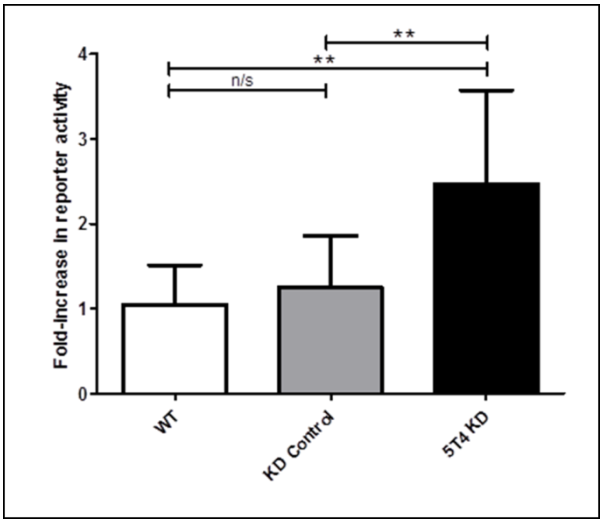

WNT3A and β-catenin nuclear activity in SKOV cells:
pBAR reporter assay shows that only 5T4-KD cells demonstrated nuclear activity when stimulated with WNT3A (100 ng/ml) for 6 hours suggesting a canonical wnt response, while both parental and KD control cells failed to respond.
Results represent pooled data from three independent experiments, error bar= SEM.

Experiment performed by Dr J Brazzatti, used with permission.

By contrast, the 5T4-KD SKOV-C3 cells did not respond to stimulation with WNT5A, which improved cell motility in the 5T4-expressing cells SKOV-3 and SKOV-CC. These results were supported by other research in our laboratory which showed, using a wound healing assay, that incubation with WNT5A improved cell motility in SKOV-C3 (5T4-KD) cells, but not in the parental or control cells[288]. Importantly, WNT5A did not act as a chemoattractant as cells did not migrate along its concentration gradient in FluoroBlok® chemotaxis assay.

Limited evidence from pilot experiments suggested that SKOV-C3 response to WNT5A activation was dose dependent and it improved chemotactic response to CXCL12. However, these limited data were generated from a single experiment which should be independently repeated in order to validate the findings.

The constitutively 5T4-negative Hoc-8 cell line and its 5T4-expressing derivative Hoc-5T4 did not respond to WNT3A or WNT5A in the experimental settings used in this study. While this could be an optimisation issue, as indicated by the relatively large error bars, or a limitation of the experimental methodology; it is possible to hypothesise that for 5T4 to exert its effect it requires a machinery of co-proteins which do not exist in constitutively 5T4 negative cells and which are not restored by the mere overexpression of 5T4.

The exact mechanism through which 5T4 KD modulates wnt signalling responses was not investigated in this project, nevertheless, parallel research by Dr J Brazzatti in the Stern laboratory, found that stimulating SKOV cells with WNT5A resulted in an increase in phosphorylated JNK (pJNK) using Western blotting in the 5T4 expressing cells but not in 5T4-KD cells **(Figure 6.11)**. This suggests that the PCP pathway is activated in cells expressing 5T4 but not 5T4-KD cells, in keeping with findings of this work. It was also found that SKOV-C3 (5T4-KD) cells showed more internalisation and phosphorylation of LRP6 in comparison with parental and control SKOV cells when stimulated with WNT3A-conditioned media. In addition, DKK-1 levels in the cell supernatant were lower in SKOV-C3 (5T4-KD) cells. These findings suggest that the mechanisms involved in 5T4 modulation of wnt signalling in these ovarian cancer cells might be different from those observed in in zebrafish and HEK293T cells where Waif1a was found to interfere with Wnt3a-induced LRP6 internalisation but not phosphorylation[26].

Figure 6.11: 5T4 KD and JNK Phosphorylation

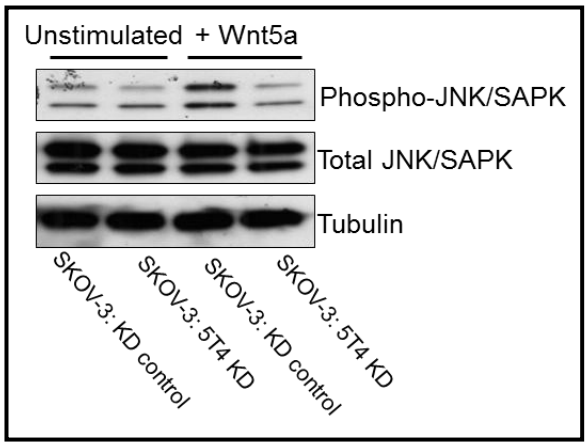

WNT5A and JNK activation in SKOv cells:
Western blot experiment shows that 5T4-KD cells failed to phosphorylate JNK protein when stimulated with WNT5A (100 ng/ml) for 6 hours while the KD control cells showed higher levels of the active JNK p-JNK suggesting a non-canonical wnt response in the presence of 5T4.

Experiment performed by Dr J Brazzatti, used with permission.

Future research could explore further a functional role for 5T4 in the wnt pathway in ovarian cancer cells by dissecting the different components of signal transduction in both canonical and non-canonical pathways. This could be achieved by generating complete 5T4 KO cells, using TALEN (Transcription Activator-Like Effector Nucleases) technology for example, and the reintroduction of full length, truncated or mutant forms of 5T4. In addition, utilising the recently available wnt inhibitors which act at different levels of the signalling pathways could help to illustrate the exact molecules involved.

WNT3A and WNT5A were exclusively used in this chapter to elucidate canonical and non-canonical activation respectively and they appeared to conform to these actions. However, both ligands have been reported to activate either pathway. Additionally other wnt ligands might reveal other roles for 5T4 expression in wnt signalling.

In this study, in situ IF provided a useful tool to explore wnt signalling in ovarian cancer cells. Quantification in IF could be achieved by presenting a particular outcome by the change in cell ratios or in the fluorescence intensities as calculated using ImageJ software for example. However, data have been presented in this study in a descriptive way rather than quantitative manner. This was chosen because cells generally appeared to respond in a uniform pattern, and showed homogeneous morphology and molecular expression as confirmed by concomitant FC data. In addition, quantitative methodology such as Western blotting and reporter assay was in use in the parallel research mentioned earlier.

Nevertheless, in spite of the generally distinct results, this does not exclude subtle changes in nuclear β-catenin which might be detectable by fluorescence intensity calculation. This could be explored in future studies utilising the recent advancement in technology such as the high throughput screening plate scanners. These machines are capable of detecting and scanning different fluorochromes simultaneously while its software could be programmed to identify nuclei and subsequently β-catenin translocation can be detected by quantifying changes in cytoplasmic and nuclear fluorescence intensity.

To conclude, 5T4 knockdown in SKOV cells resulted in canonical signal transduction in response to WNT3A stimulation with no detectable non-canonical response to WNT5A; these were reciprocal observations to the outcome of stimulating the 5T4-expressing cells separately with both ligands. These are novel findings in human cancer cells and are consistent with the observations made in zebrafish and HEK293T cells. The mechanisms of 5T4 interference in wnt signalling transduction in human cancer remains elusive and could be an interesting subject for future research.

The following chapter will investigate the role of 5T4 in human ovarian cancer spread, by probing protein expression using IHC on cancer tissues, not only for those involved in wnt signalling but also for components of CXCL12 chemotaxis and EMP; all of which have been found in this project to play a role in ovarian cancer cell line biology.

Chapter 7

RESULTS:

5T4 in Primary Ovarian Cancer

Primary Ovarian Tissues

7.1 Aim

To explore the expression of 5T4 and related molecules in paired primary human ovarian cancer tissues.

7.2 Introduction

Experiments in this study have revealed that 5T4 expression in specific ovarian cancer cell lines could have a role in the chemotactic response through the CXCL12/CXCR4 axis as well as in cell motility by influencing cellular epithelial mesenchymal plasticity (EMP) and by favouring non-canonical wnt signalling pathway. In addition, 5T4 expression has been previously found to correlate with clinical outcome and cancer stage in epithelial ovarian cancer (EOC). It is not clear, however, if 5T4 has a functional role in the spread of human EOC.

Formalin-fixed, paraffin-embedded (FFPE) human tissues sections were stained using immunohistochemistry (IHC) for 5T4, CXCL12 receptors: CXCR4 and CXCR7, EMP markers: E-cadherin, pan cytokeratins, N-cadherin, vimentin, and wnt signalling pathway proteins: β-catenin, Dkk1, JNK and phospho-JNK.

7.3 Human Tissues

In total, 11 paired (primary and metastatic) ovarian cancer specimens and five normal ovarian samples (surface epithelium and cleft epithelium) were investigated in this research. The diagnoses was reviewed and confirmed by gynaecological histopathologists in Central Manchester Hospitals prior to use.

7.3.1 EOC Specimens

None of the women in this study had been exposed to chemotherapy prior to sample collection; and in all women surgery (primary debulking) had been the first line of treatment for ovarian cancer. Five patients had high grade serous adenocarcinoma, two had carcinosarcoma, two patients had clear cell cancer, while the remaining two had high grade endometrioid carcinoma **(Table 7.1)**.

Each paired sample consisted of a specimen from the primary ovarian tumour and another specimen from a metastatic site from the same woman; making a total of 22 stained samples. Metastatic samples were from omentum in seven cases, from the contralateral ovary in three cases and from abdominal peritoneum in one woman.

Given the controversies of the cell of origin and organ of origin discussed in the introduction chapter **(Epithelial Ovarian Cancer Aetiology and Cell of Origin, 1.2.3)** specimens were selected to represent EOCs which were likely to originate from the ovaries rather than fallopian tubes or peritoneum. For this purpose only cases with a dominant ovarian tumour mass with no significant relevant pathology in the fallopian tubes were included[89, 289] **(Table 7.2)**.

In this study, fallopian tubes in the investigated tumours were assessed by a gynaecological histopathologist, fallopian tube epithelia were found abnormal only in two cases; one showed mucosal cancer deposits while the second had STIC lesions **(Table 7.2)**.

In eight cases the metastatic samples were obtained from omentum or peritoneum while metastatic samples were collected from the other ovary in three cases. In two of these three cases the primary site of the tumour was assigned to the ovary contained a tumour mass at least two fold larger than any mass on the other ovary in accordance with WHO classification[39]. The primary site of cancer was determined clinically during surgery in the remaining case as both ovaries had large tumours which were disrupted during surgery and was difficult to obtain accurate measurements on the fixed fragments.

No attempts were made to analyse data according to histological sub-type or site of metastasis given the small numbers of patients in each sub-group, however this would be of interest for future studies. At the time of writing this report (January 2014), all women but one lady were still alive with no data available regarding incidence of recurrence.

Table 7.1: Malignant Samples Characteristics

ID	Age (at operation)	Stage (pre 2014)	Grade	Histology
1	75 years	IIIc	3	High grade Serous
2	77 years	IV	3	Carcinosarcoma
3	62 years	IV	3	High grade Serous
4	55 years	IIIc	3	High grade Serous
5	76 years	IIIb	3	Clear cell
6	48 years	IIIc	3	Endometrioid
7	50 years	IIa	3	Endometrioid
8	55 years	IIIc	3	Carcinosarcoma
9	71 years	IIIc	3	Clear cell
10	77 years	IIIc	3	High grade Serous
11	76 years	IIIc	3	High grade Serous

Characteristics of malignant samples studied in this project:
11 paired samples were used; all were high grade tumours at advanced stages. For each tumour one sample was obtained from the primary cancer site and one sample from a metastatic site as shown in the table.

Table 7.2: Primary and Metastatic Sites

ID	Primary sample	Metastatic sample	Dominant tumour (cm)	Other ovary	Fallopian tube	
					Right	Left
1	Left ovary	Omentum	Left ovary, 15x11x6	5x5x2	Not identified	Not identified
2	Right ovary	Ovary	Right ovary 9x6x5	2x2x1	Not identified	Serosal invasion
3	Right ovary	Omentum	Right ovary, 17x12x10	Surface deposits	Normal	Normal
4	Right ovary	Omentum	Right ovary, 5x3x2	3x2x2	Mucosal deposits	Normal
5	Left ovary	Omentum	Left ovary, 10x7x4	No mass	Normal	Serosal deposits
6	Left ovary	Ovary	Left ovary, large*	Large*	Inflammatory changes	Normal
7	Left ovary	Ovary	Left ovary, 24x16x16	4x4x2	Normal	Normal
8	Left ovary	Omentum	Left ovary, 11x7x6	10x7x5	1 cm, para-fimbrial	Normal
9	Right ovary	Omentum	Right ovary, 18x14x13	No mass	Normal	Mesosalpinx deposit
10	Right ovary	Omentum	Right ovary, 6x4x4	No mass	STIC	Normal
11	Ovary	Peritoneum	Left Ovary, 11x10x7	6x4x3	Normal	Not identified

Sites of primary and metastatic samples studied in this project:
All samples were deemed EOC of ovarian origin as the dominant tumours were confined to the ovaries while the epithelia in all fallopian tubes were normal apart from cases (4) where cancer deposits were identified in the mucosa and case (10) which harboured STIC lesions. *: not measured as delivered in pieces to the laboratory.

7.3.2 Normal Ovarian Specimens

Normal ovary samples were obtained from women who had oophorectomy for non-malignant indications. All women but one were postmenopausal with the expected physiological atrophic changes of the ovarian surface epithelium (OSE) **(Table 7.3)**.

Table 7.3: Benign Samples Characteristics

Patient	Age (at operation)	Indication for surgery
1	60 years	Post-menopausal bleed (no cancer found)
2	55 years	Post-menopausal bleed (no cancer found)
3	43 years	Prophylactic (BRCA)
4	48 years	Pelvic pain (endometriosis)
5	52 years	Peri-menopausal bleed (no cancer found)

Characteristics of benign samples studied in this project:
5 samples were used; all but one patient were post-menopausal and none had cancer at the time of operative treatment as shown in the table.

OSE is a modified mesothelium consisting of a single cell layer covering ovaries and separated from stroma with a thin, collagen-rich zone called tunica albuginea **(Figure 7.1, A)**. Since ovarian inclusion cysts and clefts have been hypothesised as EOC precursors, therefore OSE and epithelium lining inclusion cysts / clefts were investigated separately in this study. Practically, very few inclusion cysts but several clefts were seen in the studied samples; hence epithelium lining clefts was used for comparison **(Figure 7.1, A-2)**.

OSE is often detached from ovaries and lost as a result of manipulation during surgical excision **(Figure 7.1, B)** which necessitated a meticulous inspection of ovarian surface so tunica albuginea or ovarian stroma were not confused as OSE. On the other hand, epithelia of inclusion cysts and clefts are usually preserved as they are out of the reach of surgical handling **(Figure 7.1, C & D).**

Ovarian stroma of the cortex and medulla were not analysed in this study. In addition, as only one of our samples contained sections of fallopian tube, this was not analysed in spite of its importance as epithelium of fallopian tube has been suggested as a possible source for high grade serous ovarian cancer.

Figure 7.1: Ovarian Surface Epithelium

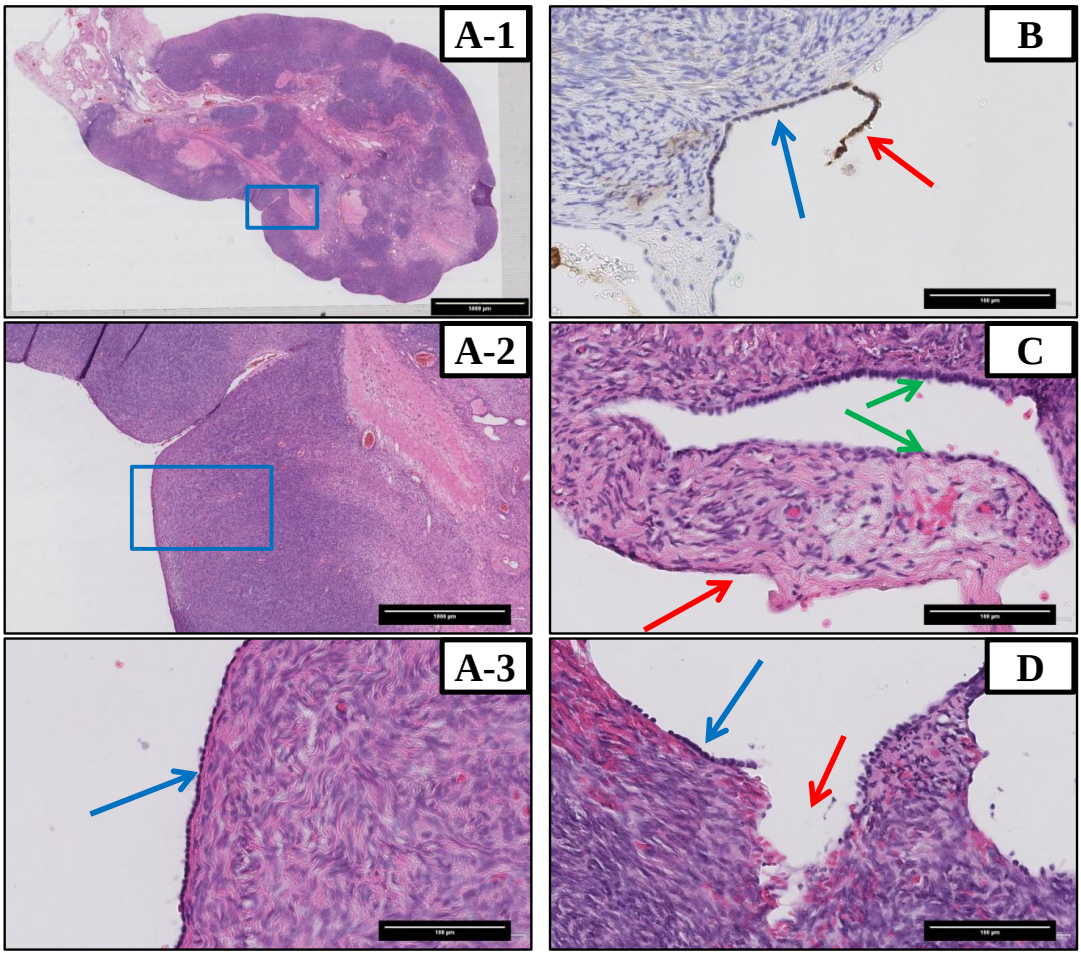

Normal ovary structure and identification of surface epithelium
A-1: a panoramic view of ovary, scale bar = 5mm; **A-2**: zoomed from A-1, shows ovarian cleft, scale bar = 1mm; **A-3:** zoomed from A-2, shows ovarian from outside to inside: surface epithelium (OSE) overlying the thin tunica albuginea (pink colour) followed by cellular ovarian stroma, scale bar 100µm;
B: shows OSE detaching in a sample perhaps caused by handling during surgery, scale bar 100µm;
C: intact surface epithelium lining an ovarian cleft (green arrows) while the OSE was lost on ovarian surface (red arrow), scale bar 100µm;
D: a further example of surgical damage of ovarian surface perhaps with surgical instrument (red arrow) and some remaining OSE nearby (blow arrow), scale bar 100µm.

7.4 Immunohistochemistry Staining

As detailed in the materials and methods chapter, Leica BOND-MAX robotic platform (Leica BIOSYSTEMS) was used for staining utilising Bond Polymer Refine Detection kit (Leica, DS9800). Once staining of all tissue sections with all studied antibodies and corresponding isotypes was completed, they were scanned with Leica SCN400 (Leica Microsystems) under the same settings to allow comparison between slides. Images were then stored and viewed with SlidePath Gateway LAN software (Leica Microsystems).

IHC staining assessment included the staining type and the staining score. In this chapter the terms ‘staining type’ and ‘type of staining’ are used to describe the sub-cellular IHC staining for a given molecule such as membranous, cytoplasmic, nuclear or mixed.

To evaluate immunohistochemistry staining, several rules were followed to assure reliable assessment across slides and to enable valid comparisons. The entire slide had to be assessed and scored at magnification power of 20X on the same computer screen with the same resolution settings for all slides. For each antibody, staining of tumour cells (or surface epithelial cells for normal ovarian specimens) assessed separately from stroma cells, however in this project only the results from tumour cells (and normal epithelium) are presented. For each antibody the type of staining was noted and categorised accordingly. Changes in the type of staining, if any, were noted when comparing primary and secondary tumours (such as a change between cytoplasmic and nuclear staining for example).

During staining, evaluating results and IHC scoring the researcher (SS) was blinded to which section was from the primary and which was from the secondary within each pair. This information was made available for final analysis after completion of all IHC assessment steps.

7.4.1 Scoring System

Scoring was performed with a semi-quantitative method[261-263]. To give staining a numeric score, five different levels of staining strength; negative, weak positive, moderate positive, strong positive and very strong positive were given the arbitrary scores of 0, 1, 2, 3, and 4 respectively. These five different levels were decided on before any scoring took place, as in **Figure 7.2**.

Subsequently the percentage of the cells at each staining level in each section was visually estimated. By so doing, all cells in the slide could be given a score for the strength of their staining and they would contribute to the final score of the slide. The score for each antibody (or isotype) in each slide was calculated as follows, with a working example is provided later in this chapter for clarification:

> IHC score = (0 x percentage of negative cells) + (1 x percentage of weak positive cells) + (2 x percentage of moderate positive cells) + (3 x percentage of strong positive cells) + (4 x percentage of very strong positive cells).

Figure 7.2: Immunohistochemistry Scoring Standards

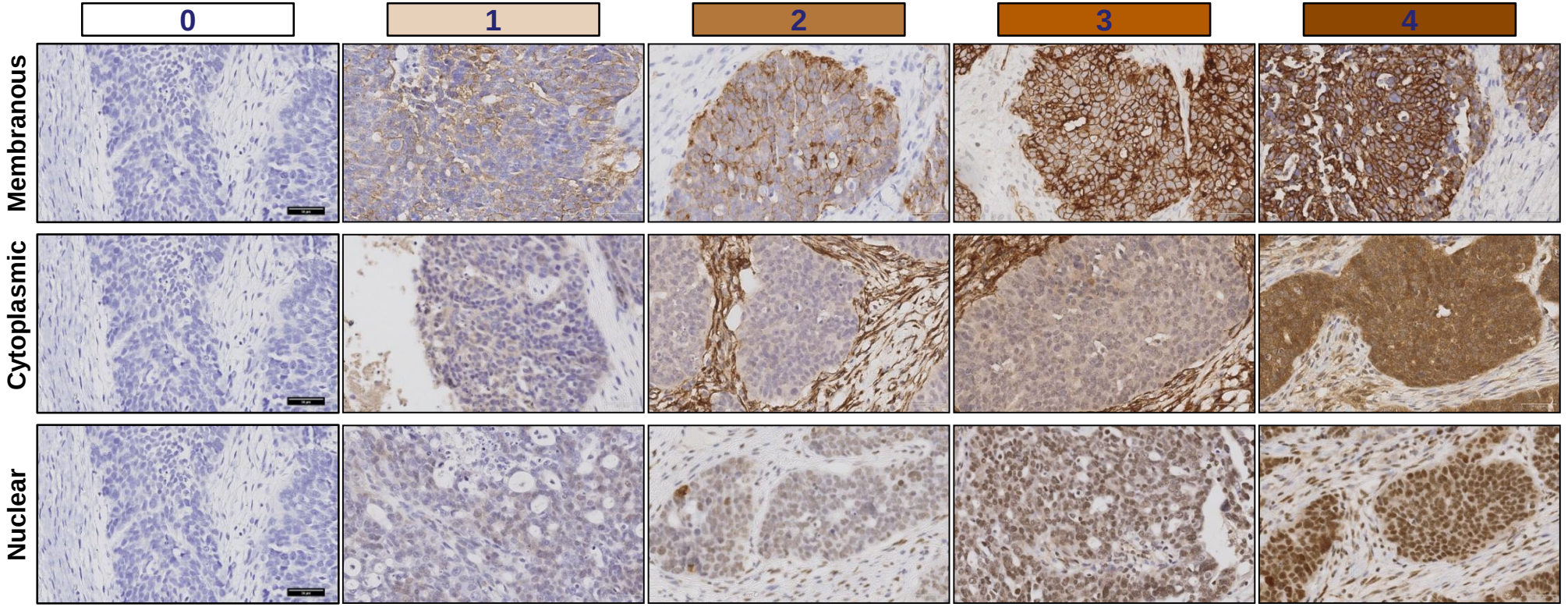

Semi-quantitative scoring in IHC

These are the standard images used to score stained tissue sections. First the type of staining was decided as membranous (first row), cytoplasmic (second row) or nuclear (third row). Occasionally staining could be a mixture of two types. Secondly, the strength of staining was decided according to the scale: 0 (being negative), 1 (weak positive), 2 (moderate positive), 3 (strong positive) and 4 (very strong positive). Scale bar = 50µm. These images were viewed at full scale, unlike here, during scoring process.

This formula gave results ranging from 0 (when all investigated cells were negative and none stained positive) to 400 (when all cells stained very strongly positive with no cells in the other staining levels). To simplify this further the results from the previous formula were divided by 4 and thus making the score range from 0 to 100.

The final staining score for a given molecule in a given section is the score of the antibody used to probe that molecule after subtracting the score of the relevant isotype.

7.4.2 Heterogeneity within Slides

Heterogeneity with cancer tissues in general and in EOC in particular is well documented. This was measured in this study by calculating the 'Homogeneity Score' for each marker which is the number of tumour sections out of a total of 22 for which at least 75% of tumour cells fit into one staining level: negative, weak positive, moderate positive, strong positive or very strong positive.

It follows that if cells are homogeneous in their expression of a protein it would be reasonable to expect that cells would stain for that antibody with the same intensity and therefore the majority would fall in a single level out of the five levels used in this study. The percentage of 75% is an arbitrary one and it was thought to be a reasonable cut off point for this study.

7.4.3 Working Example

The scoring of β-catenin staining in case (11) metastatic section is shown here as an example **(Figure 7.3)**. First the entire slide was inspected at 20X magnification; a difference between tumour cells and stroma cells was noticed in terms of the strength and type of staining. Staining in tumour cells was dominantly membranous while it was mainly cytoplasmic in the stroma cells. When compared with the membranous staining standards as in **Figure 7.2**, staining for β-catenin was scored as: negative=0%, weak positive=0%, moderate positive=0%, strong positive=75% and very strong positive=25%. The staining score therefore was calculated: (0x0)+(1x0)+(2x0)+(3x75)+(4x25)=325/400; giving a score for β-catenin staining of tumour cells in this section of 81. However, staining for the relevant isotype IgG1 was found to have as score of 3 (90% of cell were negative and 10% were weak positive; (0x90)+(1x10)=10/400. Therefore the final score for β-catenin in this sample is 78. Since in this tumour 75% of cells were in one strength level therefore staining for β-catenin of tumour cells in this specimen was considered to be homogeneous.

Figure 7.3: Immunohistochemistry Scoring Example

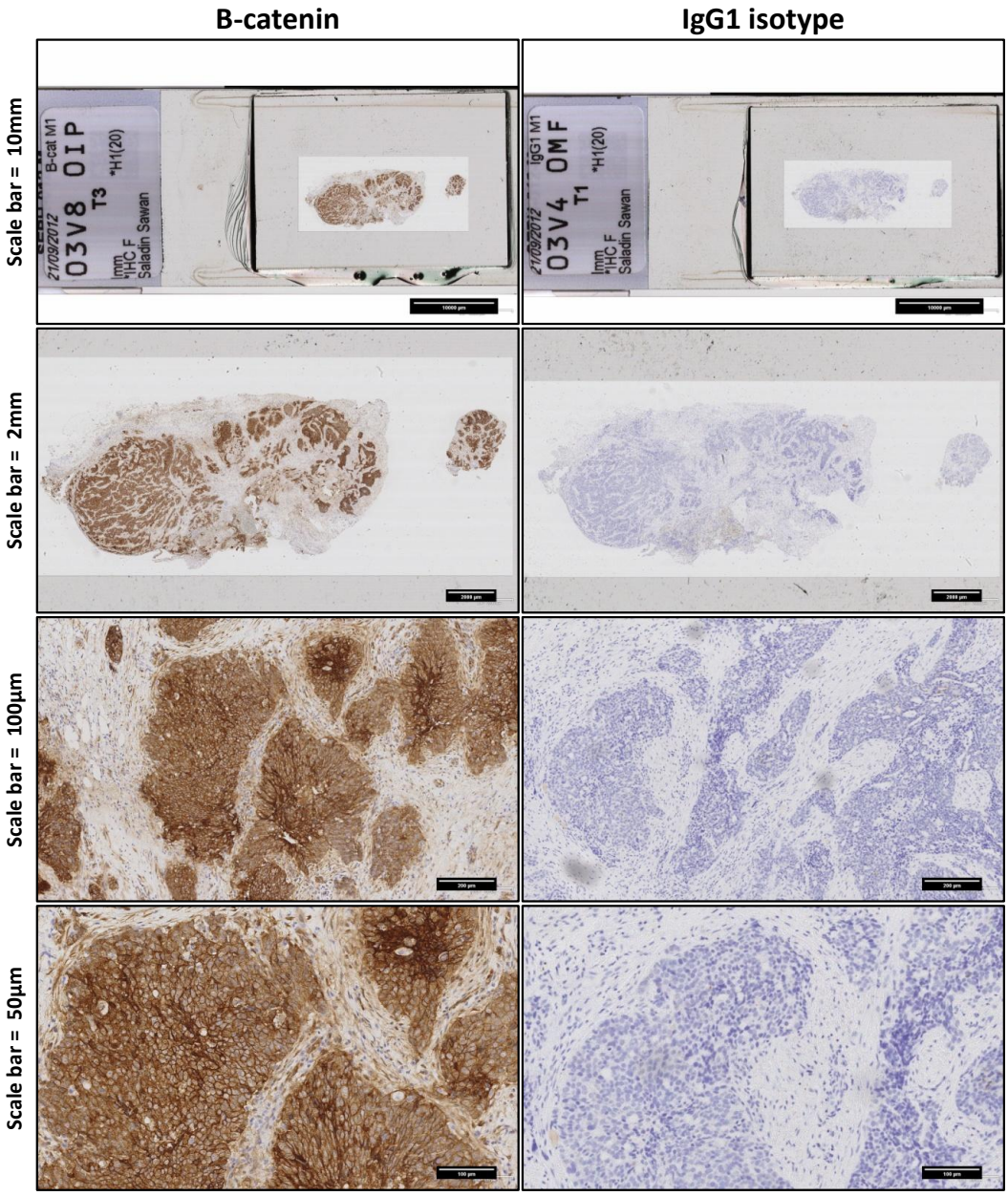

Working example of scoring of β-catenin IHC staining in a metastatic specimen

Staining for β-catenin (left column) and the relevant isotype (right column) with increasing magnifications from top down (scale bars are shown to the left of pictures). In this example 75% of cells were judged to be strong positive and 25% were very strong positive giving a score of: (3x75)+(4x25)=325/400, i.e.: 81. The staining for IgG1 isotype staining was judged to be 3 and therefore the final score for B-catenin in this sample was decided to be 78.

7.4.4 Scoring Validation

One important challenge for using IHC is the potential subjectivity in quantifying protein expression levels. In this study a semi-quantitative scoring system[261-263] was used by a single assessor (SS) who was blinded to the nature of slides in terms of primary or secondary specimens.

In hindsight the results of this chapter could have been strengthened and quality-controlled by external validation. Several methods can be used to validate IHC results such as scoring by a second assessor or by the use of specialised scoring software, such as Definiens® program, which helps to minimise operator-dependent variability. Generally, this software requires 'teaching' for each probed protein and its isotype control which requires significant time to obtain satisfactory results; as such it might be more appropriate for studies involving a large number of sections. This was impractical in this study which investigated protein expression in a relatively small number of sections.

7.5 Results

7.5.1 5T4 Expression

The staining for 5T4 in the tumour cells was membranous or mixed membranous/cytoplasmic in both the primary and the metastatic specimens. Generally there was no intra-patient variation in the type of staining (between the primary and the metastatic samples in each woman). On the other hand, 5T4 staining in the normal ovaries was dominantly cytoplasmic in OSE and the cleft epithelium **(Figure 7.4-A)**. There was a clear intra-tumour heterogeneity in the strength of staining for 5T4 with only 7 of the 22 studied cancer samples showing a dominant staining level.

Overall, all tumour samples showed positive staining for 5T4, however, with a wide inter-tumour variation. The staining score range was 7.5 - 66.3 for the primary cancers and 12.5 - 76.3 for the metastases. The means of staining scores were 34.5 and 51.6 for the primary and the metastatic specimens respectively (*P=0.004*, paired t test) **(Figure 7.4-B)**. 5T4 expression was higher in the metastatic lesions than their corresponding primary cancers in ten women while it decreased in one patient only (P=0.007, X^2 test) **(Figure 7.4-C)**. This indicates that the change within the tumour itself between the primary and the metastatic samples is more pronounced than the change in the overall averages in the studied cancers.

In the normal ovary samples 5T4 expression was lower in the surface epithelium than in the cleft epithelium with the respective score means of 13 and 71.5 (P=0.03, paired t test) **(Figure 7.4-B)**. In keeping with previous studies, 5T4 expression in the primary tumour samples was higher than that in normal surface epithelium (score means 34.5, 13 respectively, *P=0.03*, t independent test) **(Figure 7.4-B)**.

Figure 7.4: 5T4 IHC in Ovarian Specimens

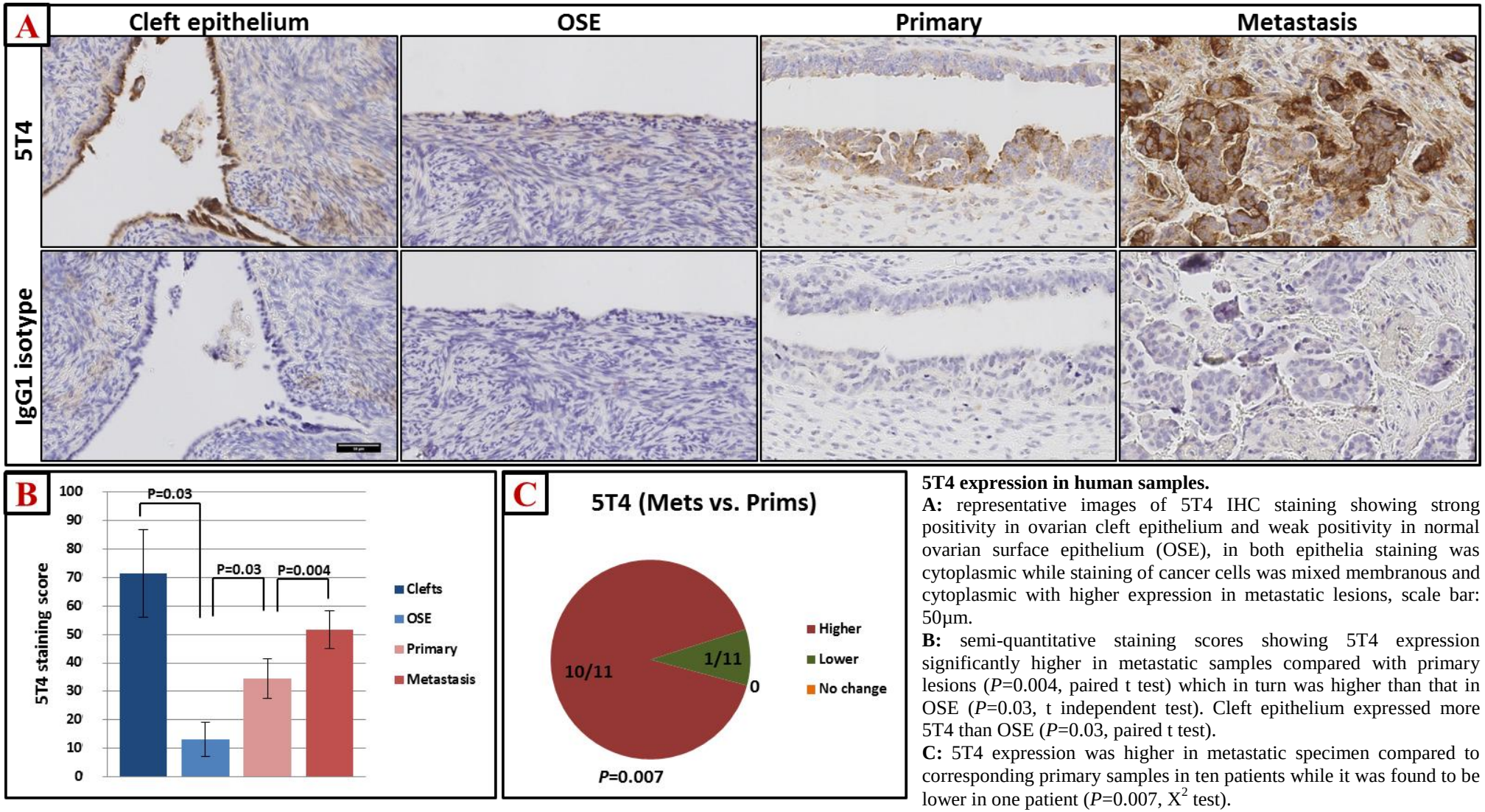

5T4 expression in human samples.

A: representative images of 5T4 IHC staining showing strong positivity in ovarian cleft epithelium and weak positivity in normal ovarian surface epithelium (OSE), in both epithelia staining was cytoplasmic while staining of cancer cells was mixed membranous and cytoplasmic with higher expression in metastatic lesions, scale bar: 50µm.

B: semi-quantitative staining scores showing 5T4 expression significantly higher in metastatic samples compared with primary lesions (P=0.004, paired t test) which in turn was higher than that in OSE (P=0.03, t independent test). Cleft epithelium expressed more 5T4 than OSE (P=0.03, paired t test).

C: 5T4 expression was higher in metastatic specimen compared to corresponding primary samples in ten patients while it was found to be lower in one patient (P=0.007, X^2 test).

7.5.2 CXCL12 Receptors

7.5.2.1 CXCR4 Expression

Staining for CXCR4 was absent in normal ovarian epithelium (OSE and clefts), whilst tumour cells which expressed CXCR4 showed membranous staining in both the primary and the metastatic specimens with no intra-patient variation in the type of staining **(Figure 7.5-A).** Overall, the majority of tumour samples did not stain for CXCR4 while others showed low staining score with 14 of the 22 studied cancer samples showing mostly negative staining.

The staining score range was 0 - 35 for the primary tumours and 0 - 45 for the metastases. The means of staining scores were 8.6 and 10.2 for the primary and the metastatic specimens respectively (*P=NS*, paired t test) **(Figure 7.5-B)**. CXCR4 expression was higher in the metastatic lesions than their corresponding primary cancers in three women, while it decreased in three women and remained unchanged in five (*P=NS*, X^2 test) **(Figure 7.5C)**.

7.5.2.2 CXCR7 Expression

The staining for CXCR7 was nuclear or mixed nuclear/cytoplasmic in all benign and malignant specimens, generally there was no intra-patient variation in the type of staining **(Figure 7.6-A)**. There was some intra-tumour homogeneity in the strength of staining for CXCR7 with 10 of the 22 studied cancer samples showing a dominant staining level.

Overall, most tumour samples showed positive staining for CXCR7, however, with a wide inter-tumour variation; the staining score range was 0 - 75 for the primary cancers and 0 - 87.5 for the metastases. The means of staining scores were 43.2 and 45.9 for the primary and the metastatic specimens respectively (*P=NS*, paired t test) **(Figure 7.6-B)**. CXCR7 expression was higher in the metastatic lesions than their corresponding primary cancers in five women while it decreased in three women and remained unchanged in three (*P=NS*, X^2 test) **(Figure 7.6-C)**.

In the normal ovary samples CXCR7 expression was lower in the surface epithelium than the cleft epithelium with respective score means of 16 and 46 but this did not reach statistical significance (*P=NS*, paired t test) **(Figure 7.6-B)**.

Figure 7.5: CXCR4 IHC in Ovarian Specimens

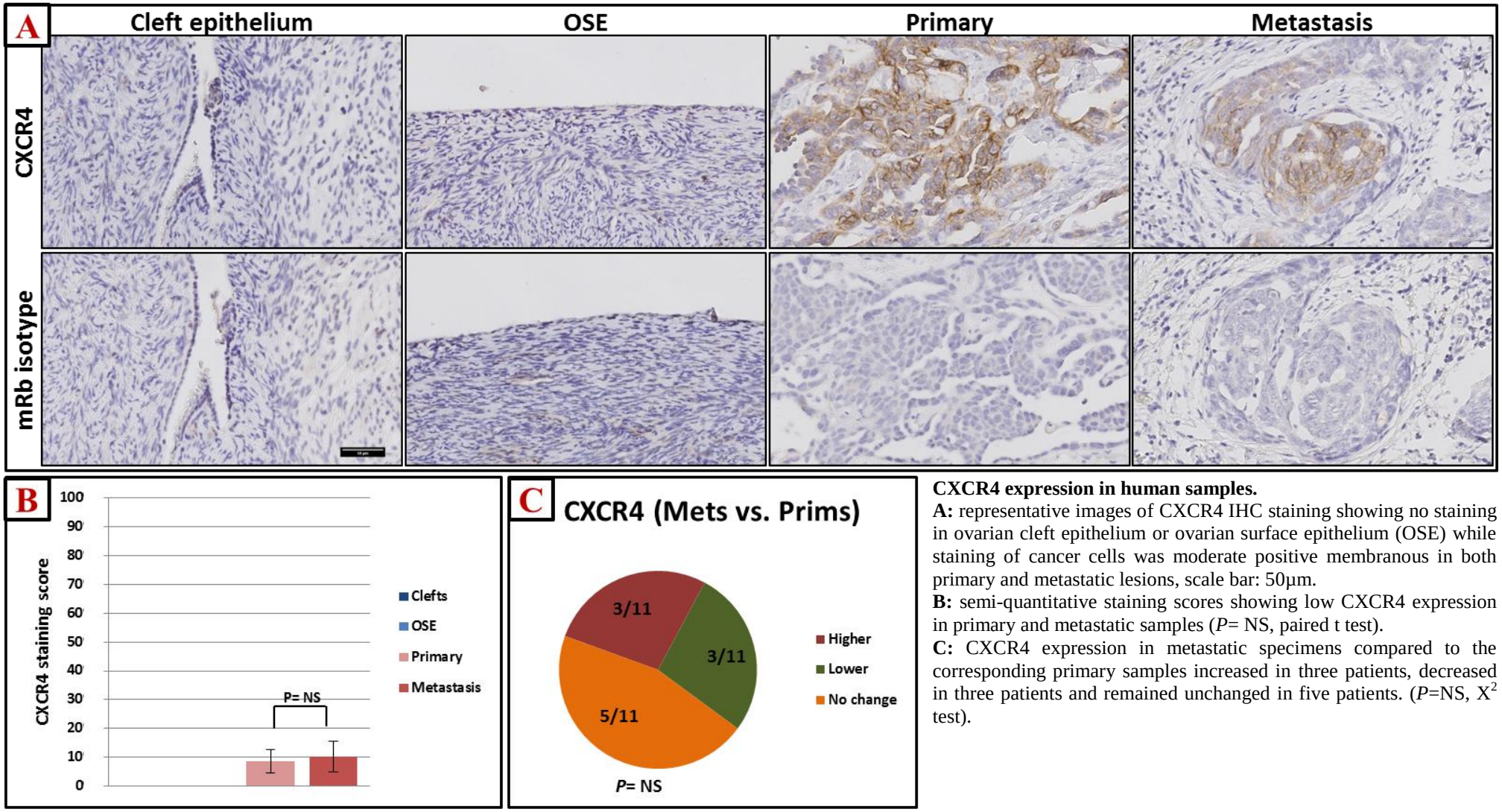

CXCR4 expression in human samples.
A: representative images of CXCR4 IHC staining showing no staining in ovarian cleft epithelium or ovarian surface epithelium (OSE) while staining of cancer cells was moderate positive membranous in both primary and metastatic lesions, scale bar: 50µm.
B: semi-quantitative staining scores showing low CXCR4 expression in primary and metastatic samples (*P*= NS, paired t test).
C: CXCR4 expression in metastatic specimens compared to the corresponding primary samples increased in three patients, decreased in three patients and remained unchanged in five patients. (*P*=NS, X^2 test).

Figure 7.6: CXCR7 IHC in Ovarian Specimens

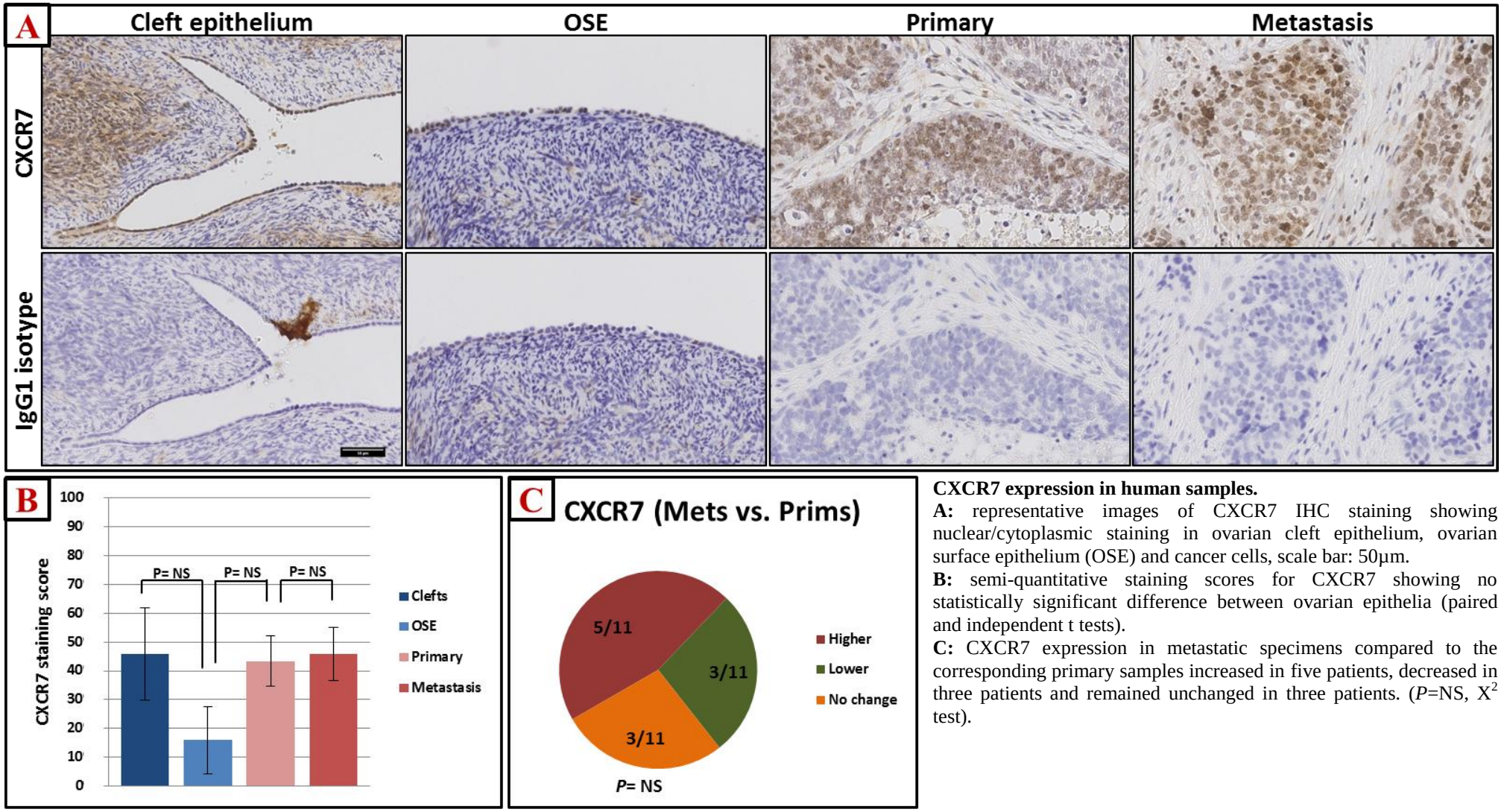

CXCR7 expression in human samples.
A: representative images of CXCR7 IHC staining showing nuclear/cytoplasmic staining in ovarian cleft epithelium, ovarian surface epithelium (OSE) and cancer cells, scale bar: 50µm.
B: semi-quantitative staining scores for CXCR7 showing no statistically significant difference between ovarian epithelia (paired and independent t tests).
C: CXCR7 expression in metastatic specimens compared to the corresponding primary samples increased in five patients, decreased in three patients and remained unchanged in three patients. (*P*=NS, X^2 test).

7.5.3 EMP Markers

7.5.3.1 Cytokeratins Expression

The staining for CK (using pan cytokeratins antibody) in the tumour cells was mixed cytoplasmic/membranous in both the primary and the metastatic specimens. Generally there was no intra-patient variation in the type of staining. CK staining in normal ovaries was also mixed membranous/cytoplasmic in OSE and the cleft epithelium **(Figure 7.7-A)**.

There was a clear intra-tumour heterogeneity in the strength of staining for CK, with only four of the 22 studied cancer samples showing a dominant staining level. Overall, all tumour samples showed positive staining for CK, however, with a wide inter-tumour variation; the staining score range was 25 - 82.5 for the primary cancers and 22.5 - 72.5 for the metastases. The means of staining scores were 58.4 and 52.9 for the primary and the metastatic specimens respectively (*P=NS*, paired t test) **(Figure 7.7-B)**. CK expression was lower in the metastatic lesions than their corresponding primary cancers in nine women while it increased in two women (*P=0.035*, X^2 test) **(Figure 7.7-C)**. This indicates that the change within the tumour itself between the primary and the metastatic samples is more pronounced than the change in the overall averages.

In the normal ovary samples, CK expression was lower in the surface epithelium than the cleft epithelium with respective score means of 56 and 95 but this did not reach statistical significance (*P=NS*, paired t test) **(Figure 7.7-B)**.

There was no statistically significant difference in CK expression between the normal OSE and the primary cancers (56, 58.4 respectively, *P=NS*, t independent test) **(Figure 7.7-B)**.

Figure 7.7: Cytokeratins IHC in Ovarian Specimens

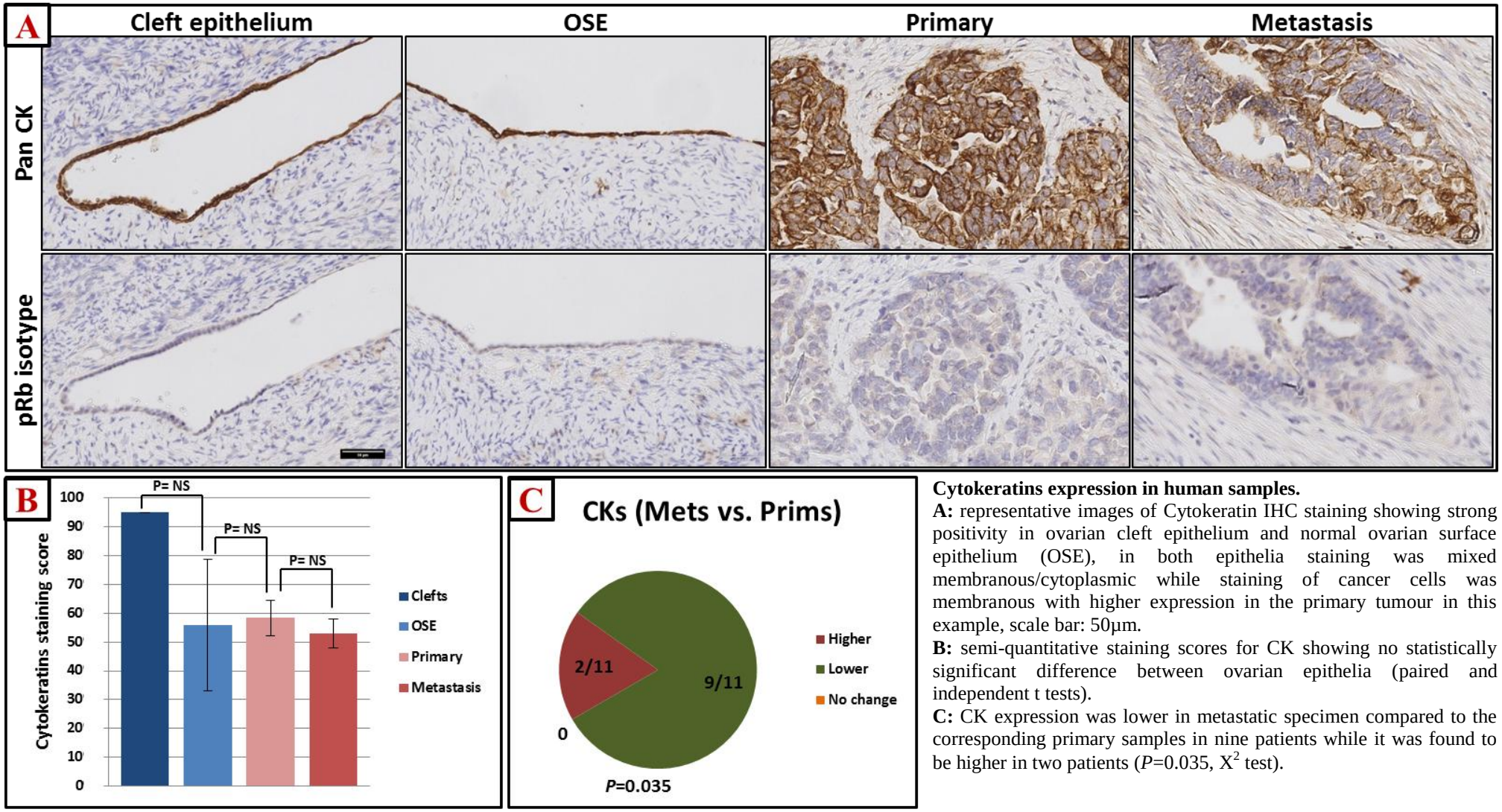

Cytokeratins expression in human samples.
A: representative images of Cytokeratin IHC staining showing strong positivity in ovarian cleft epithelium and normal ovarian surface epithelium (OSE), in both epithelia staining was mixed membranous/cytoplasmic while staining of cancer cells was membranous with higher expression in the primary tumour in this example, scale bar: 50µm.
B: semi-quantitative staining scores for CK showing no statistically significant difference between ovarian epithelia (paired and independent t tests).
C: CK expression was lower in metastatic specimen compared to the corresponding primary samples in nine patients while it was found to be higher in two patients (P=0.035, X^2 test).

7.5.3.2 E-cadherin Expression

Staining for E-cadherin was absent in the normal ovarian epithelium (OSE and clefts), while the tumour cells which expressed E-cadherin showed membranous staining in both the primary and the metastatic specimens with no intra-patient variation in the type of staining **(Figure 7.8-A)**.

Overall, the majority of the tumour samples did not stain for E-cadherin while others showed low staining scores with seven of the 22 studied cancer samples showing mostly negative staining. The staining score range was 0 - 72.5 for the primary cancers and 0 - 72.5 for the metastases. The means of staining scores were 22.5 and 18.8 for the primary and the metastatic specimens respectively (*P=NS*, paired t test) **(Figure 7.8-B)**. E-cadherin expression was higher in metastatic lesions than their corresponding primaries in three women while it decreased in four women and remained unchanged in four (*P=NS*, X^2 test) **(Figure 7.8-C)**.

7.5.3.3 Vimentin Expression

The staining for vimentin was mixed cytoplasmic/membranous in the primary and the metastatic specimens. In normal ovarian epithelia (OSE and cleft) vimentin expression was detected only in the surface epithelium of one ovary **(Figure 7.9-A)**.

Overall, the majority of the tumour samples did not stain for Vimentin with 15 of the 22 studied cancer samples showing mostly negative staining. The staining score range was 0 - 50 for the primary cancers and 0 - 33 for the metastases. The means of staining scores were 6.5 and 4.3 for the primary and the metastatic specimens respectively (*P=NS*, paired t test) **(Figure 7.9-B)**. Vimentin expression was lower in the metastatic lesions than their corresponding primary cancers in two women while it increased in one woman and remained unchanged in eight women (*P=0.02*, X^2 test) **(Figure 7.9-C)**.

There was no statistically significant difference in vimentin staining scores between the normal OSE and the primary cancer specimens (10, 6.5 respectively, *P=NS*, t independent test) **(Figure 7.9-B)**.

Figure 7.8: E-cadherin IHC in Ovarian Specimens

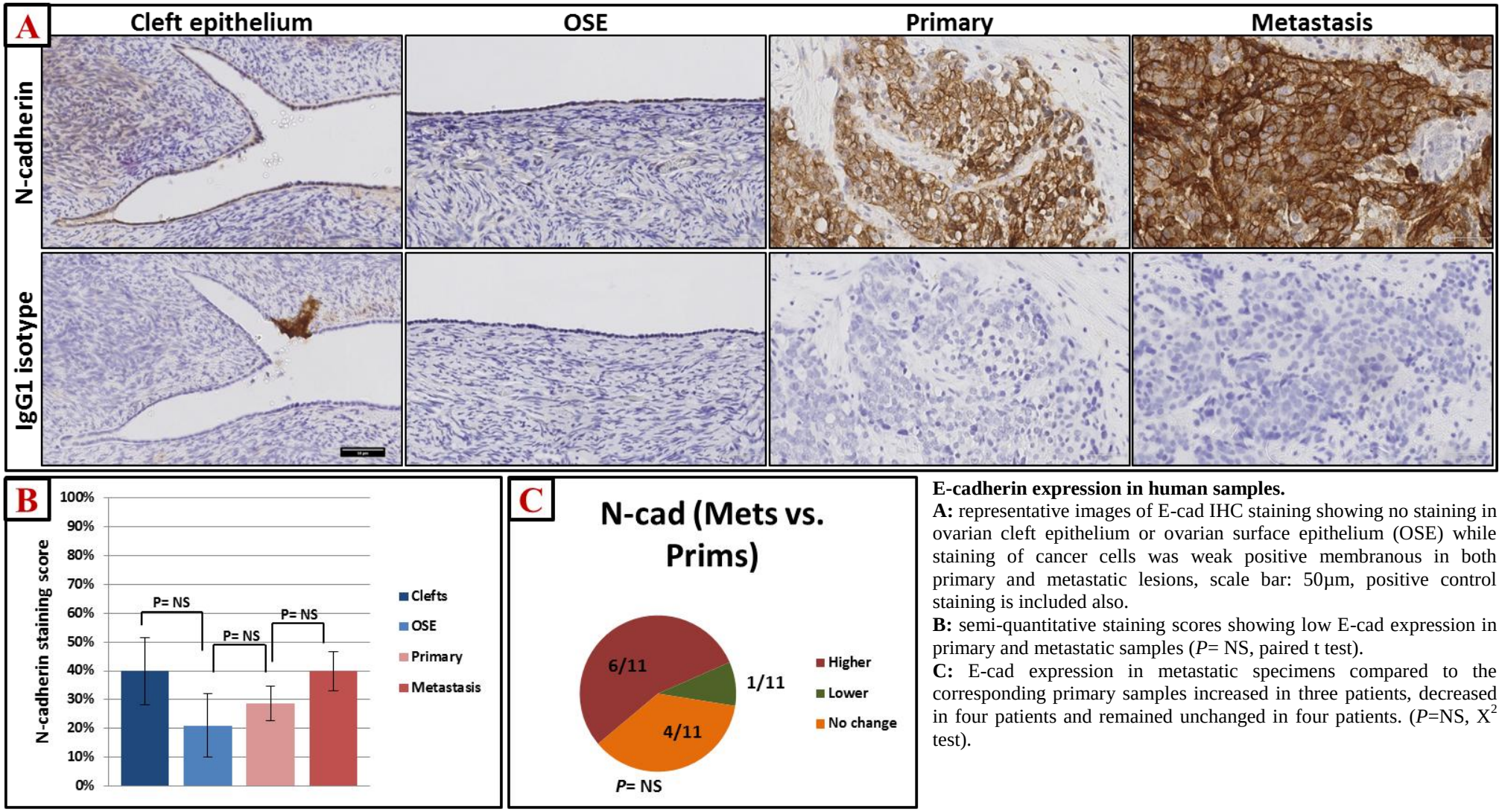

E-cadherin expression in human samples.
A: representative images of E-cad IHC staining showing no staining in ovarian cleft epithelium or ovarian surface epithelium (OSE) while staining of cancer cells was weak positive membranous in both primary and metastatic lesions, scale bar: 50µm, positive control staining is included also.
B: semi-quantitative staining scores showing low E-cad expression in primary and metastatic samples (*P*= NS, paired t test).
C: E-cad expression in metastatic specimens compared to the corresponding primary samples increased in three patients, decreased in four patients and remained unchanged in four patients. (*P*=NS, X^2 test).

Figure 7.9: Vimentin IHC in Ovarian Specimens

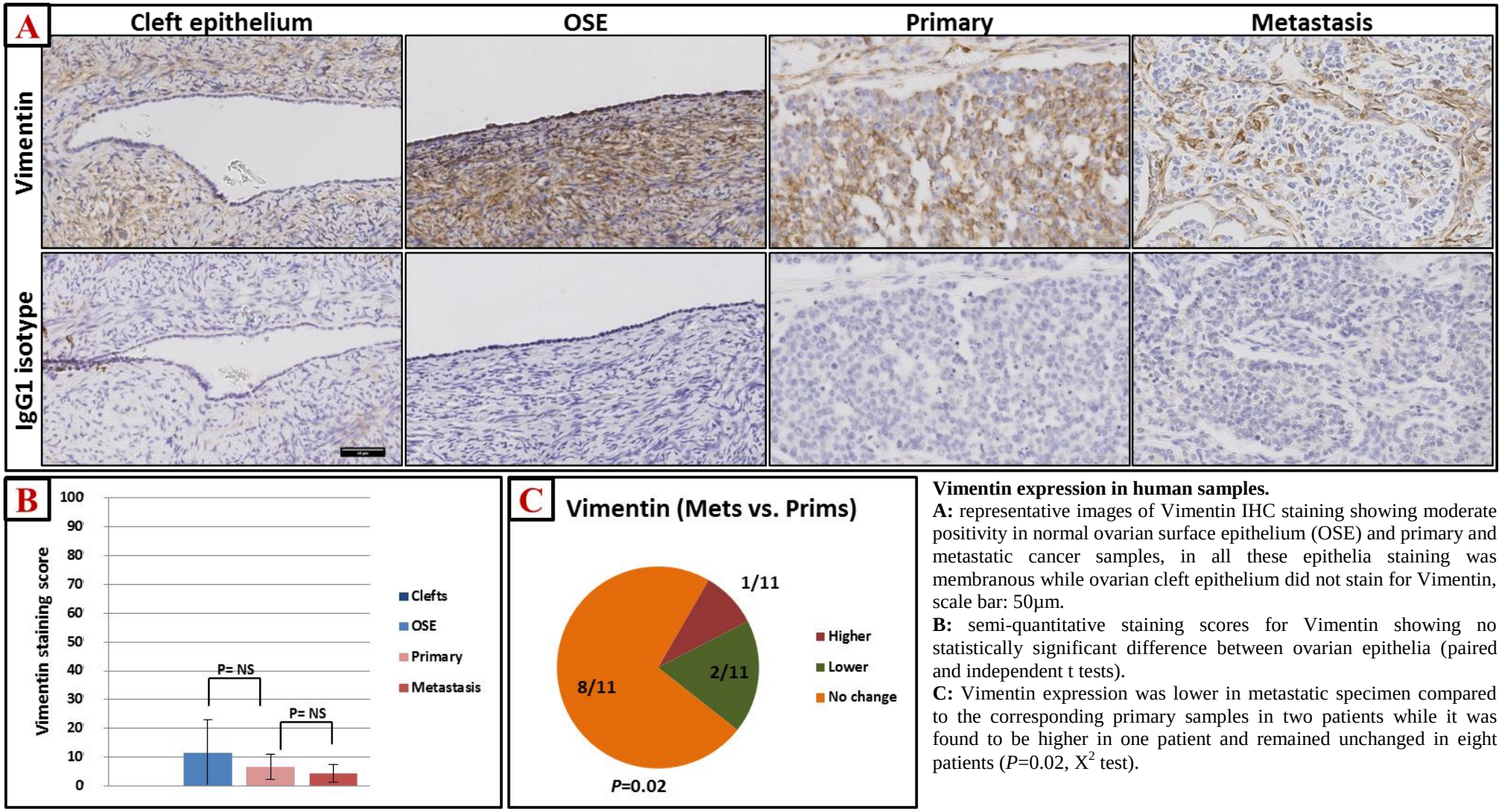

Vimentin expression in human samples.
A: representative images of Vimentin IHC staining showing moderate positivity in normal ovarian surface epithelium (OSE) and primary and metastatic cancer samples, in all these epithelia staining was membranous while ovarian cleft epithelium did not stain for Vimentin, scale bar: 50µm.
B: semi-quantitative staining scores for Vimentin showing no statistically significant difference between ovarian epithelia (paired and independent t tests).
C: Vimentin expression was lower in metastatic specimen compared to the corresponding primary samples in two patients while it was found to be higher in one patient and remained unchanged in eight patients (P=0.02, X^2 test).

7.5.3.4 N-cadherin Expression

The staining for N-cadherin in tumour cells was membranous or mixed membranous/cytoplasmic in both the primary and the metastatic specimens. Generally there was no intra-patient variation in the type of staining. On the other hand, N-cadherin staining in the normal ovaries was dominantly cytoplasmic in OSE and cleft epithelium **(Figure 7.10-A)**. There was a clear intra-tumour heterogeneity in the strength of staining for N-cadherin with only 7 of the 22 studied cancer samples showing a dominant staining level.

Overall, most tumour samples showed positive staining for N-cadherin, however, with a wide inter-tumour variation; the staining score range was 0 - 60 for the primary cancers and 0 - 75 for the metastases. The means of staining scores were 28.6 and 39.8 for the primary and the metastatic specimens respectively (*P=NS*, paired t test) **(Figure 7.10-B)**. N-cadherin expression was higher in the metastatic lesions than their corresponding primary cancers in six women while it decreased in one patient and remained unchanged in four women (*P=NS*, X^2 test) **(Figure 7.10-C)**.

In the normal ovary samples, N-cadherin expression was lower in the surface epithelium than the cleft epithelium with respective score means of 21 and 40 (*P=NS*, paired t test) **(Figure 7.10-B)**. N-cadherin expression in the primary samples was also higher than that in the normal surface epithelium with no statistical significance (28.6, 21 respectively, *P=NS*, t independent test) **(Figure 7.10-B)**.

Figure 7.10: N-cadherin IHC in Ovarian Specimens

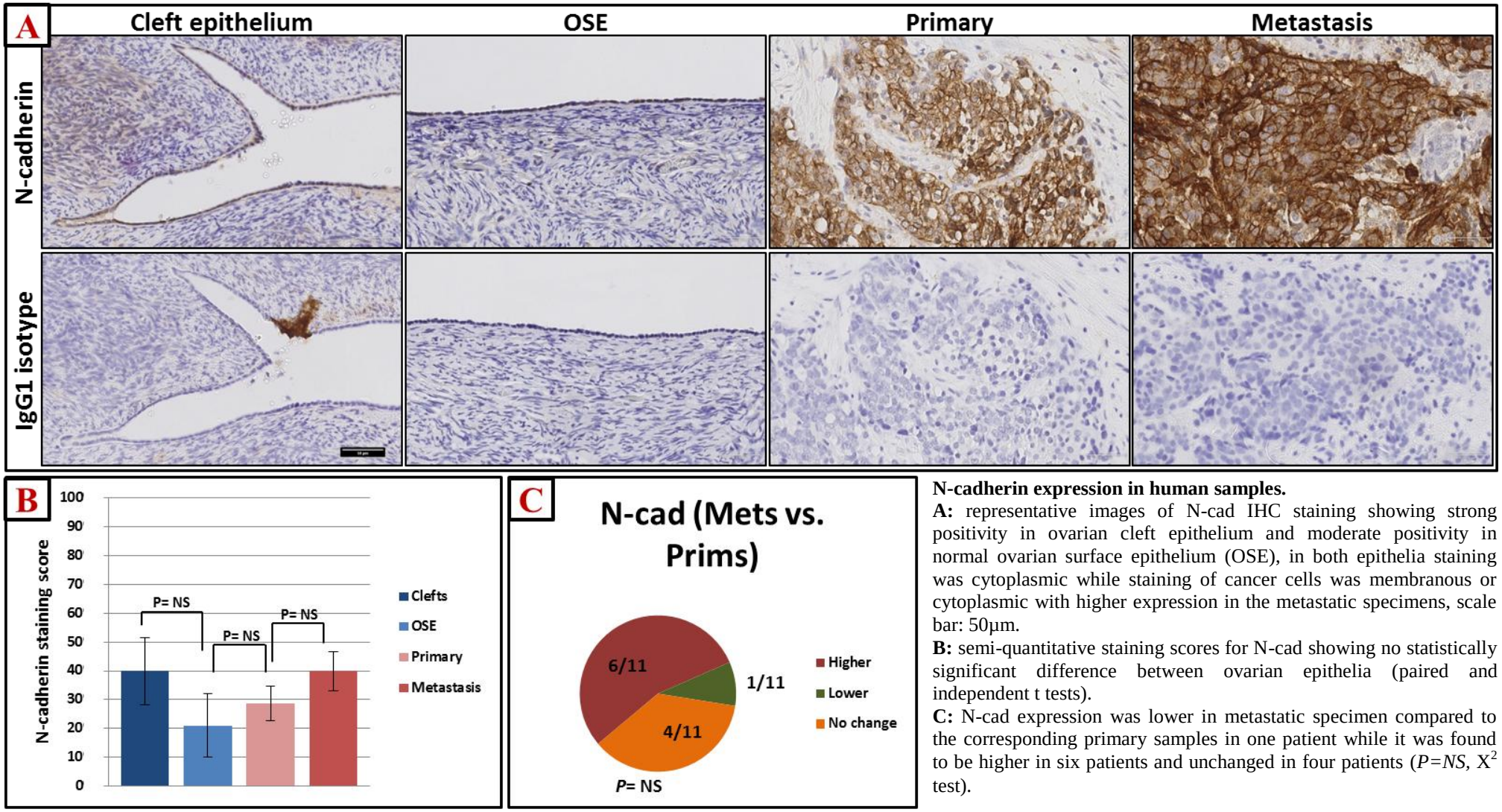

N-cadherin expression in human samples.
A: representative images of N-cad IHC staining showing strong positivity in ovarian cleft epithelium and moderate positivity in normal ovarian surface epithelium (OSE), in both epithelia staining was cytoplasmic while staining of cancer cells was membranous or cytoplasmic with higher expression in the metastatic specimens, scale bar: 50µm.
B: semi-quantitative staining scores for N-cad showing no statistically significant difference between ovarian epithelia (paired and independent t tests).
C: N-cad expression was lower in metastatic specimen compared to the corresponding primary samples in one patient while it was found to be higher in six patients and unchanged in four patients (*P=NS*, X^2 test).

7.5.4 Wnt Signalling Proteins

7.5.4.1 β-catenin Expression

The staining for B-catenin in tumour cells was mixed cytoplasmic/membranous in both the primary and the metastatic specimens. On the other hand, β-catenin staining in normal ovaries was dominantly cytoplasmic in OSE and absent in cleft epithelium **(Figure 7.11-A)**. There was a clear intra-tumour heterogeneity in the strength of staining for β-catenin with only 4 of the 22 studied cancer samples showing a dominant staining level.

Overall, most tumour samples showed positive staining for β-catenin, however with a wide inter-tumour variation; the staining score range was 0 - 70 for the primary cancers and 0 - 80 for the metastases. The means of staining scores were 28.9 and 34.2 for the primary and the metastatic specimens respectively (*P=NS*, paired t test) **(Figure 7.11-B)**. β-catenin expression was higher in the metastatic lesions than their corresponding primary cancers in seven women while it decreased in three women and remained unchanged in one woman (*P=NS*, X^2 test) **(Figure 7.11-C)**. β-catenin expression in the primary samples was higher than that in the normal surface epithelium (28.9, 1.5 respectively, *P=0.002*, t independent test) **(Figure 7.11-B)**.

7.5.4.2 DKK-1 Expression

The staining for DKK-1 was cytoplasmic in all studied epithelia **(Figure 7.12-A)**. There was clear intra-tumour heterogeneity in the strength of staining for DKK-1 with only 3 of the 22 studied cancer samples showing a dominant staining level.

Overall, all tumour samples showed strong positive staining for DKK-1 with a wide inter-tumour variation; the staining score range was 35 - 90 for the primary cancers and 42 - 87 for the metastases. The means of staining scores were 64.5 and 62.7 for the primary and the metastatic specimens respectively (*P=NS*, paired t test) **(Figure 7.12-B)**. DKK-1 expression was higher in the metastatic lesions than their corresponding primary cancers in four women while it decreased in six women and remained unchanged in one woman (*P=NS*, X^2 test) **(Figure 7.12-C)**. In the normal ovarian samples DKK-1 expression was lower in the surface epithelium than the cleft epithelium with respective score means of 32.5 and 50.5 (*P=NS*, paired t test) **(Figure 7.12-B)**. DKK-1 expression in the primary samples was higher than that in the normal surface epithelium (64.5, 32.5 respectively, *P=0.02*, t independent test) **(Figure 7.12-B)**.

Figure 7.11: β-catenin IHC in Ovarian Specimens

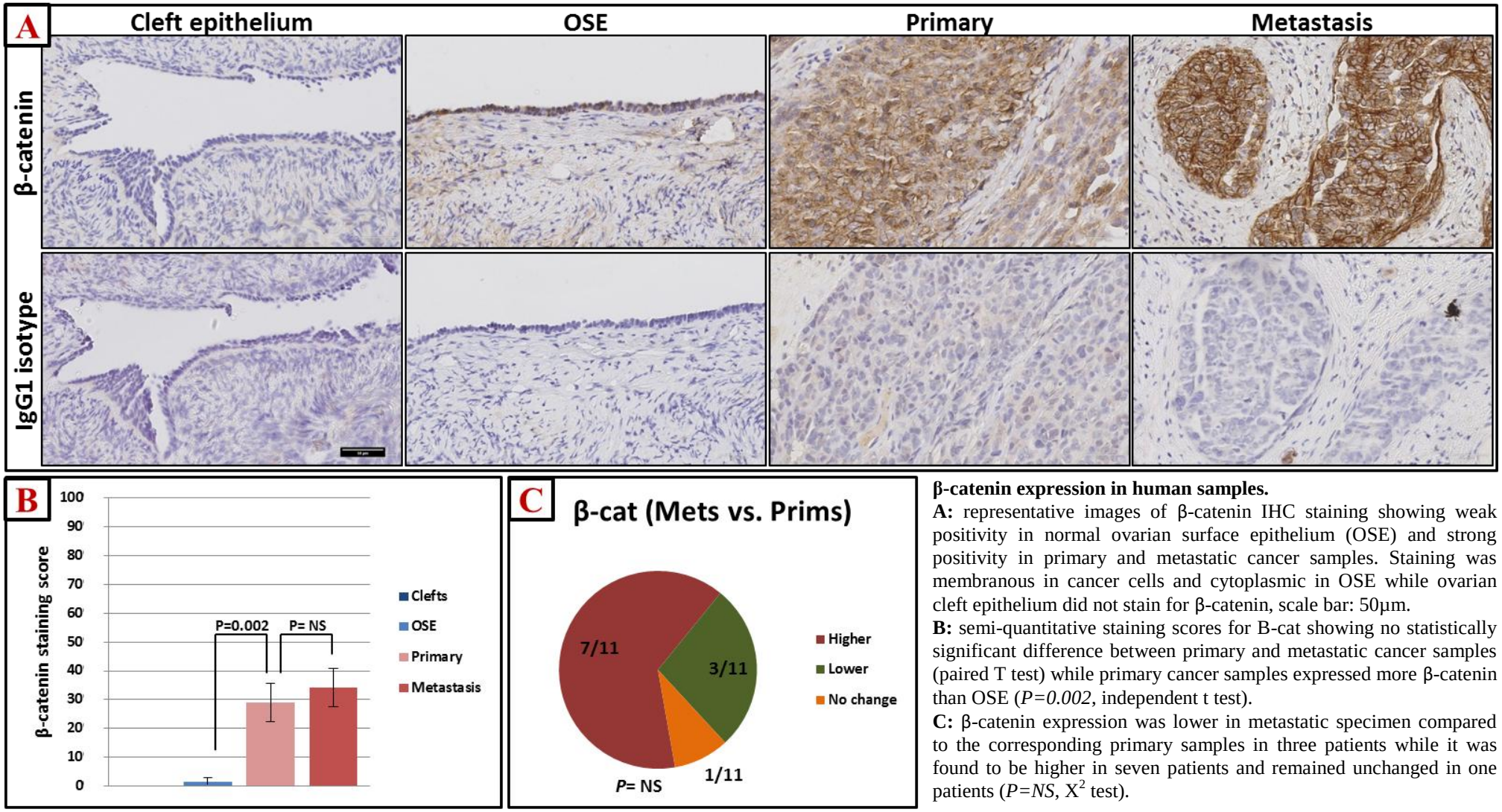

β-catenin expression in human samples.
A: representative images of β-catenin IHC staining showing weak positivity in normal ovarian surface epithelium (OSE) and strong positivity in primary and metastatic cancer samples. Staining was membranous in cancer cells and cytoplasmic in OSE while ovarian cleft epithelium did not stain for β-catenin, scale bar: 50μm.
B: semi-quantitative staining scores for B-cat showing no statistically significant difference between primary and metastatic cancer samples (paired T test) while primary cancer samples expressed more β-catenin than OSE (*P=0.002*, independent t test).
C: β-catenin expression was lower in metastatic specimen compared to the corresponding primary samples in three patients while it was found to be higher in seven patients and remained unchanged in one patients (*P=NS*, X^2 test).

Figure 7.12: DKK-1 IHC in Ovarian Specimens

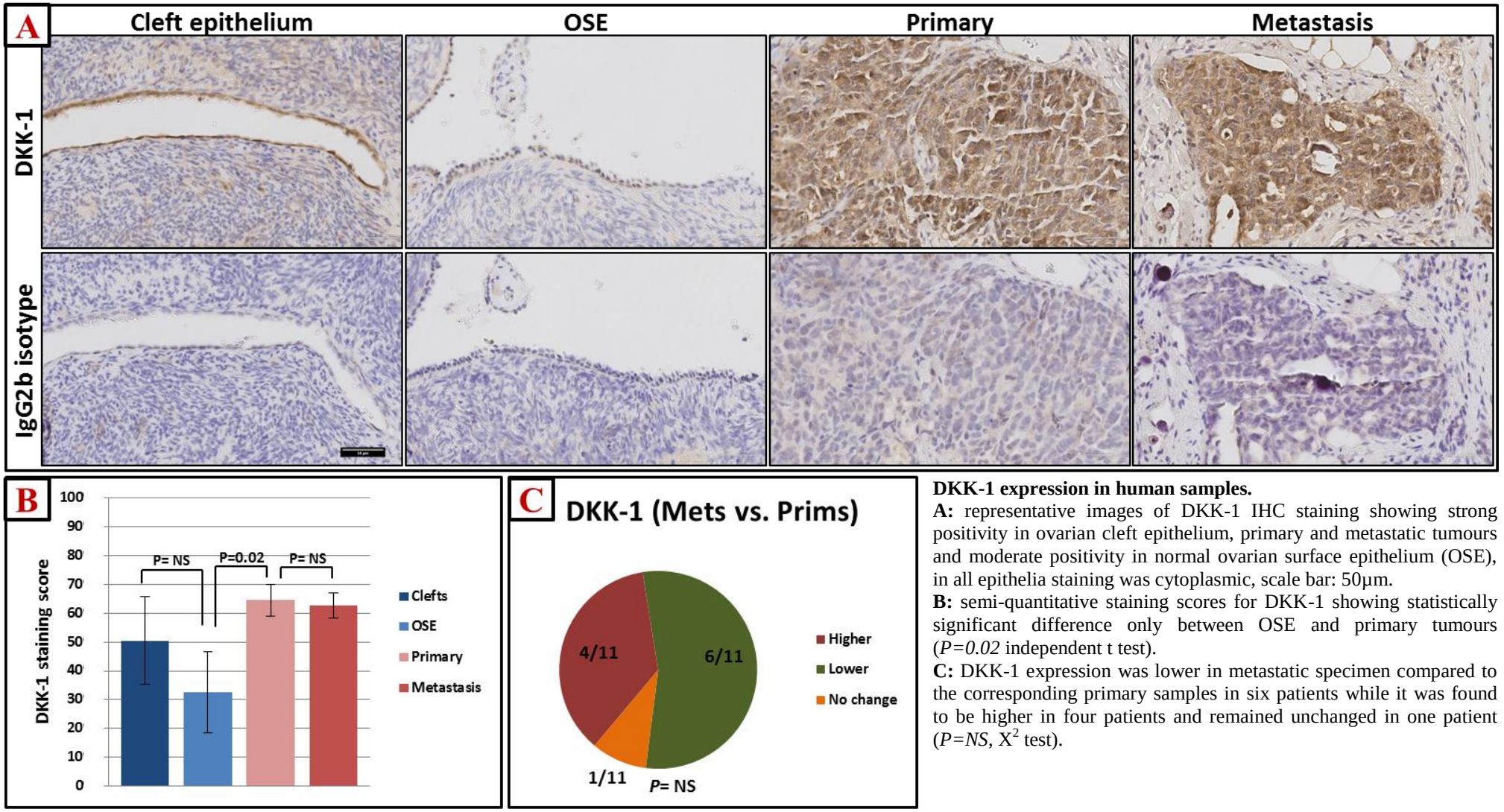

DKK-1 expression in human samples.
A: representative images of DKK-1 IHC staining showing strong positivity in ovarian cleft epithelium, primary and metastatic tumours and moderate positivity in normal ovarian surface epithelium (OSE), in all epithelia staining was cytoplasmic, scale bar: 50µm.
B: semi-quantitative staining scores for DKK-1 showing statistically significant difference only between OSE and primary tumours (*P=0.02* independent t test).
C: DKK-1 expression was lower in metastatic specimen compared to the corresponding primary samples in six patients while it was found to be higher in four patients and remained unchanged in one patient (*P=NS*, X^2 test).

7.5.4.3 JNK Expression

The staining for JNK was cytoplasmic in all studied epithelia **(Figure 7.13-A)**. There was a clear intra-tumour heterogeneity in the strength of staining for JNK with only six of the 22 studied cancer samples showing a dominant staining level.

Overall, all tumour samples showed strong positive staining for JNK, however, with a wide inter-tumour variation; the staining score range was 15 - 97.5 for the primary cancers and 25 - 72.5 for the metastases. The staining score means were 57.7 and 50.8 for the primary and the metastatic specimens respectively (*P=NS*, paired t test) **(Figure 7.13-B)**. JNK expression was lower in the metastatic lesions than their corresponding primary cancers in eight women while it increased in two women and remained unchanged in one woman (*P=0.02*, X^2 test) **(Figure 7.13-C)**. This indicates that the change in JNK expression within the tumour itself between the primary and metastatic samples was more pronounced than the change in the overall averages. In the normal ovary samples JNK expression was lower in the surface epithelium than the cleft epithelium with respective score means of 7.5 and 90 (*P=0.03*, paired T test) **(Figure 7.13-B)**. JNK expression in the primary samples was higher than that in the normal surface epithelium (57.7, 7.5 respectively, *P=0.0002*, t independent test) **(Figure 7.13-B)**.

7.5.4.4 Phospho-JNK Expression

The staining for p-JNK was nuclear in all studied epithelia **(Figure 7.14-A)**. 15 of the 22 studied cancer samples showed a dominant staining level suggesting some intra-tumour homogeneity in the strength of staining for p-JNK.

Overall, all tumour samples showed strong positive staining for p-JNK, however, with a wide inter-tumour variation; the staining score range was 37.5 - 100 for the primary cancers and 50 - 100 for the metastases. The means of staining scores were 81.5 and 80.4 for the primary and the metastatic specimens respectively (*P=NS*, paired t test) **(Figure 7.14-B)**. p-JNK expression was lower in the metastatic lesions than their corresponding primary cancers in five women while it increased in four women and remained unchanged in two women (*P=NS*, X^2 test) **(Figure 7.14-C)**.

In the normal ovarian samples p-JNK expression was lower in the surface epithelium than the cleft epithelium with respective score means of 26.5 and 85 (*P=0.04*, paired t test) **(Figure 7.14-B)**. p-JNK expression in the primary tumour samples was higher than that in the normal surface epithelium (81.5, 26.5 respectively, *P=0.02*, t test) **(Figure 7.14-B)**.

Figure 7.13: JNK IHC in Ovarian Specimens

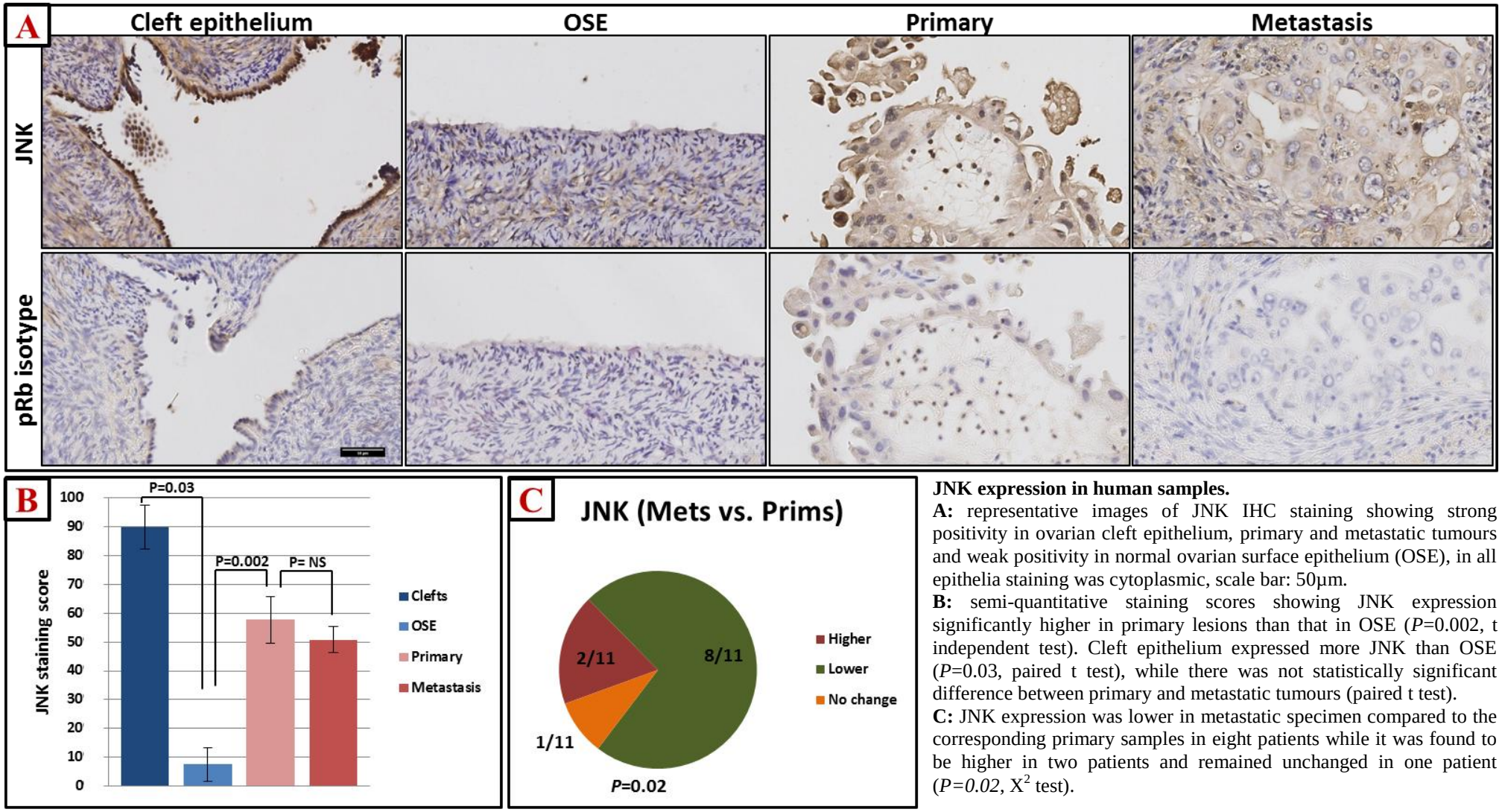

JNK expression in human samples.
A: representative images of JNK IHC staining showing strong positivity in ovarian cleft epithelium, primary and metastatic tumours and weak positivity in normal ovarian surface epithelium (OSE), in all epithelia staining was cytoplasmic, scale bar: 50µm.
B: semi-quantitative staining scores showing JNK expression significantly higher in primary lesions than that in OSE (*P*=0.002, t independent test). Cleft epithelium expressed more JNK than OSE (*P*=0.03, paired t test), while there was not statistically significant difference between primary and metastatic tumours (paired t test).
C: JNK expression was lower in metastatic specimen compared to the corresponding primary samples in eight patients while it was found to be higher in two patients and remained unchanged in one patient (*P=0.02*, X^2 test).

Figure 7.14: p-JNK IHC in Ovarian Specimens

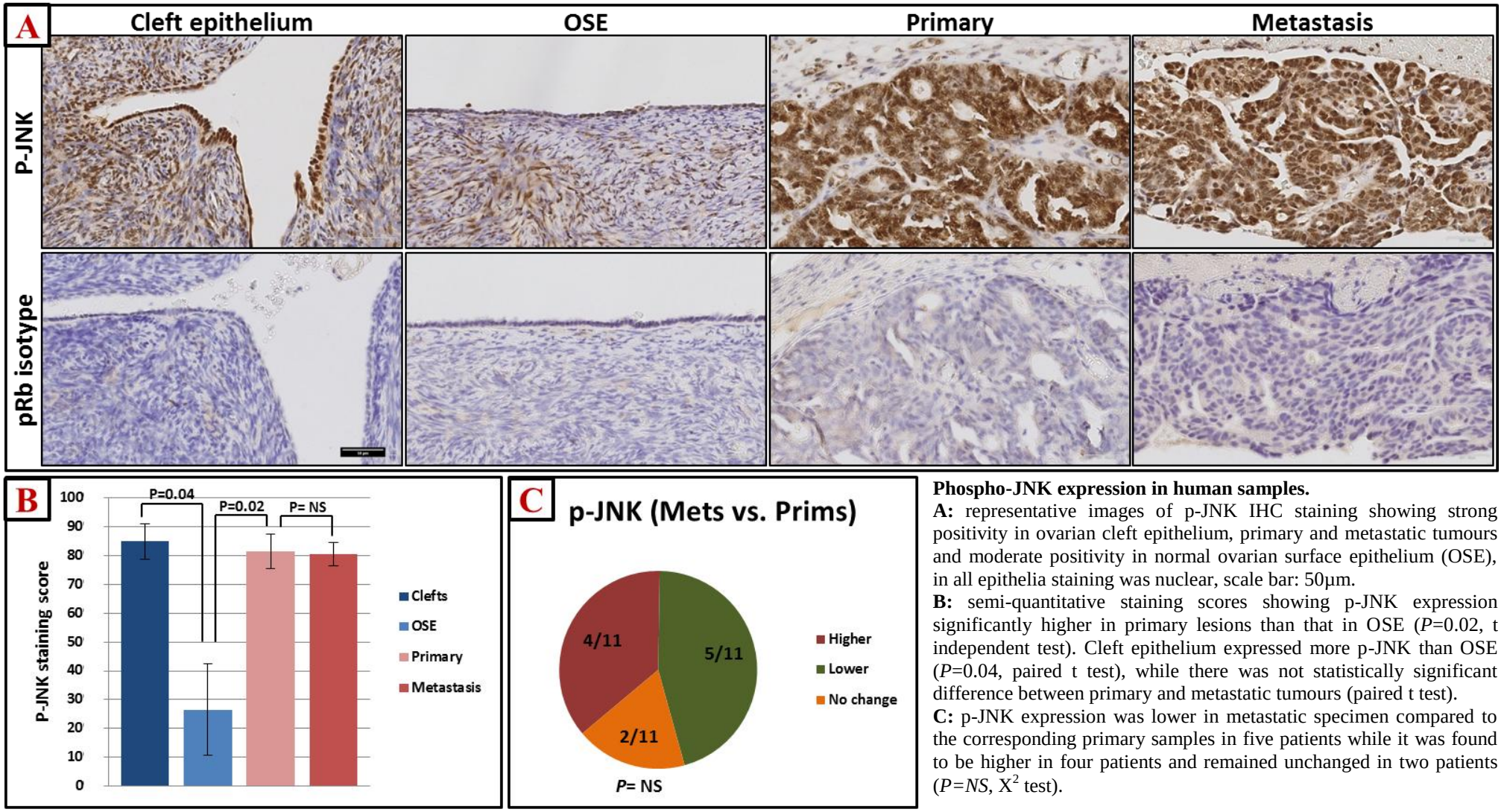

Phospho-JNK expression in human samples.
A: representative images of p-JNK IHC staining showing strong positivity in ovarian cleft epithelium, primary and metastatic tumours and moderate positivity in normal ovarian surface epithelium (OSE), in all epithelia staining was nuclear, scale bar: 50µm.
B: semi-quantitative staining scores showing p-JNK expression significantly higher in primary lesions than that in OSE (P=0.02, t independent test). Cleft epithelium expressed more p-JNK than OSE (P=0.04, paired t test), while there was not statistically significant difference between primary and metastatic tumours (paired t test).
C: p-JNK expression was lower in metastatic specimen compared to the corresponding primary samples in five patients while it was found to be higher in four patients and remained unchanged in two patients ($P=NS$, X^2 test).

7.6 Correlation Between Markers

After mapping the expression of individual molecules, it was sought to explore if there was a relationship between the expression of 5T4 and other molecules in the studied samples. There appeared to be no linear relationship between the expression of 5T4 as measured by IHC scoring and the expression of any of the other molecules when this was explored by visual examination of scatter-plots or by statistical analysis using Spearman's test **(Figure 7.15)**.

In addition, there was no recognised pattern relating the changes in 5T4 expression within the paired samples (increased in 10 of the 11 samples) to the changes in the expression of any of the other studied markers apart from JNK expression. The change in JNK expression was reciprocal to that of 5T4 in nine of the 11 studied cancers **(Table 7.4)**, (*P=0.01*, X^2 test).

Figure 7.15: Expression Correlation in Ovarian Specimens

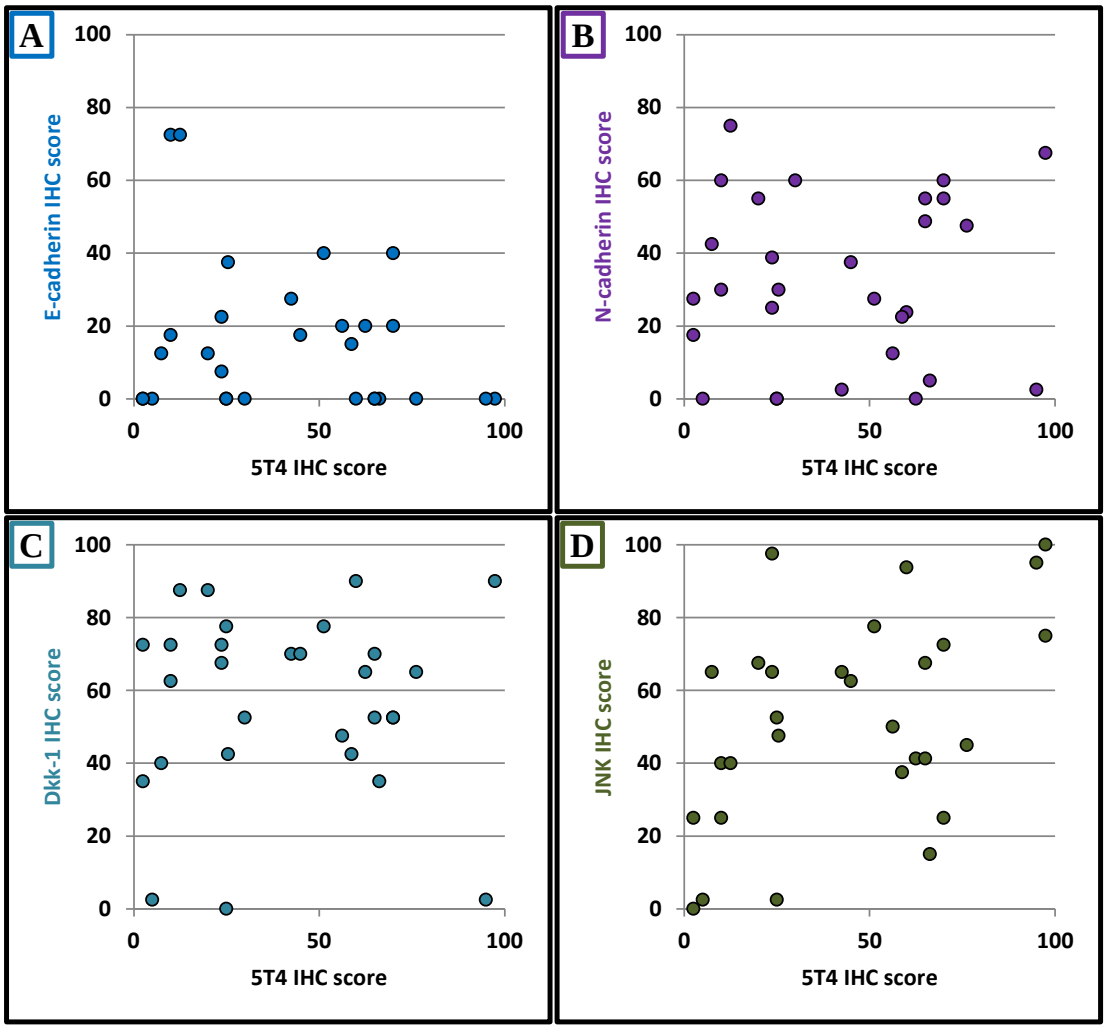

Examples of the lack of correlation between the expression of 5T4 and other molecules
Four scatter-plots of 5T4 expression against other molecules showing the lack of obvious correlation, Spearman's test also failed to show significant relationship between 5T4 expression and any of the studied molecules.

Table 7.4: IHC in Ovarian Specimens, Primary vs. Metastasis

	No change	Similar change	Reciprocal change	*P* (X^2 test)
CXCR4	5	3	3	1
CXCR7	3	4	4	1
Cytokeratins	0	3	8	0.13
E-cadherin	4	2	5	1
N-cadherin	1	5	5	1
Vimentin	8	2	1	0.56
Dkk1	1	3	6	0.21
JNK	1	1	9	**0.01***
pJNK	2	3	6	0.32
B-catenin	1	8	2	0.06

Tab 7.3: Concordance between changes of 5T4 expression and other molecules in cancer samples
Only changes in JNK expression were statistically significantly related to the changes of 5T4 expression as in most cases JNK expression increased in metastatic samples when 5T4 expression increased.

7.7 Chapter Discussion

In this final part of this study, protein expression was probed using immunohistochemistry in human tissues. The investigated proteins were 5T4, CXCL12 receptors, epithelial and mesenchymal markers, and wnt signalling proteins. The studied tissues consisted of normal ovarian surface epithelium (OSE, five samples), epithelium from ovarian clefts (five samples), and primary epithelial ovarian cancers (EOC) with paired secondary cancer lesions (11 samples). The diagnosis of both normal and malignant ovarian tissues was confirmed by a gynaecological histopathologist (RM) prior to conducting experiments. The primary and metastatic sites were also determined by the same histopathologist such as in cases where the primary and secondary tissues were sampled from the ovaries. Therefore, controversially, fallopian tube as an origin for some ovarian cancers was not taken into account in this project.

OSE samples showed low or absent 5T4 expression, in keeping with the previously published report[14]. OSE also showed a mixed epithelial/mesenchymal phenotype where it expressed cytokeratins, vimentin and N-cadherin and lacked the expression of E-cadherin in keeping with its reported mesothelial nature[62].

In comparison to OSE, matched ovarian cleft epithelia expressed significantly higher levels of 5T4, total JNK, and active (phosphorylated) JNK while, like OSE, they did not express β-catenin. The expression of DKK-1 was also higher in ovarian cleft epithelial compared to OSE but this was not statistically significant. These molecular changes could collectively indicate a non-canonical wnt activation ovarian cleft epithelia, although other pathways could not be excluded since JNK is implicated in several other pathways such as stress and cytokine pathways[195, 290].

Primary EOC samples, in comparison to OSE, showed higher levels of 5T4 and expressed membranous CXCR4 in keeping with the reported literature[14, 153, 291-293]. EOC also expressed higher levels of CXCR7, however, this was not sufficient to reach statistical significance in this small sample. CXCR7 in both epithelia was cytoplasmic and nuclear in keeping with relevant reports in ovarian and other cancers[265, 294, 295]. While CXCR7 membranous expression could not be excluded on the basis of IHC staining alone, the functional properties of nuclear/cytoplasmic CXCR7 are not clear and worthy of investigating in future studies. There has been no published report of CXCR7 expression in OSE; previous work was limited to investigating CXCR7 transcript in normal ovaries

which included surface epithelium as well as ovarian stroma which rendered the results unhelpful[295].

In addition, EOC expressed E-cadherin, which was not expressed by OSE, with no significant changes in other epithelial/mesenchymal markers. The early expression of E-cadherin in EOC is well documented and has been linked with the unusual epithelial transition in early ovarian cancer formation[170, 171].

The expression profile of wnt proteins was strikingly different between EOC and OSE. EOC expressed higher levels of both total and activated JNK and higher levels of DKK-1, all suggestive of activation of the non-canonical PCP pathway. While β-catenin was not expressed in OSE, a moderate cytoplasmic / membranous expression was detected in EOC with no measurable nuclear translocation, implying the lack of canonical wnt activation in the studied samples. The increased non-nuclear levels of β-catenin could be part of the increased levels of cadherins in EOC as β-catenin forms an essential component of the cadherin complexes, however this requires experimental confirmation.

These results are in keeping with the reported data in terms of β-catenin and DKK-1 expression in ovarian tissues[228, 229, 240]. One study which reported the expression of total and active JNK in ovarian cancer samples found pJNK levels to be correlated with improved progression free survival (PFS) using reverse phase protein array[296]. However, this is the first report of comparative expression of total and active JNK between OSE and EOC.

5T4 expression was higher in the metastatic samples in comparison to matched primary tumours in ten out of eleven women. This was accompanied by a reduction in cytokeratin expression in nine patients; both are statistically significant differences. While this could mark an epithelial to mesenchymal transition, other differences in the expression of the studied proteins including other epithelial / mesenchymal markers were not statistically significant.

The increase in 5T4 expression from primary to secondary sections in the majority of specimens (10/11) was accompanied by a reduction in total JNK expression with both changes being statistically significant. At first glance this might look contradictory to our cell line results in which 5T4 expression seem to favour the non-canonical wnt signalling. It is however, the active JNK levels, and not total JNK, which indicate the activation, or the lack of it, of the wnt PCP pathway. Changes in pJNK levels in our samples did not reach statistical significance, perhaps not surprising given the small numbers investigated

in this project. The same could be the reason of why a relationship between the expression of 5T4 and the other proteins in this study was difficult to demonstrate. This could have also resulted from the fact that staining for individual proteins was performed on sequential tissue sections and hence it was not that the same cells were stained for the different markers. These obstacles could be overcome by using multi-colour IF or IHC staining in future studies, and the recent advancement in the relevant technology could allow for this. Multiple colour staining (IHC or IF) could be used to explore further co-expression, or the lack of it, of 5T4 and other proteins at individual cell level. Such approach could avoid the difficulty in interpreting single colour IHC which in part results from the heterogeneity in EOC.

This heterogeneity might have resulted from the fact that the studied cancer samples were from several histological sub-types. Future studies might include larger numbers of patients and stratify results according to their histological, molecular or genetic aberration profile. For example, canonical wnt signalling might be of particular importance in cancers with *CTNNB1* mutations such as endometrioid sub-type[221].

Inevitably the tissue sections analysed in this study were only samples and therefore could not represent the heterogeneity of the entire tumours. A profound heterogeneity manifests at several levels in ovarian cancer: (1) at the total tumour appearance as in **Figure 1.4** which shows cystic and solid components of the same cancer, (2) at macroscopic level among the different areas of the tumour sections, (3) at microscopic level within each tumour island as suggested by the fact that only two of the eleven studied proteins showed intra-tumour homogeneity.

In addition, metastatic specimens were obtained from one of the many lesions present in each patient. It is not clear whether or not metastases could manifest different expression profiles according to their site i.e. omentum vs. mesentery. In addition, it is likely to become more difficult to obtain untreated paired samples as neo-adjuvant chemotherapy is increasingly used in patients with advanced disease.

To conclude, in this chapter it has been confirmed that 5T4 is selectively expressed in ovarian cancers of several histological sub-types and I have shown for the first time that 5T4 expression is upregulated at protein level in secondary, compared with the matched primary cancers. Limited conclusions could be drawn regarding the role of 5T4 in ovarian cancer in human from this project however it could provide a useful platform for future studies.

Chapter 8

DISCUSSION

Discussion

The potential of 5T4 as a tumour associated antigen (TAA) has long been realised and exploited leading to several cancer therapeutics targeting 5T4 in different phases of clinical trials, such as the TroVax® vaccine, anyara® a tumour targeted superantigen, and antibody conjugated drugs. Some of the functional properties of 5T4 have been unveiled in developmental biology in embryonic cells (stem cells and fibroblasts) and zebrafish embryos.

This work has identified a role for 5T4-knockdown in switching some biological properties of SKOV-3 ovarian cancer cells into a phenotype in which cells lost their CXCR4-mediated chemotactic response to CXCL12, favoured wnt canonical signalling over the non-canonical response, and demonstrated elements of mesenchymal to epithelial transition. The 5T4-KD SKOV-C3 cells became less motile and less migratory which could support a role *in vivo* for 5T4 in the effective spread of human ovarian cancer. This potential role is supported further by the finding that metastatic ovarian cancer lesions expressed higher levels of 5T4 by IHC than their paired primary cancer lesions.

The methodology used in this study is scrutinised first in this chapter and then the implications of the obtained results for future research is laid down

8.1 Cell Lines

In total, eight cell lines were investigated in this project: SKOV-3, Caov-3, OVCAR-3, OV-90, TOV-112D, TOV-21G, A2780 and Hoc-8. The choice of cell line was guided by the relevant literature and their published properties in order to fulfil the initial aims of this study in identifying EOC cells which expressed 5T4 and CXCR4 and responded chemotactically to CXCL12.

Generally, the documentation provided by the suppliers regarding the origin of these cell lines in terms of primary or metastatic site and their histological sub-type was not always clear, with evidence of conflicting reports in the literature[264, 297, 298]. Caov-3, A2780, TOV-21G and TOV-112D were established from solid tumours, but it was not determined whether they were from primary or secondary lesions. SKOV-3, Hoc-8, OV-90 and OVCAR-3 were established from ascitic effusions accompanying advanced ovarian cancers and as such they might represent metastatic or metastasising cancer cells.

Similarly, while all cell lines were derived from ovarian adenocarcinomas, the histological sub-types were known only for Hoc-8, OV-90 (both are high grade serous), TOV-21G (clear cell) and TOV-112D (endometrioid). It is possible that the lack of definition of the histological sub-type in the remaining cell lines is due to the fact that the original tumours were poorly differentiated, such that it was not possible to determine the exact histological sub-type.

A recent study has questioned the histological sub-type assigned in the literature to the commonly used ovarian cancer cell lines[264]. The authors performed comparative analyses of 47 ovarian cancer cell lines and a large number of primary ovarian cancers which included molecular profiling (gene nutation and copy number, and mRNA expression). Interestingly, the two most commonly used EOC cell lines, SKOV-3 and A2780, were found to be poor models for HGSC of the ovary since they lacked *TP53* mutations and harboured mutations found in other histological sub-types such as *ARID1A*, *BRAF*, *PIK3CA* and *PTEN* mutations[264].

The histological sub-type and the origin of cell lines can influence cell characteristics and can have implications for the interpretation of results obtained in phenotype and cell motility experiments. This project primarily intended to investigate 5T4 biology in ovarian cancer generally, therefore there was no intention to limit experiments to any particular sub-type. The eight cell lines used in this study are likely to represent the main histological sub-types of ovarian cancer (HGSC, clear cell and endometrioid) as suggested by their molecular profile[264]. Future research could expand this work by exploring 5T4 role in specific EOC sub-types (for example cancers with aberrant activation of canonical wnt signalling).

Experiments in cell lines are chosen because they are a necessary step for experimental progress when it is not possible to use human cells *in vivo*, e.g. protein expression manipulation and functional assays. Cell lines experiments however, are not a substitute for the experimentation with primary human samples. Cell lines are generally purified and highly selected cells; by the time a cell line is established it could present one cell clone of the many that co-existed in the parental cancer[299]. Cell lines could also develop new mutations during repeated culturing[300, 301]. Furthermore, media used *in vitro* for cell culturing are synthetic, aimed at enhancing cell viability and growth, which is not what cells are exposed to in their *in vivo* environment. For example human cell lines show different properties when they are cultured in media supplemented with fetal calf serum in comparison with supplementation with human serum[302-304].

While cell lines are not a perfect model for the heterogeneous ovarian cancer, the use of multiple cell lines with varying morphology, origin and gene profile[50] can be a useful model for studying ovarian cancer as they could collectively reflect some of the different aspects of ovarian cancer biology.

8.2 Protein Expression Probing Methodology

Protein expression was investigated in this project by immunostaining (FC, IF and IHC). These methods of probing protein expression are dependent on epitope integrity and its availability to interact with antibodies, as well as the choice of antibodies, which vary in terms of their sensitivity and specificity.

Flow cytometry on live cells was used to explore surface expression of the investigated molecules. An advantage of FC is the means of quantitative assessment of protein levels in a large number of cells where the expression in each individual cell is measured. The ability to control for the background fluorescence and the isotypes makes it also possible to compare results from different experiments. A limitation of FC, however, is that it requires cell suspension which in the case of adherent cells entails using trypsin, or other detaching reagents, which might affect proteins by proteolysis or modification of their conformational structure. Both of these could result in false negative results by cleaving off or masking specific recognisable epitopes. An example in this study is E-cadherin detection in Hoc-8 and SKOV-C3 cells which was possible using in situ IF but not by FC; the detected levels of E-cadherin in the non-adherent cells H146 dropped by 70% when trypsin was added to FC experiments in the optimisation experiments.

Determination of sub-cellular localisation of proteins such as cytoplasmic and nuclear is not generally possible with FC, hence intracellular protein expression was investigated in this study using IF. In situ IF has the advantage of studying cells in the constitutive state at the time of fixation, preserving cell connections with neighbouring cells and ECM (or growth substrate). However, IF assessment could be subjective as, in spite of random selection of cells, it relies on in-depth analysis of a selected number of cells. Another drawback of IF is the gradual fading of fluorescence signal during storage and microscopic examination, which can be avoided by prompt examination and restricted use of light source during assessment.

IHC scanning microscopes are at a more advanced stage than those for IF which enable processing of a large number of stained sections with minimal operator-generated variation associated with the individual assessment of sections under traditional

microscopes. For these reasons IHC was chosen for the assessment of protein expression in primary human tissues. The use of robotic staining platforms and imaging scanners for IHC have helped to improve reproducibility and reduced the potential for variation by manual staining; which is crucial in comparative studies such as in this project. IHC is still considered an important tool in studying protein expression in biological tissues as it provides, unlike IF, a clear view of cellular structures with stable staining; hence it is widely used in clinical practice.

8.3 Cell Motility Assay Methodology

There are several reported methods for assessing chemotaxis in cell lines which include generally two dimensional and three dimensional studies[273-275]. While this project used a 2D based chemotaxis assay, 3D based techniques could be of value in future research and might elucidate further aspects of the potential role of 5T4 in cell biology in ovarian cancer.

The FluoroBlok® technique was chosen as it offers continuous cell motility monitoring as well as generating end results without interference or the need to terminate experiments which is required in the traditional Boyden's methodology. FluoroBlok® was modified later to include in situ cell counting by taking advantage of a plate scanner. This novel technique provided actual cell count which enabled increasingly reliable comparisons between experiments of the different cell lines.

FluoroBlok® inserts could be utilised for invasion assays where the porous membrane is covered by a thin layer of a substance such as laminin or collagen to 'resemble' cell invasion of ECM. In this project there was no attempt to perform these studies given the peculiar nature of ovarian cancer spread within the peritoneum which does not require invasion, at least initially, where cells shed off the primary tumour into peritoneal cavity and then they attach to the peritoneal mesothelial cells or to the exposed basement membrane between dispersed cells caused by distended abdomen resulting from accumulating ascites.

Another chemotaxis technique is the Ibidi microslide[275] microfluidics method which was tested in this project and found to be unhelpful. A major disadvantage is that the number of the experimental chambers is limited to three. It is not possible to do any comparative experiments simultaneously when these chambers are used for the repeats of the same experimental setting. In addition, the need for time lapse microscopy for an extended time, typically overnight, meant increasing cost and time limitation.

An *ex vivo* chemotaxis assay is being developed as part of this work **(Appendix 5)**. Preliminary data supported a 'proof of concept' where efforts were made to establish the feasibility of measuring chemotaxis within live tissue blocks. This method investigated cell density within the tumour blocks unlike other methods which investigated cells migrating from tissue blocks into the medium they are immersed in. One experiment showed, using macro-confocal microscopy, a difference in fluorescence intensity between blocks exposed to 0% or 10% serum for 36 hours in comparison to blocks fixed immediately.

This technique requires further experimental validation such as establishing reproducibility and confirming that changes in fluorescence intensity represent changes in cell density perhaps by H&E staining of tissue sections obtained from the block centre.

8.4 Human Tissue Studies

Another aspect of this project is the static nature of experiments in human tissue samples. These studies provide a 'snap shot' capture of tissues at the time of fixation after removal from patients and they are unable to elucidate some dynamic processes such as cancer spread and dissemination.

For example, does the expression profile of cells in a metastatic site reflect that of cells which have just completed their migratory journey or of established cells in a proliferative phase? Does it have a mesenchymal appearance or does it show the phenotype of a cell which had already undergone mesenchymal to epithelial transition?

These questions can be difficult to address in human experiments. One possibility however, is the examination of cancer cells obtained from malignant ascites along with specimens from the primary and secondary lesions in the same patient. Together these samples can form, according to a proposed model[64, 305], the three steps of the natural history of EOC dissemination: primary cancer tissues, metastasising cancer cells, and metastatic cancer tissues. This approach was attempted in this project but it was difficult to achieve. Collaboration between scientists and surgeons is important in achieving this goal.

Ascitic cancer cells could help to explore the mechanisms involved in ovarian cancer adhesion and metastasis formation, an area which is under active investigations. It is not known if 5T4 has a role in ovarian cancer cell adhesion or even if ascitic cells express 5T4; phenotypic characterisation of these cells could provide a deeper insight into this crucial part of their dissemination journey. Adhesion experiments performed by Dr J Brazzatti in parallel with this study showed no difference among SKOV cell lines (parental, control and 5T4 KD) in cell adhesion to plates coated with collagen IV.

8.5 5T4 Roles

The exact mechanisms through which 5T4 KD mediates the associated changes in cell response have not been investigated in this study. Whether 5T4 exerts its effect directly or through intermediate proteins is largely unknown. The transmembranous location of 5T4 makes it unlikely to act directly as a gene activator or repressor. In addition, the transcriptional regulation of 5T4 expression is poorly understood, while *TPBG* contains potentially several binding sites in its promoter. To date, only β-catenin has been shown to activate *Waif1* in zebrafish through its wnt response element (WRE)[26].

Nonetheless, different parts of 5T4 have been suggested, or found, indispensable for its different potential roles. The extracellular domain has been found to be required for inhibition of canonical wnt signalling[26], in particular the amino acids Lys76 and Phe97 were found to be essential for this function in HEK293T cells[242]. While the transmembranous domain has been shown to be necessary for the functional expression of CXCR4 in mES[25], the cytoplasmic tail has been found to interact with TIP2/GIPC and to abrogate actin / cadherin contacts in CL-S1 cells[175]. To date there has been no confirmation of direct interaction of 5T4 with other proteins in humans with the exception of TIP2/GIPC.

Taken together, these observations suggest that 5T4 expression functional roles could be separable, however, this remains largely speculative and requires further investigation. Our data do not explain whether the consequences of 5T4 knockdown in SKOV-3 cells on chemotaxis, EMP and wnt signalling are interlinked or separable. For example, does the abrogation of the chemotactic response to CXCL12 result from direct action on CXCL12/CXCR4 axis or is it a consequence of a reduction in the inherent cell motility? Do the observed changes in epithelial/mesenchymal phenotype result from or contribute to the observed non-canonical wnt response?

There is however some evidence linking these three biological processes with each other, which unveils the complexity of interactions controlling cell motility and the possibility of involvement of multiple protein interactions and pathway crosstalk, the significance of which are yet to be discovered.

One study has shown that in T cells, CXCL12-mediated chemotactic response was accompanied by WNT5A upregulation (by PCR and WB); the canonical wnt pathway was found to be inhibited by the upregulated WNT5A through PKC (protein kinase C). In addition, WNT5A knockdown reduced CXCL12-mediated migration by 50% and significantly decreased CXCR4 expression (FC, WB and PCR)[306].

Several reports have explored the relationship between wnt signalling and EMP with conflicting results, which could suggest that wnt/EMP crosstalk is cell specific since these studies were conducted in a variety of cell lines. One study reported that WNT3a-activated wnt/β-catenin signalling in rat bone marrow-derived mesenchymal stem cells (MSC) resulted in epithelial differentiation, while blocking this signalling pathway with DKK-1 abrogated the upregulation of specific epithelial markers[307]. Consistent with that, the overexpression of E-cadherin in colorectal cancer cell lines inhibited β-catenin/TCF-dependent transcription. Furthermore, the inhibition of canonical signalling by overexpression of PDCD4 (programmed cell death 4) was accompanied with upregulation of E-cadherin while PDCD4 knockdown resulted in elevated SNAIL levels and decreased E-cadherin levels with evidence of activation of canonical wnt signalling[308].

In contrast, another study in a metastatic breast cancer cell line found that treatment with DKK-1 downregulated SLUG and SNAIL, possibly by blocking wnt canonical signal transduction, as it resulted in a reduction in nuclear β-catenin levels[309]. Likewise, inhibition of wnt signalling by overexpression of wif1 (wnt inhibitory factor 1) in prostate cancer cell lines PC-3 resulted in upregulation of E-cadherin and keratins and down regulation of N-cadherin and vimentin (MET), and reduced SLUG and TWIST expression. Wif1 inhibited canonical wnt signalling but the non-canonical pathway was not investigated in this study[310].

HGF (hepatocyte growth factor)-induced EMT in MDCK (Madin Darby canine kidney) cells enhanced canonical wnt signalling[311]. In another study, RAS/TGF-β induced EMT in the same cells, led to elevated levels of WNT5A, RhoA, Rac and JNK, and to a suppression of WNT3A-mediated canonical signalling[312]. Another study reported that, TGF-β (transforming growth factorβ 1)-induced EMT in murine renal epithelial cells caused elevated Wnt11 which mediated activation of *Zeb1* and *snail* genes. Function of Wnt11 was mediated by JNK pathway[313].

One way of dissecting the different roles of 5T4 in the different pathways could be achieved by simultaneously investigating the consequences of reintroducing complete, truncated, or mutated forms of 5T4 on the three recognised biological processes: chemotaxis, EMP and wnt signalling. This could be investigated mechanistically further by exploring the signalling transduction proteins in the different pathways, such as ERK/Akt for CXCR4, E-cadherin repressor proteins and wnt proteins.

8.6 5T4-Targeted Intraperitoneal Therapy

The results presented in this study support a potential role for 5T4 in EOC spread, and importantly, as a tumour associated antigen (TAA) expressed by both primary and metastatic ovarian cancers but not, at significant levels, by normal OSE. This raises the question as to whether an intraperitoneal targeted therapy utilising 5T4 could be worthy of investigation in EOC patients.

Several techniques could theoretically be used for intra-peritoneal 5T4-targeted therapy; one option is the use of 5T4 neutralising antibodies. However, the evidence for the efficacy of this approach are limited. In one study a 5T4 neutralising antibody was found to abrogate CXCR4-mediated chemotactic response in embryonic cells *in vitro*[25]. Another approach is to target 5T4 expression by the means of intra-peritoneal plasmid delivery to knock down 5T4 expression. A similar oral approach is currently in phase I trial using oral inactive *E.coli* in patients with familial adenomatous polyposis (FAP) to target bowel epithelium (CEQ508.FAP.01 study in FAP)[314-316]. This approach could be hazardous, however, it has the potential advantage of specificity; animal research could help to establish its safety and efficacy.

Nonetheless, it is not clear if abrogating 5T4 function, by neutralising antibodies or expression knockdown, could lead to growth and proliferation of peritoneal tumours while blocking metastasis. Our results in SKOV-3 cells do not support that, and Dr J Brazzatti has shown that there is no difference in proliferation among the three SKOV cells using an MTT assay at 3 time points (24, 48 and 72 hours). Similarly, in SCLC cell lines (H1048) we found that 5T4 KD did not result in CXCR7 expression or detectable changes in cell growth, however, 5T4 KD in MEFs led to overexpression of CXCR7 receptor and improved survival by abrogating apoptosis **(Appendix 3)**[280].

An alternative strategy for investigating intra-peritoneal 5T4-targeted therapy is the use of antibody conjugated drugs (ADC) such as calicheamicin and / or monomethylauristatin F (MMAF) both of which have been investigated in clinical trials for systemic administration[20, 21]. It is plausible that this approach could offer a useful means for controlling intra-peritoneal disease. The availability of these drugs for systemic use could prove useful also in treating extra-peritoneal disease such as lymph node and distant metastases.

Intraperitoneal 5T4-targeted therapeutics must be explored first in animal models since results obtained from cell line experiments do not necessarily apply to the complex *in vivo* environment. While *in vivo* animal models are not entirely identical to human biology,

there have been considerable recent advancements in animal models such as mice and chicken models[317, 318].

8.7 Conclusion

Overall, this study has followed a systematic approach to investigate the role of the oncofetal glycoprotein 5T4 in ovarian cancer metastasis. Initially, phenotyping according to protein expression, functional assays and protein expression manipulation were conducted in ovarian cancer cell lines. These experiments investigated three main biological processes through which 5T4 was thought to be functionally linked: CXCL12 chemotaxis, epithelial mesenchymal plasticity, and wnt signalling. Subsequently, the findings from cell line experiments were explored in human tissues, which supported the tumour associated antigen (TAA) function of 5T4 with higher expression in the metastatic lesions than matched primary cancers. Nonetheless, a direct mechanistic role for 5T4 in the studied pathways and the expressed proteins were not demonstrated by this work.

This project unveiled several novel findings such as the role of 5T4 knockdown in cancer cells which resulted in an overall less motile and less migratory phenotype. In addition, comparative studies of 5T4 and other markers, among normal ovarian surface epithelium, primary ovarian cancers and their paired metastatic lesions, have not been conducted previously.

The findings of this study can constitute a platform for future promising research into 5T4 mechanistic biology and clinical applications.

References

1. Hole N, Stern PL. A 72 kD trophoblast glycoprotein defined by a monoclonal antibody. British Journal of Cancer 1988; 57:239.

2. Southall PJ, Boxer GM, Bagshawe KD, Hole N, Bromley M, Stern PL. Immunohistological distribution of 5T4 antigen in normal and malignant tissues. British Journal of Cancer 1990; 61:89.

3. Stern PL, Beresford N, Thompson S, Johnson PM, Webb PD, Hole N. Characterization of the human trophoblast-leukocyte antigenic molecules defined by a monoclonal antibody. The Journal of Immunology 1986; 137:1604-9.

4. Lala PK, Graham CH. Mechanisms of trophoblast invasiveness and their control: the role of proteases and protease inhibitors. Cancer and Metastasis Reviews 1990; 9:369.

5. Hanahan D, Weinberg RA. The hallmarks of cancer. Cell 2000; 100:57-70.

6. Hanahan D, Weinberg Robert A. Hallmarks of Cancer: The Next Generation. Cell 2011; 144:646-74.

7. Shaw D, Woods A, Myers K, Westwater C, Rahi-Saund V, Davies M, et al. Glycosylation and epitope mapping of the 5T4 glycoprotein oncofoetal antigen. Biochemical journal 2002; 363:137.

8. Boyle JM, Grzeschik KH, Heath PR, Morten JE, Stern PL. Trophoblast glycoprotein recognised by monoclonal antibody 5T4 maps to human chromosome 6q14–q15. Human Genetics 1990; 84:455.

9. Kobe B, Kajava AV. The leucine-rich repeat as a protein recognition motif. Current Opinion in Structural Biology 2001; 11:725-32.

10. Awan A, Lucic MR, Shaw DM, Sheppard F, Westwater C, Lyons SA, et al. 5T4 Interacts with TIP-2GIPC, a PDZ Protein, with Implications for Metastasis. Biochemical and Biophysical Research Communications 2002; 290:1030.

11. Jones H, Roberts G, Hole N, McDicken IW, Stern P. Investigation of expression of 5T4 antigen in cervical cancer. British Journal of Cancer 1990; 61:96.

12. Starzynska T, Wiechowska-Kozlowska A, Marlicz K, Bromley M, Roberts SA, Lawniczak M, et al. 5T4 oncofetal antigen in gastric carcinoma and its clinical significance. European journal of gastroenterology & hepatology 1998; 10:479-84.

13. Griffiths RW, Gilham DE, Dangoor A, Ramani V, Clarke NW, Stern PL, et al. Expression of the 5T4 oncofoetal antigen in renal cell carcinoma: a potential target for T-cell-based immunotherapy. British Journal of Cancer 2005; 93:670.

14. Wrigley E, McGown AT, Rennison J, Swindell R, Crowther D, Starzynska T, et al. 5T4 oncofetal antigen expression in ovarian carcinoma. International Journal of Gynecological Cancer 1995; 5:269.

15. Ali A, Langdon J, Stern P, Partridge M. The pattern of expression of the 5T4 oncofoetal antigen on normal, dysplastic and malignant oral mucosa. Oral Oncology 2001; 37:57.

16. Amato RJ. 5T4-modified vaccinia Ankara: progress in tumor-associated antigen-based immunotherapy. Expert Opinion on Biological Therapy 2010; 10:281-7.

17. UK Clinical Research Network Study Portfolio. TRIOC: TroVax® in Relapsed Ovarian Cancer 2014.

18. Eisen T, Hedlund G, Forsberg G, Hawkins R. Naptumomab Estafenatox: Targeted Immunotherapy with a Novel Immunotoxin. Current Oncology Reports 2014; 16:1-6.

19. Shaw DM, Connolly NB, Patel PM, Kilany S, Hedlund G, Nordle O, et al. A phase II study of a 5T4 oncofoetal antigen tumour-targeted superantigen (ABR-214936) therapy in patients with advanced renal cell carcinoma. British Journal of Cancer 2007; 96:567.

20. Boghaert ER, Sridharan L, Khandke KM, Armellino D, Ryan MG, Myers K, et al. The oncofetal protein, 5T4, is a suitable target for antibody-guided anti-cancer chemotherapy with calicheamicin. International journal of oncology 2008; 32:221-34.

21. Sapra P, Damelin M, DiJoseph J, Marquette K, Geles KG, Golas J, et al. Long-term tumor regression induced by an antibody-drug conjugate that targets 5T4, an oncofetal antigen expressed on tumor-initiating cells. Molecular Cancer Therapeutics 2013; 12:38-47.

22. Starzynska T, Rahi V, Stern PL. The expression of 5T4 antigen in colorectal and gastric carcinoma. British Journal of Cancer 1992; 66:867.

23. Starzynska T, Marsh PJ, Schofield PF, Roberts SA, Myers KA, Stern PL. Prognostic significance of 5T4 oncofetal antigen expression in colorectal carcinoma. British Journal of Cancer 1994; 69:899.

24. Spencer HL, Eastham AM, Merry CLR, Southgate TD, Perez-Campo F, Soncin F, et al. E-Cadherin Inhibits Cell Surface Localization of the Pro-Migratory 5T4 Oncofetal Antigen in Mouse Embryonic Stem Cells. Molecular Biology of the Cell 2007; 18:2838-51.

25. Southgate TD, McGinn OJ, Castro FV, Rutkowski AJ, Al-Muftah M, Marinov G, et al. CXCR4 Mediated Chemotaxis Is Regulated by 5T4 Oncofetal Glycoprotein in Mouse Embryonic Cells. PLoS ONE 2010; 5:e9982.

26. Kagermeier-Schenk B, Wehner D, Ozhan-Kizil G, Yamamoto H, Li J, Kirchner K, et al. Waif1/5T4 inhibits Wnt/beta-catenin signaling and activates noncanonical Wnt pathways by modifying LRP6 subcellular localization. Dev Cell 2013; 21:1129-43.

27. Quinn M, Babb P, Brock A, Kirby L, Jones J. Cancer trends in England and Wales 1950-1999. The Office for National Statistics, 2001.

28. Trent Cancer Registry. Overview of Ovarian Cancer in England: Incidence, Mortality and Survival. In: Network NCI, ed., 2012.

29. Office for National Statistics. Cancer Incidence and Mortality in the United Kingdom, 2008-10. Office for National Statistics, 2012.

30. Walsh P, Cooper N. Cancer Atlas of the United Kingdom and Ireland. In: Office for National Statistics, ed. Ovary, 2005.

31. Mok SC, Kwong J, Welch WR, Samimi G, Ozbun L, Bonome T, et al. Etiology and pathogenesis of epithelial ovarian cancer. Disease Markers 2007; 23:367-76.

32. Doufekas K, Olaitan A. Clinical epidemiology of epithelial ovarian cancer in the UK. International Journal of Women's Health 2014; 6:537-45.

33. Sawada M, Miki T. Ovarian Germ Cell Tumors. In: Masters JW, Palsson B, eds. Human Cell Culture: Springer Netherlands, 2002:121-5.

34. Jayson GC, Kohn EC, Kitchener HC, Ledermann JA. Ovarian cancer. The Lancet 2014; 384:1376-88.

35. Antoniou A, Pharoah PDP, Narod S, Risch HA, Eyfjord JE, Hopper JL, et al. Average risks of breast and ovarian cancer associated with BRCA1 or BRCA2 mutations detected in case series unselected for family history: A combined analysis of 22 studies. American Journal of Human Genetics 2003; 72:1117-30.

36. Xiao X, Melton DW, Gourley C. Mismatch repair deficiency in ovarian cancer - Molecular characteristics and clinical implications. Gynecologic Oncology 2014; 132:506-12.

37. Jönsson JM, Bartuma K, Dominguez-Valentin M, Harbst K, Ketabi Z, Malander S, et al. Distinct gene expression profiles in ovarian cancer linked to Lynch syndrome. Familial Cancer 2014:537-45.

38. Jacobs I, Lancaster J. The molecular genetics of sporadic and familial epithelial ovarian cancer. International Journal of Gynecological Cancer 1996; 6:337-55.

39. Tavassoli FA, Devilee P. Pathology and genetics of tumours of the breast and female genital organs. Lyon: International Agency for Research on Cancer, 2003.

40. Seidman JD, Horkayne-Szakaly I, Haiba M, Boice CR, Kurman RJ, Ronnett BM. The histologic type and stage distribution of ovarian carcinomas of surface epithelial origin. International Journal of Gynecological Pathology 2004; 23:41-4.

41. Naora H. Developmental Patterning in the Wrong Context: The Paradox of Epithelial Ovarian Cancers. Cell Cycle 2005; 4:1033-5.

42. Cho KR, Shih I-M. Ovarian Cancer. Annual Review of Pathology: Mechanisms of Disease 2009; 4:287-313.

43. Dehari R, Kurman RJ, Logani S, Shih I-M. The development of high-grade serous carcinoma from atypical proliferative (borderline) serous tumors and low-grade micropapillary serous carcinoma: a morphologic and molecular genetic analysis. The American journal of surgical pathology 2007; 31:1007-12.

44. Kurman RJ, Shih I-M. Molecular pathogenesis and extraovarian origin of epithelial ovarian cancer—shifting the paradigm. Human pathology 2011; 42:918-31.

45. Köbel M, Kurman R, Seidman J. New Views of Ovarian Carcinoma Types: How Will This Change Practice? In: Ledermann JA, Creutzberg CL, Quinn MA, eds. Controversies in the Management of Gynecological Cancers: Springer London, 2014:29-38.

46. Shih I-M, Kurman RJ. Ovarian tumorigenesis: a proposed model based on morphological and molecular genetic analysis. The American journal of pathology 2004; 164:1511-8.

47. Ricciardelli C, Oehler MK. Diverse molecular pathways in ovarian cancer and their clinical significance. Maturitas 2009; 62:270-5.

48. Stack MS, Fishman DA. Ovarian Cancer. New York: Kluwer Academic 2009.

49. Walsh C, Karlan B. Molecular signatures of ovarian cancer: from detection to prognosis. Molecular Diagnosis & Therapy 2010; 14:13-22.

50. The Cancer Genome Atlas Research Network. Integrated genomic analyses of ovarian carcinoma. Nature 2011; 474:609-15.

51. Banerjee S, Kaye SB. New strategies in the treatment of ovarian cancer: current clinical perspectives and future potential. Clinical Cancer Research 2013; 19:961-8.

52. Emmanuel C, Chiew Y-E, George J, Etemadmoghadam D, Anglesio MS, Sharma R, et al. Genomic Classification of Serous Ovarian Cancer with Adjacent Borderline Differentiates RAS Pathway and TP53-Mutant Tumors and Identifies NRAS as an Oncogenic Driver. Clinical Cancer Research 2014; 20:6618-30.

53. Fathalla MF. Incessant ovulation: a factor in ovarian neoplasia? The Lancet 1971; 298:163.

54. Edmondson RJ, Monaghan JM. The epidemiology of ovarian cancer. International Journal of Gynecological Cancer 2001; 11:423-9.

55. Fredrickson TN. Ovarian tumors of the hen. Environmental health perspectives 1987; 73:35.

56. Auersperg N, Wong AST, Choi K-C, Kang SK, Leung PCK. Ovarian Surface Epithelium: Biology, Endocrinology, and Pathology. Endocr Rev 2001; 22:255-88.

57. Herrinton LJ, Stanford JL, Schwartz SM, Weiss NS. Ovarian Cancer Incidence Among Asian Migrants to the United States and Their Descendants. Journal of the National Cancer Institute 1994; 86:1336-9.

58. Healy JC, Reznek RH. The peritoneum, mesenteries and omenta: Normal anatomy and pathological processes. European Radiology 1998; 8:886-900.

59. Mutsaers SE. The mesothelial cell. The international journal of biochemistry & cell biology 2004; 36:9-16.

60. Mutsaers SE. Mesothelial cells: Their structure, function and role in serosal repair. Respirology 2002; 7:171-91.

61. Mutsaers S, Wilkosz S. Structure and Function of Mesothelial Cells. In: Ceelen W, ed. Peritoneal Carcinomatosis: Springer US, 2007:1-19.

62. Nuzhat A, Erik WT, Michael AQ. Epithelial-mesenchymal interconversions in normal ovarian surface epithelium and ovarian carcinomas: An exception to the norm. Journal of Cellular Physiology 2007; 213:581-8.

63. Scully RE. Pathology of ovarian cancer precursors. Journal of Cellular Biochemistry 1995; 59:208-18.

64. Auersperg N. Ovarian surface epithelium as a source of ovarian cancers: Unwarranted speculation or evidence-based hypothesis? Gynecologic Oncology 2013; 130:246-51.

65. Cheng W, Liu J, Yoshida H, Rosen D, Naora H. Lineage infidelity of epithelial ovarian cancers is controlled by HOX genes that specify regional identity in the reproductive tract. Nature Medicine 2005; 11:531-7.

66. Folkins AK, Jarboe EA, Roh MH, Crum CP. Precursors to pelvic serous carcinoma and their clinical implications. Gynecologic oncology 2009; 113:391-6.

67. Auersperg N. The origin of ovarian cancers—hypotheses and controversies. Front Biosci (Schol Ed) 2013; 5:709-19.

68. Dubeau L. The cell of origin of ovarian epithelial tumours. The Lancet Oncology 2008; 9:1191-7.

69. Kurman RJ, Shih I-M. The Origin and pathogenesis of epithelial ovarian cancer-a proposed unifying theory. The American journal of surgical pathology 2010; 34:433.

70. Naora H. The heterogeneity of epithelial ovarian cancers: reconciling old and new paradigms. Expert Reviews in Molecular Medicine 2007; 9:1-12.

71. Piek JMJ, van Diest PJ, Zweemer RP, Jansen JW, Poort-Keesom RJJ, Menko FH, et al. Dysplastic changes in prophylactically removed Fallopian tubes of women predisposed to developing ovarian cancer. The Journal of Pathology 2001; 195:451-6.

72. Crum CP, Drapkin R, Kindelberger D, Medeiros F, Miron A, Lee Y. Lessons from BRCA: The Tubal Fimbria Emerges as an Origin for Pelvic Serous Cancer. Clinical Medicine & Research 2007; 5:35-44.

73. Wei J-J, William J, Bulun S. Endometriosis and ovarian cancer: a review of clinical, pathologic, and molecular aspects. International Journal of Gynecologic Pathology 2011; 30:553-68.

74. Tong G-X, Devaraj K, Hamele-Bena D, Yu WM, Turk A, Chen X, et al. Pax8: A marker for carcinoma of Müllerian origin in serous effusions. Diagnostic Cytopathology 2011; 39:562-6.

75. Wang Y, Wang Y, Li J, Yuan Z, Yuan B, Zhang T, et al. PAX8: A sensitive and specific marker to identify cancer cells of ovarian origin for patients prior to neoadjuvant chemotherapy. Journal of Hematology and Oncology 2013; 6:60-7.

76. Ozcan A, Liles N, Coffey D, Shen SS, Truong LD. PAX2 and PAX8 expression in primary and metastatic müllerian epithelial tumors: a comprehensive comparison. The American journal of surgical pathology 2011; 35:1837-47.

77. Liliac L, Carcangiu ML, Canevari S, Căruntu I, Ciobanu AD, Danciu M, et al. The value of PAX8 and WT1 molecules in ovarian cancer diagnosis. Romanian journal of morphology and embryology= Revue roumaine de morphologie et embryologie 2012; 54:17-27.

78. Dubeau L. The cell of origin of ovarian epithelial tumors and the ovarian surface epithelium dogma: Does the emperor have no clothes? Gynecologic Oncology 1999; 72:437-42.

79. Dubeau L, Drapkin R. Coming into focus: The nonovarian origins of ovarian cancer. Annals of Oncology 2013; 24:viii28-viii35.

80. Lee Y, Medeiros F, Kindelberger D, Callahan MJ, Muto MG, Crum CP. Advances in the recognition of tubal intraepithelial carcinoma: Applications to cancer screening and the pathogenesis of ovarian cancer. Advances in Anatomic Pathology 2006; 13:1-7.

81. Crum CP, McKeon FD, Xian W. BRCA, the Oviduct, and the Space and Time Continuum of Pelvic Serous Carcinogenesis. International Journal of Gynecological Cancer 2012; 22:S29-S34.

82. Colgan TJ, Murphy J, Cole DE, Narod S, Rosen B. Occult carcinoma in prophylactic oophorectomy specimens: prevalence and association with BRCA germline mutation status. The American journal of surgical pathology 2001; 25:1283-9.

83. Finch A, Shaw P, Rosen B, Murphy J, Narod SA, Colgan TJ. Clinical and pathologic findings of prophylactic salpingo-oophorectomies in 159 BRCA1 and BRCA2 carriers. Gynecologic oncology 2006; 100:58-64.

84. Leeper K, Garcia R, Swisher E, Goff B, Greer B, Paley P. Pathologic findings in prophylactic oophorectomy specimens in high-risk women. Gynecologic oncology 2002; 87:52-6.

85. Carcangiu ML, Peissel B, Pasini B, Spatti G, Radice P, Manoukian S. Incidental carcinomas in prophylactic specimens in BRCA1 and BRCA2 germ-line mutation carriers, with emphasis on fallopian tube lesions: report of 6 cases and review of the literature. The American journal of surgical pathology 2006; 30:1222-30.

86. Callahan MJ, Crum CP, Medeiros F, Kindelberger DW, Elvin JA, Garber JE, et al. Primary fallopian tube malignancies in BRCA-positive women undergoing surgery for ovarian cancer risk reduction. Journal of Clinical Oncology 2007; 25:3985-90.

87. Kindelberger DW, Lee Y, Miron A, Hirsch MS, Feltmate C, Medeiros F, et al. Intraepithelial carcinoma of the fimbria and pelvic serous carcinoma: evidence for a causal relationship. The American journal of surgical pathology 2007; 31:161-9.

88. Carlson JW, Miron A, Jarboe EA, Parast MM, Hirsch MS, Lee Y, et al. Serous tubal intraepithelial carcinoma: its potential role in primary peritoneal serous carcinoma and serous cancer prevention. Journal of Clinical Oncology 2008; 26:4160-5.

89. Roh MH, Kindelberger D, Crum CP. Serous tubal intraepithelial carcinoma and the dominant ovarian mass: clues to serous tumor origin? The American journal of surgical pathology 2009; 33:376-83.

90. Przybycin CG, Kurman RJ, Ronnett BM, Shih I-M, Vang R. Are all pelvic (nonuterine) serous carcinomas of tubal origin? The American journal of surgical pathology 2010; 34:1407-16.

91. Seidman JD, Zhao P, Yemelyanova A. “Primary peritoneal” high-grade serous carcinoma is very likely metastatic from serous tubal intraepithelial carcinoma: Assessing the new paradigm of ovarian and pelvic serous carcinogenesis and its implications for screening for ovarian cancer. Gynecologic Oncology 2011; 120:470-3.

92. Leonhardt K, Einenkel J, Sohr S, Engeland K, Horn L-C. p53 signature and serous tubal in-situ carcinoma in cases of primary tubal and peritoneal carcinomas and serous borderline tumors of the ovary. International Journal of Gynecologic Pathology 2011; 30:417-24.

93. Crum CP, Herfs M, Ning G, Bijron JG, Howitt BE, Jimenez CA, et al. Through the glass darkly: intraepithelial neoplasia, top-down differentiation, and the road to ovarian cancer. The Journal of Pathology 2013; 231:402-12.

94. Reade CJ, McVey RM, Tone AA, Finlayson S, McAlpine J, Fung-Kee-Fung M, et al. The Fallopian Tube as the Origin of High Grade Serous Ovarian Cancer: Review of a Paradigm Shift. J Obstet Gynaecol Can 2014; 36:133-40.

95. Karst AM, Levanon K, Drapkin R. Modeling high-grade serous ovarian carcinogenesis from the fallopian tube. Proceedings of the National Academy of Sciences 2011; 108:7547-52.

96. Perets R, Wyant G, Muto K, Bijron J, Poole B, Chin K, et al. Transformation of the Fallopian Tube Secretory Epithelium Leads to High-Grade Serous Ovarian Cancer in Brca;Tp53;Pten Models. Cancer Cell 2013; 24:751-65.

97. Vaughan S, Coward JI, Bast RC, Berchuck A, Berek JS, Brenton JD, et al. Rethinking ovarian cancer: recommendations for improving outcomes. Nature Reviews Cancer 2011; 11:719-25.

98. Quirk JT, Natarajan N, Mettlin CJ. Age-specific ovarian cancer incidence rate patterns in the United States. Gynecologic Oncology 2005; 99:248-50.

99. Rosenblatt KA, Weiss NS, Schwartz SM. Incidence of malignant fallopian tube tumors. Gynecologic Oncology 1989; 35:236-9.

100. Stewart SL, Wike JM, Foster SL, Michaud F. The incidence of primary fallopian tube cancer in the United States. Gynecologic oncology 2007; 107:392-7.

101. Selman AE, Copeland LJ. Extraovarian Primary Peritoneal Carcinomas. Textbook of Uncommon Cancer, 2012:485-95.

102. Fellay CN, Fiche M, Delaloye J-F, Bauer J. Extraovarian primary peritoneal carcinoma. Management of Rare Adult Tumours: Springer, 2010:279-92.

103. Kalyani R, Narasimha A, Kumar H, Narayanswamy S. Extraovarian Papillary Serous Carcinoma of Peritoneum: A Report of Two Cases with Review of Literature. J South Asian Feder Obst Gynae 2013; 5:42-4.

104. Benedet JL, Bender H, Jones H, 3rd, Ngan HY, Pecorelli S. FIGO staging classifications and clinical practice guidelines in the management of gynecologic cancers. FIGO Committee on Gynecologic Oncology. International Journal of Gynaecology & Obstetrics 2000; 70:209-62.

105. Benedet J, Pecorelli S, Ngan HY, Hacker NF, Denny L, Jones III HW, et al. Staging classifications and clinical practice guidelines for gynaecological cancers. International Journal of Gynecology and Obstetrics 2000; 70:207-312.

106. Prat J. Staging classification for cancer of the ovary, fallopian tube, and peritoneum. International Journal of Gynecology and Obstetrics 2013; 124:1-5.

107. Bhoola S, Hoskins WJ. Diagnosis and management of epithelial ovarian cancer. Obstetrics & Gynecology 2006; 107:1399-410.

108. Winter-Roach BA, Kitchener HC, Lawrie TA. Adjuvant (post-surgery) chemotherapy for early stage epithelial ovarian cancer. Cochrane Database Syst Rev 2012; 3.

109. Trimbos JB, Vergote I, Bolis G, Vermorken JB, Mangioni C, Madronal C, et al. Impact of Adjuvant Chemotherapy and Surgical Staging in Early-Stage Ovarian Carcinoma: European Organisation for Research and Treatment of Cancer–Adjuvant ChemoTherapy in Ovarian Neoplasm Trial. Journal of the National Cancer Institute 2003; 95:113-25.

110. International Collaborative Ovarian Neoplasm, European Organisation for Research Treatment of Cancer. International Collaborative Ovarian Neoplasm Trial 1 and Adjuvant ChemoTherapy In Ovarian Neoplasm Trial: Two Parallel Randomized Phase III Trials of Adjuvant Chemotherapy in Patients With Early-Stage Ovarian Carcinoma. Journal of the National Cancer Institute 2003; 95:105-12.

111. International Collaborative Ovarian Neoplasm Collaborators. International Collaborative Ovarian Neoplasm Trial 1: A Randomized Trial of Adjuvant Chemotherapy in Women With Early-Stage Ovarian Cancer. Journal of the National Cancer Institute 2003; 95:125-32.

112. Armstrong DK, Bundy B, Wenzel L, Huang HQ, Baergen R, Lele S, et al. Intraperitoneal cisplatin and paclitaxel in ovarian cancer. New England Journal of Medicine 2006; 354:34-43.

113. Hall M, Gourley C, McNeish I, Ledermann J, Gore M, Jayson G, et al. Targeted anti-vascular therapies for ovarian cancer: Current evidence. British Journal of Cancer 2013; 108:250-8.

114. Davidson BA, Secord AA. Profile of pazopanib and its potential in the treatment of epithelial ovarian cancer. International Journal of Women's Health 2014; 6:289-300.

115. Ledermann J, Harter P, Gourley C, Friedlander M, Vergote I, Rustin G, et al. Olaparib maintenance therapy in platinum-sensitive relapsed ovarian cancer. New England Journal of Medicine 2012; 366:1382-92.

116. Markman M. Optimal Management of Recurrent Ovarian Cancer. International Journal of Gynecological Cancer 2009; 19:S40-S3.

117. Ledermann JA, Kristeleit RS. Optimal treatment for relapsing ovarian cancer. Annals of Oncology 2010; 21:vii218-vii22.

118. Eisenhauer EL, Zanagnolo V, Cohn DE, Salani R, O'Malley DM, Sutton G, et al. A phase II study of gemcitabine, carboplatin and bevacizumab for the treatment of platinum-sensitive recurrent ovarian cancer. Gynecologic Oncology 2014; 134:262-6.

119. Liu JF, Barry WT, Birrer M, Lee JM, Buckanovich RJ, Fleming GF, et al. Combination cediranib and olaparib versus olaparib alone for women with recurrent platinum-sensitive ovarian cancer: A randomised phase 2 study. The Lancet Oncology 2014; 15:1207-14.

120. Cancer Research UK. Ovarian cancer survival statistics. 2013.

121. Menon U. Ovarian cancer: challenges of early detection. Nature Clinical Practice Oncology 2007; 4:498-9.

122. Bast RC, Jr., Brewer M, Zou C, Hernandez MA, Daley M, Ozols R, et al. Prevention and early detection of ovarian cancer: mission impossible? Recent Results in Cancer Research 2007; 174:91-100.

123. Usha M, Aleksandra G-M, Rachel H, Andy R, Matthew B, Aarti S, et al. Sensitivity and specificity of multimodal and ultrasound screening for ovarian cancer, and stage distribution of detected cancers: results of the prevalence screen of the UK Collaborative Trial of Ovarian Cancer Screening (UKCTOCS). The Lancet Oncology 2009; 10:327.

124. Janczar S, Graham JS, Paige AJ, Gabra H. Targeting locoregional peritoneal dissemination in ovarian cancer. Expert Review of Obstetrics & Gynecology 2009; 4:133-47.

125. Tan DSP, Agarwal R, Kaye SB. Mechanisms of transcoelomic metastasis in ovarian cancer. The Lancet Oncology 2006; 7:925-34.

126. Lengyel E. Ovarian Cancer Development and Metastasis. The American journal of pathology 2010; 177:1053.

127. Clark R, Krishnan V, Schoof M, Rodriguez I, Theriault B, Chekmareva M, et al. Milky Spots Promote Ovarian Cancer Metastatic Colonization of Peritoneal Adipose in Experimental Models. The American Journal of Pathology 2013; 183:576-91.

128. Morris V, Schmidt E, MacDonald I, Groom A, Chambers A. Sequential steps in hematogenous metastasis of cancer cells studied by in vivo videomicroscopy. Invasion & metastasis 1996; 17:281-96.

129. Chambers AF, Naumov GN, Varghese HJ, Nadkarni KV, MacDonald IC, Groom AC. Critical steps in hematogenous metastasis: An overview. Surgical Oncology Clinics of North America 2001; 10:243-55.

130. Labelle M, Hynes RO. The initial hours of metastasis: The importance of cooperative host-tumor cell interactions during hematogenous dissemination. Cancer Discovery 2012; 2:1091-9.

131. Tarin D, Price JE, Kettlewell MGW, Souter RG, Vass ACR, Crossley B. Mechanisms of Human Tumor Metastasis Studied in Patients with Peritoneovenous Shunts. Cancer Research 1984; 44:3584-92.

132. Morice P, Joulie F, Camatte S, Atallah D, Rouzier R, Pautier P, et al. Lymph node involvement in epithelial ovarian cancer: analysis of 276 pelvic and paraaortic lymphadenectomies and surgical implications. Journal of the American College of Surgeons 2003; 197:198-205.

133. Moser B, Wolf M, Walz A, Loetscher P. Chemokines: multiple levels of leukocyte migration control. Trends in Immunology 2004; 25:75.

134. Moser B, Loetscher P. Lymphocyte traffic control by chemokines. Nat Immunol 2001; 2:123.

135. Sharma M. Chemokines and their receptors: orchestrating a fine balance between health and disease. Critical Reviews in Biotechnology 2010; 30:1-22.

136. O'Hayre M, Salanga CL, Handel TM, Allen SJ. Chemokines and cancer: migration, intracellular signalling and intercellular communication in the microenvironment. Biochem J 2008; 409:635-49.

137. Balkwill FR. The chemokine system and cancer. The Journal of Pathology 2012; 226:148-57.

138. Tassone L, Notarangelo LD, Bonomi V, Savoldi G, Sensi A, Soresina A, et al. Clinical and genetic diagnosis of warts, hypogammaglobulinemia, infections, and myelokathexis syndrome in 10 patients. Journal of Allergy and Clinical Immunology 2009; 123:1170.

139. Furusato B, Mohamed A, Uhlén M, Rhim JS. CXCR4 and cancer. Pathology International 2010; 60:497-505.

140. Delgado MB, Clark-Lewis I, Loetscher P, Langen H, Thelen M, Baggiolini M, et al. Rapid inactivation of stromal cell-derived factor-1 by cathepsin G associated with lymphocytes. European Journal of Immunology 2001; 31:699-707.

141. Teicher BA, Fricker SP. CXCL12 (SDF-1)/CXCR4 Pathway in Cancer. Clinical Cancer Research 2010; 16:2927-31.

142. Christopherson KW, Hangoc G, Broxmeyer HE. Cell surface peptidase CD26/dipeptidylpeptidase IV regulates CXCL12/stromal cell-derived factor-1α-mediated

chemotaxis of human cord blood CD34+ progenitor cells. The Journal of Immunology 2002; 169:7000-8.

143. Sun YX, Pedersen EA, Shiozawa Y, Havens AM, Jung Y, Wang J, et al. CD26/dipeptidyl peptidase IV regulates prostate cancer metastasis by degrading SDF-1/CXCL12. Clinical and Experimental Metastasis 2008; 25:765-76.

144. Crump MP, Gong J-H, Loetscher P, Rajarathnam K, Amara A, Arenzana-Seisdedos F, et al. Solution structure and basis for functional activity of stromal cell-derived factor-1; dissociation of CXCR4 activation from binding and inhibition of HIV-1. EMBO J 1997; 16:6996-7007.

145. McQuibban GA, Butler GS, Gong J-H, Bendall L, Power C, Clark-Lewis I, et al. Matrix Metalloproteinase Activity Inactivates the CXC Chemokine Stromal Cell-derived Factor-1. Journal of Biological Chemistry 2001; 276:43503-8.

146. Holland JD, Kochetkova M, Akekawatchai C, Dottore M, Lopez A, McColl SR. Differential Functional Activation of Chemokine Receptor CXCR4 Is Mediated by G Proteins in Breast Cancer Cells. Cancer Research 2006; 66:4117-24.

147. Sohy D, Parmentier M, Springael J-Y. Allosteric Transinhibition by Specific Antagonists in CCR2/CXCR4 Heterodimers. Journal of Biological Chemistry 2007; 282:30062-9.

148. Burns JM, Summers BC, Wang Y, Melikian A, Berahovich R, Miao Z, et al. A novel chemokine receptor for SDF-1 and I-TAC involved in cell survival, cell adhesion, and tumor development. The Journal of experimental medicine 2006; 203:2201-13.

149. Levoye A, Balabanian K, Baleux F, Bachelerie F, Lagane B. CXCR7 heterodimerizes with CXCR4 and regulates CXCL12-mediated G protein signaling. Blood 2009; 113:6085-93.

150. Thelen M, Thelen S. CXCR7, CXCR4 and CXCL12: An eccentric trio? Journal of Neuroimmunology 2008; 198:9.

151. Maksym RB, Tarnowski M, Grymula K, Tarnowska J, Wysoczynski M, Liu R, et al. The role of stromal-derived factor-1/ CXCR7 axis in development and cancer. European Journal of Pharmacology 2009; 625:31.

152. Muller A, Homey B, Soto H, Ge N, Catron D, Buchanan ME, et al. Involvement of chemokine receptors in breast cancer metastasis. Nature 2001; 410:50.

153. Jiang Y-p, Wu X-h, Shi B, Wu W-x, Yin G-r. Expression of chemokine CXCL12 and its receptor CXCR4 in human epithelial ovarian cancer: An independent prognostic factor for tumor progression. Gynecologic Oncology 2006; 103:226-33.

154. Scotton CJ, Wilson JL, Milliken D, Stamp G, Balkwill FR. Epithelial Cancer Cell Migration: a role for chemokine receptors? Cancer Research 2001; 61:4961-5.

155. Scotton CJ, Wilson JL, Scott K, Stamp G, Wilbanks GD, Fricker S, et al. Multiple Actions of the Chemokine CXCL12 on Epithelial Tumor Cells in Human Ovarian Cancer. Cancer Research 2002; 62:5930-8.

156. Hiroaki K, Kiyosumi S, Mikio T, Kazuhiko I, Akihiro N, Fumitaka K. Involvement of SDF-1alpha/CXCR4 axis in the enhanced peritoneal metastasis of epithelial ovarian carcinoma. International Journal of Cancer 2008; 122:91-9.

157. Lamouille S, Xu J, Derynck R. Molecular mechanisms of epithelial–mesenchymal transition. Nat Rev Mol Cell Biol 2014; 15:178-96.

158. Cervantes-Arias A, Pang L, Argyle D. Epithelial-mesenchymal transition as a fundamental mechanism underlying the cancer phenotype. Veterinary and comparative oncology 2013; 11:169-84.

159. Yang J, Weinberg RA. Epithelial-Mesenchymal Transition: At the Crossroads of Development and Tumor Metastasis. Developmental Cell 2008; 14:818.

160. Iwatsuki M, Mimori K, Yokobori T, Ishi H, Beppu T, Nakamori S, et al. Epithelial-mesenchymal transition in cancer development and its clinical significance. Cancer Science 2010; 101:293-9.

161. Tarin D. The Fallacy of Epithelial Mesenchymal Transition in Neoplasia. Cancer Research 2005; 65:5996-6001.

162. Thompson EW, Newgreen DF. Carcinoma Invasion and Metastasis: A Role for Epithelial-Mesenchymal Transition? Cancer Research 2005; 65:5991-5.

163. Tsai JH, Yang J. Epithelial–mesenchymal plasticity in carcinoma metastasis. Genes & development 2013; 27:2192-206.

164. Kalluri R, Weinberg R. The basics of epithelial-mesenchymal transition. The Journal of Clinical Investigation 2009; 119:1420-8.

165. Garber K. Epithelial-to-mesenchymal transition is important to metastasis, but questions remain. J Natl Cancer Inst 2008; 100:232 - 3.

166. Hugo H, Ackland ML, Blick T, Lawrence MG, Clements JA, Williams ED, et al. Epithelial-mesenchymal and mesenchymal-epithelial transitions in carcinoma progression. J Cell Physiol 2007; 213:374 - 83.

167. Davies BR, Worsley SD, Ponder BAJ. Expression of E-cadherin, α-catenin and β-catenin in normal ovarian surface epithelium and epithelial ovarian cancers. Histopathology 1998; 32:69-80.

168. Ahmed N, Thompson EW, Quinn MA. Epithelial-mesenchymal interconversions in normal ovarian surface epithelium and ovarian carcinomas: An exception to the norm. Journal of Cellular Physiology 2007; 213:581-8.

169. Vergara D, Merlot B, Lucot J-P, Collinet P, Vinatier D, Fournier I, et al. Epithelial-mesenchymal transition in ovarian cancer. Cancer Letters 2009; 291:59.

170. Imai T, Horiuchi A, Shiozawa T, Osada R, Kikuchi N, Ohira S, et al. Elevated expression of E-cadherin and α-, β-, and γ-catenins in metastatic lesions compared with primary epithelial ovarian carcinomas. Human pathology 2004; 35:1469-76.

171. Hudson L, Zeineldin R, Stack MS. Phenotypic plasticity of neoplastic ovarian epithelium: unique cadherin profiles in tumor progression. Clinical & Experimental Metastasis 2008; 25:643-55.

172. Eastham A, Spencer H, Soncin F, Ritson S, Merry CLR, Stern P, et al. Epithelial-mesenchymal transition events during human embryonic stem cell differentiation. Cancer research 2007; 67:11254.

173. Kim Y-S, Yi B-R, Kim N-H, Choi K-C. Role of the epithelial-mesenchymal transition and its effects on embryonic stem cells. Exp Mol Med 2014; 46:e108.

174. Ward CM, Barrow K, Woods AM, Stern PL. The 5T4 oncofoetal antigen is an early differentiation marker of mouse ES cells and its absence is a useful means to assess pluripotency. Journal of Cell Science 2003; 116:4533-42.

175. Carsberg CJ, Myers KA, Stern PL. Metastasis-associated 5T4 antigen disrupts cell-cell contacts and induces cellular motility in epithelial cells. International Journal of Cancer 1996; 68:84-92.

176. Nusse R, Varmus HE. Many tumors induced by the mouse mammary tumor virus contain a provirus integrated in the same region of the host genome. Cell 1982; 31:99-109.

177. Korzh V. Winding roots of Wnts. Zebrafish 2008; 5:159-68.

178. Polakis P. An Introduction to Wnt Signaling. In: Goss KH, Kahn M, eds. Targeting the Wnt Pathway in Cancer: Springer New York, 2011:1-18.

179. Nusse R. Wnt Signaling. Cold Spring Harbor Perspectives in Biology 2012; 4:a011163.

180. Reya T, Clevers H. Wnt signalling in stem cells and cancer. Nature 2005; 434:843-50.

181. Berridge MJ. wnt signalling pathway. Cell Signalling Pathways. Cell Signalling Biology: Portland Press Limited, 2014:http://www.biochemj.org/csb/002/csb.htm#Wnt_signalling_pathways.

182. Baarsma HA, Königshoff M, Gosens R. The WNT signaling pathway from ligand secretion to gene transcription: molecular mechanisms and pharmacological targets. Pharmacology & therapeutics 2013; 138:66-83.

183. Saito-Diaz K, Chen TW, Wang X, Thorne CA, Wallace HA, Page-McCaw A, et al. The way Wnt works: Components and mechanism. Growth Factors 2013; 31:1-31.

184. Aberle H, Bauer A, Stappert J, Kispert A, Kemler R. β-catenin is a target for the ubiquitin–proteasome pathway. The EMBO journal 1997; 16:3797-804.

185. Clevers H, Nusse R. Wnt/β-Catenin Signaling and Disease. Cell 2012; 149:1192-205.

186. Biechele TL, Moon RT. Assaying β-catenin/TCF transcription with β-catenin/TCF transcription-based reporter constructs. Wnt Signaling: Springer, 2008:99-110.

187. Biechele TL, Adams AM, Moon RT. Transcription-Based Reporters of Wnt/β-Catenin Signaling. Cold Spring Harbor Protocols 2009; 2009:5223.

188. Chuang K, Lieu C, Tsai W, Wu M, Chen Y, Liao J, et al. Evaluation of anti-Wnt/β-catenin signaling agents by pGL4-TOP transfected stable cells with a luciferase reporter system. Brazilian Journal of Medical and Biological Research 2010; 43:931-41.

189. Hatzis P, van der Flier LG, van Driel MA, Guryev V, Nielsen F, Denissov S, et al. Genome-Wide Pattern of TCF7L2/TCF4 Chromatin Occupancy in Colorectal Cancer Cells. Molecular and Cellular Biology 2008; 28:2732-44.

190. Gómez-Orte E, Sáenz-Narciso B, Moreno S, Cabello J. Multiple functions of the noncanonical Wnt pathway. Trends in Genetics 2013; 29:545-53.

191. Semenov MV, Habas R, MacDonald BT, He X. SnapShot: Noncanonical Wnt Signaling Pathways. Cell 2007; 131:1378.e1-.e2.

192. McNeill H, Woodgett JR. When pathways collide: collaboration and connivance among signalling proteins in development. Nat Rev Mol Cell Biol 2010; 11:404-13.

193. Wynshaw-Boris A. Dishevelled: In Vivo Roles of a Multifunctional Gene Family During Development. In: Yingzi Y, ed. Current Topics in Developmental Biology: Academic Press, 2012:213-35.

194. Ishida-Takagishi M, Enomoto A, Asai N, Ushida K, Watanabe T, Hashimoto T, et al. The Dishevelled-associating protein Daple controls the non-canonical Wnt/Rac pathway and cell motility. Nature communications 2012; 3:859.

195. Cui J, Zhang M, Zhang Y-q, Xu Z-h. JNK pathway: diseases and therapeutic potential. Acta Pharmacol Sin 2007; 28:601-8.

196. van Amerongen R, Nusse R. Towards an integrated view of Wnt signaling in development. Development 2009; 136:3205-14.

197. Christian JL, McMahon JA, McMahon AP, Moon RT. Xwnt-8, a Xenopus Wnt-1/int-1-related gene responsive to mesoderm-inducing growth factors, may play a role in ventral mesodermal patterning during embryogenesis. Development 1991; 111:1045-55.

198. Du SJ, Purcell SM, Christian JL, McGrew LL, Moon RT. Identification of distinct classes and functional domains of Wnts through expression of wild-type and chimeric proteins in Xenopus embryos. Molecular and cellular biology 1995; 15:2625-34.

199. Moon RT, Campbell RM, Christian JL, McGrew LL, Shih J, Fraser S. Xwnt-5A: a maternal Wnt that affects morphogenetic movements after overexpression in embryos of Xenopus laevis. Development 1993; 119:97-111.

200. Wong GT, Gavin BJ, McMahon AP. Differential transformation of mammary epithelial cells by Wnt genes. Mol Cell Biol 1994; 14:6278-86.

201. Willert K, Nusse R. Wnt proteins. Cold Spring Harbor perspectives in biology 2012; 4:a007864.

202. Cruciat C-M, Niehrs C. Secreted and transmembrane wnt inhibitors and activators. Cold Spring Harbor perspectives in biology 2013; 5:a015081.

203. Niehrs C. Function and biological roles of the Dickkopf family of Wnt modulators. Oncogene 2006; 25:7469-81.

204. Huelsken J, Behrens J. The Wnt signalling pathway. J Cell Sci 2002; 115:3977-8.

205. Kuhl M, Geis K, Sheldahl LC, Pukrop T, Moon RT, Wedlich D. Antagonistic regulation of convergent extension movements in Xenopus by Wnt/beta-catenin and Wnt/Ca2+ signaling. Mech Dev 2001; 106:61-76.

206. McEwen DG, Peifer M. Wnt signaling: Moving in a new direction. Curr Biol 2000; 10:R562-4.

207. Klingelhofer J, Troyanovsky RB, Laur OY, Troyanovsky S. Exchange of catenins in cadherin-catenin complex. Oncogene 2003; 22:1181-8.

208. Gottardi CJ, Gumbiner BM. Distinct molecular forms of β-catenin are targeted to adhesive or transcriptional complexes. The Journal of Cell Biology 2004; 167:339-49.

209. Joiner DM, Ke J, Zhong Z, Xu HE, Williams BO. LRP5 and LRP6 in development and disease. Trends in Endocrinology & Metabolism 2013; 24:31-9.

210. Sabapathy K. Role of the JNK Pathway in Human Diseases. In: Shirish S, ed. Progress in Molecular Biology and Translational Science: Academic Press, 2012:145-69.

211. Simons M, Mlodzik M. Planar cell polarity signaling: from fly development to human disease. Annual review of genetics 2008; 42:517.

212. MacDonald BT, Tamai K, He X. Wnt/β-Catenin Signaling: Components, Mechanisms, and Diseases. Developmental Cell 2009; 17:9-26.

213. Prosperi J, Luu H, Goss K. Dysregulation of the Wnt Pathway in Solid Tumors. In: Goss KH, Kahn M, eds. Targeting the Wnt Pathway in Cancer: Springer New York, 2011:81-128.

214. Müschen M. WNT/β-Catenin Signaling in Leukemia. In: Goss KH, Kahn M, eds. Targeting the Wnt Pathway in Cancer: Springer New York, 2011:129-42.

215. Bodmer W, Bailey C, Bodmer J, Bussey H, Ellis A, Gorman P, et al. Localization of the gene for familial adenomatous polyposis on chromosome 5. Nature 1987; 328:614 - 6.

216. Goss KH, Groden J. Biology of the adenomatous polyposis coli tumor suppressor. Journal of Clinical Oncology 2000; 18:1967-79.

217. Huang C-L, Liu D, Ishikawa S, Nakashima T, Nakashima N, Yokomise H, et al. Wnt1 overexpression promotes tumour progression in non-small cell lung cancer. European Journal of Cancer 2008; 44:2680-8.

218. Marsit CJ, McClean MD, Furniss CS, Kelsey KT. Epigenetic inactivation of the SFRP genes is associated with drinking, smoking and HPV in head and neck squamous cell carcinoma. International journal of cancer 2006; 119:1761-6.

219. Lindvall C, Zylstra CR, Evans N, West RA, Dykema K, Furge KA, et al. The Wnt co-receptor Lrp6 is required for normal mouse mammary gland development. PLoS One 2009; 4:e5813.

220. Björklund P, Svedlund J, Olsson A-K, Åkerström G, Westin G. The internally truncated LRP5 receptor presents a therapeutic target in breast cancer. PloS one 2009; 4:e4243.

221. Wu R, Zhai Y, Fearon ER, Cho KR. Diverse mechanisms of β-catenin deregulation in ovarian endometrioid adenocarcinomas. Cancer Research 2001; 61:8247-55.

222. Arend RC, Londoño-Joshi AI, Straughn Jr JM, Buchsbaum DJ. The Wnt/β-catenin pathway in ovarian cancer: A review. Gynecologic Oncology 2013; 131:772-9.

223. Wang Y, Hewitt S, Liu S, Zhou X, Zhu H, Zhou C, et al. Tissue microarray analysis of human FRAT1 expression and its correlation with the subcellular localisation of β-catenin in ovarian tumours. British journal of cancer 2006; 94:686-91.

224. Sagae S, Kobayashi K, Nishioka Y, Sugimura M, Ishioka S, Nagata M, et al. Mutational Analysis of β-Catenin Gene in Japanese Ovarian Carcinomas: Frequent Mutations in Endometrioid Carcinomas. Cancer Science 1999; 90:510-5.

225. Karbova E, Davidson B, Metodiev K, Tropé CG, Nesland JM. Adenomatous polyposis coli (APC) protein expression in primary and metastatic serous ovarian carcinoma. International journal of surgical pathology 2002; 10:175-80.

226. Lee CM, Shvartsman H, Deavers MT, Wang S-C, Xia W, Schmandt R, et al. β-Catenin nuclear localization is associated with grade in ovarian serous carcinoma. Gynecologic oncology 2003; 88:363-8.

227. Gatcliffe T, Monk B, Planutis K, Holcombe R. Wnt signaling in ovarian tumorigenesis. International Journal of Gynecological Cancer 2008; 18:954-62.

228. Rask K, Nilsson A, Brannstrom M, Carlsson P, Hellberg P, Janson PO, et al. Wnt-signalling pathway in ovarian epithelial tumours: increased expression of beta-catenin and GSK3beta. British Journal of Cancer 2003; 89:1298-304.

229. Badiglian Filho L, Oshima CTF, De Oliveira Lima F, De Oliveira Costa H, De Sousa Damião R, Gomes T, et al. Canonical and noncanonical Wnt pathway: a comparison among normal ovary, benign ovarian tumor and ovarian cancer. Oncology Reports 2009; 21:313.

230. Pukrop T, Binder C. The complex pathways of Wnt 5a in cancer progression. J Mol Med (Berl) 2008; 86:259-66.

231. Weeraratna AT, Jiang Y, Hostetter G, Rosenblatt K, Duray P, Bittner M, et al. Wnt5a signaling directly affects cell motility and invasion of metastatic melanoma. Cancer Cell 2002; 1:279-88.

232. Yamamoto H, Kitadai Y, Yamamoto H, Oue N, Ohdan H, Yasui W, et al. Laminin gamma2 mediates Wnt5a-induced invasion of gastric cancer cells. Gastroenterology 2009; 137:242-52.

233. Pourreyron C, Reilly L, Proby C, Panteleyev A, Fleming C, McLean K, et al. Wnt5a is strongly expressed at the leading edge in non-melanoma skin cancer, forming active gradients, while canonical Wnt signalling is repressed. PloS one 2012; 7:e31827.

234. Yu M, Ting DT, Stott SL, Wittner BS, Ozsolak F, Paul S, et al. RNA sequencing of pancreatic circulating tumour cells implicates WNT signalling in metastasis. Nature 2012; 487:510–3.

235. Ford CE, Punnia-Moorthy G, Henry CE, Llamosas E, Nixdorf S, Olivier J, et al. The non-canonical Wnt ligand, Wnt5a, is upregulated and associated with epithelial to mesenchymal transition in epithelial ovarian cancer. Gynecologic Oncology 2014; 134:338-45.

236. Bitler BG, Nicodemus JP, Li H, Cai Q, Wu H, Hua X, et al. Wnt5a Suppresses Epithelial Ovarian Cancer by Promoting Cellular Senescence. Cancer Research 2011; 71:6184-94.

237. Jacob F, Ukegjini K, Nixdorf S, Ford CE, Olivier J, Caduff R, et al. Loss of secreted frizzled-related protein 4 correlates with an aggressive phenotype and predicts poor outcome in ovarian cancer patients. PloS one 2012; 7:e31885.

238. Ford CE, Jary E, Ma SSQ, Nixdorf S, Heinzelmann-Schwarz VA, Ward RL. The Wnt gatekeeper SFRP4 modulates EMT, cell migration and downstream Wnt signalling in serous ovarian cancer cells. PloS one 2013; 8:e54362.

239. Menezes ME, Devine DJ, Shevde LA, Samant RS. Dickkopf1: a tumor suppressor or metastasis promoter? International Journal of Cancer 2012; 130:1477-83.

240. Wang S, Zhang S. Dickkopf-1 is frequently overexpressed in ovarian serous carcinoma and involved in tumor invasion. Clinical & experimental metastasis 2011; 28:581-91.

241. Caneparo L, Huang Y-L, Staudt N, Tada M, Ahrendt R, Kazanskaya O, et al. Dickkopf-1 regulates gastrulation movements by coordinated modulation of Wnt/βcatenin and Wnt/PCP activities, through interaction with the Dally-like homolog Knypek. Genes & development 2007; 21:465-80.

242. Zhao Y, Malinauskas T, Harlos K, Jones EY. Structural Insights into the Inhibition of Wnt Signaling by Cancer Antigen 5T4/Wnt-Activated Inhibitory Factor 1. Structure 2014; 22:612-20.

243. Filmus J, Trent JM, Pullano R, Buick RN. A Cell Line from a Human Ovarian Carcinoma with Amplification of the K-ras Gene. Cancer Research 1986; 46:5179-82.

244. American Type Culture Collection. 2014.

245. European Collection of Cell Cultures. 2014.

246. Viray JL. Implementation of Applied Biosystems AmpFlSTR® MiniFiler™ Amplification Kit For Forensic Casework: Validation, Inhibition, and Contact DNA Studies. Forensic Science. UNIVERSITY OF CALIFORNIA: University of California, Davis, 2008.

247. Lazic S. The problem of pseudoreplication in neuroscientific studies: is it affecting your analysis? BMC Neuroscience 2010; 11:5.

248. Cumming G, Fidler F, Vaux DL. Error bars in experimental biology. The Journal of Cell Biology 2007; 177:7-11.

249. Vaux DL, Fidler F, Cumming G. Replicates and repeats—what is the difference and is it significant? EMBO reports 2012; 13:291-6.

250. Shapiro HM. Practical flow cytometry. John Wiley & Sons, 2005.

251. Herzenberg LA, Tung J, Moore WA, Herzenberg LA, Parks DR. Interpreting flow cytometry data: a guide for the perplexed. Nature immunology 2006; 7:681-5.

252. Parikh HH, Li WC, Ramanathan M. Evaluation of an alternative to the Kolmogorov–Smirnov test for flow cytometric histogram comparisons. Journal of immunological methods 1999; 229:97-105.

253. Cox C, Reeder JE, Robinson RD, Suppes SB, Wheeless LL. Comparison of frequency distributions in flow cytometry. Cytometry 1988; 9:291-8.

254. Bagwell B. A journey through flow cytometric immunofluorescence analyses—finding accurate and robust algorithms that estimate positive fraction distributions. Clinical Immunology Newsletter 1996; 16:33-7.

255. Boyden S. The chemotactic effect of mixtures of antibody and antigen on polymorphonuclear leucocytes. The Journal of experimental medicine 1962; 115:453-66.

256. Senn S. Analysis of serial measurements in medical research. BMJ: British Medical Journal 1990; 300:680.

257. Matthews J, Altman DG, Campbell M, Royston P. Analysis of serial measurements in medical research. BMJ: British Medical Journal 1990; 300:230.

258. Buddug Rhiannon Thomas. 5T4 Oncofoetal Glycoprotein and Hepatocyte Growth Factor Influence on Breast and Ovarian Carcinoma cells. School of Medicine: University of Manchester, 2000.

259. Berahovich RD, Penfold MET, Schall TJ. Nonspecific CXCR7 antibodies. Immunology Letters 2010; 133:112-4.

260. Fischer T, Nagel F, Jacobs S, Stumm R, Schulz S. Reassessment of CXCR4 chemokine receptor expression in human normal and neoplastic tissues using the novel rabbit monoclonal antibody UMB-2. PLoS One 2008; 3:e4069.

261. Matos LLd, Stabenow E, Tavares MR, Ferraz AR, Capelozzi VL, Pinhal MAdS. Immunohistochemistry quantification by a digital computer-assisted method compared to semiquantitative analysis. Clinics 2006; 61:417-24.

262. Taylor C, Levenson R. Quantification of immunohistochemistry—issues concerning methods, utility and semiquantitative assessment II. Histopathology 2006; 49:411-24.

263. Walker R. Quantification of immunohistochemistry—issues concerning methods, utility and semiquantitative assessment I. Histopathology 2006; 49:406-10.

264. Domcke S, Sinha R, Levine DA, Sander C, Schultz N. Evaluating cell lines as tumour models by comparison of genomic profiles. Nat Commun 2013; 4:3126-35.

265. Yu Y, Li H, Xue B, Jiang X, Huang K, Ge J, et al. SDF-1/CXCR7 Axis Enhances Ovarian Cancer Cell Invasion by MMP-9 Expression Through p38 MAPK Pathway. DNA and cell biology 2014; 33:543-9.

266. Kajiyama H, Kikkawa F, Khin E, Shibata K, Ino K, Mizutani S. Dipeptidyl Peptidase IV Overexpression Induces Up-Regulation of E-Cadherin and Tissue Inhibitors of Matrix Metalloproteinases, Resulting in Decreased Invasive Potential in Ovarian Carcinoma Cells. Cancer Research 2003; 63:2278-83.

267. Li J, Jiang K, Qiu X, Li M, Hao Q, Wei L, et al. Overexpression of CXCR4 is significantly associated with cisplatin-based chemotherapy resistance and can be a prognostic factor in epithelial ovarian cancer. BMB Reports 2014; 47:33-8.

268. Zhu ZB, Makhija SK, Lu B, Wang M, Kaliberova L, Liu B, et al. Transcriptional targeting of adenoviral vector through the CXCR4 tumor-specific promoter. Gene Ther 2004; 11:645-8.

269. Wang H, Liu W, Wei D, Hu K, Wu X, Yao Y. Effect of the LPA-mediated CXCL12-CXCR4 axis in the tumor proliferation, migration and invasion of ovarian cancer cell lines. Oncology Letters 2014; 7:1581-5.

270. Giri S, Karakoti A, Graham RP, Maguire JL, Reilly CM, Seal S, et al. Nanoceria: a rare-earth nanoparticle as a novel anti-angiogenic therapeutic agent in ovarian cancer. PloS one 2013; 8:e54578.

271. McLeod C, Anderson DWJ, Katz W. Preparation of foetal calf serum for use in tissue culture. Journal of Biological Standardization 1980; 8:263-70.

272. Mitchell CG, Eddleston ALWF. The importance of selecting suitable foetal calf serum for use in the leucocyte migration test. Transplantation 1973; 16:689-91.

273. Pujic Z, Mortimer D, Feldner J, Goodhill G. Assays for eukaryotic cell chemotaxis. Combinatorial chemistry & high throughput screening 2009; 12:580.

274. Roca-Cusachs P, Sunyer R, Trepat X. Mechanical guidance of cell migration: lessons from chemotaxis. Current Opinion in Cell Biology 2013; 25:543-9.

275. Wu J, Wu X, Lin F. Recent developments in microfluidics-based chemotaxis studies. Lab on a Chip 2013; 13:2484-99.

276. Georgi Valeriev Marinov. Trafficking And Functional Interactions Of The Oncofoetal Trophoblast Glycoprotein 5t4. School of Medicine. Manchester: University of Manchester, 2012.

277. Richard R. Neubig. Pharmacology of G Protein Coupled Receptors. Amsterdam: Academic Press, 2011.

278. Penela P, Murga C, Ribas C, Tutor AS, Peregrín S, Mayor F. Mechanisms of regulation of G protein-coupled receptor kinases (GRKs) and cardiovascular disease. Cardiovascular research 2006; 69:46-56.

279. Maurice P, Guillaume J-L, Benleulmi-Chaachoua A, Daulat AM, Kamal M, Jockers R. GPCR-interacting proteins, major players of GPCR function. Advances in pharmacology 2011; 62:349.

280. McGinn OJ, Marinov G, Sawan S, Stern PL. CXCL12 receptor preference, signal transduction, biological response and the expression of 5T4 oncofoetal glycoprotein. Journal of Cell Science 2012; 125:5467-78.

281. Santiago Y, Chan E, Liu P-Q, Orlando S, Zhang L, Urnov FD, et al. Targeted gene knockout in mammalian cells by using engineered zinc-finger nucleases. Proceedings of the National Academy of Sciences 2008; 105:5809-14.

282. Pan Y, Xiao L, Li ASS, Zhang X, Sirois P, Zhang J, et al. Biological and biomedical applications of engineered nucleases. Molecular Biotechnology 2013; 55:54-62.

283. Andrzej Jerzy Rutkowski. Investigation of a novel locus encoding a putative paralogue of 5T4 oncofoetal glycoprotein. School of Cancer and Enabling Sciences. Manchester: University of Manchester, 2012.

284. Gurdon J, Lemaire P, Kato K. Community effects and related phenomena in development. Cell 1993; 75:831-4.

285. Jouanneau J, Moens G, Bourgeois Y, Poupon M, Thiery J. A minority of carcinoma cells producing acidic fibroblast growth factor induces a community effect for tumor progression. Proceedings of the National Academy of Sciences 1994; 91:286-90.

286. Thiery JP, Chopin D. Epithelial cell plasticity in development and tumor progression. Cancer and Metastasis Reviews 1999; 18:31-42.

287. Ward CM, Eastham AM, Stern PL. Cell surface 5T4 antigen is transiently upregulated during early human embryonic stem cell differentiation: effect of 5T4 phenotype on neural lineage formation. Experimental cell research 2006; 312:1713-26.

288. Stern PL, Brazzatti J, Sawan S, McGinn OJ. Understanding and exploiting 5T4 oncofoetal glycoprotein expression. Seminars in Cancer Biology 2014; 29:13-20.

289. Kotsopoulos J, Terry KL, Poole EM, Rosner B, Murphy MA, Hecht JL, et al. Ovarian cancer risk factors by tumor dominance, a surrogate for cell of origin. International Journal of Cancer 2013; 133:730-9.

290. Bogoyevitch MA, Kobe B. Uses for JNK: the many and varied substrates of the c-Jun N-terminal kinases. Microbiology and Molecular Biology Reviews 2006; 70:1061-95.

291. Zhu G, Zhang M, Duan Z, Liu Y. Expression and significance of chemokine SDF-1 and its receptor CXCR4 in human epithelial ovarian tumours. Journal of Xi'an Jiaotong University (Medical Sciences) 2008; 29:223-6.

292. Popple A, Durrant L, Spendlove I, Scott PRI, Deen S, Ramage J. The chemokine, CXCL12, is an independent predictor of poor survival in ovarian cancer. British journal of cancer 2012; 106:1306-13.

293. Barbolina MV, Kim M, Liu Y, Shepard J, Belmadani A, Miller RJ, et al. Microenvironmental Regulation of Chemokine (C-X-C-Motif) Receptor 4 in Ovarian Carcinoma. Molecular Cancer Research 2010; 8:653-64.

294. Heinrich EL, Lee W, Lu J, Lowy AM, Kim J. Chemokine CXCL12 activates dual CXCR4 and CXCR7-mediated signaling pathways in pancreatic cancer cells. J Transl Med 2012; 10:68-77.

295. Jaszczynska-Nowinka K, Rucinski M, Ziolkowska A, Markowska A, Malendowicz LK. Expression of SDF-1 and CXCR4 transcript variants and CXCR7 in epithelial ovarian cancer. Oncology Letters 2014; 7:1618-24.

296. Vivas-Mejia P, Benito JM, Fernandez A, Han H-D, Mangala L, Rodriguez-Aguayo C, et al. c-Jun-NH2-kinase-1 inhibition leads to antitumor activity in ovarian cancer. Clinical cancer research 2010; 16:184-94.

297. Anglesio MS, Wiegand KC, Melnyk N, Chow C, Salamanca C, Prentice LM, et al. Type-Specific Cell Line Models for Type-Specific Ovarian Cancer Research. PLoS ONE 2013; 8:e72162.

298. Jacob F, Nixdorf S, Hacker NF, Heinzelmann-Schwarz VA. Reliable in vitro studies require appropriate ovarian cancer cell lines. Journal of Ovarian Research 2014; 7:60.

299. Wilding JL, Bodmer WF. Cancer Cell Lines for Drug Discovery and Development. Cancer Research 2014; 74:2377-84.

300. Gillet JP, Varma S, Gottesman MM. The clinical relevance of cancer cell lines. Journal of the National Cancer Institute 2013; 105:452-8.

301. Tveit K, Pihl A. Do cell lines in vitro reflect the properties of the tumours of origin? A study of lines derived from human melanoma xenografts. British journal of cancer 1981; 44:775.

302. Tateishi K, Ando W, Higuchi C, Hart D, Hashimoto J, Nakata K, et al. Comparison of human serum with fetal bovine serum for expansion and differentiation of human synovial MSC: potential feasibility for clinical applications. Cell transplantation 2008; 17:549-57.

303. Emerman JT, Fiedler EE, Tolcher AW, Rebbeck PM. Effects of Defined Medium, Fetal Bovine Serum, and Human Serum on Growth and Chemosensitivities of Human Breast Cancer Cells in Primary Culture: Inference for in vitro Assays. In Vitro Cellular & Developmental Biology 1987; 23:134-40.

304. Isaac C, Mattos CNd, Rêgo FMPd, Cardim LN, Altran SC, Paggiaro AO, et al. Replacement of fetal calf serum by human serum as supplementation for human fibroblast culture. Revista Brasileira de Cirurgia Plástica 2011; 26:379-84.

305. Flesken-Nikitin A, Hwang C-I, Cheng C-Y, Michurina TV, Enikolopov G, Nikitin AY. Ovarian surface epithelium at the junction area contains a cancer-prone stem cell niche. Nature 2013; 495:241-5.

306. Ghosh MC, Collins GD, Vandanmagsar B, Patel K, Brill M, Carter A, et al. Activation of Wnt5A signaling is required for CXC chemokine ligand 12–mediated T-cell migration. Blood 2009; 114:1366-73.

307. Wang Y, Sun Z, Qiu X, Li Y, Qin J, Han X. Roles of Wnt/β-catenin signaling in epithelial differentiation of mesenchymal stem cells. Biochemical and biophysical research communications 2009; 390:1309-14.

308. Wang Q, Sun Z-X, Allgayer H, Yang H-S. Downregulation of E-cadherin is an essential event in activating β-catenin/Tcf-dependent transcription and expression of its target genes in Pdcd4 knockdown cells. Oncogene 2010; 29:128-38.

309. DiMeo TA, Anderson K, Phadke P, Feng C, Perou CM, Naber S, et al. A Novel Lung Metastasis Signature Links Wnt Signaling with Cancer Cell Self-Renewal and Epithelial-Mesenchymal Transition in Basal-like Breast Cancer. Cancer Research 2009; 69:5364-73.

310. Yee DS, Tang Y, Li X, Liu Z, Guo Y, Ghaffar S, et al. Research The Wnt inhibitory factor 1 restoration in prostate cancer cells was associated with reduced tumor growth, decreased capacity of cell migration and invasion and a reversal of epithelial to mesenchymal transition. Molecular Cancer 2010; 9:162-76.

311. Howard S, Deroo T, Fujita Y, Itasaki N. A positive role of cadherin in Wnt/β-catenin signalling during epithelial-mesenchymal transition. PloS one 2011; 6:e23899.

312. Chen Y-S, Mathias RA, Mathivanan S, Kapp EA, Moritz RL, Zhu H-J, et al. Proteomics Profiling of Madin-Darby Canine Kidney Plasma Membranes Reveals Wnt-5a Involvement during Oncogenic H-Ras/TGF-β-mediated Epithelial-Mesenchymal Transition. Molecular & Cellular Proteomics 2011; 10:M110.

313. Zhang P, Cai Y, Soofi A, Dressler GR. Activation of Wnt11 by transforming growth factor-β drives mesenchymal gene expression through non-canonical Wnt protein signaling in renal epithelial cells. Journal of Biological Chemistry 2012; 287:21290-302.

314. Landesman-Milo D, Peer D. Toxicity profiling of several common RNAi-based nanomedicines: A comparative study. Drug Delivery and Translational Research 2014; 4:96-103.

315. Lares MR, Rossi JJ, Ouellet DL. RNAi and small interfering RNAs in human disease therapeutic applications. Trends in Biotechnology 2010; 28:570-9.

316. Draz MS, Fang BA, Zhang P, Hu Z, Gu S, Weng KC, et al. Nanoparticle-Mediated Systemic Delivery of siRNA for Treatment of Cancers and Viral Infections. Theranostics 2014; 4:872-92.

317. House CD, Hernandez L, Annunziata CM. Recent technological advances in using mouse models to study ovarian cancer. Frontiers in Oncology 2014; 4:1-7.

318. Tiwari A, Hadley JA, Hendricks GL, III, Elkin RG, Cooper T, Ramachandran R. Characterization of Ascites-Derived Ovarian Tumor Cells from Spontaneously Occurring Ovarian Tumors of the Chicken: Evidence for E-Cadherin Upregulation. PLoS ONE 2013; 8:e57582.

Appendices:

Appendix 1: FIGO staging (pre 2014) of Ovarian Cancer[104]

FIGO Stage		TNM Category
	Primary tumour cannot be assessed	TX
	No evidence of primary tumour	T0
I	Tumour limited to the ovaries	T1
IA	Tumour limited to one ovary; capsule intact, no tumour on ovarian surface; no malignant cells in ascites or peritoneal washings	T1a
IB	Tumour limited to both ovaries; capsule intact, no tumour on ovarian surface; no malignant cells in ascites or peritoneal washings	T1b
IC	Tumour limited to one or both ovaries with any of the following: capsule ruptured, tumour on ovarian surface, malignant cells in ascites or peritoneal washings	T1c
II	Tumour involves one or both ovaries with pelvic extension	T2
IIA	Extension and / or implants on uterus and / or tubes.; no malignant cells in ascites or peritoneal washings	T2a
IIB	Extension to other pelvic tissues; no malignant cells in ascites or peritoneal washings	T2b
IIC	Pelvic extension (IIA or IIB) with malignant cells in ascites or peritoneal washings	T2c
III	Tumour involves one or both ovaries with microscopically confirmed peritoneal metastasis outside the pelvis and / or regional lymph node metastasis	T3/N1
IIIA	Microscopic peritoneal metastasis beyond pelvis	T3a
IIIB	Macroscopic peritoneal metastasis beyond pelvis 2 cm or less in greatest dimension	T3b
IIIC	Peritoneal metastasis beyond pelvis more than 2 cm in greatest dimension and / or regional lymph node metastasis	T3c/N1
IV	Distant metastasis excludes peritoneal metastasis.	M1

Ovarian cancer staging according to the International Federation of Gynecology & Obstetrics (FIGO)[104].

Appendix 2: Ethical Approval

North West 8 Research Ethics Committee – Greater Manchester East
3rd Floor, Barlow House
4 Minshull Street
Manchester
M1 3DZ

Telephone: 0161 625 7820

2 December 2010

Private & Confidential
Dr S Sawan, Clinical Research Fellow
The Paterson Institute for Cancer Research
Wilmslow Road
Manchester
M20 4BX

Dear Dr Sawan

Full title of study:	**The Role of the Oncofetal Glycoprotein 5T4 in Ovarian Cancer Microenvironment**
REC reference number:	**10/H1013/66**
Protocol number:	**RDP920**

Thank you for your response to the Committee's letter of 25 October 2010. I can confirm the REC has received the documents listed below as evidence of compliance with the approval conditions detailed in our letter dated 25 October 2010. Please note these documents are for record purposes only and have not been reviewed by the Committee.

Documents received

The documents received were as follows:

Document	*Version*	*Date*
Participant Information Sheet: Patients	SEPH	16 November 2010
Participant Information Sheet: Controls	SEPH	16 November 2010
Participant Consent Form	SEPH	16 November 2010

You should ensure that the sponsor has a copy of the final documentation for the study. It is the sponsor's responsibility to ensure that the documentation is made available to R&D offices at all participating sites.

10/H1013/66 **Please quote this number on all correspondence**

Yours sincerely

Ms Elaine Hutchings
Committee Co-ordinator
E-mail: elaine.hutchings@northwest.nhs.uk

Copy to: Mohammed Zabair, R&D
University of Manchester

North West 8 Research Ethics Committee – Greater Manchester East
Research Ethics Office
Barlow House
4 Minshull Street
Manchester
M1 3DZ

Telephone: 0161 625 7828

25 October 2010

Dr Saladin Sawan
Clinical Research Fellow
The University of Manchester
The Paterson Institute for cancer research
Wilmslow Road
Manchester
M20 4BX

Dear Dr Sawan

Study Title:	**The Role of the Oncofetal Glycoprotein 5T4 in Ovarian Cancer Microenvironment**
REC reference number:	**10/H1013/66**
Protocol number:	**RDP920**

The Research Ethics Committee reviewed the above application at the meeting held on 19 October 2010. Thank you for attending to discuss the study.

Discussion

The Committee asked how long participants would have between being approached to participate and giving consent.

You advised that it would usually be a week however in some instances patients would be fast tracked for the operation and they would only have 24 hours to consent.

The Committee agreed the minimum time for consent of 24 hours which you planned to allow was acceptable.

The Committee asked how you would ensure non-English speaking participants could understand what was expected of them.

You advised that in a previous, similar study there had been very few people who required an interpreter. You advised that if someone did require an interpreter you would use the translators available at St Mary's Hospital.

The Committee asked what volume of blood would be used in the research.

You explained that 40ml would be sufficient.

The Committee agreed the participant should know exactly how much blood would be taken.

The Committee asked why the peritoneal sample was being taken and how big it would be.

You advised that the peritoneum was the covering of the ovary and you believed that the origination of ovarian cancer was caused by this covering. The size would be approximately 1.5cm by 5cm.

The Committee agreed the size was acceptable however agreed this should be made clear on the PIS.

The Committee queried who would store the blood samples.

You advised that the samples would likely be stored in the Patterson. You clarified that further ethical approval would be undertaken for the use of the samples in future research.

The Committee agreed the term *'gifting'* should be explained in the PIS and used on the consent form.

The Committee agreed the findings of the study could be put on a website for participants to access rather than having to store contact details and re-contact them at a later date.

Professor Stern agreed and advised this was normally done anyway.

Decision – Favourable Opinion

The members of the Committee present gave a favourable ethical opinion of the above research on the basis described in the application form, protocol and supporting documentation, subject to the conditions specified below.

Ethical review of research sites

The favourable opinion applies to all NHS sites taking part in the study, subject to management permission being obtained from the NHS/HSC R&D office prior to the start of the study (see "Conditions of the favourable opinion" below).

Conditions of the favourable opinion

The favourable opinion is subject to the following conditions being met prior to the start of the study.

1. Under the heading, *'What will happen to me if I take part?', the following sentences should be added:*

   'When you come into hospital for your treatment, you will have some blood tests. 40ml of blood will be taken.

   'We require a small sample, approximately 1.5cm by 5cm, which will be done by your surgeon…'

2. The following sentence should be added to the PIS under the heading *'What will happen to any samples I give?'*:

   'Samples stored will have no name on them and will be kept in St Mary's Hospital according to the relevant legislation. I understand that by gifting my samples I will be donating the samples for use in future research studies'.

3. The following sentence should be added to the consent form instead of the sentence detailed at point 5:

   'I agree to donate my samples as a gift for future research'

4. The following sentence in the PIS under the heading *'Why have I been invited?'* should be removed:

   'We knew about you because we are members of the clinical team here in St Mary's Hospital'.

Management permission or approval must be obtained from each host organisation prior to the start of the study at the site concerned.

For NHS research sites only, management permission for research ("R&D approval") should be obtained from the relevant care organisation(s) in accordance with NHS research governance arrangements. Guidance on applying for NHS permission for research is available in the Integrated Research Application System or at http://www.rdforum.nhs.uk. Where the only involvement of the NHS organisation is as a Participant Identification Centre, management permission for research is not required but the R&D office should be notified of the study. Guidance should be sought from the R&D office where necessary.

Sponsors are not required to notify the Committee of approvals from host organisations.

It is responsibility of the sponsor to ensure that all the conditions are complied with before the start of the study or its initiation at a particular site (as applicable).

You should notify the REC in writing once all conditions have been met (except for site approvals from host organisations) and provide copies of any revised documentation with updated version numbers.

Approved documents

The documents reviewed and approved at the meeting were:

Document	*Version*	*Date*
Investigator CV	Dr S Sawan	20 September 2010
Investigator CV	P L Stern	16 September 2010
Protocol	SEPH-15	23 August 2010
REC application	3.0	20 September 2010
Covering Letter		20 September 2010
Participant Information Sheet: Patients	SEPH-15	23 August 2010
Participant Information Sheet: Controls	SEPH-15	23 August 2010
Participant Consent Form	SEPH-15	23 August 2010
Peer Review		12 June 2010
Evidence of insurance or indemnity		15 September 2010

Membership of the Committee

The members of the Ethics Committee who were present at the meeting are listed on the attached sheet.

Statement of compliance

The Committee is constituted in accordance with the Governance Arrangements for Research Ethics Committees (July 2001) and complies fully with the Standard Operating Procedures for Research Ethics Committees in the UK.

After ethical review

Now that you have completed the application process please visit the National Research Ethics Service website > After Review

You are invited to give your view of the service that you have received from the National Research Ethics Service and the application procedure. If you wish to make your views known please use the feedback form available on the website.

The attached document "After ethical review – guidance for researchers" gives detailed guidance on reporting requirements for studies with a favourable opinion, including:

- Notifying substantial amendments
- Adding new sites and investigators
- Progress and safety reports
- Notifying the end of the study

The NRES website also provides guidance on these topics, which is updated in the light of changes in reporting requirements or procedures.

We would also like to inform you that we consult regularly with stakeholders to improve our service. If you would like to join our Reference Group please email referencegroup@nres.npsa.nhs.uk.

10/H1013/66	Please quote this number on all correspondence

With the Committee's best wishes for the success of this project

Yours sincerely

Mr Francis Chan
Chair

Email: stephen.tebbutt@northwest.nhs.uk

Enclosures: List of names and professions of members who were present at the meeting and those who submitted written comments

"After ethical review – guidance for researchers"

Copy to: Mr Mohammed Zubair, University of Manchester

North West 8 Research Ethics Committee – Greater Manchester East

Attendance at Committee meeting on 19 October 2010

Committee Members:

Name	*Profession*	*Present*	*Notes*
Mr David Asher	Community Locum Pharmacist (Lay Member)	Yes	
Mr James Burns	Retired	Yes	
Ms Samantha Byers	Senior Pharmacist	No	
Mr Francis Chan	Consultant Orthopaedic Surgeon	Yes	
Mrs Jacqueline Crowther	Postgraduate Student	No	
Mrs Mary Dolan	Nurse Lecturer	Yes	
Dr Michael Hollingsworth	Honorary Senior Lecturer in Pharmacology	Yes	
Mr Christopher Houston	Lay Member	Yes	
Mr Simon Jones	Podiatrist	Yes	
Dr Priyadarshan Joshi	Consultant Psychiatrist	Yes	
Dr Philip Lewis	Consultant Cardiologist	No	
Professor Janet Marsden	Professor of Ophthalmology and Emergency Care	Yes	
Mr Jasper Palmier-Claus	PhD Student	No	
Dr Om Sanehi	Consultant in Anaesthesia	No	
Mr Howard Shilton	Lecturer in Nursing	No	
Mrs Mary Speake	Renal Research Sister	Yes	
Rev Philip Winn	Hospital Chaplain	Yes	

Also in attendance:

Name	*Position (or reason for attending)*
Helen Cochrane	Observer
Jane McConniffe	Observer
Mr Stephen Tebbutt	Co-ordinator

Appendix 3: Published Article I[280]

CXCL12 receptor preference, signal transduction, biological response and the expression of 5T4 oncofoetal glycoprotein

Owen J. McGinn, Georgi Marinov, Saladin Sawan and Peter L. Stern*

Immunology Group, Paterson Institute for Cancer Research, University of Manchester, Manchester M13 9PT, UK

*Author for correspondence (Pstern@picr.man.ac.uk)

Accepted 1 August 2012
Journal of Cell Science 125, 5467–5478

doi: 10.1242/jcs.109488

Summary

CXCL12 is a pleiotropic chemokine capable of eliciting multiple signal transduction cascades and functions, via interaction with either CXCR4 or CXCR7. Factors that determine CXCL12 receptor preference, intracellular signalling route and biological response are poorly understood but are of central importance in the context of therapeutic intervention of the CXCL12 axis in multiple disease states. We have recently demonstrated that 5T4 oncofoetal glycoprotein facilitates functional CXCR4 expression leading to CXCL12 mediated chemotaxis in mouse embryonic cells. Using wild type (WT) and 5T4 knockout (5T4KO) murine embryonic fibroblasts (MEFs), we now show that CXCL12 binding to CXCR4 activates both the ERK and AKT pathways within minutes, but while these pathways are intact, they are non-functional in 5T4KO cells treated with CXCL12. Importantly, in the absence of 5T4 expression, CXCR7 is upregulated and becomes the predominant receptor for CXCL12, activating a distinct signal transduction pathway with slower kinetics involving transactivation of the epidermal growth factor receptor (EGFR), eliciting proliferation rather than chemotaxis. Thus the surface expression of 5T4 marks the use of the CXCR4 rather than the CXCR7 receptor, with distinct consequences for CXCL12 exposure, relevant to the spread and growth of a tumour. Consistent with this hypothesis, we have identified human small cell lung carcinoma cells with similar 5T4/CXCR7 reciprocity that is predictive of biological response to CXCL12 and determined that 5T4 expression is required for functional chemotaxis in these cells.

Key words: 5T4, TPBG, CXCR7, Proliferation, Chemotaxis, Signalling, Src, EGFR

Journal of Cell Science

Introduction

The 5T4 trophoblast oncofoetal glycoprotein is expressed by many different carcinomas while showing only low levels in some normal tissues (Hole and Stern, 1988; Southall et al., 1990). 5T4 expression has been shown to influence cell adhesion, cytoskeletal organisation and motility (Awan et al., 2002; Carsberg et al., 1996), properties which might account for its association with poorer clinical outcome in some cancers (Mulder et al., 1997; Starzynska et al., 1994; Starzynska et al., 1998; Wrigley et al., 1995). 5T4 molecules are highly N-glycosylated transmembrane glycoproteins whose extracellular domain contains two regions of leucine-rich repeats (LRR) and associated flanking regions, separated by an intervening hydrophilic sequence (King et al., 1999). LRR are found in proteins with diverse functions and are frequently associated with protein-protein interactions (Kobe and Kajava, 2001).

5T4 oncofoetal antigen is associated with very early embryonic stem (ES) cell differentiation and altered motility (Ward et al., 2003) and is also a part of this coordinated process of epithelial-mesenchymal transition (EMT) (Eastham et al., 2007; Spencer et al., 2007). EMT is associated with key morphogenetic events in embryonic development but are also considered contributory to the metastatic spread of epithelial tumours. We have recently shown that 5T4 glycoprotein facilitates functional CXCR4 expression leading to CXCL12 mediated chemotaxis in differentiating ES cells, MEFs and cancer cells (Castro et al., 2012; Southgate et al., 2010).

CXCL12 is a pleiotropic chemokine regulating cellular survival, proliferation as well as chemotaxis but has also been associated with cancer metastasis (Balkwill, 2004; Vandercappellen et al., 2008). CXCL12 was originally identified as the only monogamous chemokine in the CXC family, binding specifically to the widely expressed cell surface seven transmembrane domain G-protein coupled receptor (GPCR) CXCR4 (Burger and Kipps, 2006; Nagasawa et al., 1996). This exclusivity was challenged by discrepancies of CXCL12 binding in the absence of CXCR4 which led to the identification of the orphan receptor RDC1, subsequently established in the CXC chemokine family as CXCR7 (Burns et al., 2006). In addition to CXCL12, CXCR7 binds with low affinity to the chemokine CXCL11 (I-TAC) (Burns et al., 2006).

Biological responses elicited following chemokine binding to the specific receptors involve G protein coupled signalling. For example, upon CXCL12 binding, CXCR4 undergoes a conformational change that facilitates activation of heterotrimeric G proteins and signalling effectors at the plasma membrane (Marchese, 2006). This initiates signalling cascades along multiple pathways including PI3K and MAPK resulting in downstream phosphorylation of proteins such as AKT and ERK respectively (Ganju et al., 1998; Zhang et al., 2005). However, CXCR7 lacks the consensus DRYLAIV motif of the CXC family on the second

intracellular loop of the receptor that is purportedly involved directly in G protein coupling. It also fails to activate G protein mediated GTP hydrolysis or initiate calcium mobilization in response to ligand binding (Burns et al., 2006). These data have supported the view that CXCR7 functions as a decoy receptor. However, CXCR7 significantly increases cell proliferation and elevates cellular adhesion in response to CXCL12 in other conditions (Begley et al., 2007; Burns et al., 2006; Miao et al., 2007; Tripathi et al., 2009). Whether CXCR7 functions like a GPCR in mediating a signal transduction process has been a topic of continued debate (Rajagopal et al., 2010). It has been proposed that CXCR7 acts to scavenge or sequester CXCL12, thereby generating gradients of CXCL12 that lead to differential signalling through CXCR4 (Boldajipour et al., 2008; Dambly-Chaudière et al., 2007). Since CXCR4 and CXCR7 can form heterodimers, at least when transiently overexpressed in transfected cells, the possibility that CXCR7 serves as a co-receptor for CXCR4 leading to enhanced CXCL12 mediated G-protein signalling has been proposed (Levoye et al., 2009; Sierro et al., 2007). These mechanisms all involve ligand binding to CXCR7 requiring crosstalk with CXCR4 to activate intracellular signalling pathways (Hartmann et al., 2008). Importantly it has now been shown that CXCR7 interacts with β-arrestin in a ligand-dependent manner (Kalatskaya et al., 2009; Luker et al., 2009; Rajagopal et al., 2010) providing the first confirmed mechanism of direct CXCR7 mediated signal transduction.

Using WT and 5T4KO MEFs, we have investigated CXCL12 receptor preference, signalling pathways and biological responses. In WT MEFs, CXCL12 binds CXCR4, activating both the ERK and AKT pathways within minutes. However in the absence of 5T4 expression, CXCL12 binds CXCR7 which is upregulated, activating a distinct signal transduction pathway with slower kinetics involving the transactivation of the EGFR and eliciting proliferation rather than chemotaxis. The reciprocal relationship between 5T4 and CXC7 is also described in certain small cell lung carcinoma (SCLC) cell lines in which 5T4 is required for chemotaxis to CXCL12.

Results

CXCL12 stimulation of the MAPK and PI3K pathways are disrupted in 5T4 KO but not WT MEFs

In WT MEFs CXCL12 activated dose-dependent signal transduction cascades along both the PI3K and MAPK pathways, with kinetics characteristic of a G-protein coupled response, leading to phosphorylation of AKT and ERK respectively (Fig. 1A,B). However, in 5T4KO MEFs no such cascade was activated in response to CXCL12 (Fig. 1A,B). Data from three independent experiments were compiled and densitometric analysis confirmed that no significant ERK or AKT activation could be observed in 5T4KO MEFs in response to CXCL12 (Fig. 1C–F).

The pathways of signal transduction in WT MEFs complied with classical PI3K and MAPK routes, as phosphorylation of AKT and ERK were significantly disrupted by inhibition of canonical upstream kinases in each pathway, PI3K (80% inhibition) and MEK, respectively (70% inhibition) (Fig. 2). Uncoupling of G-proteins from the cell surface receptors with pertussis toxin (PTX) also resulted in signal transmission inhibition (78%), confirming that each pathway was activated by a GPCR (Fig. 2). The GPCR in question was confirmed to be CXCR4 with the use AMD3100 (AMD), a specific CXCR4 antagonist, which disrupted both PI3K (79%) and MAPK (78%) signalling in these cells. A specific CXCR7 antagonist, CCX733 (CCX), had no effect (Fig. 2).

Although CXCL12 elicited no signal along the PI3K or MAPK pathways in 5T4KO MEFs, the absence of the 5T4 gene in these cells did not cause a gross defect in either signalling pathway. Both PI3K and MAPK networks were intact in 5T4KO MEFs and were inducible by other well-characterised ligands that act independently of chemokine receptors. MAPK signalling was activated by phorbol 12-myristate 13-acetate (PMA) in both WT and 5T4KO MEFs equally (Fig. 2A), and PI3K signalling was similarly activated by insulin in MEFs from both genotypes (Fig. 2B). These data confirmed that the signalling defects reported in 5T4KO MEFs were attributable to dysfunctional CXCR4 rather than disrupted signalling networks.

CXCL12 induces chemotaxis in WT but not 5T4KO MEFs and proliferation of 5T4KO but not WT MEFs

CXCL12 has a well defined role as a chemo-attractant; however, while both WT and 5T4KO MEFs display similar levels of overall migration in a 10% serum gradient (Fig. 3A), only WT MEFS show significant chemotaxis to CXCL12 ($P<0.001$). This migration is dependent upon CXCR4 activity and can be inhibited by AMD3100 ($P=0.001$) (Fig. 3B). CXCL12 has been demonstrated to elicit multiple cellular functions beyond chemotaxis, including the survival and proliferation of normal and cancerous cells. Accordingly we investigated the influence of CXCL12 on the growth of WT and 5T4KO MEFs. Interestingly we observed that despite an apparent failure to elicit a G protein-coupled signal transduction cascade (Fig. 1), CXCL12 was able to enhance the proliferation of 5T4KO MEFs under limiting growth conditions as assessed by counting cell numbers (Fig. 3C). This proliferative response was specific to the 5T4KO MEFs as their WT counterparts did not display enhanced proliferation in response to the chemokine (Fig. 3C). Proliferation was further assessed over a range of times (Fig. 3D) and CXCL12 concentrations (Fig. 3E) by MTT analysis.

CXCL12 induced 5T4KO MEF proliferation is mediated by upregulated CXCR7 expression

The proliferative response of 5T4KO MEFs to CXCL12 is clearly not associated with the typical time course reported for GPCR activation of signalling cascades, so any influence on the downstream pathways over longer time courses post stimulation was investigated. We found that a delayed transmission of signal along the MAPK pathway in response to CXCL12 existed in both WT and 5T4KO MEFs (Fig. 4A). In WT MEFs, in addition to the classical G protein-coupled early response (Fig. 1), a signal was also observed around 60 minutes. In 5T4KO MEFs responses to CXCL12 along the MAPK axis were principally seen at ~30 and 120 minutes (Fig. 4A). Specific CXCR antagonists showed that signal transduction was mediated by CXCR4 in WT and CXCR7 in 5T4KO MEFs, respectively (Fig. 4B). Consistent with this, FACs (Fig. 4C) and western blot (Fig. 4D) analyses showed that while CXCR4 cell surface and overall protein levels are similar across the genotypes, CXCR7 is upregulated in 5T4KO compared to WT MEFs and is only present at the cell surface of 5T4KO MEFs. To corroborate these findings, and confirm the specific function of the CXCR7 antagonist CCX733, physical knockdown of CXCR7 expression in 5T4KO MEFs by specific shRNAs was performed. Relative to

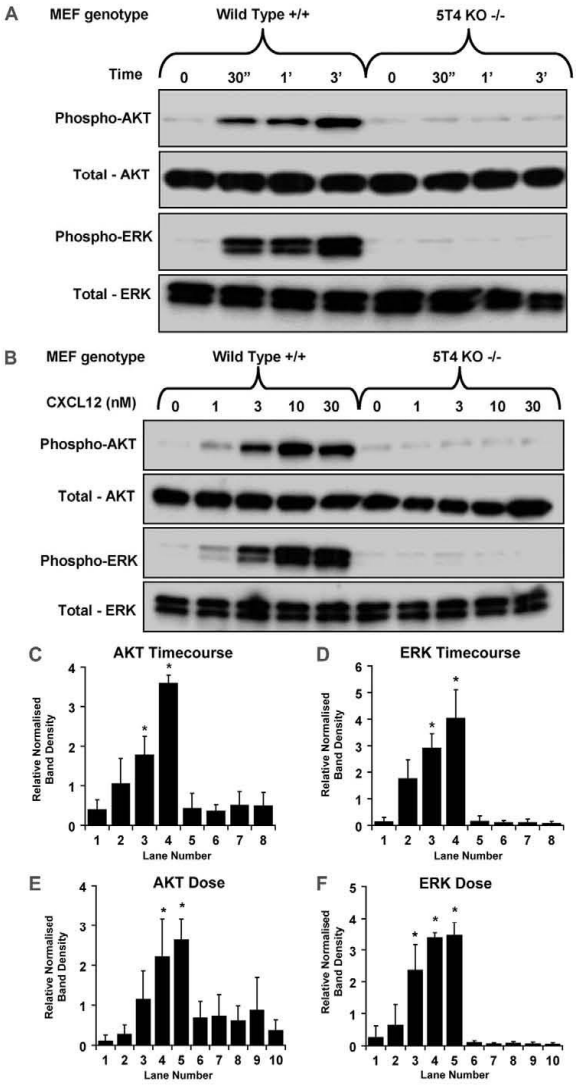

Fig. 1. CXCL12 stimulation of the MAPK and PI3K pathways is disrupted in 5T4 KO but not WT MEFs. WT or 5T4KO MEFs CXCL12 dose and time dependent levels of total and activated (phosphorylated) signalling proteins determined by western blotting using specific antibodies. (**A**) CXCL12 (12.5 nm) stimulated a rapid increase in both AKT and ERK phosphorylation in WT but not 5T4KO MEFs. (**B**) The rapid activation (3 minutes) of both AKT and ERK was CXCL12 dose dependent in WT MEFs but absent in 5T4KO MEFs. (**C–F**) Relative, normalised densitometric analyses of three independent experiments are presented, with significant phosphorylation ($P<0.05$) marked with an asterisk for; (C) AKT time course, (D) ERK time course, (E) AKT dose response and (F) ERK dose response.

scrambled control shRNA infected cells, CXCR7 expression was significantly reduced by 69% (Fig. 4E) which correlated with a 46% reduction in CXCL12 induced ERK phosphorylation in these cells (Fig. 4F).

These observations correlated functionally as the CXCL12 induced proliferation in 5T4KO MEFs was blocked by CXCR7 but not CXCR4 antagonism (Fig. 4G). While expression of 5T4 enhances CXCL12/CXCR4 functionality its absence also marks reduced expression of the alternate CXCR7 receptor. Thus 5T4 may act to alter the equilibrium of CXCL12 receptor preference between the higher affinity CXCR7, inducing proliferation, and the pro-migratory CXCR4.

CXCR7 signalling and biological function in 5T4KO MEFs is specific to CXCL12

While CXCR4 binds only CXCL12, CXCR7 can bind both CXCL12 and CXCL11, a chemokine that is shared with the CXCR3 receptor (Qin et al., 1998). We investigated these alternative ligands and receptors in the MEF signalling networks. CXCR3 was not detected at the surface of either WT or 5T4KO MEFs by flow cytometry (Fig. 5A). Since CXCR3 may not be at the surface of these cells, and is primarily expressed on activated leukocytes, a leukaemic cell line (SD1) was added to the analyses as a positive control and whole cell lysates were probed by western blot. CXCR3 was expressed in

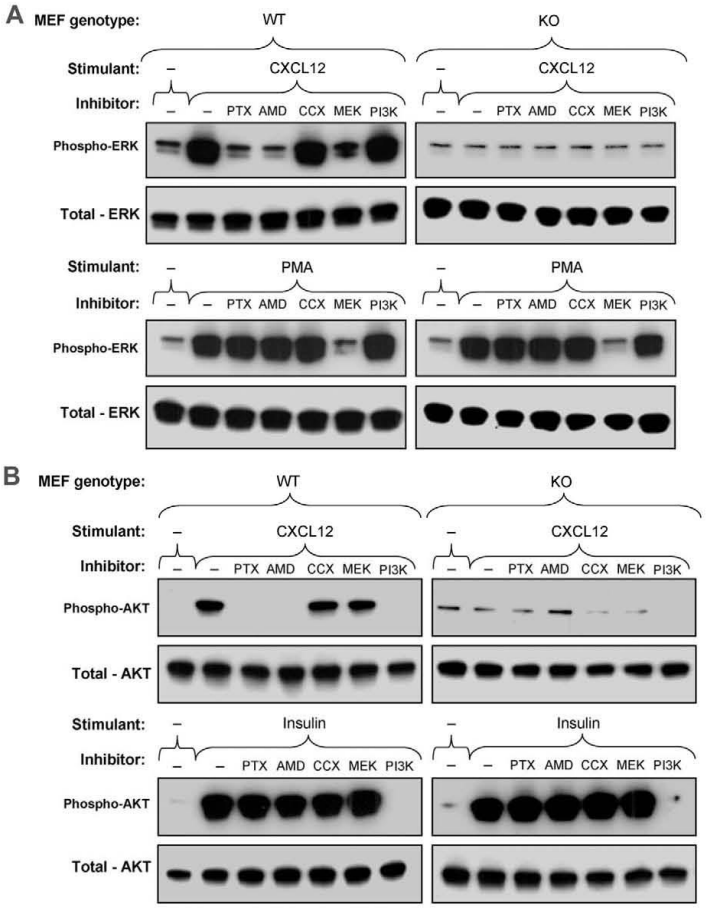

Fig. 2. CXCL12 stimulates PI3K and MAPK cascades via CXCR4 in WT MEFs. CXCL12 activation of ERK (**A**) and AKT (**B**) in WT MEFs is blocked by CXCR4 inhibitor AMD3100 (AMD) whereas CXCR7 specific inhibitor CCX733 (CCX) had no effect on either pathway. MEK (A) and PI3K (B) inhibitors disrupt CXCL12 stimulated ERK and AKT activation respectively confirming that CXCL12 induces canonical MAPK and PI3K signal transduction in WT MEFs. Signal transduction is also dependent upon G protein-coupling as pertussis toxin (PTX) disrupts both pathways (A,B). PMA and insulin induced ERK (A) and AKT (B) activation respectively in both WT and 5T4KO MEFs demonstrates that the signalling pathways are intact in 5T4KO MEFs and indicates a failure of CXCL12 to activate a G protein-coupled signal cascade.

the control SD1 cell line but displayed limited expression in whole cell lysates from both MEF genotypes (Fig. 5B). These data suggest that any CXCL11 effect on signal transduction or function would have to be delivered via the CXCR7 receptor. However, CXCL11 did not activate the MAPK pathway with early or late kinetics (Fig. 5C) nor enhance the proliferation of WT or 5T4KO MEFs (Fig. 5D). However, CXCL11 has been shown to compete with CXCL12 for CXCR7 binding, and in so doing inhibit CXCL12 driven biological functions, thereby acting as a CXCR7 antagonist (Zabel et al., 2011; Zabel et al., 2009). Accordingly, pre-incubation with CXCL11 blocked CXCL12 proliferation in 5T4KO MEF in a dose dependent manner (Fig. 5E), indicating competitive inhibition of CXCL12 binding to CXCR7. These data confirm that the CXCR7 dependent signal transduction and biological response in 5T4KO MEFs is mediated by CXCL12.

CXCR7 activation of the MAPK pathway involves transactivation of EGFR and depends upon Src kinase

Chemokine receptors have been reported to activate G protein-independent signal transduction mechanisms that rely upon the activation of Src kinases (Daaka et al., 1997; Luttrell et al., 1999) but they can also transactivate various growth factor receptors including the EGFR (Porcile et al., 2004). Here we show that CXCR7 signal transduction in 5T4KO MEFs, manifest as late phosphorylation of ERK, is blocked by both specific Src and EGFR tyrosine kinase inhibitors. CXCR7 signalling along the MAPK pathway is dependent upon EGFR activity in these cells, and can be blocked by the EGFR tyrosine kinase inhibitor Tyrphostin (Fig. 6A). It is well established that tyrosine kinase inhibitors can have off-target effects due to a lack of specificity, we therefore validated our pharmaceutical approach by knockdown of the EGFR in these cells. EGFR expression was significantly reduced (62%) in 5T4KO MEFs relative to scrambled control shRNA infected MEFs (Fig. 6B), which correlated with a 49% reduction in ERK phosphorylation in response to CXCL12 (Fig. 6C). Furthermore, CXCL12 activation of 5T4KO MEFs results in phosphorylation of the EGFR with similar kinetics to those observed for ERK activation (Fig. 6D), which can be prevented by knockdown (69%) or antagonism (97%) of the CXCR7 receptor, confirming that CXCR7 activity is responsible for EGFR activation (Fig. 6E,F).

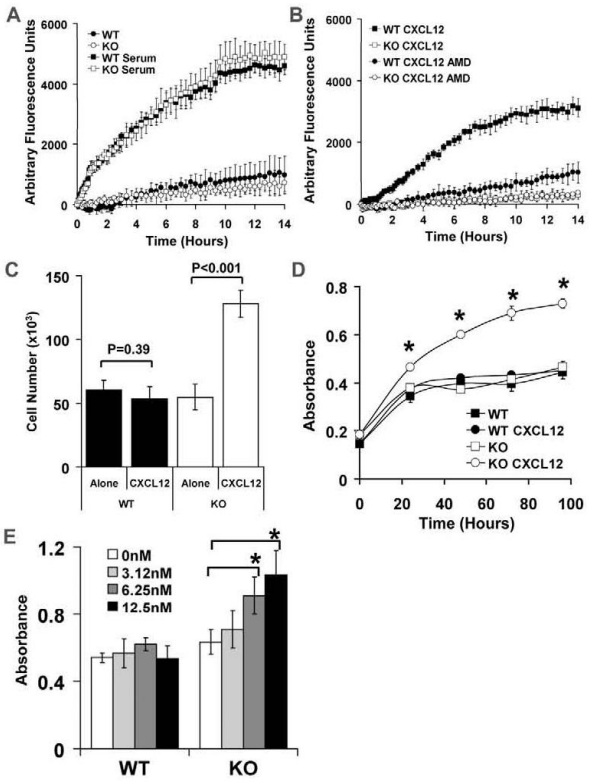

Fig. 3. CXCL12 induces chemotaxis in WT but proliferation in 5T4 KO MEFs. (**A**) No differences were observed in the overall migration rates of WT and 5T4KO MEFs along a serum gradient. (**B**) Chemotaxis was significant in WT ($P=0.001$) but not 5T4KO MEFs ($P=0.44$) in a CXCL12 gradient which was blocked by CXCR4 inhibitor AMD3100 (AMD). (**C**) CXCL12 stimulated significant proliferation of 5T4KO ($P<0.001$) but not WT ($P=0.39$) MEFs as determined by total cell numbers. (**D**) MTT analysis shows CXCL12 induced proliferation in 5T4KO but not WT MEFs over a 4-day time course and (**E**) CXCL12 dose dependent proliferation of 5T4 KO (significance determined as $P<0.05$ and marked *) but not WT MEFs.

CXCR7 signal transduction in these cells is also dependent upon Src kinase activity and can be blocked with a pan Src inhibitor PP1 (Fig. 6G). CXCR7 mediated phosphorylation of the EGFR can also be blocked by PP1 suggesting that Src kinase acts downstream of CXCR7 but upstream of the EGFR in this novel signal transduction pathway (Fig. 6G). Finally, this pathway was confirmed to be of functional significance as intervention with Tyrphostin disrupted CXCL12 mediated proliferation in 5T4KO MEFs (Fig. 6H).

5T4 and CXCR7 expression in human small cell lung carcinomas (SCLC)

If there is a reciprocal relationship between 5T4 and CXCR7 then it might be predictive of CXCL12 biological function in human cancer. Small cell lung carcinoma lines (H69, H82, H146, H345, H524, H526, H1048, H1963 and DMS114) were screened for expression of 5T4, CXCR4 and CXCR7 by flow cytometry or western blotting. Only DMS114 and H524 cells were found to be 5T4 negative, while all lines expressed CXCR4 (not shown). These 5T4 negative cell lines were paired with a morphologically similar, 5T4 positive SCLC cell line, H1048 and H146, respectively, and the reciprocal relationship between 5T4 and CXCR7 at the cell surface was investigated by flow cytometry. We discovered that, as in MEFs, CXCR7 was only detected at the surface of the 5T4 negative cells, DMS114 and H524 (Fig. 7A).

H1048 and DMS114 are both adherent and have a similar morphology and behaviour in culture so we used these cells to test whether 5T4 expression also marks different biological responses to CXCL12.

H1048 (Fig. 7B) but not DMS114 (Fig. 7C) cells showed significant CXCL12 chemotaxis which could be blocked by AMD3100 but not CCX733 ($P<0.005$ data not shown). Under the limiting culture conditions employed, enhanced growth with CXCL12 was not observed however there was a greater CXCL12 dose dependent survival of DMS114 (up to ~80%) compared to H1048 cells (up to ~30%) (Fig. 7D). The improved survival of DMS114 cells was significantly inhibited by anti-CXCR7 (9C4) blocking antibody pre-treatment (Hartmann et al., 2008) (Fig. 7D) and by the small molecule CXCR7 antagonist CCX733 but not AMD3100 (Fig. 7E). The limited protection seen in H1048 cells was not influenced by either of these treatments and appears unrelated to CXCR4 or CXCR7 interaction (Fig. 7D,E).

In conjunction with greater CXCL12 induced survival, DMS114 but not H1048 cells were significantly protected from both late and early stages of apoptosis as determined by annexin staining by flow cytometry (Fig. 7F) and detection of cleaved Caspase-3 by western blot (Fig. 7G). Only the CXCR7 positive, 5T4 negative DMS114 cells were protected from Caspase-3 activation by CXCL12. Furthermore, pre-incubation of DMS114

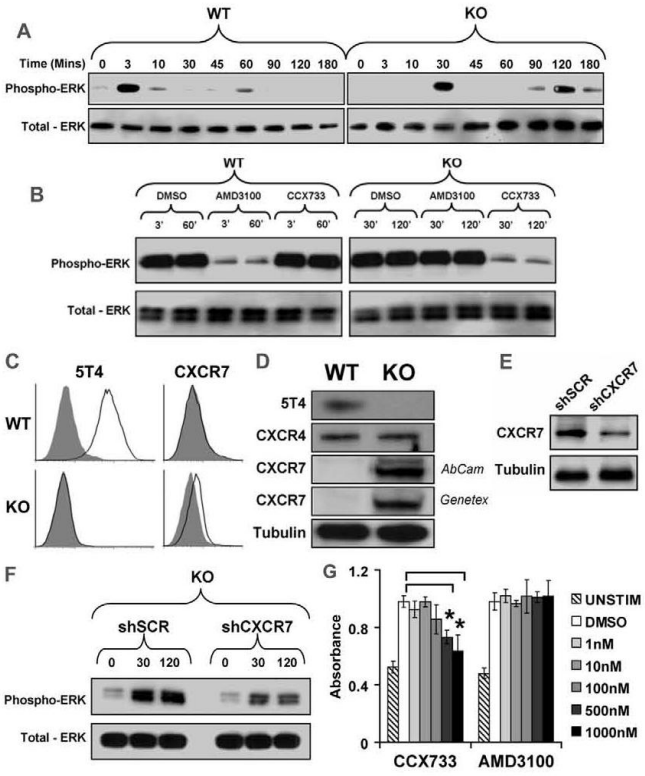

Fig. 4. CXCL12 induced 5T4KO MEF proliferation is mediated by upregulated CXCR7 expression and activation of a novel signal transduction cascade. (**A**) In WT MEFs, CXCL12 induced a typical G protein-coupled rapid (3 minute) activation of the MAPK pathway and a delayed response at about 60 min. 5T4KO MEFs showed no rapid response but delayed activation of ERK in response to CXCL12 after 30 and 120 min which was not seen in WT MEFs. (**B**) In WT MEFs, activation of the MAPK pathway was inhibited by AMD3100 and not CCX733, conversely in 5T4 KO MEFs all MAPK signalling was inhibited by CCX733 but not AMD3100. (**C**) Flow cytometry analyses show that CXCR7 is upregulated at the cell surface of 5T4KO compared to WT. (**D**) Western blot analyses show that while total CXCR4 protein levels are similar across MEF genotypes, CXCR7 total protein is significantly greater in 5T4KO MEFs than WT. (**E**) Knockdown of CXCR7 in 5T4KO MEFs by lentiviral shRNA particles (shCXCR7) reduced CXCR7 expression compared to scrambled control particles (shSCR). (**F**) CXCL12 activated phosphorylation of ERK is reduced in CXCR7 knockdown cells (shCXCR7) relative to scrambled control cells (shSCR). (**G**) CXCL12 induced significant proliferation in 5T4KO MEFs (*P<0.05) inhibited in a dose dependent manner by CCX733 but not AMD3100.

cells with CCX733 precluded the anti-apoptotic effects of CXCL12 in these assays (Fig. 7G), confirming that in all cases the biological responses of CXCL12 were mediated by CXCR7.

In order to confirm a direct role for 5T4 in the biological functions examined in the SCLC cells, we used a panel of shRNAs to knock down the expression of 5T4 in the H1048 cells. Relative to scrambled controls we were able to reduce the expression of 5T4 by fivefold (Fig. 8A) and assessed these cells for the expression of both CXCR7 and EMT markers. Knockdown of 5T4 in H1048 cells had no effect on cell surface levels of CXCR7 or CXCR4; however, we did observe that expression of the mesenchymal marker N-Cadherin was reduced (Fig. 8A). Importantly, while migration across a serum gradient was unaffected, chemotaxis toward CXCL12 was reduced in the 5T4 knock down H1048 cells (Fig. 8B), relative to scrambled controls (Fig. 8C).

Discussion

We have previously demonstrated that 5T4 oncofoetal glycoprotein facilitates functional CXCR4 expression leading to CXCL12 mediated chemotaxis in mouse embryonic cells (Southgate et al., 2010) and certain human tumours (Castro et al., 2012). Here, we show that in the absence of 5T4 the alternate CXCL12 receptor, CXCR7, is upregulated in MEFs and its activation elicits a different pathway of signal transduction with an altered functional cellular response.

In WT MEFs CXCL12 binds to CXCR4, initiating an immediate G-protein coupled signal via the MAPK and PI3K pathways resulting in cellular chemotaxis. In 5T4KO MEFs activation is propagated along the same pathways but with distinct kinetics atypical of GPCR responses and leads to increased cell proliferation. Using specific receptor antagonists we demonstrated that CXCR7, and not CXCR4, transduces the response to CXCL12 in 5T4KO MEFs. It is worthy of note that the CXCR4 antagonist AMD3100 has been shown in some cases to have partial agonistic activity on CXCR7 (Kalatskaya et al., 2009); however, this observation is not a consensus view, and in our system at least AMD3100 does not appear to promote CXCR7 function. This observation does, however, serve to illustrate the apparent distinction between CXCR4 and CXCR7 in potentiation of cellular responses to CXCL12, namely chemotaxis and proliferation/survival, respectively. A CXCR7 influence on survival and efficient differentiation of B cells into antibody producing cells has been reported (Infantino et al., 2006). A proliferative activity associated with CXCR7 has been shown in fibroblasts with ectopic expression supporting tumour formation in nude mice (Raggo et al., 2005). In experimental acute renal failure there is upregulation of CXCL12 which recruits progenitor cells for tissue repair where CXCR7 is critical for CXCL12-mediated survival, whereas CXCR4 is involved in chemotaxis (Mazzinghi et al., 2008). In addition, CXCR7 is also expressed by a variety of tumour cell lines (Burns et al., 2006;

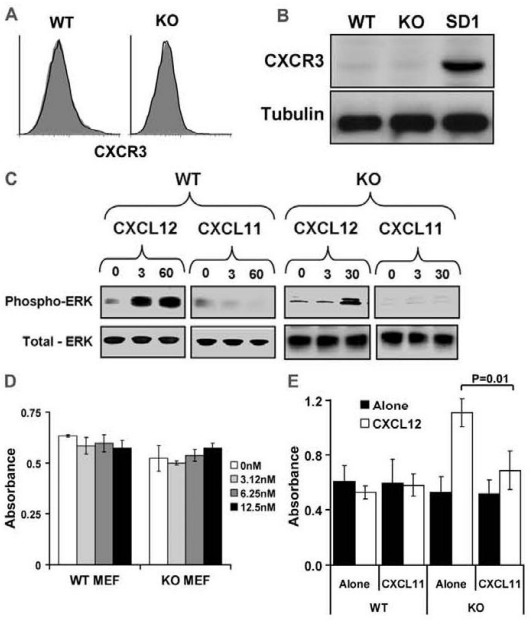

Fig. 5. CXCR7 signalling and biological function in 5T4KO MEFs is specific to CXCL12. (**A**) CXCR3 is not expressed at the surface of either WT or 5T4KO MEFs, as determined by flow cytometry. (**B**) CXCR3 protein is not detectable in whole cell lysates from WT or 5T4KO MEFs but is present in the control cell line SD1. (**C**) CXCL12 but not CXCL11 elicits a rapid (3 min) and delayed (60 min) activation of ERK in WT MEFs and a delayed activation (30 min) in KO MEFs. (**D**) CXCL11 fails to induce significant cellular proliferation (MTT) of either WT or 5T4KO MEFs. (**E**) CXCL12 (white bars) increased proliferation of 5T4KO MEFs and was inhibited by pre-incubation with CXCL11 (P=0.01); CXCL12 with or without CXCL11 pre-incubation did not stimulate growth of WT MEFs.

Miao et al., 2007) as well as in primary human tumours (Goldmann et al., 2008; Schutyser et al., 2007; Wang et al., 2008) where the tumour growth and aggressiveness can correlate with receptor expression.

Although some overexpression studies have implied that CXCR7 and CXCR4 may act in concert, via the formation of heterodimeric receptor pairs (Levoye et al., 2009; Sierro et al., 2007), our data in MEFs show independence of signalling and function. Coordinated but discrete roles of the two receptors have been described in primordial cell migration in the formation of the lateral line during Zebrafish development. Here, the spatial distribution of CXCR4 and CXCR7 expression is crucial since disruption of the segregation of the receptors results in primordial cell stalling (Dambly-Chaudière et al., 2007). In B cell development, CXCR7 has an established role and is a marker of mature B cells (Infantino et al., 2006) while CXCR4 is detectable at the cell surface during all stages of development it is only weakly responsive in mature B cells (D'Apuzzo et al., 1997; Honczarenko et al., 1999). In human placenta there is also a reciprocal expression pattern of the CXCL12 receptors. CXCR4 expression is higher in early (8–10 weeks) compared to term placenta (Kumar et al., 2004) conversely CXCR7 expression is higher in term rather than early placenta (Tripathi et al., 2009). In mouse embryonic stem cells there is reciprocity of CXCR7 and CXCR4 membrane expression marked by 5T4. Undifferentiated ES cells are 5T4 negative and express membrane CXCR7 but its biological function here is unknown. Upon differentiation CXCR7 is downregulated and 5T4 upregulated transcriptionally which provides for functional chemotaxis to CXCL12 through CXCR4 (Southgate et al., 2010).

In mouse embryonic cells there is a correlation of 5T4 expression with CXCR4 predominance over CXCR7 although how the latter is regulated is not known. It is likely that the balance of CXCL12 receptor expression will be dynamically controlled to provide the morphogenetic requirements of cells and tissues. There are several factors that are likely to influence the receptor that CXCL12 will bind. Firstly, CXCR7 has more than a ten-fold higher affinity for the chemokine than CXCR4 (Balabanian et al., 2005; Burns et al., 2006). Furthermore, the enzyme peptidylarginine deiminase (PAD) has been demonstrated to differentially reduce the binding affinity of CXCL12 for its cognate receptors. PAD sequentially citrullinates the three N-terminal arginines of CXCL12 to produce CXCL12 isoforms with altered citrullination patterns. Interestingly, mono-citrullination on Arg(8) has no effect on CXCL12 binding to CXCR7 but reduces CXCR4 binding by 30 fold; the triple citrullinated isoform Arg(8, 12 and 20) cannot bind CXCR4 but still has reduced affinity for CXCR7 (Struyf et al., 2009). It is perhaps not surprising that CXCL12 appears to favour binding CXCR7 over CXCR4 given that CXCR4 is so widely expressed. It would be detrimental for all cells to respond chemotactically to CXCL12, for example epithelia would become dispersed and tissue integrity compromised. 5T4 is one factor that acts to bias the CXCL12 response in favour of CXCR4 but this is only manifest in the context of coincident CXCR7 downregulation for which the mechanisms are unknown. It is tempting to speculate that CXCR7 and 5T4 may be co-regulated.

These observations are further complicated by the increasing number of non-cognate CXCL12 receptors, and CXCR4/7 ligands, all of which have the potential to offset the equilibrium of the CXCL12 axis. For example, syndecan has recently been shown to interact with both the CXCR4 receptor and the CXCL12 ligand (Schanz et al., 2011), and macrophage migration inhibitory factor (MIF) can bind to both CXCL12 receptors, acting as a non-cognate ligand to prevent CXCL12 driven metastasis (Tarnowski et al., 2010). Indeed a protein of similar structure to 5T4, LRRC4, has been shown to influence CXCR4 signalling kinetics and function in glioblastoma (Wu et al., 2008). It is our contention that 5T4 is another of these factors that govern the CXCL12 receptor predominance equilibrium.

In this study, CXCL12/CXCR4 elicited a typical GPCR signal along canonical routes. A canonical route of signalling for CXCR7 has not been described and indeed the capacity to activate secondary messenger systems has been questioned. Thus some studies have provided evidence that CXCR7 represents a silent or decoy receptor responsible for either sequestering extracellular CXCL12 (Mahabaleshwar et al., 2008; Tiveron and Cremer, 2008) or modulating CXCR4 signalling by forming heterodimers (Levoye et al., 2009; Sierro et al., 2007). Although virtually all reports have agreed that CXCR7 does not couple to G proteins, functional roles for the receptor that belie a signalling event suggest a non-classical positive signalling role for this

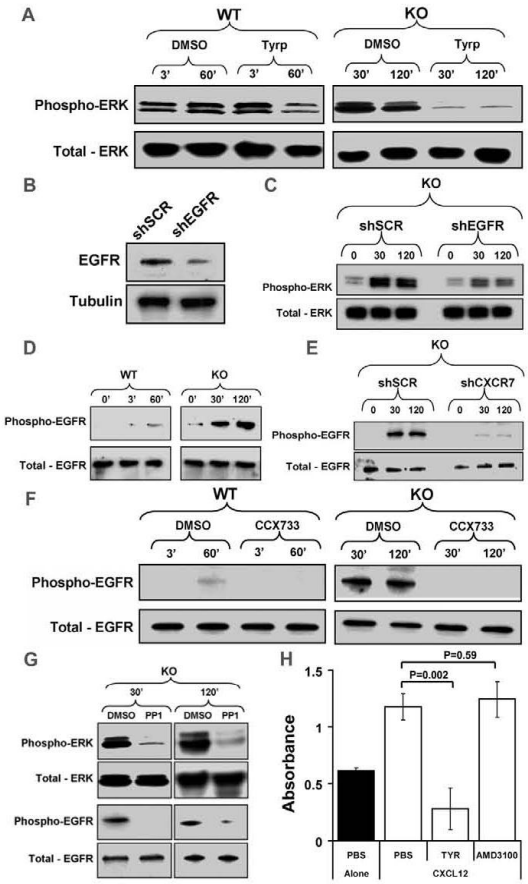

Fig. 6. CXCR7 activation of the MAPK pathway involves transactivation of EGFR via Src kinase. Delayed ERK activation by CXCL12 in 5T4KO MEFs is dependent upon EGFR transactivation; (**A**) disruption of MAPK signal transduction in the presence of the EGFR inhibitor Tyrphostin (Tyr). (**B**) Knockdown of EGFR in 5T4KO MEFs by lentiviral shRNA particles (shEGFR) reduced EGFR expression compared to scrambled control particles (shSCR). (**C**) CXCL12 activated phosphorylation of ERK is reduced in EGFR knockdown cells (shEGFR) relative to scrambled control cells (shSCR). (**D**) Phosphorylation of the EGFR by CXCL12 with similar kinetics to ERK activation, which can be prevented by; (**E**) CXCR7 knockdown or (**F**) antagonism with the CXCR7 inhibitor CCX733. (**G**) CXCR7 activation of the EGFR and signalling along the MAPK pathway are prevented by the pan Src kinase inhibitor PP1. (**H**) CXCL12/CXCR7 induced proliferation in 5T4KO MEFs is dependent upon EGFR activity, and can be blocked with Tyrphostin (P=0.002).

receptor. Importantly direct CXCR7 mediated signalling, can occur through β-arrestin. Initial studies indicated an interaction between CXCR7 and β-arrestin in a ligand dependent manner (Luker et al., 2009). Subsequently it was determined that CXCR7 can signal directly through β-arrestin and act as an endogenous β-arrestin-biased receptor (Rajagopal et al., 2010). The concept of β-arrestin biased receptors is well supported and it is believed that a balance exists between G protein- and β-arrestin-mediated pathways. Agonist binding typically results in signalling mediated by G proteins and β-arrestins accompanied by receptor desensitisation and internalisation by β-arrestins. This is in contrast to a system with biased signalling, where signalling is mediated selectively through only one of these two pathways. Interestingly, biased receptors have been genetically engineered from balanced receptors by mutation of key residues involved in G protein coupling, such as mutations of the highly conserved DRY motif of the angiotensin II type 1A receptor (AT1AR) to generate the variant AT1AR(DRY/AAY) (Wei et al., 2003) or mutations of three highly conserved residues in the β2 adrenergic receptor to generate the β-arrestin biased β2AR(TYY) (Shenoy et al., 2007). Surprisingly, similar mutations are observed naturally in decoy receptors including CXCR7, which lacks a typical sequence surrounding the DRY motif (Graham, 2009), suggesting that biased receptors have evolved in the genome, that CXCR7 may be one of them and that other receptors that are currently thought to be orphans or decoys may also signal through non-G-protein-mediated mechanisms (Rajagopal et al., 2010).

These observations suggest that CXCR7 may represent a naturally β-arrestin biased receptor. Recent studies of the β-adrenergic (β2AR) GPCR have demonstrated a mechanism of β-arrestin mediated signalling which is consistent with our observations on CXCR7 signal transduction. This work shows a role of β-arrestins in β2AR directed MAPK activation which varies with cell type, agonist dose and time course. The β2AR can couple to both Gαs and Gαi proteins, as well as β-arrestin; early studies suggested that both coupling to Gαi and β-arrestin resulted in ERK activation (Daaka et al., 1997; Luttrell et al., 1999). Careful dissection of the β2AR MAPK pathway in HEK293 cells, showed early ERK activation (between 0 and 5 min) was reduced by treatment with pertussis toxin (and was therefore G protein-dependent), while late ERK activation (between 5 and 60 min) was inhibited by knockdown of either β-arrestin-1 or -2 (Shenoy et al., 2007). The phenomenon of late ERK activation is analogous to our findings in 5T4KO MEFs and supports a role for β-arrestin mediated signal transduction. Perhaps most interestingly, the mechanism of late MAPK pathway signal transduction involves activation of Src kinase. The implication is that β-arrestin is able to recruit Src kinase as part of a larger scaffold which, following ligand binding, allows the activation of the kinase by β-arrestin. Furthermore, it has also been suggested that the β2AR can interact directly with Src kinase to facilitate delayed activation of the MAPK pathway (Huang et al., 2004; Sun et al., 2007).

We propose (at least in MEFs) that CXCL12 binding to CXCR7 activates, via β-arrestin, intracellular Src kinase which then transactivates the EGFR leading to signalling along the MAPK pathway. Unfortunately, it is difficult to directly test the role of β-arrestin with no specific inhibitor available. Other approaches such as RNAi knockdown or overexpression would have global effects or generate non physiological interactions likely to make interpreting the results difficult. Our demonstration that CXCR7 activation in 5T4KO cells is able to induce transactivation of the EGFR via activation of Src is not without precedent. There are multiple examples of GPCR and chemokine receptor activation leading to growth factor receptor transactivation. CXCR4 for example has been demonstrated to transactivate both HER2 and the EGFR both via a Src kinase

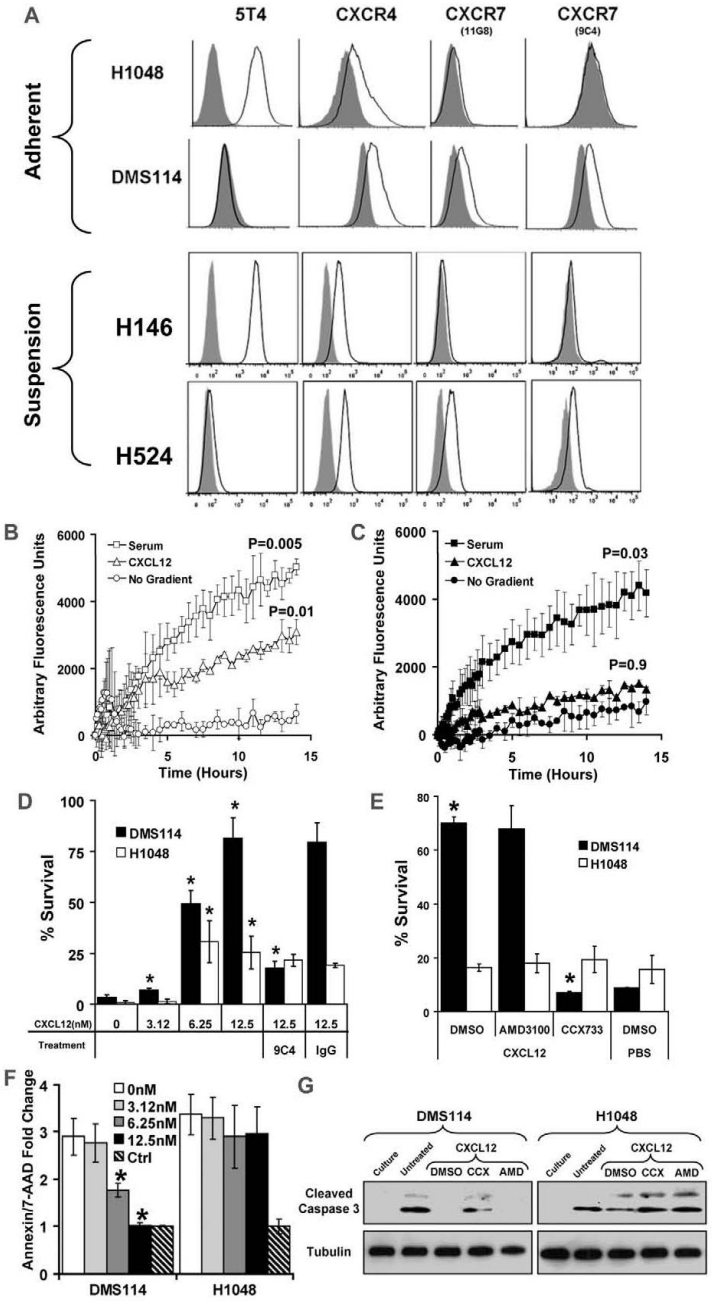

Fig. 7. 5T4 and CXCR7 reciprocity in human SCLC. (**A**) Flow cytometry revealed that the SCLC cell lines DMS114/H524 and H1048/H146 were reciprocally cell surface positive for CXCR7 (9C4 and 11G8) and 5T4, respectively. While both cell lines migrate equally in a serum gradient (**B**,**C**), 5T4 positive H1048 (B) showed significantly greater CXCL12 chemotaxis (56% of control) than (C) DMS114 (10% of control). (**D**,**E**) Under limiting culture conditions, CXCL12 was able to promote significantly greater survival in DMS114 compared to H1048 cells (*P<0.05); improved survival of DMS114 but not H1048 cells is significantly inhibited by anti-CXCR7 blocking antibody (9C4) pre-treatment (D), CCX733 (E) but not AMD3100 (E). DMS114 but not H1048 cells are also significantly protected against apoptosis by CXCL12 as determined by decreased surface expression of Annexin (**F**) and reduced Caspase-3 activation (**G**) in response to CXCL12 stimulation. The anti-apoptotic effects of CXCL12 in DMS114 cells could be blocked by CXCR7 antagonism with CCX733 (G).

dependent mechanism (Chinni et al., 2008; Porcile et al., 2004); furthermore, CXCL12 has been shown to activate both Src and the EGFR in non-transformed N15C6 prostate epithelial cells (Kasina et al., 2009).

Src transactivates the EGFR by phosphorylation at Tyr845 in the kinase domain, stabilising the activation loop, maintaining the active enzyme state, and providing a binding surface for substrate proteins (Cooper and Howell, 1993; Hubbard et al., 1994). Singh

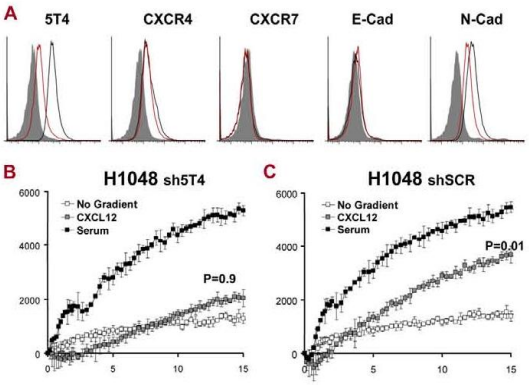

Fig. 8. Direct role of 5T4 in human SCLC response to CXCL12. (**A**) 5T4 expression was knocked down in H1048 SCLC cells using shRNA constructs as determined by flow cytometry, CXCR4/7 expression was not affected by 5T4 knockdown, but N-Cadherin expression was also reduced (shaded histograms are IgG controls, black histograms are scrambled control H1048 cells, red histograms are 5T4 knockdown H1048 cells). (**B**) Knockdown of 5T4 expression in H1048 cells (H1048 sh5T4) reduces chemotaxis to CXCL12, relative to (**C**) scrambled control H1048 cells (H1048 shSCR).

et al. (Singh and Lokeshwar, 2011) have shown in prostate cancer cell lines that CXCR7 can be co-precipitated with and is essential for function of the EGFR, but they did not observe any CXCL12 activated EGFR activity. This may be due to activating mutations of the EGFR which circumvent the requirement for CXCR7 directed phosphorylation of the EGFR by Src. Such mutations have been described in the EGFR, for example the L858R missense mutant which resulted in high levels of basal phosphorylation at Tyr845 (Sordella et al., 2004), and multiple mutations within the EGFR activation loop have been identified in prostate cancer (Cai et al., 2008), a disease that is consistently linked with EGFR hyperactivity.

This study builds upon the role of the 5T4 oncofoetal antigen in the CXCL12 chemokine axis. Our data suggest that 5T4 is not only involved in the positive function of CXCR4, but that also its absence reciprocally marks CXCR7 function. Taken together our data suggest that 5T4 may play a role in breaking the natural CXCR7 receptor bias of the chemokine CXCL12 and provides for a switch in homeostatic function induced by the chemokine. We have also begun to decipher the signal transduction mechanisms utilised by the CXCR7 receptor, clarifying multiple observations of an apparent role for CXCR7 in survival/proliferation. Preliminary studies in SCLC suggest that our observations in MEFs may be of functional relevance to human cancer although more detailed studies of the signalling pathways will need to be performed. One might speculate that in a primary tumour, 5T4 surface expression by cells at the periphery would provide for chemotaxis to CXCL12 secreting endothelial cells and metastatic spread whereas in the heart of the tumour preferential CXCR7 expression could detect lower levels of chemokine and promote cell growth. Therapeutic approaches, targeting selective inhibition of CXCR7 and CXCR4 signalling exploiting 5T4 dependency, might provide for better tumour selectivity.

Materials and Methods

5T4 Knockout (KO) mice

The 5T4KO heterozygote C57BL/6 animals were crossed and the progeny genotyped as previously described (Southgate et al., 2010).

Generation and propagation of MEFs

MEFs were prepared and genotyped 5T4KO or WT from day 13 mouse embryos from mating 5T4KO heterozygote C57BL/6 mice. Each embryo was dispersed and trypsinized for 25 min at 37℃, and the resulting cells were grown for 1 day in T-150 flask. These cells were designated as passage number 0 (P0). Cells were passaged every 2-3 days and experiments were generally performed on passages 4 7. MEFs were cultured in Dulbecco's modified Eagle's medium (DMEM) supplemented with 10% fetal bovine serum, 2 mM L-glutamine, 100 units/ml penicillin and 100 ug/ml streptomycin at 37℃ under 5% CO_2.

Human small cell lung carcinoma cell lines

Small cell lung carcinoma (SCLC) cell lines were obtained from ATCC; H69, H82, DMS114, H196, H526, H1048, H1963 and were grown and authenticated as previously described (Dean et al., 2011). The cells were screened for expression of 5T4, CXCR4 and CXCR7 by flow cytometry or western blotting as previously described (Southgate et al., 2010). Cell suspensions were prepared and labelled with mouse monoclonal antibody to human 5T4 (mAb-h5T4), rabbit anti-CXCR7 (Ab72100, Abcam), rabbit anti-CXCR4 (Ab2074, Abcam) or relevant IgG controls (DAKO) and subsequently with secondary reagents, goat anti-mouse IgG1 (A21121, Invitrogen) or AF488 goat anti-rabbit IgG (A11034, Invitrogen).

Chemotaxis assay

Chemotaxis was assessed using transwell chambers as previously described for cellular motility assays with variations described below (Spencer et al., 2007). Briefly, the FluoroBlok system (BD Biosciences) was employed to assess the kinetic migration of MEFs. FluoroBlok cell culture inserts are designed with a patented light-tight PET membrane that efficiently blocks the transmission of light within the range of 490 700 nm, allowing fluorescence detection in a simplified and non-destructive manner. Fluorescently labelled cells present in the top chamber of the insert are shielded from bottom-reading fluorescence plate readers and microscopes by the BD FluoroBlok membrane. Once labelled cells migrate through the membrane, they are easily detected by a bottom-reading fluorescence plate reader thereby eliminating cell scraping and manual cell counting to enable analysis of both kinetic and end point migration and invasion assays.

The transwells (8-μm pore size) were immersed in gelatine solution overnight (0.1% in PBS) and rinsed in PBS. Transwells were blocked in BSA for 30 min at 37℃/5% CO_2 and washed in PBS. MEFs were cultured as described above, serum starved for 24 hours and labelled with DiIl16 dye (Cambridge Biotech) for 1 hour at 37℃. Excess dye was removed by washing in PBS; cells were then counted, and resuspended in phenol red-free, 1% serum culture medium, and added to the transwell plates onto a preformed chemotactic gradient (CXCL12 at 30 ng/ml or serum containing 10% FCS as a positive control) and incubated for up to 24 hours at 37℃/5% CO_2. Fluorescent readings were taken from the bottom of the plate every 30 min at an excitation wavelength of 549 nm and an emission wavelength of 565 nm. In all experiments there was no evidence of differential plating with varying conditions; chemotaxis was presented as fluorescent intensity over the indicated time course. *P*-values were calculated using unpaired Student's *t*-test. All chemotactic experiments were performed at least three times with triplicates for each condition.

Proliferation assay

Proliferation was determined by MTT analysis, enumeration of live cells (as qualified by the exclusion of trypan blue) and brightfield microscopy. WT or 5T4KO MEFs were serum starved for 24 hours prior to chemokine stimulation and commencement of analysis for up to 96 hours. At the indicated time points cells were imaged prior to counting or MTT analysis. MTT solution in PBS was added to each well for 4 hours. After removal of the medium, DMSO was added to each well to dissolve the formazan crystals. The absorbance at 540 nm was determined using a micro plate reader (Molecular Devices). WT and 5T4KO MEFs showed identical metabolism of MTT enabling the use of this assay to assess growth over time and with different chemokine doses. Triplicate wells were assayed for each condition. Inhibition studies were performed in the presence of AMD3100 (Sigma) for CXCR4, 9C4 (Calltag) and CCX733 and 11G8 (ChemoCentryx) for CXCR7, tyrphostin (Sigma) for the EGFR and CXCL11 (R&D) for competitive inhibition studies.

Detection of intracellular signal transduction by SDS-polyacrylamide gel electrophoresis (PAGE) and western blotting

Signal transduction was assessed by the phosphorylation (activation) of canonical intracellular mediators of signal transduction. WT and 5T4 KO MEFs were serum starved for up to 48 hours prior to stimulation with different ligands for different times with reactions terminated by ice cold PBS. The compounds PD98059

(50 μM), LY294002 (50 μM) (both Cell Signaling Technology), CCX733 (1 μM), AMD3100 (10 μM), PP1 or tyrphostin (all Sigma), in order to inhibit MEK1, PI3 kinase, CXCR7, CXCR4, Src kinase or the EGFR respectively, were applied to cells for 1 hour prior to CXCL12, CXCL11 (12.5 nM), phorbol 12-myristate 13-acetate (PMA) (50 nM) (Sigma) or insulin stimulation. Cells were lysed in M-PER supplemented with protease and phosphatase inhibitor cocktails, (Thermo Fisher). Samples were prepared in reducing or non-reducing PAGE loading buffer as appropriate (Thermo Fisher), heated to 100℃ for 3 minutes and loaded on to a preformed 10% or 4 15% gradient gel (BioRad) and run in Laemmli buffer (25 mM Tris-base, 192 mM glycine, 0.1% SDS). Western transfer to PVDF membranes used a BioRad Mini-PROTEAN Tetra cell system. For western probing, primary antibody concentrations were selected in accordance with the supplier's instructions, antibodies used were: anti-m5T4 (B3F1 (Southgate et al., 2010)), polyclonal rabbit anti-CXCR4 (Abcam), anti-CXCR7 antibodies from Abcam (Ab72100), Genetex (GTX82935) and Calltag (9C4), anti-CXCR3 (R&D), anti-ERK1/2, phospho-ERK1/2 (Thr202/Tyr204), AKT and phospho-AKT (Thr308), anti-cleaved caspase-3 (Asp175) (all Cell Signaling Technology) and anti-Tubulin (Abcam). Following secondary antibody labelling using appropriate HRP conjugates, (AbSerotec) hybridising bands were detected using SuperSignal West Dura (Thermo Fisher).

Flow cytometry

CXCR7 expression at the surface of cells was determined by flow cytometry using two layer immunofluorescence with anti CXCR7 antibodies (as described) or an isotype matched control at 4℃ for 1 hour followed by rabbit anti-mouse immunoglobulins/RPE F(ab')2 (Dako) at 4℃ for 30 min. The samples were analysed using FACSCalibur Flow cytometer.

ShRNA knockdowns

In primary murine embryonic fibroblasts the expression of CXCR7 and EGFR was knocked down using lentiviral shRNA vectors from Santa Cruz Biotechnology (CXCR7 sc-142643-V, EGFR sc-29302-V and Control sc-108080). Briefly, 5T4 KO MEFs were incubated with lentiviral particles (MOI=3), coding shRNA for CXCR7 and EGFR overnight in the presence of polybrene (4 ug/ml) in full DMEM media. The cells were then incubated in fresh full DMEM media for 72 hours and expression of CXCR7 and EGFR was evaluated.

For knockdown of human 5T4, four shRNA plasmids were designed, using an experimentally validated algorithm, to knock down 5T4 by RNA interference in addition to one negative control plasmid. Each vector was tagged with a puromycin-resistance gene. H1048 cells (p:23) were transfected at 70% confluence. DNA from each plasmid was mixed separately with FuGENE6 transfection agent (Roche, 11814443001) in a ratio of 2 μg DNA/6 μl transfection agent for a total 100 μl by using serum-free Opti-MEM medium (Gibco, 51985). The plasmid/transfection agent mixture was left at room temperature for 30 minutes before addition to growth media. 48 hours later growth medium was changed to fresh one supplemented with 0.5 μg/ml puromycin (Sigma, P9620-10). Only successfully transfected cells survived in wells with puromycin. Puromycin dose was determined by a minimum dose-to-kill experiment (puromycin added to 70% confluent cells at increasing dose from 0.1 μg/ml to 10 μg/ml and the lowest concentration which successfully killed all cells after 5 days was used). The cells were allowed to grow in the presence of puromycin and then passaged before 5T4 expression was determined.

Densitometry

For all western blot data, densitometric analyses were performed using ImageJ software on at least three independent blots per experiment. Band density, relative to loading controls were normalised and compared statistically by Student's *t*-test or ANOVA, significant data are described in the Results sections.

Statistical analysis

Means and standard deviations are presented. Statistical significance was calculated by either two-tailed unpaired Student's *t*-test or ANOVA as appropriate.

Acknowledgements

We thank Jian-Mei Hou for the initial SCLC screen, Mark Penfold at Chemocentryx for the generous provision of CCX733, 11G8 antibody and for useful discussions, and all people involved in the PICR core facilities.

Funding

This work was supported by a programme grant from Cancer Research UK [grant number C480/A12328]; and S.S. was supported by the Wigan Cancer Research Fund as a Joseph Starkey Clinical Research Fellow.

References

Awan, A., Lucic, M. R., Shaw, D. M., Sheppard, F., Westwater, C., Lyons, S. A. and Stern, P. L. (2002). 5T4 interacts with TIP-2/GIPC, a PDZ protein, with implications for metastasis. *Biochem. Biophys. Res. Commun.* **290**, 1030-1036.

Balabanian, K., Lagane, B., Infantino, S., Chow, K. Y., Harriague, J., Moepps, B., Arenzana-Seisdedos, F., Thelen, M. and Bachelerie, F. (2005). The chemokine SDF-1/CXCL12 binds to and signals through the orphan receptor RDC1 in T lymphocytes. *J. Biol. Chem.* **280**, 35760-35766.

Balkwill, F. (2004). The significance of cancer cell expression of the chemokine receptor CXCR4. *Semin. Cancer Biol.* **14**, 171-179.

Begley, L. A., MacDonald, J. W., Day, M. L. and Macoska, J. A. (2007). CXCL12 activates a robust transcriptional response in human prostate epithelial cells. *J. Biol. Chem.* **282**, 26767-26774.

Boldajipour, B., Mahabaleshwar, H., Kardash, E., Reichman-Fried, M., Blaser, H., Minina, S., Wilson, D., Xu, Q. and Raz, E. (2008). Control of chemokine-guided cell migration by ligand sequestration. *Cell* **132**, 463-473.

Burger, J. A. and Kipps, T. J. (2006). CXCR4: a key receptor in the crosstalk between tumor cells and their microenvironment. *Blood* **107**, 1761-1767.

Burns, J. M., Summers, B. C., Wang, Y., Melikian, A., Berahovich, R., Miao, Z., Penfold, M. E., Sunshine, M. J., Littman, D. R., Kuo, C. J. et al. (2006). A novel chemokine receptor for SDF-1 and I-TAC involved in cell survival, cell adhesion, and tumor development. *J. Exp. Med.* **203**, 2201-2213.

Cai, C. Q., Peng, Y., Buckley, M. T., Wei, J., Chen, F., Liebes, L., Gerald, W. L., Pincus, M. R., Osman, I. and Lee, P. (2008). Epidermal growth factor receptor activation in prostate cancer by three novel missense mutations. *Oncogene* **27**, 3201-3210.

Carsberg, C. J., Myers, K. A. and Stern, P. L. (1996). Metastasis-associated 5T4 antigen disrupts cell-cell contacts and induces cellular motility in epithelial cells. *Int. J. Cancer* **68**, 84-92.

Castro, F. V., McGinn, O. J., Krishnan, S., Marinov, G., Li, J., Rutkowski, A. J., Elkord, E., Burt, D. J., Holland, M., Vaghjiani, R. et al. (2012). 5T4 oncofetal antigen is expressed in high risk of relapse childhood pre-B acute lymphoblastic leukemia and is associated with a more invasive and chemotactic phenotype. *Leukemia* **26**, 1487-1498.

Chinni, S. R., Yamamoto, H., Dong, Z., Sabbota, A., Bonfil, R. D. and Cher, M. L. (2008). CXCL12/CXCR4 transactivates HER2 in lipid rafts of prostate cancer cells and promotes growth of metastatic deposits in bone. *Mol. Cancer Res.* **6**, 446-457.

Cooper, J. A. and Howell, B. (1993). The when and how of Src regulation. *Cell* **73**, 1051-1054.

D'Apuzzo, M., Rolink, A., Loetscher, M., Hoxie, J. A., Clark-Lewis, I., Melchers, F., Baggiolini, M. and Moser, B. (1997). The chemokine SDF-1, stromal cell-derived factor 1, attracts early stage B cell precursors via the chemokine receptor CXCR4. *Eur. J. Immunol.* **27**, 1788-1793.

Daaka, Y., Luttrell, L. M. and Lefkowitz, R. J. (1997). Switching of the coupling of the beta2-adrenergic receptor to different G proteins by protein kinase A. *Nature* **390**, 88-91.

Dambly-Chaudière, C., Cubedo, N. and Ghysen, A. (2007). Control of cell migration in the development of the posterior lateral line: antagonistic interactions between the chemokine receptors CXCR4 and CXCR7/RDC1. *BMC Dev. Biol.* **7**, 23.

Dean, E. J., Cummings, J., Roulston, A., Berger, M., Ranson, M., Blackhall, F. and Dive, C. (2011). Optimization of circulating biomarkers of obatoclax-induced cell death in patients with small cell lung cancer. *Neoplasia* **13**, 339-347.

Eastham, A. M., Spencer, H., Soncin, F., Ritson, S., Merry, C. L., Stern, P. L. and Ward, C. M. (2007). Epithelial-mesenchymal transition events during human embryonic stem cell differentiation. *Cancer Res.* **67**, 11254-11262.

Ganju, R. K., Brubaker, S. A., Meyer, J., Dutt, P., Yang, Y., Qin, S., Newman, W. and Groopman, J. E. (1998). The alpha-chemokine, stromal cell-derived factor-1alpha, binds to the transmembrane G-protein-coupled CXCR-4 receptor and activates multiple signal transduction pathways. *J. Biol. Chem.* **273**, 23169-23175.

Goldmann, T., Drömann, D., Radtke, J., Marwitz, S., Lang, D. S., Schultz, H. and Vollmer, E. (2008). CXCR7 transcription in human non-small cell lung cancer and tumor-free lung tissues; possible regulation upon chemotherapy. *Virchows Arch.* **452**, 347-348.

Graham, G. J. (2009). D6 and the atypical chemokine receptor family: novel regulators of immune and inflammatory processes. *Eur. J. Immunol.* **39**, 342-351.

Hartmann, T. N., Grabovsky, V., Pasvolsky, R., Shulman, Z., Buss, E. C., Spiegel, A., Nagler, A., Lapidot, T., Thelen, M. and Alon, R. (2008). A crosstalk between intracellular CXCR7 and CXCR4 involved in rapid CXCL12-triggered integrin activation but not in chemokine-triggered motility of human T lymphocytes and CD34+ cells. *J. Leukoc. Biol.* **84**, 1130-1140.

Hole, N. and Stern, P. L. (1988). A 72 kD trophoblast glycoprotein defined by a monoclonal antibody. *Br. J. Cancer* **57**, 239-246.

Honczarenko, M., Douglas, R. S., Mathias, C., Lee, B., Ratajczak, M. Z. and Silberstein, L. E. (1999). SDF-1 responsiveness does not correlate with CXCR4 expression levels of developing human bone marrow B cells. *Blood* **94**, 2990-2998.

Huang, J., Sun, Y. and Huang, X. Y. (2004). Distinct roles for Src tyrosine kinase in beta2-adrenergic receptor signaling to MAPK and in receptor internalization. *J. Biol. Chem.* **279**, 21637-21642.

Hubbard, S. R., Wei, L., Ellis, L. and Hendrickson, W. A. (1994). Crystal structure of the tyrosine kinase domain of the human insulin receptor. *Nature* **372**, 746-754.

Infantino, S., Moepps, B. and Thelen, M. (2006). Expression and regulation of the orphan receptor RDC1 and its putative ligand in human dendritic and B cells. *J. Immunol.* **176**, 2197-2207.

Kalatskaya, I., Berchiche, Y. A., Gravel, S., Limberg, B. J., Rosenbaum, J. S. and Heveker, N. (2009). AMD3100 is a CXCR7 ligand with allosteric agonist properties. *Mol. Pharmacol.* **75**, 1240-1247.

Kasina, S., Scherle, P. A., Hall, C. L. and Macoska, J. A. (2009). ADAM-mediated amphiregulin shedding and EGFR transactivation. *Cell Prolif.* **42**, 799-812.

King, K. W., Sheppard, F. C., Westwater, C., Stern, P. L. and Myers, K. A. (1999). Organisation of the mouse and human 5T4 oncofoetal leucine-rich glycoprotein genes and expression in foetal and adult murine tissues. *Biochim. Biophys. Acta* **1445**, 257-270.

Kobe, B. and Kajava, A. V. (2001). The leucine-rich repeat as a protein recognition motif. *Curr. Opin. Struct. Biol.* 11, 725-732.

Kumar, A., Kumar, S., Dinda, A. K. and Luthra, K. (2004). Differential expression of CXCR4 receptor in early and term human placenta. *Placenta* **25**, 347-351.

Levoye, A., Balabanian, K., Baleux, F., Bachelerie, F. and Lagane, B. (2009). CXCR7 heterodimerizes with CXCR4 and regulates CXCL12-mediated G protein signaling. *Blood* **113**, 6085-6093.

Luker, K. E., Gupta, M., Steele, J. M., Foerster, B. R. and Luker, G. D. (2009). Imaging ligand-dependent activation of CXCR7. *Neoplasia* 11, 1022-1035.

Luttrell, L. M., Ferguson, S. S., Daaka, Y., Miller, W. E., Maudsley, S., Della Rocca, G. J., Lin, F., Kawakatsu, H., Owada, K., Luttrell, D. K. et al. (1999). Beta-arrestin-dependent formation of beta2 adrenergic receptor-Src protein kinase complexes. *Science* **283**, 655-661.

Mahabaleshwar, H., Boldajipour, B. and Raz, E. (2008). Killing the messenger: The role of CXCR7 in regulating primordial germ cell migration. *Cell Adh. Migr.* **2**, 69-70.

Marchese, A. (2006). Assessment of degradation and ubiquitination of CXCR4, a GPCR regulated by EGFR family members. *Methods Mol. Biol.* **327**, 139-145.

Mazzinghi, B., Ronconi, E., Lazzeri, E., Sagrinati, C., Ballerini, L., Angelotti, M. L., Parente, E., Mancina, R., Netti, G. S., Becherucci, F. et al. (2008). Essential but differential role for CXCR4 and CXCR7 in the therapeutic homing of human renal progenitor cells. *J. Exp. Med.* **205**, 479-490.

Miao, Z., Luker, K. E., Summers, B. C., Berahovich, R., Bhojani, M. S., Rehemtulla, A., Kleer, C. G., Essner, J. J., Nasevicius, A., Luker, G. D. et al. (2007). CXCR7 (RDC1) promotes breast and lung tumor growth in vivo and is expressed on tumor-associated vasculature. *Proc. Natl. Acad. Sci. USA* **104**, 15735-15740.

Mulder, W. M., Stern, P. L., Stukart, M. J., de Windt, E., Butzelaar, R. M., Meijer, S., Adér, H. J., Claessen, A. M., Vermorken, J. B., Meijer, C. J. et al. (1997). Low intercellular adhesion molecule 1 and high 5T4 expression on tumor cells correlate with reduced disease-free survival in colorectal carcinoma patients. *Clin. Cancer Res.* **3**, 1923-1930.

Nagasawa, T., Nakajima, T., Tachibana, K., Iizasa, H., Bleul, C. C., Yoshie, O., Matsushima, K., Yoshida, N., Springer, T. A. and Kishimoto, T. (1996). Molecular cloning and characterization of a murine pre-B-cell growth-stimulating factor/stromal cell-derived factor 1 receptor, a murine homolog of the human immunodeficiency virus 1 entry coreceptor fusin. *Proc. Natl. Acad. Sci. USA* **93**, 14726-14729.

Porcile, C., Bajetto, A., Barbero, S., Pirani, P. and Schettini, G. (2004). CXCR4 activation induces epidermal growth factor receptor transactivation in an ovarian cancer cell line. *Ann. N. Y. Acad. Sci.* **1030**, 162-169.

Qin, S., Rottman, J. B., Myers, P., Kassam, N., Weinblatt, M., Loetscher, M., Koch, A. E., Moser, B. and Mackay, C. R. (1998). The chemokine receptors CXCR3 and CCR5 mark subsets of T cells associated with certain inflammatory reactions. *J. Clin. Invest.* **101**, 746-754.

Raggo, C., Ruhl, R., McAllister, S., Koon, H., Dezube, B. J., Früh, K. and Moses, A. V. (2005). Novel cellular genes essential for transformation of endothelial cells by Kaposi's sarcoma-associated herpesvirus. *Cancer Res.* **65**, 5084-5095.

Rajagopal, S., Kim, J., Ahn, S., Craig, S., Lam, C. M., Gerard, N. P., Gerard, C. and Lefkowitz, R. J. (2010). Beta-arrestin- but not G protein-mediated signaling by the "decoy" receptor CXCR7. *Proc. Natl. Acad. Sci. USA* **107**, 628-632.

Schanz, A., Baston-Bust, D., Krussel, J. S., Heiss, C., Janni, W. and Hess, A. P. (2011). CXCR7 and syndecan-4 are potential receptors for CXCL12 in human cytotrophoblasts. *J. Reprod. Immunol.* **89**, 18-25.

Schutyser, E., Su, Y., Yu, Y., Gouwy, M., Zaja-Milatovic, S., Van Damme, J. and Richmond, A. (2007). Hypoxia enhances CXCR4 expression in human microvascular endothelial cells and human melanoma cells. *Eur. Cytokine Netw.* **18**, 59-70.

Shenoy, S. K., Barak, L. S., Xiao, K., Ahn, S., Berthouze, M., Shukla, A. K., Luttrell, L. M. and Lefkowitz, R. J. (2007). Ubiquitination of beta-arrestin links seven-transmembrane receptor endocytosis and ERK activation. *J. Biol. Chem.* **282**, 29549-29562.

Sierro, F., Biben, C., Martínez-Muñoz, L., Mellado, M., Ransohoff, R. M., Li, M., Woehl, B., Leung, H., Groom, J., Batten, M. et al. (2007). Disrupted cardiac development but normal hematopoiesis in mice deficient in the second CXCL12/SDF-1 receptor, CXCR7. *Proc. Natl. Acad. Sci. USA* **104**, 14759-14764.

Singh, R. K. and Lokeshwar, B. L. (2011). The IL-8-regulated chemokine receptor CXCR7 stimulates EGFR signaling to promote prostate cancer growth. *Cancer Res.* **71**, 3268-3277.

Sordella, R., Bell, D. W., Haber, D. A. and Settleman, J. (2004). Gefitinib-sensitizing EGFR mutations in lung cancer activate anti-apoptotic pathways. *Science* **305**, 1163-1167.

Southall, P. J., Boxer, G. M., Bagshawe, K. D., Hole, N., Bromley, M. and Stern, P. L. (1990). Immunohistological distribution of 5T4 antigen in normal and malignant tissues. *Br. J. Cancer* **61**, 89-95.

Southgate, T. D., McGinn, O. J., Castro, F. V., Rutkowski, A. J., Al-Muftah, M., Marinov, G., Smethurst, G. J., Shaw, D., Ward, C. M., Miller, C. J. et al. (2010). CXCR4 mediated chemotaxis is regulated by 5T4 oncofetal glycoprotein in mouse embryonic cells. *PLoS ONE* **5**, e9982.

Spencer, H. L., Eastham, A. M., Merry, C. L., Southgate, T. D., Perez-Campo, F., Soncin, F., Ritson, S., Kemler, R., Stern, P. L. and Ward, C. M. (2007). E-cadherin inhibits cell surface localization of the pro-migratory 5T4 oncofetal antigen in mouse embryonic stem cells. *Mol. Biol. Cell* **18**, 2838-2851.

Starzynska, T., Marsh, P. J., Schofield, P. F., Roberts, S. A., Myers, K. A. and Stern, P. L. (1994). Prognostic significance of 5T4 oncofetal antigen expression in colorectal carcinoma. *Br. J. Cancer* **69**, 899-902.

Starzynska, T., Wiechowska-Kozlowska, A., Marlicz, K., Bromley, M., Roberts, S. A., Lawniczak, M., Kolodziej, B., Zyluk, A. and Stern, P. L. (1998). 5T4 oncofetal antigen in gastric carcinoma and its clinical significance. *Eur. J. Gastroenterol. Hepatol.* **10**, 479-484.

Struyf, S., Noppen, S., Loos, T., Mortier, A., Gouwy, M., Verbeke, H., Huskens, D., Luangsay, S., Parmentier, M., Geboes, K. et al. (2009). Citrullination of CXCL12 differentially reduces CXCR4 and CXCR7 binding with loss of inflammatory and anti-HIV-1 activity via CXCR4. *J. Immunol.* **182**, 666-674.

Sun, Y., McGarrigle, D. and Huang, X. Y. (2007). When a G protein-coupled receptor does not couple to a G protein. *Mol. Biosyst.* **3**, 849-854.

Tarnowski, M., Grymula, K., Liu, R., Tarnowska, J., Drukala, J., Ratajczak, J., Mitchell, R. A., Ratajczak, M. Z. and Kucia, M. (2010). Macrophage migration inhibitory factor is secreted by rhabdomyosarcoma cells, modulates tumor metastasis by binding to CXCR4 and CXCR7 receptors and inhibits recruitment of cancer-associated fibroblasts. *Mol. Cancer Res.* **8**, 1328-1343.

Tiveron, M. C. and Cremer, H. (2008). CXCL12/CXCR4 signalling in neuronal cell migration. *Curr. Opin. Neurobiol.* **18**, 237-244.

Tripathi, V., Verma, R., Dinda, A., Malhotra, N., Kaur, J. and Luthra, K. (2009). Differential expression of RDC1/CXCR7 in the human placenta. *J. Clin. Immunol.* **29**, 379-386.

Vandercappellen, J., Van Damme, J. and Struyf, S. (2008). The role of CXC chemokines and their receptors in cancer. *Cancer Lett.* **267**, 226-244.

Wang, J., Shiozawa, Y., Wang, J., Wang, Y., Jung, Y., Pienta, K. J., Mehra, R., Loberg, R. and Taichman, R. S. (2008). The role of CXCR7/RDC1 as a chemokine receptor for CXCL12/SDF-1 in prostate cancer. *J. Biol. Chem.* **283**, 4283-4294.

Ward, C. M., Barrow, K., Woods, A. M. and Stern, P. L. (2003). The 5T4 oncofoetal antigen is an early differentiation marker of mouse ES cells and its absence is a useful means to assess pluripotency. *J. Cell Sci.* **116**, 4533-4532.

Wei, H., Ahn, S., Shenoy, S. K., Karnik, S. S., Hunyady, L., Luttrell, L. M. and Lefkowitz, R. J. (2003). Independent beta-arrestin 2 and G protein-mediated pathways for angiotensin II activation of extracellular signal-regulated kinases 1 and 2. *Proc. Natl. Acad. Sci. USA* **100**, 10782-10787.

Wrigley, E., McGown, A. T., Rennison, J., Swindell, R., Crowther, D., Starzynska, T. and Stern, P. L. (1995). 5T4 oncofetal antigen expression in ovarian carcinoma. *Int. J. Gynecol. Cancer* **5**, 269-274.

Wu, M., Chen, Q., Li, D., Li, X., Li, X., Huang, C., Tang, Y., Zhou, Y., Wang, D., Tang, K. et al. (2008). LRRC4 inhibits human glioblastoma cells proliferation, invasion, and proMMP-2 activation by reducing SDF-1 alpha/CXCR4-mediated ERK1/2 and Akt signaling pathways. *J. Cell. Biochem.* **103**, 245-255.

Zabel, B. A., Wang, Y., Lewén, S., Berahovich, R. D., Penfold, M. E., Zhang, P., Powers, J., Summers, B. C., Miao, Z., Zhao, B. et al. (2009). Elucidation of CXCR7-mediated signaling events and inhibition of CXCR4-mediated tumor cell transendothelial migration by CXCR7 ligands. *J. Immunol.* **183**, 3204-3211.

Zabel, B. A., Lewén, S., Berahovich, R. D., Jaén, J. C. and Schall, T. J. (2011). The novel chemokine receptor CXCR7 regulates trans-endothelial migration of cancer cells. *Mol. Cancer* **10**, 73.

Zhang, J., Sarkar, S. and Yong, V. W. (2005). The chemokine stromal cell derived factor-1 (CXCL12) promotes glioma invasiveness through MT2-matrix metalloproteinase. *Carcinogenesis* **26**, 2069-2077.

Appendix 4: Published Article II[288]

G Model
YSCBI-1156; No. of Pages 8
ARTICLE IN PRESS

Seminars in Cancer Biology xxx (2014) xxx–xxx

Contents lists available at ScienceDirect

Seminars in Cancer Biology

journal homepage: www.elsevier.com/locate/semcancer

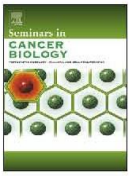

Review

Understanding and exploiting 5T4 oncofoetal glycoprotein expression

Peter L. Stern*, Julie Brazzatti, Saladin Sawan, Owen J. McGinn

Institute of Cancer Sciences, University of Manchester, UK

ARTICLE INFO

Keywords:
5T4 oncofoetal antigen
CXC12 chemokine
Wnt signalling
Epithelial mesenchymal transition
5T4-immunotherapy

ABSTRACT

Oncofoetal antigens are present during foetal development with generally limited expression in the adult but are upregulated in cancer. These molecules can sometimes be used to diagnose or follow treatment of tumours or as a target for different immunotherapies. The 5T4 oncofoetal glycoprotein was identified by searching for shared surface molecules of human trophoblast and cancer cells with the rationale that they may function to allow survival of the foetus as a semi-allograft in the mother or a tumour in its host, potentially influencing growth, invasion or altered immune surveillance of the host. 5T4 tumour selective expression has stimulated the development of 5T4 vaccine, 5T4 antibody targeted-superantigen and 5T4 antibody-drug therapies through preclinical and into clinical studies. It is now apparent that 5T4 expression is a marker of the use (or not) of several cellular pathways relevant to tumour growth and spread. Thus 5T4 expression is mechanistically associated with the directional movement of cells through epithelial mesenchymal transition, facilitation of CXCL12/CXCR4 chemotaxis, blocking of canonical Wnt/beta-catenin while favouring non-canonical pathway signalling. These processes are highly regulated in development and in normal adult tissues but can contribute to the spread of cancer cells. Understanding the differential impact of these pathways marked by 5T4 can potentially improve existing, or aid development of novel cancer treatment strategies.

1. 5T4 trophoblast glycoprotein is an oncofoetal antigen

The 5T4 oncofoetal glycoprotein was identified by searching for shared surface molecules of human trophoblast and cancer cells with the rationale that they may function to allow survival of the foetus as a semi-allograft in the mother or a tumour in its host. It was hypothesized that such functions would be likely to include those concerned with growth, invasion or altered immune surveillance in the host.

Purified glycoproteins from human trophoblast syncytio-microvillous plasma membranes were used as an immunogen to raise monoclonal antibodies which were screened for binding to trophoblast and different tumour cell lines, but not normal human peripheral blood mononuclear cells [1]. Subsequently, immunohistochemistry established that the specific monoclonal antibody detected expression by many different types of carcinoma but only low levels in some normal tissue epithelia [2,3]. Indeed primary and metastatic cancers from cervix, colorectal, gastric, ovarian, oral, prostate, lung and renal sites showed a useful tumour expression profile. For colorectal, gastric and ovarian cancer there was evidence of tumour expression levels correlating with poorer clinical outcome [3].

Further biochemical and genomic studies established the molecule as an approximately 72 kD heavily N-glycosylated protein encoded on the long arm of chromosome 6 at q14-15 [4–6]. The gene coding for the 5T4 protein is a member of the leucine rich repeat (LRR) containing family of proteins [7]. The latter motif is associated with protein–protein interactions of a functionally diverse set of molecules [8]. The extracellular part of the 5T4 molecule has ~3.5 LRRs in two domains separated by a short hydrophilic sequence with each domain having N- and C-terminal LRR flanking regions; there is a transmembrane domain and a short cytoplasmic sequence. A reported crystal structure of the extracellular domain at 1.8 Å resolution predicts a highly glycosylated rigid core comprising 8 LLRs which form a platform for conserved surface residues in the terminal LRR region [9].

Overexpression of the 5T4 gene in different cell types indicated a possible function relevant to cancer spread. In murine fibroblasts, overexpressed h5T4 induced a more spindle shaped morphology, disruption of cell contacts and a reduction in adherence [10] while in normal murine epithelial cells there were similar changes plus evidence of E-cadherin down-regulation, increased motility and cytoskeletal disruption dependent on the intracellular part of 5T4

* Corresponding author at: Institute of Cancer Sciences, University of Manchester, Paterson Building, Wilmslow Road, Manchester M20 4BX, UK.
Tel.: +44 161 446 3127; fax: +44 161 446 3109.
E-mail addresses: Peter.Stern@manchester.ac.uk, pstern@picr.man.ac.uk (P.L. Stern).

http://dx.doi.org/10.1016/j.semcancer.2014.07.004
1044-579X/

Please cite this article in press as: Stern PL, et al. Understanding and exploiting 5T4 oncofoetal glycoprotein expression. Semin Cancer Biol (2014), http://dx.doi.org/10.1016/j.semcancer.2014.07.004

[11]. Subsequently, a yeast two hybrid screen using the 5T4 cytoplasmic domain as a probe identified a PDZ domain containing interactor, TIP2/GPIC, which is known to mediate links to the actin cytoskeleton [12]. The isolation of the murine 5T4 gene confirmed its evolutionary conservation and provided additional tools for evaluating 5T4 function and immune targeting [13,14].

2. 5T4 and epithelial mesenchymal transition (EMT)

EMT occurs during embryonic development and is important for the metastatic spread of epithelial tumours [15]. The 5T4 oncofoetal antigen is an early marker of differentiation of mouse and human embryonic stem (ES) cell [16–18]. This process is also an EMT-like event characterized by the differentiation of ES cells in monolayer culture associated with an E- to N-cadherin switch, upregulation of E-cadherin repressor molecules (Snail and Slug proteins), increased matrix metalloproteinase (MMP-2 and MMP-9) activity and motility [19,20]. Interestingly, undifferentiated E-Cadherin KO ES cells constitutively express surface 5T4, while abrogation of E-cadherin mediated cell-cell contact in undifferentiated ES cells using neutralizing antibodies results in increased motility, altered actin cytoskeleton arrangement and a mesenchymal phenotype with cell surface expression of 5T4 molecules. Overall it appears that 5T4 overexpression in epithelial cells is associated with downregulation of E-cadherin, with the latter acting to prevent cell surface localization of 5T4 possibly by stabilizing cortical actin cytoskeletal organization.

To further study this EMT process we conducted a comparative microarray analysis of undifferentiated ($5T4^{-ve}$) and early differentiating ($5T4^{+ve}$) murine ES cells. 5T4 is up-regulated at an earlier stage of ES differentiation than the widely used down-regulation of the SSEA-1 marker, and thus cell sorting for surface 5T4 expression provided an additional level of stringency in the definition of ES cell populations compared to stratifications used in some other microarray studies [21]. Any transcriptional changes may be important in governing the balance of self-renewal/pluripotency and differentiation in ES cells, or in the regulation of 5T4 cell surface expression. Such properties may also be functionally important in tumour progression. Analysis of the microarray data from undifferentiated and differentiating ES cells identified >2-fold up or down regulation of transcripts in 143 and 245 genes respectively. There was a pattern of transcriptional changes relating to loss of pluripotency in ES cells with significant downregulation of *Klf4*, *Oct4* and *Sox2*. Many genes known to bind these transcription factors and forming part of the extended transcriptional network influencing pluripotency of ES cells were also found to be downregulated. The complex changes in transcription seen in the differentiating ES cells analyzed reflect the several different pathways that can control ES cell pluripotency and self-renewal [21].

One significant transcriptional change identified was the downregulation of transcripts for the dipeptidyl peptidase IV, CD26, which codes for a cell surface protease that cleaves the chemokine CXCL12 [22]. Interestingly, differentiating ES cells also showed an upregulation of CXCL12 transcription. CXCL12 has been shown to regulate many biological processes but also plays an important role in tumourigenesis [23–25]. CXCL12 binds to the widely expressed cell surface seven transmembrane domain G-protein coupled receptor CXCR4 [26] and to the recently identified receptor CXCR7/RDC1 [27]. Upon ligand binding, the CXCR4 undergoes a conformational change that facilitates activation of heterotrimeric G proteins and signalling effectors at the plasma membrane [28]. This initiates a signalling cascade resulting in downstream phosphorylation of proteins such as ERK1/2 and AKT [29,30]. These activities are dependent on CXCR4 expression at the plasma membrane and cellular events that reduce the latter can abrogate the biological effects. Following activation, CXCR4 undergoes β-arrestin-mediated endocytotosis and although recycling of CXCR4 can occur this receptor can also be ubiquitinated and directed to lysosomes where it is degraded [31]. Both CXCL12 and CXCR4 expression have been associated with tumourigenesis in many cancers including breast, ovarian, renal, prostate, and neuroblastoma [23–25]. These CXCR4 expressing tumours preferentially spread to tissues that highly express CXCL12, including lung, liver, lymph nodes and bone marrow. Therefore, the inverse correlation between 5T4 and CXCL12 with CD26 transcript levels during mouse ES cell differentiation, and the known roles of these molecules in cell migration/motility, may suggest that particular regulatory processes are common to both ES cell differentiation and tumour metastasis. It is therefore significant that 5T4 molecules have been shown to modulate the functional expression of CXCR4 at the cell surface of mouse embryonic cells as well as some human tumour cells [21].

3. 5T4 and CXCL12 chemokine signalling

5T4 and CXCR4 molecules are co-localized at the cell surface in differentiating ES cells and mouse embryo fibroblasts (MEF) which both exhibit CXCL12 specific chemotaxis. However, the same cell types derived from 5T4KO mice show principally intracellular CXCR4 expression and no chemotaxis. The rescue of 5T4 expression in KO cells using an adenovirus encoding mouse 5T4 restores CXCL12 chemotaxis and significant surface co-localization with CXCR4. Further experiments using a series of chimeric constructs with interchanged domains of 5T4 and the glycoprotein CD44 identified the 5T4 transmembrane domain as necessary to enable optimal CXCR4 cell surface expression and chemotaxis. Nocodazole disruption of the microtubules in MEF led to intracellular accumulation and loss of cell surface CXCR4 while 5T4 remained detectable at the plasma membrane albeit at a diminished level. One hour after drug washout both antigens were detectable at the cell surface with marked co-localization. By contrast, disruption of the Golgi or the actin cytoskeleton did not significantly affect 5T4/CXCR4 co-localization at the plasma membrane. Importantly, some monoclonal antibodies against m5T4 can inhibit CXCL12 chemotaxis of mouse embryonic cells which implies a molecular interaction of 5T4 and CXCR4 occurring at the cell surface that facilitates the biological response to CXCL12. It is apparent that 5T4 is not a chaperone that merely trafficks the receptor to the cell surface since CXCR4 surface expression depends on microtubules whereas 5T4 does not. Further, FRET studies do not support a direct interaction between the molecules while preliminary proteomic analysis following cross linking of 5T4 molecules indicate many cytoskeleton associated interactions [32]. This regulation of CXCR4 surface expression by 5T4 molecules provides a novel means to control responses to the chemokine CXCL12, for example during embryogenesis, but can also be selected to advantage the spread of a 5T4 positive tumour from its primary site [21]. A role for receptor associated membrane proteins in controlling other GPCR has been documented and exploited for developing intervention strategies [33].

3.1. CXCL12 receptor preference, signal transduction, biological response and the expression of 5T4 oncofoetal glycoprotein

Using WT (wild type) and 5T4KO (knockout) MEFs, it was established that CXCL12 binding to CXCR4 activates both the MAPK (ERK) and PI3K (AKT) pathways within minutes but while these pathways are intact they are non-functional in 5T4KO cells treated with CXCL12. Further, in the absence of 5T4 expression, CXCR7 is upregulated and becomes the predominant receptor for CXCL12, activating a distinct signal transduction pathway with slower kinetics

Please cite this article in press as: Stern PL, et al. Understanding and exploiting 5T4 oncofoetal glycoprotein expression. Semin Cancer Biol (2014), http://dx.doi.org/10.1016/j.semcancer.2014.07.004

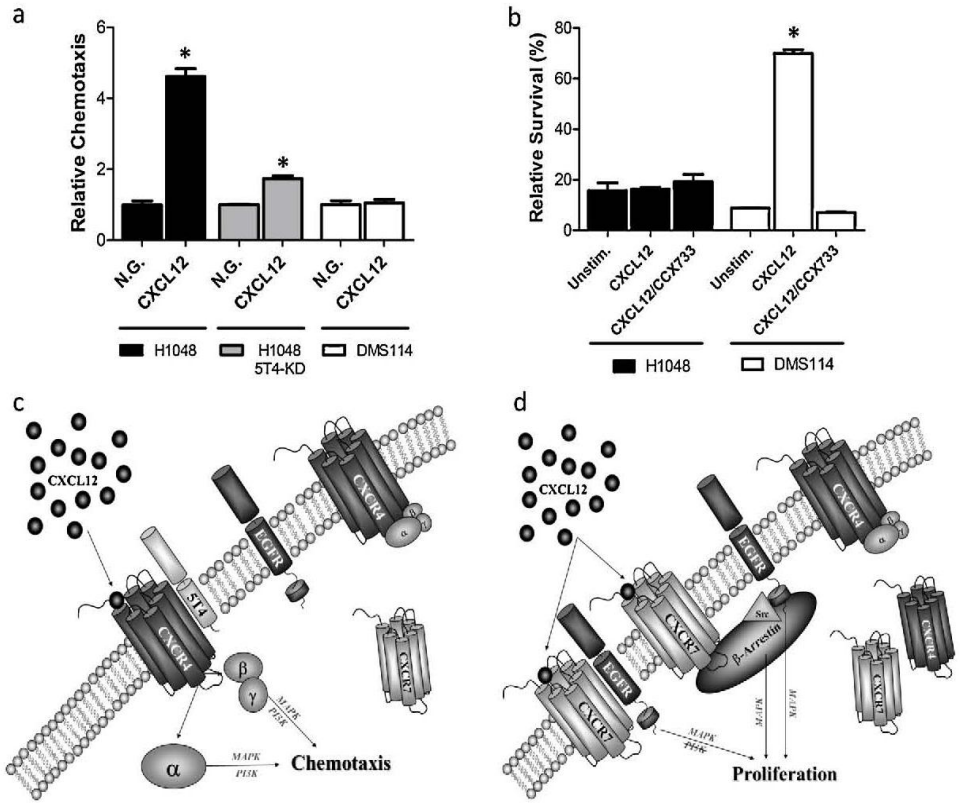

Fig. 1. 5T4 and CXCL12 receptor preference, signal transduction and biological responses. (a) Chemotaxis assays [21,34,38] show CXCL12 directional migration of H1048 (5T4 positive) but not 5T4KD H1048 or 5T4 negative DMS114 human small cell carcinoma cells. No gradient (NG); $^*p < 0.05$. (b) Survival analysis [34] shows only 5T4 negative DMS114 but not 5T4 positive H1048 have enhanced survival in CXCL12 mediated through the CXCR7 receptor (blocking with specific inhibitor CCX733). (c) In 5T4 positive cells some 5T4 and CXCR4 co-localize at the plasma membrane, this facilitates the response to a CXCL12 gradient leading to activation of the ERK/AKT signalling pathways within minutes which subsequently results in directional movement (chemotaxis). Certain 5T4 mAbs can block such chemotaxis. Such 5T4 influence can contribute to human tumour spread through potentiating chemotaxis. (d) In 5T4 negative cells the cells respond to CXCL12 by proliferation and/or increased survival in limiting conditions. In this circumstance, the alternative CXCL12 receptor CXCR7 is utilized but the ERK signalling pathway activated has much with slower kinetics derivative from CXCL12/CXCR7 transactivation of the EGFR through Src. Thus the absence of 5T4 marks the use of CXCR7 for CXCL12 signalling and a differential biological response in human tumour cells.

involving transactivation of the EGFR, eliciting proliferation rather than chemotaxis. Thus the surface expression of 5T4 marks the use of the CXCR4 rather than the CXCR7 receptor, with distinct consequences for CXCL12 exposure relevant to the spread and growth of a tumour [34]. It is possible that 5T4 plays a role in breaking the natural CXCR7 receptor bias of the chemokine CXCL12 (tenfold higher affinity) and provides for a switch in homeostatic function induced by the chemokine. The functional relevance to human cancer is supported by data with 5T4 negative and positive human small cell lung carcinoma cell lines which show respectively CXCL12/CXCR7 mediated improved survival and CXCL12/CXCR4 chemotaxis (Fig. 1a and b). Thus one might speculate that in a primary tumour, 5T4 surface expression by cells at the periphery would result in chemotaxis to CXCL12 secreting endothelial cells and metastatic spread. Whereas in the centre of the tumour preferential CXCR7 expression could compensate for the lower levels of chemokine and promote cell growth/survival (Fig. 1c and d). Therapeutic approaches, targeting selective inhibition of CXCR7 and CXCR4 signalling exploiting 5T4 dependency might improve tumour selectivity.

3.2. 5T4 oncofoetal antigen expression in childhood pre-B acute lymphoblastic leukaemia (B-ALL)

Most leukemic cells of B-cell origin express CXCR4 and a functional CXCR4 receptor appears to be critical for homing of pre-B acute lymphoblastic cells to the marrow niche [35] but mature hematopoietic cells are 5T4 negative [3]. However, 5T4 transcripts are detectable during B cell development at the pro- and pre-B cell phases [36] so using data from global gene expression profiling we looked for any correlation between 5T4 and CXCR4 expression in patients with pre-B acute lymphoblastic leukaemia (B-ALL). 5T4 but not CXCR4 transcription was significantly higher in patients with cytogenetic subtypes characteristic of high risk of relapse of pre-B ALL. It is these patients who have an increased risk of therapeutic failure and often have disease in extramedullary sites which express CXCL12 [37]. 5T4/CXCR4 positive pre B-ALL cells of high-risk cytogenetic type may have enhanced ability to home to extramedullary compartments that produce CXCL12. Using 5T4+ve and 5T4−ve cells derived from a high risk cytogenetics *BCR-ABL+* pre-B ALL line, we have shown that 5T4 expression correlates with increased invasion, adhesion and CXCR4/CXCL12 chemotaxis in vitro and differential infiltration of extramedullary sites following intraperitoneal challenge of immunocompromised mice [38]. Again CXCL12/CXCR4 chemotaxis is associated with 5T4 expression and can be blocked by certain monoclonal antibodies to 5T4. Even with the current successful B-ALL treatments, approximately 1 in 4 children will relapse with recurrence frequently characterized by the occurrence of disease at extra-medullary sites such as the central nervous system and gonads [39]. We are currently evaluating whether 5T4 expression can be used as a prognostic marker

Please cite this article in press as: Stern PL, et al. Understanding and exploiting 5T4 oncofoetal glycoprotein expression. Semin Cancer Biol (2014), http://dx.doi.org/10.1016/j.semcancer.2014.07.004

of leukemic spread, its mechanistic involvement and utility as a target for 5T4 antibody delivered immunotherapies [38].

4. 5T4 modulation of Wnt signalling

Intercellular signalling by Wnt proteins regulates numerous cellular processes during animal development, homeostasis and regeneration, while misregulated Wnt signalling causes disease, including cancer [40–47]. The most characterized pathway is the canonical Wnt/β-catenin pathway. In the absence of Wnt stimulation, β-catenin is associated with a destruction complex formed by proteins including Axin, adenomatous polyposis coli (APC) and glycogen synthase kinase 3 (GSK-3) which keep levels of cytoplasmic β-catenin low and localized in the cytoplasm. GSK-3 phosphorylates β-catenin, targeting it for ubiquitination and subsequent destruction by the proteasome. Upon Wnt ligand binding to a member of the Frizzled (Fzd) G-protein coupled receptor family complexed to a low-density lipoprotein receptor-related protein (LRP5/6), the destruction complex is inhibited, blocking phosphorylation of β-catenin by GSK-3. Hypophosphorylated β-catenin accumulates in the cytoplasm before translocating to the nucleus where it regulates expression of target genes including those involved in cell cycle and proliferation through partnerships with the T-cell-specific transcription factor/lymphoid enhancer-binding factor 1 (TCF/LEF) transcription factor family members. The canonical Wnt pathway is regulated by various secreted factors which bind to Wnt ligands and block their interaction with Fzd receptors including the Dickkopf (Dkk) family, which inhibit canonical Wnt signalling by inhibiting Fzd-LRP6 complex formation and by inducing LRP endocytosis. The other pathways (the planar cell polarity (PCP) and Ca^{2+} pathways) together are classified as non-canonical Wnt signalling as there is no discernible involvement of β-catenin. In the PCP pathway, Fzd receptor stimulation with Wnt ligands activates JNK and directs cytoskeletal rearrangement and coordinated polarization of cells within the plane of an epithelial sheet. There are two groups of ligands activating either the canonical or non-canonical pathways respectively Wnt1, Wnt3a, Wnt8 and Wnt8b and Wnt4, Wnt5a and Wnt11.

In Zebrafish, the homologue of mammalian 5T4, Wnt-activated inhibitory factor 1 (Waif1) interferes with Wnt/β-catenin signalling and concomitantly activates non-canonical Wnt pathways. Waif1a/5T4 interferes with β-catenin signalling in Wnt receiving cells by blocking Wnt-dependent LRP6 internalization without affecting LRP6 phosphorylation [48]. Thus, Waif1a/5T4 uses a novel mechanism of β-catenin signalling inhibition based on modulation of LRP6 availability in signalling-promoting intracellular compartments. Waif1/5T4 also enhances the activation of β-catenin-independent Wnt signalling possibly via stimulation of a non-canonical function of Dkk1 (Fig. 2a). Waif1/5T4 is involved in regulating Wnt pathway selection and could contribute to 5T4 influences on adhesion, cytoskeletal organization and motility thereby contributing to cancer spread and subsequently poorer clinical outcome. Interestingly, β-catenin-independent signalling activated by Wnt5a enhances motility and invasion of melanoma, breast cancer and gastric cancer cells [43,49–51]. This tempts speculation that 5T4 expression marks spread of cells by enhancing non-canonical Wnt signalling through a cell autonomous PCP type pathway which can drive the modulation of actin and microtubular skeletons, actions prerequisite for cell movement in development or cancer [52].

We have begun to investigate the role of Wnt signalling pathways in ovarian cancer where 5T4 expression is associated with a poorer clinical outcome [53]. Using SKOV-3 (WT and/or control KD) and 5T4 knockdown (KD) SKOV-3 ovarian cell lines we have established that Wnt3a treatment in wild type (WT) or control KD compared to 5T4 KD SKOV-3 cells demonstrates a 5T4 associated down-regulation of pBAR Wnt canonical pathway reporter activity (Fig. 2b). Derivative from crystal structure and amino acid alignment of 5T4 molecules from different species it has now been shown that amino acids K76 and F97, are essential for canonical Wnt inhibitory function of human 5T4 [9]. The non-canonical response is favoured in WT compared to 5T4KD cells as illustrated by the in vitro wound healing response to Wnt5a (Fig. 2c). Further, 5T4KD cells show enhanced JNK/SAPK phosphorylation (Fig. 2d), typical of the PCP pathway, as well as increased secretion of Dkk-1 (not shown) which acts to potentiate the non-canonical pathway. Immunohistochemistry analysis of primary and metastatic ovarian cancer samples has shown 5T4 expression increased with spread compared to surface epithelium of the ovary (Fig. 3a and b). Interestingly, non-canonical ligand Wnt5a expression has been linked to poor prognosis in women with ovarian neoplasia, where high expression of Wnt5a correlated with malignancy and poor survival outcomes [54]. Wnt5a expression has also been linked to chemoresistance to anti-cancer drugs with miRNA knockdown of Wnt5a in SKOV-3 cells leading to an increase in chemosensitivity [55]. Additionally, SKOV-3 cells have been shown to preferentially express non-canonical Wnt ligands [54]. All this supports a contributory role for non-canonical Wnt signalling activation in ovarian cancer with 5T4 expression a potential marker of this pathway. Both CXCL12 activation of CXCR4 and Wnt5a non-canonical Wnt signalling have been linked to poor prognosis in metastatic malignancy. Given that our work has demonstrated an association for 5T4 in the ability of cancer cells to activate both routes, it is feasible that 5T4 is involved in the synergy of these two important pathways. Indeed, there is data that suggest a synergistic role for Wnt and CXCR4-mediated signalling in cancer [56–58].

5. Exploiting 5T4 expression for cancer therapy

The selective pattern of 5T4 tumour expression, the association with a tumour initiating phenotype providing for improved therapy even within a heterogeneously 5T4 expressing tumour plus a putative mechanistic involvement with cancer spread through particular signalling pathways make this an attractive target for immunotherapeutic strategies. Three different 5T4 based immunotherapeutic strategies have been developed and are being tested in clinical studies.

5.1. Vaccine

Vaccine immunotherapy aims to maximize the immunogenicity of 5T4 by presenting the antigens in a foreign viral vector with the principle goal of generating effector T cells able to kill 5T4 positive tumours. Lack of high avidity T cell receptors (TCRs) in the T cell repertoire and specific or non-specific T regulatory cells may be major limiting factors for vaccine immunogenicity and effectiveness. The highly attenuated and modified vaccinia virus ankara (MVA) strain expressing either human or mouse 5T4 was used to evaluate immunogenicity and anti-tumour activity in preclinical studies [59].

Vaccination of mice with MVA-m5T4, was able to break tolerance (induction of antibodies) and control the growth of autologous B16 melanoma cells expressing m5T4 in a tumour protection scenario. Furthermore, mice vaccinated with MVA-m5T4 showed no signs of autoimmune toxicity. Additional studies established human CD4 and CD8 T cell 5T4 repertoires although the presence of specific Treg cells could limit their activity [60–63]. The preclinical data supported the development of TroVax (MVA-h5T4) for tumour immunotherapy. A succession of phase I or II clinical trials in colorectal, prostate and renal cell carcinoma patients (including

Please cite this article in press as: Stern PL, et al. Understanding and exploiting 5T4 oncofoetal glycoprotein expression. Semin Cancer Biol (2014), http://dx.doi.org/10.1016/j.semcancer.2014.07.004

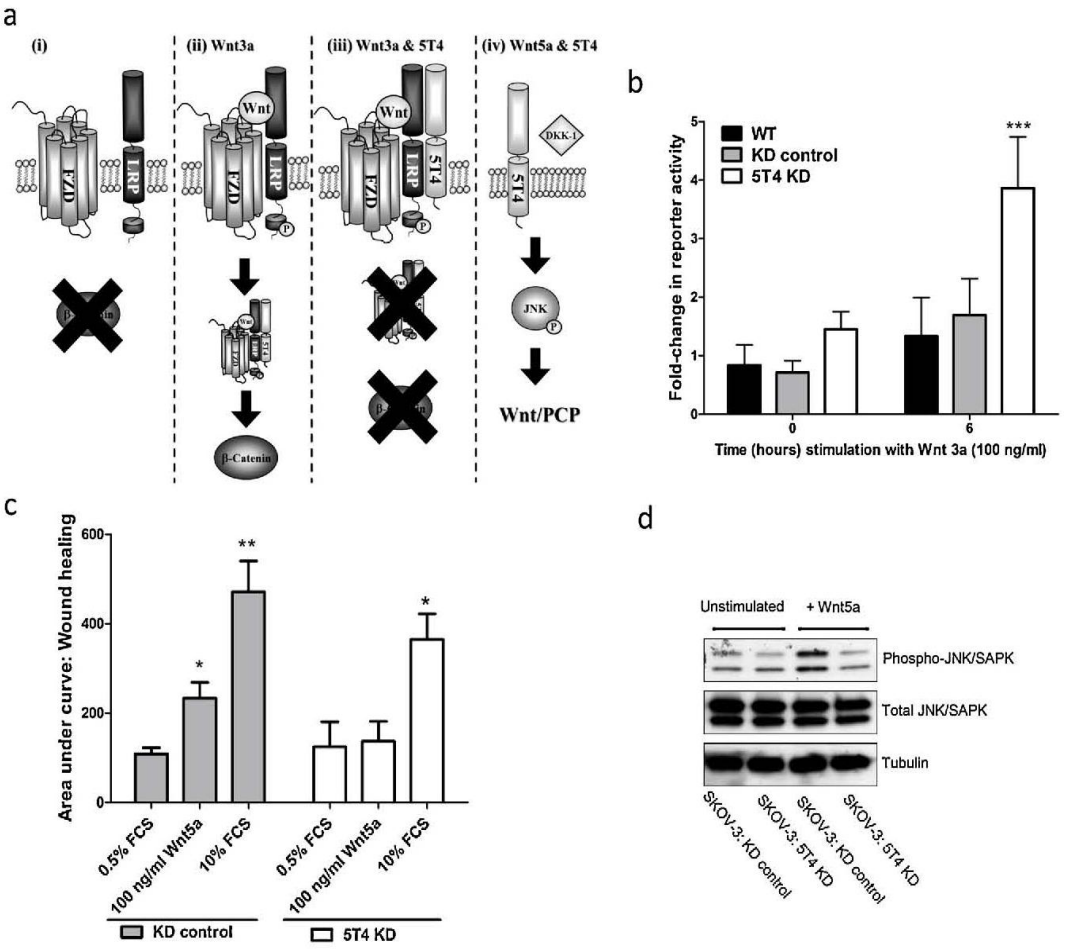

Fig. 2. 5T4 modulation of Wnt signalling. (a) Kagermeier-Schenk et al. [48] showed that Waif1a/5T4 interferes with β-catenin signalling in Wnt receiving cells by blocking Wnt-dependent LRP6 internalization without effecting LRP6 phosphorylation. This is a novel mechanism of β-catenin signalling inhibition based on modulation of LRP6 availability in signalling-promoting intracellular compartments. Waif1/5T4 also enhances the activation of β-catenin-independent Wnt signalling possibly via stimulation of a non-canonical function of Dkk1. Using SKOV-3 WT, KD control or 5T4KD ovarian carcinoma cells Wnt3a β-catenin signalling in a reporter assay was shown to blocked by 5T4 expression (b); Wnt5a driven in vitro wound healing [73] is correlated with 5T4 expression (c) and increased Wnt5a JNK/SAPK phosphorylation (d).

with chemotherapy or cytokine treatments) established the optimal dose and route of vaccination as well as safety, tolerability, and vaccine immunogenicity (serology, lymphocyte proliferation and ELISPOT assays) [3]. Following these studies, a phase III trial in renal cell carcinoma (RCC) patients was designed to determine if the addition of TroVax to available standard of care (SOC) therapy could improve survival for patients with metastatic RCC [63]. While TroVax was safe and well tolerated in all these patients, it failed to meet its primary endpoint as there was no significant difference in the survival for the TroVax and placebo treated groups. However, in the subset of patients with a good prognosis and receiving IL-2, there was a significantly improved survival with TroVax compared to the placebo group. Analysis of a selected group of 50 TroVax vaccinated patients with the highest increase in 5T4 antibody responses showed a favourable survival compared to placebo patients while a similar group with the highest increase in MVA antibody did not. Indeed, a high antibody response was associated with longer survival within TroVax treated clinical trial populations [64]. The latter result tempts speculation that these antibodies might be mechanistically involved by preventing spread through interference with 5T4 associated function. However, the induced antibodies are low titre and have not yet been assessed in any functional assay. Further trials of TroVax are ongoing but ultimately such vaccine approaches may require integration with the use of immunomodulators designed to interfere with regulatory controls of immunity through CTLA-4 and/or PD-1 checkpoint blockade [65,66].

5.2. Antibody directed superantigen therapy

Bacterial superantigens such as Staphylococcal Enterotoxin A (SEA) can activate T cells by linking the latter through binding to a particular family of V-beta chain containing TCRs to major histocompatibility complex (MHC) class II molecules on antigen presenting cells. With an antibody–superantigen fusion protein, large amounts of cytotoxic and cytokine producing T cells can be targeted by the antibody specificity for a tumour associated antigen (TAA) for in vivo tumour treatment. 5T4 was selected as a suitable target and the challenges overcoming the toxicity associated with MHC class II binding and any pre-existing immunity to the bacterial protein have been addressed in successive candidate drug developments [67]. In phase II studies of the first generation 5T4Fab-SEA

Please cite this article in press as: Stern PL, et al. Understanding and exploiting 5T4 oncofoetal glycoprotein expression. Semin Cancer Biol (2014), http://dx.doi.org/10.1016/j.semcancer.2014.07.004

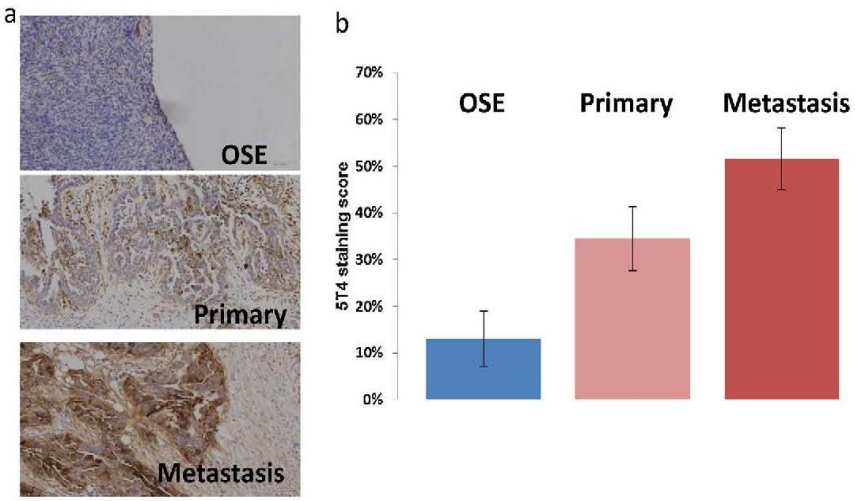

Fig. 3. Immunohistochemical analysis of 5T4 expression in paired primary and metastatic ovarian cancers. (a) Immunohistochemistry of FFPE sections following antigen retrieval (pH9) and labelling with R&D mouse monoclonal 4975 (5T4) and anti-mouse IgG-HRP. 5T4 labelling of normal surface epithelium of ovary, (OSE), a primary ovarian cancer and a paired metastatic deposit. (b) Immunoscoring of 5T4 expression in OSE and 11 paired ovarian cancer biopsies by immunoscoring shows there is a significant increase in expression with spread ($p < 0.05$).

drug in RCC patients, the treatment cycle was repeated after one month and survival was significantly prolonged compared to that expected. Patents receiving higher drug exposure had greater disease control and lived almost twice as long as expected, whereas low drug exposure patients survived as expected and where sustained IL-2 production at day 2 appeared to be a biomarker for the clinical effect [68]. This led to the development of an improved variant (ANYARA or naptumomab estafenatox) which incorporated a hybrid SEA/E-120 superantigen sequence with additional point mutations reducing MHC class II binding and antigenicity [69]. A Phase II/III study of ANYARA in combination with interferon-alpha versus interferon-alpha alone in 513 advanced RCC patients has been conducted. The safety profile was good but survival benefit was only seen by excluding patients with high levels of pre-formed antibodies. Additional analyses of the ANYARA Phase II/III study data are on-going with future development strategies aiming at a pivotal phase II/III study with ANYARA in combination with a tyrosine kinase inhibitor in the favourable RCC subgroup. Recent preclinical studies have shown the potential for use of ANYARA in treatment of pre B-ALL [38].

5.3. *Antibody drug conjugates (ADC)*

ADCs chemically combine the specificity of the antibody with a cytotoxic drug. The challenge is to produce an efficacious and safe agent and this demands optimizing the properties of a suitable TAA specific antibody in combination with the linkage chemistry and the payload characteristics. 5T4 is a particularly attractive target as it provides for delivery of therapeutic activity to a population of cells near the top of the cellular hierarchy through its expression by tumour initiating cells [70]. A 5T4 humanized monoclonal antibody (A1) linked by sulfydryl-based conjugation to deliver a tubulin inhibitor, monomethyllauristan F (MMAF) via a maleimidocaproyl showed potent in vivo activity in a variety of tumour models, with induction of long term regression after the last dose [71]. Evidence of the selective accumulation of the 5T4 (but not control) conjugates with release of the payload and consequent mitotic arrest in the tumour tissue was demonstrated. Depending on the particular tumour, 3–10 mg/kg doses given every 4 days were sufficient to produce a complete pathogenic response; this was independent of the degree of heterogeneity in 5T4 expression. This effect was shown to be consistent with the targeting of tumour initiating cells within the tumours. Primate studies have shown that the A1mcMMAF provides sufficient targeted payload to the tumour tissue with limited non-specific exposure of the cytotoxic agent. The overall therapeutic value is enhanced by the targeting of the most aggressive and tumourigenic populations within tumours (TICs), the study of which in a clinical setting is now in progress.

6. Conclusion

The functional biology of 5T4 molecules is consistent with a role in the directional movement of cells. These processes are highly regulated in normal developing and adult tissues. It seems reasonable to hypothesize that 5T4 is a marker and functional contributor to a cell type which might be described as a stem cell in motion. In adult tissues, 5T4 would only be expressed by stem cells which are required to move to deal with normal tissue replacement or damage. This 5T4 expression would be down-regulated again by normal tissue architecture and with the recovery of the appropriate stem cell niche. In cancer, this tissue homeostasis would be disrupted and 5T4 positive cancer stem cells would be enabled to move until a suitable niche was established. Thus it is likely that 5T4 expression would be a dynamic property and overlapping with stem cell capability. In early development, it has been hypothesized that Wnt signalling is the primary response of ES cells to differentiation signals. As such, expression of 5T4 should be correlated to the activation of Wnt signalling and reflect fate [72]. Obviously 5T4 is only one of many complimentary and independent functional modulators of cellular behaviour relevant to development and cancer. Nether the less widespread 5T4 tumour expression and link to a cancer stem cell phenotype make it a particularly attractive target for antibody based therapies.

Conflict of interest

P.L. Stern received milestone payments in respect of the development of TroVax and ANYARA.

Please cite this article in press as: Stern PL, et al. Understanding and exploiting 5T4 oncofoetal glycoprotein expression. Semin Cancer Biol (2014), http://dx.doi.org/10.1016/j.semcancer.2014.07.004

Acknowledgements

This work was supported by funds from Cancer Research UK, Leukemia and Lymphoma Research (Grant number 12054) and Wigan Cancer Research Fund.

References

[1] Hole N, Stern PL. A 72 kD trophoblast glycoprotein defined by a monoclonal antibody. Br J Cancer 1988;57(3):239–46.
[2] Southall PJ, Boxer GM, Bagshawe KD, Hole N, Bromley M, Stern PL. Immunohistological distribution of 5T4 antigen in normal and malignant tissues. Br J Cancer 1990;61(1):89–95.
[3] Stern P. Immunotherapies targeting 5T4 oncofoetal glycoprotein. In: Rezaei N, editor. Bench to bedside immunotherapy of cancers, Vol. 2. Berlin: Springer; 2014 [chapter 23].
[4] Hole N, Stern PL. Isolation and characterization of 5T4, a tumour-associated antigen. Int J Cancer 1990;45(1):179–84.
[5] Shaw DM, Woods AM, Myers KA, Westwater C, Rahi-Saund V, Davies MJ, et al. Glycosylation and epitope mapping of the 5T4 glycoprotein oncofoetal antigen. Biochem J 2002;363(Pt 1):137–45.
[6] Boyle JM, Grzeschik KH, Heath PR, Morten JE, Stern PL. Trophoblast glycoprotein recognised by monoclonal antibody 5T4 maps to human chromosome 6q14-q15. Hum Genet 1990;84(5):455–8.
[7] Myers KA, Rahi-Saund V, Davison MD, Young JA, Cheater AJ, Stern PL. Isolation of a cDNA encoding 5T4 oncofetal trophoblast glycoprotein. An antigen associated with metastasis contains leucine-rich repeats. J Biol Chem 1994;269(12):9319–24.
[8] Bella J, Hindle KL, McEwan PA, Lovell SC. The leucine-rich repeat structure. Cell Mol Life Sci 2008;65(15):2307–33.
[9] Zhao Y, Malinauskas T, Harlos K, Jones EY. Structural insights into the inhibition of Wnt signaling by cancer antigen 5T4/Wnt-activated inhibitory factor 1. Structure 2014;22(4):612–20.
[10] Carsberg CJ, Myers KA, Evans GS, Allen TD, Stern PL. Metastasis-associated 5T4 oncofoetal antigen is concentrated at microvillus projections of the plasma membrane. J Cell Sci 1995;108(Pt 8):2905–16.
[11] Carsberg CJ, Myers KA, Stern PL. Metastasis-associated 5T4 antigen disrupts cell–cell contacts and induces cellular motility in epithelial cells. Int J Cancer 1996;68(1):84–92.
[12] Awan A, Lucic MR, Shaw DM, Sheppard F, Westwater C, Lyons SA, et al. 5T4 interacts with TIP-2/GIPC: a PDZ protein, with implications for metastasis. Biochem Biophys Res Commun 2002;290(3):1030–6.
[13] King KW, Sheppard FC, Westwater C, Stern PL, Myers KA. Organisation of the mouse and human 5T4 oncofoetal leucine-rich glycoprotein genes and expression in foetal and adult murine tissues. Biochim Biophys Acta 1999;1445(3):257–70.
[14] Woods AM, Wang WW, Shaw DM, Ward CM, Carroll MW, Rees BR, et al. Characterization of the murine 5T4 oncofoetal antigen: a target for immunotherapy in cancer. Biochem J 2002;366(Pt 1):353–65.
[15] Nieto MA, Cano A. The epithelial–mesenchymal transition under control: global programs to regulate epithelial plasticity. Semin Cancer Biol 2012;22(5–6):361–8.
[16] Barrow KM, Ward CM, Rutter J, Ali S, Stern PL. Embryonic expression of murine 5T4 oncofoetal antigen is associated with morphogenetic events at implantation and in developing epithelia. Dev Dyn 2005;233(4):1535–45.
[17] Ward CM, Barrow K, Woods AM, Stern PL. The 5T4 oncofoetal antigen is an early differentiation marker of mouse ES cells and its absence is a useful means to assess pluripotency. J Cell Sci 2003;116(Pt 22):4533–42.
[18] Ward CM, Eastham AM, Stern PL. Cell surface 5T4 antigen is transiently upregulated during early human embryonic stem cell differentiation: effect of 5T4 phenotype on neural lineage formation. Exp Cell Res 2006;312(10):1713–26.
[19] Eastham AM, Spencer H, Soncin F, Ritson S, Merry CL, Stern PL, et al. Epithelial–mesenchymal transition events during human embryonic stem cell differentiation. Cancer Res 2007;67(23):11254–62.
[20] Spencer HL, Eastham AM, Merry CL, Southgate TD, Perez-Campo F, Soncin F, et al. E-cadherin inhibits cell surface localization of the pro-migratory 5T4 oncofetal antigen in mouse embryonic stem cells. Mol Biol Cell 2007;18(8):2838–51.
[21] Southgate TD, McGinn OJ, Castro FV, Rutkowski AJ, Al-Muftah M, Marinov G, et al. CXCR4 mediated chemotaxis is regulated by 5T4 oncofetal glycoprotein in mouse embryonic cells. PLoS ONE 2010;5(4):e9982.
[22] Christopherson 2nd KW, G. Hangoc, Mantel CR, Broxmeyer HE. Modulation of hematopoietic stem cell homing and engraftment by CD26. Science 2004;305(5686):1000–3.
[23] Balkwill F. The significance of cancer cell expression of the chemokine receptor CXCR4. Semin Cancer Biol 2004;14(3):171–9.
[24] Burger JA, Kipps TJ. CXCR4: a key receptor in the crosstalk between tumor cells and their microenvironment. Blood 2006;107(5):1761–7.
[25] Vandercappellen J, Van Damme J, Struyf S. The role of CXC chemokines and their receptors in cancer. Cancer Lett 2008;267(2):226–44.
[26] Nagasawa T, Nakajima T, Tachibana K, Iizasa H, Bleul CC, Yoshie O, et al. Molecular cloning and characterization of a murine pre-B-cell growth-stimulating factor/stromal cell-derived factor 1 receptor: a murine homolog of the human immunodeficiency virus 1 entry coreceptor fusin. Proc Natl Acad Sci USA 1996;93(25):14726–9.
[27] Burns JM, Summers BC, Wang Y, Melikian A, Berahovich R, Miao Z, et al. A novel chemokine receptor for SDF-1 and I-TAC involved in cell survival: cell adhesion, and tumor development. J Exp Med 2006;203(9):2201–13.
[28] Marchese A. Assessment of degradation and ubiquitination of CXCR4, a GPCR regulated by EGFR family members. Methods Mol Biol 2006;327:139–45.
[29] Ganju RK, Brubaker SA, Meyer J, Dutt P, Yang Y, Qin S, et al. The alpha-chemokine: stromal cell-derived factor-1alpha, binds to the transmembrane G-protein-coupled CXCR-4 receptor and activates multiple signal transduction pathways. J Biol Chem 1998;273(36):23169–75.
[30] Zhang J, Sarkar S, Yong VW. The chemokine stromal cell derived factor-1 (CXCL12) promotes glioma invasiveness through MT2-matrix metalloproteinase. Carcinogenesis 2005;26(12):2069–77.
[31] Marchese A, Raiborg C, Santini F, Keen JH, Stenmark H, Benovic JL. The E3 ubiquitin ligase AIP4 mediates ubiquitination and sorting of the G protein-coupled receptor CXCR4. Dev Cell 2003;5(5):709–22.
[32] Marinov G. Trafficking and functional interactions of the oncofoetal trophoblast glycoprotein 5T4. Manchester: Institute of Cancer Sciences, University of Manchester; 2012.
[33] Hay DL, Poyner DR, Sexton PM. GPCR modulation by RAMPs. Pharmacol Ther 2006;109(1-2):173–97.
[34] McGinn OJ, Marinov G, Sawan S, Stern PL. CXCL12 receptor preference, signal transduction, biological response and the expression of 5T4 oncofoetal glycoprotein. J Cell Sci 2012;125(Pt 22):5467–78.
[35] Crazzolara R, Kreczy A, Mann G, Heitger A, Eibl G, Fink FM, et al. High expression of the chemokine receptor CXCR4 predicts extramedullary organ infiltration in childhood acute lymphoblastic leukaemia. Br J Haematol 2001;115(3):545–53.
[36] van Zelm MC, van der Burg M, de Ridder D, Barendregt BH, de Haas EF, Reinders MJ, et al. Ig gene rearrangement steps are initiated in early human precursor B cell subsets and correlate with specific transcription factor expression. J Immunol 2005;175(9):5912–22.
[37] Moorman AV, Ensor HM, Richards SM, Chilton L, Schwab C, Kinsey SE, et al. Prognostic effect of chromosomal abnormalities in childhood B-cell precursor acute lymphoblastic leukaemia: results from the UK Medical Research Council ALL97/99 randomised trial. Lancet Oncol 2010;11(5):429–38.
[38] Castro FV, McGinn OJ, Krishnan S, Marinov G, Li J, Rutkowski AJ, et al. 5T4 oncofetal antigen is expressed in high risk of relapse childhood pre-B acute lymphoblastic leukemia and is associated with a more invasive and chemotactic phenotype. Leukemia 2012;26(7):1487–98.
[39] van den Berg H, de Groot-Kruseman HA, Damen-Korbijn CM, de Bont ES, Schouten-van Meeteren AY, Hoogerbrugge PM. Outcome after first relapse in children with acute lymphoblastic leukemia: a report based on the Dutch Childhood Oncology Group (DCOG) relapse all 98 protocol. Pediatr Blood Cancer 2011;57(2):210–6.
[40] Nusse R. Wnt signaling in disease and in development. Cell Res 2005;15(1):28–32.
[41] Gordon MD, Nusse R. Wnt signaling: multiple pathways, multiple receptors, and multiple transcription factors. J Biol Chem 2006;281(32):22429–33.
[42] Huelsken J, Behrens J. The Wnt signalling pathway. J Cell Sci 2002;115(Pt 21):3977–8.
[43] Pourreyron C, Reilly L, Proby C, Panteleyev A, Fleming C, McLean K, et al. Wnt5a is strongly expressed at the leading edge in non-melanoma skin cancer, forming active gradients, while canonical Wnt signalling is repressed. PLoS ONE 2012;7(2):e31827.
[44] Ho HY, Susman MW, Bikoff JB, Ryu YK, Jonas AM, Hu L, et al. Wnt5a-Ror-Dishevelled signaling constitutes a core developmental pathway that controls tissue morphogenesis. Proc Natl Acad Sci USA 2012;109(11):4044–51.
[45] McEwen DG, Peifer M. Wnt signaling: moving in a new direction. Curr Biol 2000;10(15):R562–4.
[46] Sheldahl LC, Slusarski DC, Pandur P, Miller JR, Kuhl M, Moon RT. Dishevelled activates Ca^{2+} flux: PKC, and CamKII in vertebrate embryos. J Cell Biol 2003;161(4):769–77.
[47] van Amerongen R, Nusse R. Towards an integrated view of Wnt signaling in development. Development 2009;136(19):3205–14.
[48] Kagermeier-Schenk B, Wehner D, Ozhan-Kizil G, Yamamoto H, Li J, Kirchner K, et al. Waif1/5T4 inhibits Wnt/beta-catenin signaling and activates noncanonical Wnt pathways by modifying LRP6 subcellular localization. Dev Cell 2011;21(6):1129–43.
[49] Pukrop T, Binder C. The complex pathways of Wnt 5a in cancer progression. J Mol Med (Berl) 2008;86(3):259–66.
[50] Weeraratna AT, Jiang Y, Hostetter G, Rosenblatt K, Duray P, Bittner M, et al. Wnt5a signaling directly affects cell motility and invasion of metastatic melanoma. Cancer Cell 2002;1(3):279–88.
[51] Yamamoto H, Kitadai Y, Yamamoto H, Oue N, Ohdan H, Yasui W, et al. Laminin gamma2 mediates Wnt5a-induced invasion of gastric cancer cells. Gastroenterology 2009;137(1):242–52, 252.e1–6.
[52] Clark CE, Nourse CC, Cooper HM. The tangled web of non-canonical Wnt signalling in neural migration. Neurosignals 2012;20(3):202–20.
[53] Wrigley E, McGown AT, Rennison J, Swindell R, Crowther D, Starzynska T, et al. 5T4 oncofetal antigen expression in ovarian carcinoma. Int J Gynecol Cancer 1995;5(4):269–74.
[54] Peng C, Zhang X, Yu H, Wu D, Zheng J. Wnt5a as a predictor in poor clinical outcome of patients and a mediator in chemoresistance of ovarian cancer. Int J Gynecol Cancer 2011;21(2):280–8.
[55] Badiglian Filho L, Oshima CT, De Oliveira Lima F, De Oliveira Costa H, De Sousa Damiao R, Gomes TS, et al. Canonical and noncanonical Wnt pathway:

Please cite this article in press as: Stern PL, et al. Understanding and exploiting 5T4 oncofoetal glycoprotein expression. Semin Cancer Biol (2014), http://dx.doi.org/10.1016/j.semcancer.2014.07.004

a comparison among normal ovary, benign ovarian tumor and ovarian cancer. Oncol Rep 2009;21(2):313–20.
[56] Dimitriadis A, Vincan E, Mohammed IM, Roczo N, Phillips WA, Baindur-Hudson S. Expression of Wnt genes in human colon cancers. Cancer Lett 2001;166(2):185–91.
[57] Ghosh MC, Collins GD, Vandanmagsar B, Patel K, Brill M, Carter A, et al. Activation of Wnt5A signaling is required for CXC chemokine ligand 12-mediated T-cell migration. Blood 2009;114(7):1366–73.
[58] Tamura M, Sato MM, Nashimoto M. Regulation of CXCL12 expression by canonical Wnt signaling in bone marrow stromal cells. Int J Biochem Cell Biol 2011;43(5):760–7.
[59] Mulryan K, Ryan MG, Myers KA, Shaw D, Wang W, Kingsman SM, et al. Attenuated recombinant vaccinia virus expressing oncofetal antigen (tumor-associated antigen) 5T4 induces active therapy of established tumors. Mol Cancer Ther 2002;1(12):1129–37.
[60] Smyth LJ, Elkord E, Taher TE, Jiang HR, Burt DJ, Clayton A, et al. CD8 T-cell recognition of human 5T4 oncofetal antigen. Int J Cancer 2006;119(7):1638–47.
[61] Elkord E, Burt DJ, Drijfhout JW, Hawkins RE, Stern PL. CD4+ T-cell recognition of human 5T4 oncofoetal antigen: implications for initial depletion of CD25+ T cells. Cancer Immunol Immunother 2008;57(6):833–47.
[62] Elkord E, Dangoor A, Burt DJ, Southgate TD, Daayana S, Harrop R, et al. Immune evasion mechanisms in colorectal cancer liver metastasis patients vaccinated with TroVax (MVA-5T4). Cancer Immunol Immunother 2009;58(10):1657–67.
[63] Amato RJ, Hawkins RE, Kaufman HL, Thompson JA, Tomczak P, Szczylik C, et al. Vaccination of metastatic renal cancer patients with MVA-5T4: a randomized, double-blind, placebo-controlled phase III study. Clin Cancer Res 2010;16(22):5539–47.
[64] Harrop R, Shingler W, Kelleher M, de Belin J, Treasure P. Cross-trial analysis of immunologic and clinical data resulting from phase I and II trials of MVA-5T4 (TroVax) in colorectal: renal, and prostate cancer patients. J Immunother 2010;33(9):999–1005.
[65] Binder DC, Schreiber H. Dual blockade of PD-1 and CTLA-4 combined with tumor vaccine effectively restores T-cell rejection function in tumors—letter. Cancer Res 2014;74(2):632, discussion 635.
[66] Ott PA, Hodi FS, Robert C. CTLA-4 and PD-1/PD-L1 blockade: new immunotherapeutic modalities with durable clinical benefit in melanoma patients. Clin Cancer Res 2014;19(19):5300–9.
[67] Hedlund G, Forsberg G, Nederman T, Sundstedt A, Dahlberg L, Tiensuu M. Tumour targeted superantigens. In: Schmidt S, editor. Fusion protein technologies for biopharmaceuticals: applications and challenges. Hoboken, NJ, USA: John Wiley & Sons, Inc.; 2013.
[68] Shaw DM, Connolly NB, Patel PM, Kilany S, Hedlund G, Nordle O, et al. A phase II study of a 5T4 oncofoetal antigen tumour-targeted superantigen (ABR-214936) therapy in patients with advanced renal cell carcinoma. Br J Cancer 2007;96(4):567–74.
[69] Eisen T, Hedlund G, Forsberg G, Hawkins R. Naptumomab estafenatox: targeted immunotherapy with a novel immunotoxin. Curr Oncol Rep 2014;16(2):370.
[70] Damelin M, Geles KG, Follettie MT, Yuan P, Baxter M, Golas J, et al. Delineation of a cellular hierarchy in lung cancer reveals an oncofetal antigen expressed on tumor-initiating cells. Cancer Res 2011;71(12):4236–46.
[71] Sapra P, Damelin M, Dijoseph J, Marquette K, Geles KG, Golas J, et al. Long-term tumor regression induced by an antibody-drug conjugate that targets 5T4: an oncofetal antigen expressed on tumor-initiating cells. Mol Cancer Ther 2013;12(1):38–47.
[72] Martinez Arias A, Brickman JM. Gene expression heterogeneities in embryonic stem cell populations: origin and function. Curr Opin Cell Biol 2011;23(6):650–6.
[73] Chen S, Wang J, Gou WF, Xiu YL, Zheng HC, Zong ZH, et al. The involvement of RhoA and Wnt-5a in the tumorigenesis and progression of ovarian epithelial carcinoma. Int J Mol Sci 2013;14(12):24187–99.

Please cite this article in press as: Stern PL, et al. Understanding and exploiting 5T4 oncofoetal glycoprotein expression. Semin Cancer Biol (2014), http://dx.doi.org/10.1016/j.semcancer.2014.07.004

Appendix 5: *ex vivo* Chemotaxis Methodology

Fresh ovarian cancer samples were obtained during surgical treatment and transferred in serum and phenol-red free RPMI supplemented with antibiotics and fungizone on ice to the laboratory in sterile tube. Tissue were cut into small, identical in size blocks using 4mm Miltex punch biopsy (Fisher Scientific, 33-34) while tissues were kept in the same transfer media. 21 blocks were selected and randomised, using SPSS random number generator function, to the type of experimental media in 48 well plate. One experiment included exposure to 0%, 1% or 10% serum and incubated for 12, 24 or 36 hours. Blocks were then fixed in formalin overnight, incubated with SYBR Gold nuclear stain (Life technologies, S-11494) overnight to allow penetration. Block transparency was achieved by treatment with methyl salicylate (Sigma, M6752) when blocks were imaged using macro-confocal microscope with ultra violet (UV) light source which allowed determination of cell density (via stained nuclei) within blocks by sectional imaging at 25 µm interval across the block axis.